HHS Public Access

Author manuscript

Chem Rev. Author manuscript; available in PMC 2019 February 14.

Published in final edited form as:

Chem Rev. 2018 February 14; 118(3): 1253–1337. doi:10.1021/acs.chemrev.7b00205.

Chemical Biology of H_2S Signaling through Persulfidation

Milos R. Filipovic[*,†,‡], **Jasmina Zivanovic**[†,‡], **Beatriz Alvarez**[§], and **Ruma Banerjee**[‖]

[†]Univeristy of Bordeaux, IBGC, UMR 5095, F-33077 Bordeaux, France

[‡]CNRS, IBGC, UMR 5095, F-33077 Bordeaux, France

[§]Laboratorio de Enzimología, Facultad de Ciencias and Center for Free Radical and Biomedical Research, Universidad de la Republica, 11400 Montevideo, Uruguay

[‖]Department of Biological Chemistry, University of Michigan Medical School, Ann Arbor, Michigan 48109-0600, United States

Abstract

Signaling by H_2S is proposed to occur via persulfidation, a posttranslational modification of cysteine residues (RSH) to persulfides (RSSH). Persulfidation provides a framework for understanding the physiological and pharmacological effects of H_2S. Due to the inherent instability of persulfides, their chemistry is understudied. In this review, we discuss the biologically relevant chemistry of H_2S and the enzymatic routes for its production and oxidation. We cover the chemical biology of persulfides and the chemical probes for detecting them. We conclude by discussing the roles ascribed to protein persulfidation in cell signaling pathways.

Graphical abstract

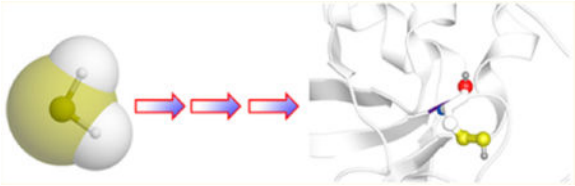

1. INTRODUCTION

Hydrogen sulfide (H_2S) is inextricably tied to the emergence of life on Earth. The recent discovery of unanalyzed samples from Miller's 1958 experiment confirmed that sulfur-containing molecules (including the amino acids cysteine and methionine) could have been formed under the atmospheric conditions of early Earth from H_2S, which is released in volcanic emissions and from other geothermal activity.[1] It is postulated that RNA, protein,

[*]**Corresponding Author:** milos.filipovic@ibgc.cnrs.fr.

Special Issue: Posttranslational Protein Modifications

ORCID

Milos R. Filipovic: 0000-0003-0060-0041

Notes

The authors declare no competing financial interest.

and lipid precursors have common origins in a cyanosulfidic protometabolism.[2] It is possible to create nucleic acid precursors on metal centers starting with hydrogen cyanide, H_2S, and ultraviolet light. Furthermore, the conditions that produced nucleic acid precursors likely also created the starting materials for natural amino acids and lipids suggesting that a simple set of reactions could have given rise to most of life's building blocks.[2]

Early life forms likely thrived in an H_2S-rich environment. H_2S would have been useful for synthetic purposes but also as a source of metabolic energy. One of the first reported examples of lithothrophy, i.e., the ability to utilize inorganic substrates for energy generation, is of the H_2S-oxidizing bacterium *Beggiatoa*, discovered by Winogradsky.[3] In this organism, H_2S provides the reducing power for CO_2 fixation via the Calvin cycle. Furthermore, green and purple sulfur bacteria use H_2S as an electron donor for photosynthetic CO_2 reduction. High levels of H_2S are lethal to most animals, but a few like pupfish, poeciliids, molluscs, and giant tubeworms are specialized to flourish in H_2S-rich habitats like marshes and deep-sea hydrothermal vents.

In medicine, perhaps the earliest reference to H_2S, even before its identity was established, was in a 1713 publication titled *De Morbis Artificum Diatribes* (Disease of Workers) by the Italian physician, Bernardino Ramazzini.[4] He described an occupation hazard that manifested as a painful inflammation in the eye in workers who were chronically exposed to an unknown "acidic vapor" while cleaning privies and cesspits. Ramazzini also noted that this acidic vapor was responsible for coating silver and copper coins in the pockets of ill workers with a black substance (presumably silver sulfide and copper sulfide).[4] While experimenting with pyrite ore (FeS_2) and mineral acid, the Swedish pharmacist Carl Wilhelm Scheele generated H_2S, which he described as "sulfur air" (Schwefelluft) in 1777.[5]

The historical reputation of H_2S as a poisonous gas endured until 1996, when Abe and Kimura first demonstrated that H_2S plays a role as an endogenous neuromodulator.[6] Kimura's group was also the first to report that H_2S acts as a smooth muscle relaxant,[7] although the beneficial effects of H_2S on blood vessels had been known for a while. Thus, several Russian publications in the 1960s reported the beneficial effects of H_2S baths on coronary vasodilation and peripheral blood circulation after reconstructive operations on major arteries,[8–10] and the effect of H_2S on isolated rabbit aorta was reported by Kruszina and colleagues in 1985.[11] The vasodilatory property of endogenously generated H_2S was demonstrated in mice lacking γ-cystathionine (CSE),[12] as they developed profound age-related hypertension, with some parallels to another gas signaling molecule, nitric oxide ($NO^{\bullet}$). These early observations propelled the current explosion of research on H_2S biology and signaling.

Another serendipitous discovery that put H_2S in the spotlight was the report that exposure of mice to subtoxic H_2S levels (20–80 ppm) decreased energy expenditure within a few minutes and induced a suspended animation-like state.[13] The body temperature dropped by almost 20 °C, and the respiration rate decreased to 10% of normal. Remarkably, these effects were completely reversible, and the animals showed no apparent deficits upon recovery.[13] This observation has spurred interest in the potential therapeutic development of H_2S to "buy time" for treating trauma patients.[14]

The past decade has witnessed a burgeoning literature on the physiological effects of H_2S and its role in many disease states, which are covered in several excellent reviews.[15–17] The proposal that signaling by H_2S involves postranslational modification of cysteine residues (i.e., Cys-SSH) provided a framework for understanding its physiological and pharmacological effects.[18,19] Protein persulfidation (erroneously described as sulfhydration) is also involved in biosynthetic pathways that require sulfur transfer, e.g., iron–sulfur clusters, biotin, thiamine, lipoic acid, molybdopterin, and sulfur-containing bases in RNA. The presence of the persulfide modification at a proteomic level was first examined only recently.[18–20]

Due to its inherent instability, persulfide chemistry remains understudied. In this review, we introduce the biologically relevant chemistry of H_2S, cover the enzymatic routes for its production and oxidation, discuss the chemical biology of persulfides and review progress on the development of chemical probes for persulfide labeling and visualization. We conclude by discussing how persulfidation can control protein function and cell signaling pathways.

2. CHEMICAL PROPERTIES OF H_2S

H_2S is a flammable gas with the smell of rotten eggs. The water–H_2S system strictly obeys Henry's law.[21–23] Some basic physicochemical properties of H_2S are given in Table 1. H_2S is a highly toxic gas. The human nose is considered to be one of the most sensitive H_2S sensors with a detection threshold of 0.02–0.03 ppm.[24,25] At 10 ppm, H_2S leads to eye soreness;[26] 20 ppm is the maximal allowable concentration for a daily 8 h exposure,[27] while exposure to 50 ppm of H_2S lead to conjunctival and mild respiratory irritation.[24,27,28] At 100 ppm, H_2S leads to olfactory loss within 3–15 min,[27] 150 ppm to olfactory nerve paralysis,[24,27,28] and exposure to 300–500 ppm represents an imminent threat to life leading to pulmonary edema.[29] Exposure to ≥500 ppm of H_2S leads to rapid loss of consciousness, cessation of respiration, and death.[30]

2.1. Nomenclature

Formerly called hydrosulfuric acid or sulfhydric acid due to the acidic nature of its aqueous solutions, dihydrogen sulfide and sulfane are now the names recommended for H_2S by IUPAC. For HS^-, the IUPAC recommended names are sulfanide or hydrogen(sulfide)(1−); for S^{2-}, sulfide(2−), or sulfanediide. The term "H_2S" is used in this review for the gas and for the mixture of H_2S and HS^- in aqueous solution at a certain pH, unless otherwise specified.

The term "sulfanes", according to the IUPAC Gold Book, includes polysulfanes, hydropolysulfides, and polysulfides, but its use is discouraged to avoid confusion with the newer systematic name sulfane for H_2S and the names derived therefrom. In the literature on the biological effects of H_2S, the term sulfane sulfur, sometimes abbreviated S^0, is used to refer to a sulfur atom that is covalently bonded to two or more sulfur atoms (e.g., $RS(S)_nSR$, where $(S)_n$ represents sulfane sulfurs) or to a sulfur atom and an ionizable hydrogen (e.g., Cys-SSH).[31,32] Some compounds containing sulfane sulfur are thiosulfate ($S_2O_3^{2-}$ or ^-S-SO_3^-), persulfides (RSSH), inorganic and organic polysulfanes (HSS_nSH, RSS_nSR, and

RSS$_n$H), polythionates ($^-$SO$_3$–S$_n$–SO$_3^-$), and cyclooctasulfur (S$_8$). Sulfane sulfur has six valence electrons in contrast to sulfide sulfur, which has eight, and is incorrectly referred to as “zero valence” sulfur, although it is always attached to other sulfur atoms or to an ionizable hydrogen. Sulfane sulfur can also be defined as sulfur that can tautomerize to the thiosulfoxide form (i.e., RSSH to RS(S)H). Sulfane sulfur usually has an oxidation state of zero.[33,34] It can be transferred to cyanide (CN^-) to form thiocyanate (SCN^-) and it can be reduced to H_2S by thiols (RSH). In this review, the term sulfane sulfur will be used to refer to a sulfur covalently bonded to two or more sulfur atoms or to a sulfur atom and an ionizable hydrogen. Elemental sulfur, that can be present in many different allotropic states of which the most abundant is S_8, will be abbreviated S_n.

2.2. Physicochemical Properties of H_2S

H_2S is a covalent hydride. Its structure is analogous to that of water, the hydride that is formed with oxygen, the companion to sulfur in the chalcogen group together with selenium and tellurium. However, the bond angles in H_2S are smaller than in water (93 versus 104°).[35] The frontier orbitals for the bent H_2S molecule are well described.[35,36] The molecular orbitals for H_2S result from the linear combination of the 1s orbital of the hydrogen atom and the 3s and 3p orbitals of the sulfur atom.[35,37] The energies of orbitals for H_2S versus HS^- are an important feature that defines the differences in their reactivity. For example the HOMO orbital of HS^- is less stable (−2.37 eV calculated and −2.31 eV measured)[38,39] than of H_2S (−10.47 eV) indicating that HS^- is more nucleophilic and basic than H_2S, which is consistent with their known reactivities. Because the HOMO is so stable, H_2S is not an excellent one-electron donor. The LUMO orbital for H_2S (+0.509 eV calculated and −1.1 eV based on electron affinity data) suggests that H_2S can be an excellent electron acceptor.[35,37] However, because LUMO is an antibonding orbital in the bent H_2S, electrons added to this orbital cause a weakening of both S–H bonds.[35]

Interestingly, H_2S forms relatively strong hydrogen bonds with HS^- in aprotic solvents. At low temperatures H_2S reacts with triethylammonium hydrosulfide and with tetramethylammonium hydrosulfide to form complexes containing, respectively, 2 and 3 mol of H_2S per mole of salt. The energy of the hydrogen bond in $HSH\cdots SH^-$ is greater than 29 kJ/mol and possibly as large as 58 kJ/mol.[40] At pressures above 90 GPa (Gigapascal), H_2S becomes a metallic conductor of electricity. When subjected to extremely high pressures (~1.5 million atmospheres (150 GPa)) and cooled below 203 K, H_2S displays the classic hallmarks of superconductivity: zero electrical resistance and a phenomenon known as the Meissner effect. The Meissner effect occurs when a superconducting material is placed in an external magnetic field and there is no field inside the sample, unlike in normal materials.[41]

H_2S has three low-temperature (ambient pressure) thermodynamic crystalline phases. IR spectra of crystalline phase III shows low-frequency bending vibration ν_2 at 1169, 1184, and 1189 cm^{-1}, higher frequency stretching vibrations, a symmetric stretch, ν_1 at 2525 and 2536 cm^{-1}, and an asymmetric stretch ν_3 at 2548 cm^{-1}.[42]

Sulfur is larger than oxygen (covalent radius of 105 against 66), has a lower electronegativity (2.58 against 3.44 in the Pauling scale), and is more polarizable. As a consequence, the dipolar moment is lower for H_2S than for water (0.97 versus 1.85 D) and

the intermolecular interactions are weaker. Thus, H_2S is a gas at room temperature and normal pressure, while water is a liquid (boiling points of −60 °C versus 100 °C). Nevertheless, H_2S has relatively high solubility in water (110 mM atm^{-1} at room temperature and 210 mM atm^{-1} at 0 °C).[43,44]

H_2S is a weak diprotic acid (eqs 1 and 2).

$$H_2S \rightleftharpoons HS^- + H^+ \quad (1)$$

$$HS^- \rightleftharpoons S^{2-} + H^+ \quad (2)$$

In aqueous solution, the pK_a valuesof the first dissociation (eq 1) are 6.98 and 6.76 at 25 and 37 °C, respectively. Different values for the second dissociation constant for HS^- have been reported. The original data indicated a pK_2 value at 25 °C ranging from 12.5 to 15.[43,45–49] However, Giggenbach pointed out that polysulfides formed at higher pH due to the oxidation of HS^- interfere with the determination of pK_2.[50,51] Based on optical spectra of highly alkaline, oxygen free, HS^- solution, Giggenbach estimated pK_2 to be 17 ± 0.1 at 24 °C.[51] Meyer et al., confirmed this based on Raman spectroscopic monitoring of the H−S stretch in an oxygen-free HS^- solution with sodium hydroxide concentrations ranging from 5 to 22 M.[52] Licht and Mansen proposed 17.3 for pK_2 of H_2S, based on pH measurements of highly alkaline K_2S solutions.[53] Using weak acid theory, which predicts a difference of 12.3 between pK_1 and pK_2 for an acid in which the negative charge resulting from the first dissociation step is localized on the same atom to which the second proton is bonded, Myers calculated a pK_2 value of 19 ± 2.[54] Extrapolating from the thermodynamic data for the dissociation of polysulfides and avoiding the experimental and theoretical difficulties associated with measurements in highly alkaline HS^- solutions, Schoonen and Barnes calculated pK_2 to be 18.51 ± 0.56.[55] Thus, although reference to the original values for pK_2 (12–15) persists in the biochemical literature, it is in fact higher (17–19).

At the physiological pH of 7.4 and at 37 °C, H_2S is in fast equilibrium with HS^-, and the proportions of HS^- and H_2S are 81 and 19%, respectively. The concentration of S^{2-} is negligible (1.7×10^{-12} M) but still sufficient to cause precipitation of metal sulfides, due to very low product solubility constants. Solutions of H_2S in water are mildly acidic with a pH of ~4, solutions of NaHS are alkaline, and solutions of Na_2S are strongly alkaline. This information needs to be taken into consideration when adding H_2S or its salts to chemical or biological assays. The concentration of the HS^- anion can be determined from its absorption at 230 nm,[56] using a molar absorptivity of 8000 M^{-1} cm^{-1}. However, air oxidation and polysulfide formation can complicate accurate determination.

2.3. Concentration in Membranes and Permeation of H_2S

The signaling actions of H_2S in compartments where it is not generated will be greatly influenced by its ability to concentrate in and diffuse across membranes. The partition coefficients (i.e., the ratio of its concentration in organic solvent/buffer) of H_2S between the

organic solvents octanol or hexane and water are 2.1 ± 0.2 and 1.9 ± 0.5, respectively, at 25 °C and pH 3.8, a pH where the diprotonated H_2S form predominates.[57] These values indicate that H_2S is slightly hydrophobic since it is twice as soluble in organic solvents as in water. When the pH is increased to the more physiological value of 7.4, the partition coefficient decreases to 0.64 ± 0.05 (for octanol), due to the ionization of H_2S to HS^- in the aqueous phase.[57] Consistent with the values in organic solvents, the partition coefficient between dilauroylphosphatidylcholine liposomes and water is 2.0 ± 0.6 (pH 3.8, 25 °C).[57] This relatively high solubility in a membrane model is consistent with the high permeability of H_2S across biological membranes. Experimental estimates, comparison with other molecules, and molecular dynamics studies suggest that membrane permeability is as high as 11.9 cm s^{-1} and that aquaporins or other protein facilitators are not needed for H_2S to cross membranes.[57–59] Nevertheless, according to mathematical models, biological membranes are expected to slow down H_2S transport resulting in local increases at sites of formation.[57]

2.4. Reactivity of H_2S

The ability of HS^- to donate a pair of electrons and form a covalent bond, i.e., its nucleophilicity, is very good. This can be explained by its negative charge, by its high polarizability, and by the relatively low electronegativity of sulfur. Furthermore, HS^- is highly available at neutral pH due to the pK_1 value of H_2S being ~7.

A generic reaction of HS^- with an electrophile (E_1^+) is represented in eq 3. In contrast to the analogous reactions of thiolates (RS^-, where the sulfur is bound to a carbon), the product formed from the reaction of HS^- with an electrophile can ionize and react with a second electrophile (E_2^+) leading to a distinct product (eq 4). This differential reactivity between HS^- and thiolates is the basis of several methods for H_2S detection (see section 3).

$$HS^- + E_1^+ \rightarrow E_1 - SH \quad (3)$$

$$E_1 - S^- + E_2^+ \rightarrow E_1 - S - E_2 \quad (4)$$

The measure of nucleophilicity is a kinetic one and is estimated by comparing reaction rates, i.e. the faster the reaction, the greater the nucleophilicity. In this regard, it is interesting to compare the nucleophilicity of HS^- with that of alkyl thiolates (RS^-). This comparison is biochemically relevant, since thiolates are abundant in biological systems. The rate constants of the reactions of HS^- with different disulfides (eq 5) are about 1 order of magnitude smaller than the corresponding reactions of thiolates (eq 6).[60]

$$HS^- + R_1SSR_2 \rightarrow R_1SSH + R_2S^- \quad (5)$$

$$RS^- + R_1SSR_2 \rightarrow R_1SSR + R_2S^- \quad (6)$$

Equation 6 represents a thiol disulfide exchange reaction. These reactions occur through a concerted mechanism in which the attack of HS^- or RS^- on one of the sulfurs in the disulfide is accompanied by the release of the other as a thiolate. The lower rate constants in the case of HS^- versus RS^- can be attributed to the lack of an inductive effect by the adjacent methylene, to differences in polarizability, or to solvation effects.[60] Accordingly, computational calculations show that the energy of the highest occupied Kohn–Shan orbital, an indicator of nucleophilicity, is lower for HS^- than for thiolates, while the chemical hardness is higher.[60] The reactivity of HS^- toward hydrogen peroxide and peroxynitrite is also lower than that of thiolates.[61,62]

The two-electron reduction potential $E^{\circ\prime}(HS_2^-, H^+/2HS^-)$ is −0.23 V (versus SHE), which means that H_2S is a strong reductant.[63,64] The value is similar to the potentials for the cysteine and glutathione redox couples.[63,64] Importantly, the reaction of H_2S with two-electron oxidants such as hydroperoxides does not yield a disulfide (HSSH/HSS^-) directly. Instead, sulfenic acid (HSOH) is formed as an intermediate (see section 5).

The one-electron reduction potential $E^{\circ\prime}(S^{\bullet-}, H^+/HS^-)$ is estimated to be +0.91 V based on the thermodynamic parameters for these two species: $\Delta_f G^\circ(S^{\bullet-})$ = +140 kJ/mol, $\Delta_f G^\circ(HS^-)$ = +12 kJ/mol, pK_a ($HS^\bullet$) = 3.4[64] and is identical to the experimentally determined value of 0.92 V.[65] The value compares well with the values for thiols ($E^{\circ\prime}(RS^\bullet, H^+/RSH)$ = +0.96 V).[63,64] Given that pK_1 of H_2S is ~7, the Gibbs energies of formation of H_2S and HS^- are identical at pH 7. The bond dissociation energy of H_2S is 90 kcal mol^{-1} or 377 kJ mol^{-1}.[66] For comparison, the bond dissociation energy of H_2O is 118 kcal mol^{-1} or 494 kJ mol^{-1} and the one-electron reduction potential is $E^{\circ\prime}(HO^\bullet, H^+/H_2O)$ = +2.32 V.[67]

The one-electron oxidation of H_2S to the sulfyil radical ($HS^\bullet$) by biological oxidants is expected to be difficult given the high reduction potential of the $S^{\bullet-}/HS^-$ couple. Yet, H_2S is known to decay in air and is also oxidized by metals. The discrepancy is explained by the high reactivity of the resulting $HS^\bullet/S^{\bullet-}$ radicals. $HS^\bullet$ (λ_{max} = 240 nm) dimerizes to give H_2S_2,[65,68] which in turn, readily decomposes to give S_n and H_2S (eq 7, 8),[69,70] both of which are removed from the system pulling the redox equilibrium in the direction of H_2S oxidation.

$$S^{\bullet-} + HS^\bullet \rightarrow HS_2^- \quad k = 9 \times 10^9 M^{-1}s^{-1} \quad (7)$$

$$HS_2^- + H^+ \rightarrow \frac{1}{n}S_{n(s)} + H_2S(g) \quad (8)$$

At pH > 5, $^{\bullet}SH/S^{\bullet-}$ reacts with HS^- ($k_f = 4 \times 10^9\ M^{-1}\ s^{-1}$, $k_r = 5 \times 10^5\ s^{-1}$) to form disulfanuidyl (or dihydrogen disulfide radical anion), $HSSH^{\bullet-}/HSS^{\bullet 2-}$ (λ_{max} = 380 nm) (eq 9).[65,68]

$$S^{\bullet -} + HS^- \rightleftharpoons HSS^{\bullet 2-} k_f = 4 \times 10^9 M^{-1} s^{-1},\ k_r = 5.3 \times 10^5 s^{-1} \quad (9)$$

Both $HS^{\bullet}/S^{\bullet-}$ and $HSSH^{\bullet-}/HSS^{\bullet 2-}$ react with oxygen (eq 10–12). $HSS^{\bullet 2-}$ is a weaker oxidant than $S^{\bullet-}$ ($E^{\circ\prime}(HSS^{\bullet 2-}, H^+/HS^-) = +0.67$ V). EPR studies have identified the $^{\bullet}SH$ radical in irradiated glassy solutions of sulfides and determined that its reaction with O_2 leads to formation of $OSO^{\bullet-}$ (λ_{max} = 255 nm) and not $^-SOO^{\bullet}$.[71]

$$S^{\bullet -} + O_2 \rightarrow SO_2^{\bullet -}\ k = 5 \times 10^9 M^{-1} s^{-1} \quad (10)$$

$$SO_2^{\bullet -} + O_2 \rightarrow SO_2 + O_2^{\bullet -}\ k = 1 \times 10^8 M^{-1} s^{-1} \quad (11)$$

$$HSS^{\bullet 2-} + O_2 \rightarrow HSS^- + O_2^{\bullet -}\ k = 4 \times 10^8 M^{-1} s^{-1} \quad (12)$$

A major technical problem while working with H_2S solutions is the propensity for autoxidation. When H_2S or Na_2S are added to oxygen-free water a clear solution is formed. If the solution contains oxygen and trace metals in the pH range 6–9, a yellow-green color develops. The intensity of the color depends upon the concentration of elemental sulfur, S_n. Upon acidification, a whitish colloidal sulfur suspension forms.

Although the one-electron reduction of oxygen by HS^- (eq 13) is not thermodynamically favored, as reflected by the reduction potential $E^{\circ\prime}(O_2/O_2^{\bullet-}) = -0.35$ V (−0.18 V for a 1 M O_2 standard state), H_2S oxidation nonetheless occurs, albeit slowly.[72–76]

$$HS^- + O_2 \rightarrow S^{\bullet -} + HO_2^{\bullet}\ \Delta E^{\circ\prime} = -1.26\ V \quad (13)$$

The reaction between H_2S and O_2 is expected to be very slow from a kinetic point of view due to a spin barrier. O_2 has a triplet electronic ground state and a diradical character, which promotes its reactions with species with unpaired electrons but slows its reactions with species with paired electrons as in H_2S. The oxidation of H_2S (HS^- and S^{2-}) by O_2 has a complicated stoichiometry with an array of products and metastable intermediates being produced. Products of all sulfur oxidation states have been reported: polysulfide ions (S_4^{2-} and S_5^{2-}), sulfur (colloidal or orthotrombic), $S_4O_6^{2-}$), $S_2O_3^{2-}$, SO_3^{2-}, $S_2O_6^{2-}$and SO_4^{2-}. Elemental sulfur, sulfite, sulfate, and thiosulfate are the major product observed in many studies and are usually formed in the stoichiometries shown in eqs 14–17:[72–76]

$$8H_2S + 4O_2 \rightarrow S_8 + 8H_2O \quad (14)$$

$$H_2S + \frac{3}{2}O_2 \rightarrow 2H^+ + SO_3^{2-} \quad (15)$$

$$SO_3^{2-} + \frac{1}{8}S_8 \rightarrow S_2O_3^{2-} \quad (16)$$

$$H_2S + 2O_2 \rightarrow 2H^+ + SO_4^{2-} \quad (17)$$

Transition metal ions and complexes are effective catalysts as they are able to lower the activation energy for redox reactions.[77] This chemistry is exploited during industrial removal of H_2S, which is a corrosive gas, from sour waters and wastewaters, from gaseous streams, and from raw oil. For large industrial scale cleaning applications (especially for sour gases), the Claus process is employed, converting H_2S to S_n in two steps. In the first step, H_2S gets oxidized to SO_2, which symproportionates in a second reaction with another mole of H_2S to elemental sulfur of high purity (>99.5%).[78,79]

For smaller applications and quantities, diverse setups and methods have been employed and patented. Some well-described applications include H_2S removal by bacteria, ultrasonic irradiation[80] bare iron or iron oxide surfaces,[81,82] iron solutions ($Fe_2(SO_4)_3$), or iron chelated agents (e.g., EDTA and CDTA).[83–85] Interestingly, addition of the heavy metal ion chelator DTPA (diethylenetriaminepentaacetic acid), which unlike EDTA completely chelates iron, stabilizes H_2S in solution and prevents its oxidation. The use of DTPA is highly recommended when working with H_2S (Na_2S or NaHS) solutions.[86]

Inorganic polysulfides and sulfur formed during H_2S oxidation could have biological effects of their own. Inorganic polysulfides and their biological effects are covered in detail in section 8.4.

The chemistry of sulfur has been reviewed extensively.[87–89] Sulfur exists in many allotropic forms of which cyclic S_8 is the most stable.[87–89] In polar solvents such as methanol or acetonitrile, S_8 is partially transformed to S_7 and S_6 at ambient temperatures.[90] In aprotic solvents, hydroxide ion reacts with elemental sulfur S_8 to give the trisulfur anion radical $S_3^{\bullet-}$ as the major product.[91] $S_3^{\bullet-}$ is highly reactive (see section 8.5). The allotropic composition of elemental sulfur is further perturbed by light.[92] Sulfur can also exist as polymeric sulfur (S_∞). During oxidation of H_2S solutions, sulfur sol can arise, which consists of a sulfur core with hydrophilic polythionate ($S_x(SO_3^-3)_2$) tails that enhance solubility and give rise to the characteristic yellow color.[87–89] Sulfur also has biological effects akin to H_2S. Intravenous

injection of sulfur in rabbits led to the immediate detection of H_2S in breath.[93] Addition of colloidal sulfur to liver extracts led to its reduction to H_2S and to increased oxygen uptake.[94] Red blood cells can reduce sulfur in an NADPH- and glutathione-dependent manner, leading to H_2S release.[95] Some elemental sulfur preparations have entered preclinical trials recently, as H_2S donors.[96]

3. WORKING WITH H_2S

Several methods are available for the qualitative and/or quantitative detection of H_2S. Before describing the different analytical methods, important considerations such as H_2S source, handling and safety precautions, and possible interferences in the measurements are discussed.

3.1. Handling Precautions

Although H_2S is relatively soluble in water and the pH dependent ionization to HS^- and S^{2-} increases the concentration of total H_2S species in the aqueous phase, solutions of H_2S or its salts, NaHS and Na_2S, lose H_2S to the gas phase. This loss is more significant when solutions are acidic rather than alkaline (pK_a of H_2S = 6.98, 25 °C) and when containers have large headspaces. Therefore, it is necessary to use sealed vials and to transfer H_2S-containing solutions using gastight syringes.[97] In addition, since H_2S tends to oxidize, particularly in the presence of metal ion contaminants, it is necessary to prepare solutions in anaerobic water or buffers, free of trace metals.[97] Storage of H_2S solutions is not recommended and solutions should be prepared immediately before use.

H_2S is highly toxic and should be handled in fume hoods. Investigators should not rely on their sense of smell for monitoring H_2S, because, although it can be detected at concentrations as low as 0.02 ppm, the inability to smell H_2S is one of the first signs of H_2S toxicity. Before discarding H_2S-containing solutions, a quenching solution containing zinc acetate (30 g/L), sodium citrate (9 g/L), and NaOH (12 g/L) can be used that results in insoluble ZnS formation. The safety aspects of working with H_2S have been reviewed recently.[86,98]

3.2. Inorganic Sources of H_2S for Reference and Experiments

H_2S from commercially available gas cylinders can be a very pure source of this gas. Solutions are usually prepared by dissolving the gas in a deoxygenated solvent. A saturated solution containing ~0.1 M H_2S and with a pH of ~4 can be prepared in water. HS^- solutions can be prepared in buffer solutions with pH ~9. The gas flow-through should be trapped as ZnS to avoid H_2S release into the atmosphere.[86] Alternatively, H_2S solutions can be prepared by mixing sulfide salts with acid in variations of Kipp's apparatus for the preparation of gases.[99] In addition, concentrated solutions of H_2S (0.8 M) in tetrahydrofuran are commercially available.

Sulfide salts rather than H_2S gas are in fact often used for practical reasons. The salts that are usually used are sodium hydrogen sulfide ($NaSH{\cdot}xH_2O$) and disodium sulfide, either anhydrous (Na_2S) or nonahydrate ($Na_2S{\cdot}9H_2O$). The purity of the salts is an important consideration, particularly in the case of the NaSH salts.[86,97,98,100,101] Being highly

hygroscopic, these salts bind water from air and become liquid with time if kept outside of a glovebox. Of particular concern is the use of salts with unidentified numbers of water molecules (commercially available as $NaSH \cdot xH_2O$, where $x = 1–10$), as it is unclear how researchers can calculate H_2S concentrations without a defined molecular weight. Recently the preparation of tetrabutylammonium hydrosulfide (NBu_4SH) was reported, which is a potentially useful source of HS^- in experiments performed in organic solvents.[102] However, NBu_4SH is very hygroscopic and should also be handled with care in a glovebox. Frequent impurities found in all these sources are water, elemental sulfur, polysulfides, and other oxidation products such as sulfite and thiosulfate. Another concern is the alkaline pH of the solutions of the salts, particularly Na_2S, in water. The salts should be white, anhydrous powders and should be stored in desiccators under vacuum or in an argon box. It is convenient to wash the crystals with distilled water to remove oxidation products from the surface.[86] To eliminate sulfane sulfur contaminants, stock solutions can be treated with immobilized phosphines[103] or with cyanide.[100,101]

Several natural and synthetic compounds can slowly liberate H_2S to potentially simulate its formation in biological systems. Various chemical groups and release mechanisms are involved, and this subject has been extensively reviewed.[104–110] NaSH and Na_2S salts are sometimes incorrectly referred to as H_2S donors; slow release of H_2S from them cannot be invoked. The acid base equilibration of these salts is extremely fast and consequently, the corresponding concentrations of HS^- and H_2S exist in solution with their ratio depending on the pH.

3.3. H_2S Donors

Recent advances in H_2S donor design have led to the development of several classes of donors that are showing very promising pharmacological effects. One main difference between these donors and sulfide salts is the slow release of H_2S, potentially mimicking physiological H_2S production. Significant problems with H_2S donors are that the chemistry of H_2S release is often unclear (for some, their pharmacologically similar effects to H_2S are used as an indication of their H_2S donor ability) and that the decomposition products could be reactive. The chemistry and biological applications of H_2S releasing agents has been extensively covered.[104–110] In this section, we summarize the main classes of H_2S donors, which are grouped based on the mechanism of their H_2S release: (i) donors that require thiols to release H_2S, (ii) donors that release H_2S by hydrolysis (with or without light), (iii) donors that release H_2S in reaction with bicarbonate, and (iv) COS-releasing donors that yield H_2S in the presence of carbonic anhydrase (Figure 1).

The simplest and oldest known thiol-activated H_2S donors are active principles of garlic.[111] Their chemistry is covered in section 8.6 as these compounds also release low molecular weight persulfides. The first synthetic thiol-activated donors were compounds based on the *N*-mercapto template (Figure 1A).[112] Since *N*-SH species are unstable, acyl groups were introduced to protect the mercapto group and enhance stability. In the presence of thiols such as GSH or cysteine, these compounds decompose to give H_2S. Similarly to *N*-SH donors, tertiary perthiol-based compounds were reported as H_2S donors, e.g., pencillamine-perthiol (Figure 1B).[113] It is important to note, however, that H_2S release from these donors also

results in the formation of mixed disulfides, which could introduce other modifications on proteins and initiate signaling. Nonetheless, the protective effects of pencillamine-perthiol based H_2S donors in myocardial ischemia/reperfusion injury have been reported. Dithioperoxyanhydrides were also recently reported as potential thiol-activated H_2S donors.[114] Again, these compounds require 2 mol of thiol and release 1 mol of H_2S and a mixed disulfide (Figure 1C). Arylthioamides represent the fourth class of thiol-activated H_2S donors (Figure 1D). However, these compounds show very weak H_2S formation even in the presence of high concentrations of glutathione or cysteine.[115] Nonetheless, when administered orally to rats, they induced a drop in blood pressure, reminiscent of the effect of H_2S. *S*-Aroylthiooximes have also been proposed as H_2S donors in the presence of aminothiols and show potential for the preparation of H_2S releasing materials (Figure 1E).[116,117]

Some compounds, such as Lawesson's reagent (2,4-bis(4-methoxyphenyl)-1,3,2,4-dithiadiphosphetane-2,4-disulfide) are known to release H_2S by spontaneous hydrolysis in aqueous solution.[118] In fact, this compound was shown to be beneficial in regulating colon ulceration in a rat colitis model.[119] A derivative of Lawesson's reagent, GYY4137 (morpholin-4-ium metoxyphenyl(morpholino) phosphino-dithioate) is one of the most widely used H_2S donors (Figure 1F).[120–124] The pH-sensitive H_2S release (the lower the pH the greater the release) has been confirmed both colorimetrically and amperometrically, and the mechanism of H_2S generation recently elucidated.[125] This is a two-step process; the first, faster step involves straightforward sulfur–oxygen exchange with water, while the second, slower step, results in complete hydrolysis to an arylphosphonate (Figure 1F). GYY4137 has vasodilatory and anti-inflammatory effects akin to H_2S, and considering the time scale for most of its reported biological effects, the probable source of H_2S is the first reaction step (Figure 1F).[125] Using a core structure of GYY4137 or the phosphorothioate as a template, new compounds that undergo pH-dependent cyclization and subseqent H_2S release have been reported recently. Such donors could have particular application in ischemia-reperfusion injury where a pH drop is expected in ischemic tissues (Figure 1G).[126]

1,2-Dithiole-3-thiones represent another class of H_2S-releasing molecules[127] that is widely used in the design of H_2S donors and is often coupled to some other pharmacologically active moiety, e.g., nonsteroidal anti-inflammatory drugs,[128–130] adenosine,[131] or targeted to mitochondria with the lipophilic triphenylphosphonium cation (Figure 1H).[132–134] Hydrolysis is proposed to be involved in the mechanism of H_2S release, and the hydrolysis products were recently identified by mass spectrometry. Furthermore, this class of molecules was shown to directly persulfidate glutathione,[131] while mitochondrially targeted AP39 (Figure 1H), even at nanomolar concentrations, increased intracellular persulfide levels more strongly than any H_2S donor.[135] Some NSAID conjugated hybrids have entered phase I clinical trial.[136] Some effort has been made in preparing photocleavable gemdithiol based H_2S donors, which then undergo hydrolysis to release H_2S (Figure 1I).[137]

Thio-amino acids (thioglycine and thiovaline) reportedly react with bicarbonate and are converted to the corresponding *N*-carboxyanhydrides with concomitant release of H_2S (Figure 1J).[138] Considering the high concentration of bicarbonate in the biological milieu and its common use as a buffer in cell culture media, these compounds could potentially be

useful as H_2S donors. Unlike other reported classes, these donors reach their plateau after 1 h and could be classified as donors with moderate-to-fast H_2S release.

Some compounds are able to release carbonyl sulfide (COS; e.g., thiocarbamates and *N*-thiocarboxyanhydrides). COS is converted into H_2S by the action of the ubiquitous enzyme carbonic anhydrase (Figure 1K).[139,140] This chemistry has been explored to create molecules that release COS (and subsequently H_2S) upon light activation or intracellular reaction with reactive oxygen and nitrogen species.[141,142]

The first metal complex-based H_2S donor has been reported recently, ammonium tetrathiomolybdate (Figure 1L).[143] $(NH_4)_2MoS_4$ was shown to slowly release H_2S in buffers and cell culture[143] and exhibited cytoprotective effects in a rat model of ischemia-reperfusion injury.[144]

3.4. Methods for H_2S Measurement

Unlike H_2S, the deprotonated species, HS^- and S^{2-}, absorb in the ultraviolet region with absorption coefficients at 230 nm of 8.0×10^3 and 4.6×10^3 M^{-1} cm^{-1}, respectively, at 25 °C.[145] In principle, H_2S solutions can be diluted in buffer at pH ~9.6 (e.g., carbonate buffer), where H_2S is predominantly in the HS^- form, and the concentration can be determined from the absorbance at 230 nm.[86] This approximation is, however, useful only for very pure solutions since the presence of H_2S oxidation products as well as other components in the case of complex mixtures can cause interference.

To standardize stock solutions, classical iodometric titrations can be performed. For this, H_2S is trapped in zinc acetate to minimize its diffusion and then reacted with excess iodine in acidic medium. The remaining iodine is titrated with sodium thiosulfate, using starch as an indicator (eqs 18 and 19). However, the presence of other reductants can lead to error.

$$S^{2-} + I_2 \rightarrow S + 2I^- \quad (18)$$

$$I_2 + 2S_2O_3^{2-} \rightarrow 2I^- + S_4O_6^{2-} \quad (19)$$

The development of H_2S detection tools has been rapidly expanding and has been covered in several review articles. In the following sections, an overview of the most widely used methods for H_2S detection is provided.

3.4.1. Methylene Blue Method—This method is based on the synthesis of methylene blue from H_2S and *N*,*N*-dimethyl-*p*-phenylenediamine in the presence of acid and ferric chloride (Chart 1). The oxidative coupling of two molecules of the diamine with H_2S involves the initial one- or two-electron oxidation of the diamine to the cation radical or diimine intermediates, respectively, followed by nucleophilic attack of H_2S to form a thiophenol derivative that reacts with a second molecule of the oxidized intermediate.[146,147] Zinc chloride is also included in the assays to prevent H_2S volatilization. The concentration

of methylene blue is measured at 670 nm and compared to calibration curves obtained with samples of known concentrations of H_2S that were similarly processed.[148–150] Variations of this method include chromatographic separation of methylene blue[151] and mass spectrometric detection.[152] The methodological details and potential pitfalls of this method have been reviewed.[32,101,153] Some of the key drawbacks are its low sensitivity (in the μM range), the release of sulfides from acid-labile stores (like iron sulfur clusters) that can lead to a gross overestimation of H_2S, limited linear range for absorbance of methylene blue on concentration, and the potential for interference due to the presence of thiols or due to the turbidity of biological samples.

3.4.2. Lead Acetate—A simple way to follow the enzymatic synthesis of H_2S is to use lead acetate and measure the formation of insoluble lead sulfide by the increase in turbidity at 390 nm. H_2S concentrations are determined by comparison to a calibration curve generated with known concentrations of lead sulfide. Lead acetate is also useful for activity staining in gels; enzymes that produce H_2S are identified as dark spots by soaking native gels in solutions containing the appropriate H_2S-generating substrate(s) plus lead acetate.[154] An alternative approach is to use lead acetate-soaked filter paper and to measure the appearance of black spots using densitometry.[155,156] However, this method provides only semiquantitive data, and the sensitivity is quite low.

3.4.3. Electrochemical Sensors—Two types of sensors have been used: ion-selective electrodes and polarographic sensors. The H_2S ion-selective electrodes use a silver sulfide membrane that specifically interacts with S^{2-} creating a change in potential across the membrane. The electrodes are inexpensive, easy to operate, and highly selective. However, they require a long equilibration time and frequent reconditioning to remove interfering materials. Furthermore, they require a high pH that could interfere by releasing H_2S from proteins. Second, the polarographic H_2S sensors are based on measurement of the current produced from the oxidation of H_2S by ferricyanide.[157] These sensors contain a membrane through which H_2S permeates into an internal solution of alkaline potassium ferricyanide, where chemical oxidation of H_2S occurs concomitant with the reduction of ferricyanide to ferrocyanide. The latter is then reoxidized electrochemically. The polarographic sensors have a shorter response time and higher sensitivity, allowing for real-time monitoring of H_2S down to ~10 nM. However, they have the tendency to leak easily and have large residual currents due to impurities. Enzyme-based electrochemical H_2S sensors have also been proposed and reviewed recently.[158]

3.4.4. Gas Chromatography—The determination of H_2S in aqueous samples can be carried out following derivatization (e.g., to bis(pentafluorobenzyl)sulfide), extraction into organic solvents, and gas chromatography analysis with different detection systems.[32,101] Alternatively, gas chromatography can be used for the direct determination of H_2S gas removed from the headspace of reaction vessels and analyzed using a flame photometric detector or a sulfur chemiluminiscence detector that has high sensitivity.[32,159,160] The concentration of H_2S in the aqueous phase of the assay mixture at a given pH is then calculated based on mass conservation considerations knowing the pH of the solution, pK_1 for H_2S, and its solubility at the assay temperature. A big advantage of this method is that,

when coupled to a sulfur chemiluminiscence detector, very low amounts of H_2S (0.5 pmol) can be measured. Handling of the samples, however, requires particular care and gastight equipment.

3.4.5. Monobromobimane Derivatization—The fluorogenic reagent monobromobimane, which was originally introduced to label thiols (RSH),[161] can also be used to measure H_2S in the namolar range.[162–164] Both thiols and H_2S react with monobromobimane via a nucleophilic substitution process. In the case of thiols, a thioether is formed, while in the case of H_2S, a bimane-substituted thiol is formed, which can react with a second monobromobimane forming dibimane sulfide (Chart 2). The latter can be detected by its fluorescence during HPLC separation or by mass spectrometry. This method has found a broad use lately; however, an important consideration with monobromobimane-based detection is the relatively slow reaction rate ($k \approx 10\ M^{-1}\ s^{-1}$ at pH 8).[162] Monobromobimane has also been used to quantify polysulfides and persulfides by mass spectrometry.[165] The preparation of the corresponding standards is, however, challenging due to their instability; bimane polysulfides may be unstable too.

3.4.6. Other Fluorescent Probes—The growing interest in detecting H_2S in biological samples is spurring the development of H_2S probes for tissue, cellular, and subcellular imaging. Such probes usually contain a fluorescence quencher that can be modified or removed by H_2S. Various reactions and molecular scaffolds have been used, with different reaction rates, selectivity, and potential limitations. Since these probes have been recently reviewed,[98,166–168] only selected examples are provided in Charts 3–5. One strategy is to detect the reduction of azide groups by H_2S to amines in a variety of scaffolds including rhodamine, dansyl, and naphthalimide scaffolds (Chart 3A).[169–171] Alternatively, the reduction of nitro groups to amines has been used[171] (Chart 3B). A limitation of these probes is their slow reaction rates and the possible interference of other species, particularly thiols. Furthermore, the quantification of H_2S from biological samples is not really possible. Considering that most of the probes react with H_2S irreversibly, they actually remove sulfide from the intracellular pool and reach saturation rapidly giving a potentially incorrect impression of high intracellular steady state levels of H_2S. Future development of reversible probes would permit measurements of actual changes in H_2S levels.

To improve the selectivity over thiols, the double nucleophilicity of H_2S can be exploited, as in the case of the reaction with monobromobimane (Chart 2). Probes have been developed that contain two electrophilic centers; for example, an aldehyde and an acrylate. H_2S first reacts with the aldehyde forming a thiohemiacetal group that then undergoes a Michael addition reaction with the acrylate group (Chart 4A).[172] Alternatively, the two electrophilic centers can be a disulfide and an ester. In the example shown in Chart 4B, H_2S reacts with an activated disulfide forming a persulfide and a thiol. The persulfide then attacks the ester liberating a fluorophore and benzodithiolone.[173]

Another property that can be exploited for H_2S detection is its high affinity for metals. Probes have been developed that contain a fluorophore bound to Cu^{2+}, which quenches fluorescence. Binding of H_2S to the metal ion results in CuS precipitation and an increase in fluorescence (Chart 5).[174]

3.5. Endogenous Concentration of H_2S

The methods described above can be used with appropriate precautions to detect and quantify H_2S in simple solutions. However, their use with biological samples can be confounded by side reactivity, leading to highly variable estimates of H_2S concentration. These differences can arise from the nature of the standards used, from sample loss due to the volatility and oxidation lability of H_2S, from interference from species with similar reactivity (e.g., thiols and persulfides), and from the release of H_2S from labile pools during sample handling (e.g., acidification, alkalinization, reduction). Biological samples contain labile sulfur compounds that release H_2S upon certain chemical treatments.[32,101] For example, exposure to acidic pH, which is associated with some analytical methods, liberates H_2S from iron sulfur clusters. Addition of reductants such as dithiothreitol liberates H_2S from sulfane sulfur compounds, particularly from persulfides, polysulfides, and elemental sulfur. Alkaline conditions result in H_2S release from various sulfur-containing species, particularly thiols and disulfides. This potential for introducing artifacts has contributed to the estimates of H_2S concentration in biological samples varying over 5 orders of magnitude.

As pointed out by Olson,[153,175] it is important to critically evaluate the reliability of the reported values for H_2S in biological samples. The concentration of H_2S in tissues is often expressed as moles of H_2S per gram protein or as moles of H_2S per gram of wet weight. Cells are typically 10–20% protein and 60–75% water. Thus, 1 nmol of H_2S (mg protein)$^{-1}$ is equivalent to ~200 μM H_2S, and 1 nmol of H_2S (mg wet weight)$^{-1}$ is equivalent to ~1500 μM. In cultured cells, H_2S concentration is sometimes expressed as moles per cell. Considering that a human cell has a volume of the order of 10^{-12} L (i.e., 10^3 fL or 10^3 μm^3), then 1 nmol of H_2S (10^6 cells)$^{-1}$ is equivalent to ~1000 μM. Since, the human nose can detect ~1 μM H_2S in solutions,[159,176] many reports of H_2S concentrations in biological samples are undoubtedly in error.

Before 1996, when H_2S was recognized as a physiological mediator, essentially all measurements of blood H_2S had either failed to detect it or yielded extremely low values, consistent with the fact that H_2S cannot be smelled in blood. Since 1996, reports of blood H_2S concentrations had risen to an average of ~50 μM.[175,176] However, the use of more sensitive methods, e.g., polarographic sensor or gas chromatography coupled to a sulfur chemiluminiscence detector, together with greater rigor in sample preparation, are revealing that the concentration of H_2S in blood is <100 nM and may be as low as ~100 pM.[159,177]

Gas chromatography coupled to chemiluminiscence detection has revealed that the basal tissue H_2S levels are quite low. According to one study, the basal H_2S level is ~10−15 nM in murine liver and brain.[159] Another study reported levels of 0.004–0.055 μmol H_sS kg^{-1} or 0.03–0.39 μmol (kg protein)$^{-1}$, corresponding to 6–80 nM, in murine liver, brain, heart, muscle, esophagus, and kidney.[178] In agreement with these low estimates, the steady-state concentration extrapolated from measurements of H_2S production and consumption rates in murine liver, kidney, and brain were calculated to be 9–29 nM.[179] Curiously, H_2S levels in aorta are significantly higher (~1.5 μM).[178]

The steady state concentration of H_2S is the net result of its formation and decay rates. Production rates have been estimated to be 0.45, 0.3, and 0.1 pmol min^{-1} (mg tissue)$^{-1}$ (i.e., ~0.6, 0.4, and 0.2 μM min^{-1}) in intact colon muscle, brain, and liver of mice in the presence of 10 mM cysteine; the production rate increased to 8, 7, and 20 pmol min^{-1} (mg tissue)$^{-1}$ (i.e., ~11, 10, and 28 μM min^{-1}) respectively, in homogenized tissue.[180] Another study reported H_2S production rates by murine liver and brain homogenates of 106 and 1.2 nmol min^{-1} (g tissue)$^{-1}$ (i.e., ~151 and 1.7 μM min^{-1}), respectively, in the presence of 10 mM cysteine.[159] At a more physiologically relevant concentration of 0.1 mM cysteine, H_2S production rates of 48 μmol h^{-1} (kg tissue)$^{-1}$ (i.e., ~ 12 μM min^{-1}) and 29 μmol h^{-1} (kg tissue)$^{-1}$ (i.e., 0.7 μM min^{-1}) by murine liver and brain homogenates, respectively, were reported.[179] The decay rates of H_2S are high, and as expected, they decrease dramatically under hypoxic conditions.[179] The apparent first order rate constant of H_2S decay in murine liver under aerobic conditions was reported to be 277 min^{-1} at 37 °C.[179] Thus, the very low steady-state tissue concentrations of H_2S are primarily due to the high rate of its oxidation.[179]

4. ENZYMES INVOLVED IN H_2S BIOGENESIS

At least three enzymes in the mammalian sulfur metabolic network have the potential to synthesize H_2S.[181–185] Two of these enzymes, cystathionine β-synthase (CBS) and CSE, comprise the transsulfuration pathway. The latter provides an avenue for synthesizing cysteine from the essential amino acid methionine, via the metabolic intermediate, homocysteine. The transsulfuration pathway enzymes exist predominantly in the cytoplasm although, under some conditions, they are reportedly located in other compartments such as the nucleus[186] or the mitochondrion.[187,188] The third enzyme, mercaptopyruvate sulfurtransferase (MST), resides in both mitochondrial and cytoplasmic compartments.[189] It converts 3-mercaptopyruvate, derived from cysteine transamination, to pyruvate and transfers sulfur to a thiophilic acceptor forming a persulfide from which H_2S can be released. In this section, an overview of the recent literature on the structure, mechanism, and regulation of these three enzymes is discussed with an emphasis on the recent literature pertaining to H_2S biogenesis by the human enzymes.

4.1. Reactions Catalyzed by CBS

Located at the crossroads of the methionine cycle and the transsulfuration pathway, CBS commits sulfur to cysteine synthesis and catabolism, which in turn influences H_2S biogenesis. CBS exhibits substrate promiscuity and catalyzes a multitude of reactions at the β-carbon of the substrates, serine and cysteine (Chart 6).[154,185,190–192] In its role in the transsulfuration pathway, CBS catalyzes the β-replacement of serine by homocysteine forming cystathioninine and eliminating H_2O (Chart 6, [1]). It can also catalyze the β-replacement of cysteine by homocysteine [2], by a second mole of cysteine [3], or by water [4], forming cystathionine, lanthionine, or serine, respectively, and eliminating H_2S in the process. Finally, CBS can catalyze the β-elimination of cystine forming cysteine persulfide (Cys-SSH) [5]. Mutations in CBS are the most common cause of hereditary homocystinuria, an autosomal recessive disorder.[193]

4.1.1. Organization of CBS and Properties of the Heme Cofactor—Human CBS is a homodimer with a subunit molecular weight of ~63 kDa. Its propensity for aggregation leads to its isolation as higher order oligomers ranging from 4-to 16-mers. The crystal structures of full-length human[194,195] and *Drosophila*[196] CBS have been obtained for the dimers. CBS is unique in being the only known PLP enzyme that is also a hemeprotein.[197] It is a modular protein with an N-terminal domain spanning ~70 residues, which binds a regulatory heme b cofactor (Figure 2A). This is followed by a middle catalytic core (spanning residues 71–411, human numbering), which houses the PLP cofactor and resembles the fold II or β-class of PLP enzymes.[198] The catalytic core is conserved across organisms regardless of whether CBS contains or lacks the heme domain. A Cys272-X-X-Cys275 motif present in the catalytic core is seen in the reduced dithiol and oxidized disulfide state in two structures[199,200] and could potentially render CBS sensitive to regulation by metal ions or to oxidation. CBS is reportedly inhibited by free copper (10–25 μM), although a connection between this observation and chelation by the CXXC motif has not been made.[201] The C-terminal domain (spanning residues 412–551) comprises a tandem repeat of two "CBS domains", which is a β–α–β–β–α secondary structure motif found in diverse proteins that often binds adenosine derivatives and is associated with energy sensing.[202] In CBS, the C-terminal domain binds *S*-adenosylmethionine (AdoMet),[203] an allosteric activator.[204] Hence, ~40% of the protein is involved in the N- and C-terminal regulatory domains, which exert allosteric control over the CBS-catalyzed reaction.

Three structures of full-length CBS have been reported: two of human CBS in the presence and absence of AdoMet[194,195] and a third of *Drosophila* CBS,[196] which does not bind AdoMet and exists in a hyperactivated state.[205] These structures reveal that AdoMet binding elicits a remarkable conformational rearrangement. In the absence of AdoMet, an intersubunit crossover of the C-terminal domains places each by the active site entrance of the other subunit, impeding substrate access (Figure 2B). In the presence of AdoMet, the C-terminal domain dimerizes atop the catalytic domains (Figure 2C). This structural rearrangement explains why AdoMet binding[204] or truncation of the C-terminal domain entirely,[206] activates CBS, i.e., by facilitating substrate access to the active site.

Although held by an unstructured N-terminal loop and relatively exposed, the heme in CBS is tightly bound. The first structures of truncated CBS lacking the C-terminal regulatory domain revealed that Cys52 and His65 coordinate the heme iron (Figure 3).[199,200] The low-spin heme iron retains these ligands in both the ferric and ferrous oxidation states. Upon reduction, the Soret peak shifts from 428 to 448 nm while the α/β absorption bands shift from a broad feature centered at ~550 nm (in ferric CBS) to 571 and 540 nm (in ferrous CBS).[207] Early NMR, pulsed EPR,[208] and resonance Raman[209,210] studies had ruled out a catalytic role for the heme. ^{31}P NMR studies demonstrated that the spin–lattice relaxation rates in the paramagnetic ferric (6.34 ± 0.01 s) and diamagnetic ferrous (5.04 ± 0.06 s) states were similar, indicating that the PLP and heme cofactors are not proximal to each other.[208] The crystal structures revealed that an ~20 Å distance separates the heme and PLP sites (Figure 3)[199,200] and that this distance is not modulated by the presence or absence of the C-terminal regulatory domain or its allosteric effector, AdoMet.[194,195] Yeast CBS lacks the heme cofactor but is highly active,[211] further arguing against a catalytic role for this

cofactor. In fact, deletion of the N-terminal 69 residues in human CBS results in a heme-less variant, which albeit less stable, retains ~40% of wild-type activity.[212]

A rhombic EPR signal is associated with ferric CBS with g values of 2.5, 2.3, and 1.86, which is similar to that of model heme complexes and heme proteins with imidazole/thiolate ligands.[213] Resonance Raman studies using ^{34}S-labeled CBS identified the ν(Fe–S) vibration at 312 cm^{-1}.[209] Exposure to mercuric chloride, a thiol chelator, resulted in CBS converting from a 6-coordinate low-spin to 5-coordinate high-spin state with a Soret maximum at 395 nm and a rhombic g = 6 EPR signal.[213] The spin-state change induced by mercuric chloride was correlated with a loss of CBS activity,[210] consistent with long-range communication between the heme and PLP sites. ^{31}P NMR studies also provided evidence for long-range signal transmission by revealing that the chemical shift of the phosphorus nucleus in PLP shifted from 5.4 to 2.2 ppm upon reduction of the heme iron.[208]

The ferric heme in CBS, which is coordinately saturated, is relatively inert to exchange by exogenous ligands.[214] The reduction potential of the Fe^{3+}/Fe^{2+} couple is −350 ± 4 mV for full-length CBS[215] and −291 ± 5 mV for truncated CBS[216] lacking the C-terminal regulatory domain. Following reduction, ferrous CBS can bind exogenous ligands such as CO, NO$^{\bullet}$, cyanide, and various isonitriles.[217–219] The heme cofactor reduces nitrite to ferrous heme-bound NO$^{\bullet}$.[220] Binding of these ligands is associated with loss of activity, where characterized. Despite the low reduction potential for the heme iron in full-length CBS, it can be reduced by an NADPH-driven flavin oxidoreductase when coupled to carbonylation by CO, establishing the potential physiological relevance of this reaction.[221] Ferrous CBS does not bind O_2; instead it undergoes rapid oxidation (1.1×10^5 M^{-1} s^{-1}) apparently by an outer sphere mechanism generating superoxide radical and ferric heme.[216] Reoxidation of the ferrous-nitrosyl heme on CBS leads to peroxynitrite formation.[222] Thus, the heme redox activity makes CBS a potential source of both reactive oxygen ($O_2^{\bullet-}$) and nitrogen ($ONOO^-$) species.

AdoMet increases the affinity of the CBS heme for NO$^{\bullet}$ (2-fold) and CO (5-fold) and thereby sensitizes the enzyme to inhibition.[223] Hence, in the interplay between the N- and C-terminal regulatory domains, heme supersedes AdoMet as an allosteric regulator. AdoMet activates ferric CBS but potentiates the inhibition of ferrous CBS by CO or NO$^{\bullet}$. Together with the effect of the C-terminal domain on the heme redox potential discussed above, the effect of AdoMet on the affinity of the heme ligands, CO and NO$^{\bullet}$, hints at long-range communication between the N- and C-terminal domains, which are >50 Å apart in the structure of AdoMet-bound CBS.[195]

4.1.2. Catalytic Mechanism of CBS—The ping pong reaction cycle of CBS involves the following steps: (i) binding of the first substrate (serine or cysteine), which results in displacement of Lys119 and formation of the corresponding external aldimine, (ii) abstraction of the α-proton by Lys119 leading to a resonance stabilized carbanion, (iii) elimination of water or H_2S leading to aminoacrylate formation, (iv) addition of the second substrate (homocysteine, cysteine, or water) to give the corresponding product external aldimine, and (v) reformation of the Schiff base with Lys119 leading to product release (Chart 7). Support for this reaction mechanism has been obtained by stopped-flow kinetic

studies on human[224] and yeast[225] enzymes as well as from kinetic studies on a heme-less variant of human CBS.[212] Since the absorbance of the heme cofactor obscures the PLP cofactor, difference stopped flow spectrometry had to be used to monitor PLP-bound reaction intermediates in the human enzyme.[224] Mutation of Lys119 to alanine reduces CBS activity ~1000-fold and the exogenous base, ethylamine, leads to a 2-fold higher activity, consistent with the role of Lys119 as a general base in addition to its involvement in Schiff base formation.[212]

The active site of CBS displays a constellation of conserved interactions common to members of the fold II family of PLP enzymes. PLP is tethered via Lys119 forming an internal aldimine in the resting human enzyme. At the other end of the PLP ring, the side chain of Ser349 is positioned to interact with the pyridinium nitrogen while Asn149 hydrogen bonds with the oxygen. Electrostatic contacts made between conserved threonine residues (Thr257 and Thr260) in a glycine-rich loop and the phosphate group of PLP further lock the cofactor in place. High resolution structures of *Drosophila* CBS have captured two reaction intermediates, the carbanion and the aminoacrylate species, providing detailed insights into the mechanism of their stabilization.[196] A zwitterionic interaction between the ε-NH_3^+ group of the lysine, which forms a Schiff base with PLP in the resting enzyme, and the Cα (at 2.0 Å distance) and C4A (at 3.0 Å distance) stabilizes the carbanion intermediate (Chart 7B). In the aminoacrylate intermediate, the ε-NH_3^+ of the lysine, which is no longer needed to stabilize charge at Cα/C4A, is instead, parked near the phosphate group of PLP, with which it interacts (Chart 7C).

Synthesis of Cys-SSH from cystine represents a β-elimination reaction. It is expected to proceed via a similar reaction sequence up to the formation of the aminoacrylate intermediate, which is accompanied by elimination of the Cys-SSH product. After this point, a transschiffization (rather than a β-replacement) reaction regenerates the resting internal adimine form of the enzyme and releases the eneamine product, which is hydrolyzed in solution to the α-keto acid, pyruvate, and ammonia.

4.1.3. Relative Efficacy of H_2S versus Cys-SSH Synthesis by CBS—Rat[165] and human[226] CBS catalyze the β-elimination of cystine, the oxidized form of cysteine, to form Cys-SSH. The kinetic parameters for human CBS catalyzed Cys-SSH formation are k_{cat} = 0.11 s^{-1} and k_{cat}/K_m = 85 M^{-1} s^{-1} at pH 7.4 and 37 °C. Under V_{max} conditions, the most efficient reaction for H_2S synthesis by human CBS is the β-replacement of cysteine by homocysteine with the following kinetic parameters: k_{cat} = 19.6 s^{-1} and k_{cat}/Km(Cys) = 2882 M^{-1} s^{-1} at pH 7.4 and 37 °C. Since the intracellular milieu is reducing and the concentration of cystine is significantly lower than of cysteine, substrate levels regulate H_2S synthesis from cysteine versus Cys-SSH synthesis from cystine. Kinetic simulations of reaction rates at physiologically relevant concentrations of cysteine, cystine, and homocysteine revealed that the contribution of CBS to Cys-SSH synthesis is negligible under these conditions being ~30 000-fold lower than H_2S synthesis.[226] This analysis suggests that CBS is unlikely to be a significant source of Cys-SSH in cells.

4.2. Regulation of CBS

CBS is a busy hub of regulation, which is fitting since it directs sulfur away from the cycle of an essential amino acid, methionine, to other sulfur metabolites such as cysteine, glutathione (GSH), taurine, and H_2S. Embedded in the CBS structure itself are two domains at the N- and C-termini, which exert their regulation in distinct ways and also appear to impact each other in ways that are poorly understood. In the following section, modulation of CBS activity by its regulatory domains and by posttranslational modifications is discussed.

4.2.1. Heme-Dependent Allosteric Regulation of CBS—The ferric heme in CBS, which is coordinately saturated, is relatively inert to exchange by exogenous ligands.[214] On the other hand, ferrous CBS binds exogenous ligands such as CO and NO• with concomitant loss of activity.[217,218] Binding of NO• to ferrous CBS is accompanied by a shift in the Soret peak from 448 to 390 nm[218] and leads to a 5-coordinate heme from which both Cys52 and His65 are dissociated (Chart 9). Wild-type CBS exhibits a monophasic binding isotherm for NO• and a $K_D \leq 0.23\ \mu M$.[227] The rate constant for NO• binding to CBS exhibits a linear dependence on NO• concentration ($8 \times 10^3\ M^{-1}\ s^{-1}$, pH 7.0 and 25 °C) and is enhanced ~2-fold in the presence of AdoMet together with a 1.3-fold decrease in k_{off}. CO displaces the Cys52 ligand and forms a 6-coordinate low-spin ferrous-CO species with a maximum at 420 nm (Chart 8). Binding of NO• is ~100-fold faster than of CO, which is limited by the dissociation of Cys52 from the heme iron.[228] Thus, NO• is presumed to bind by initial displacement of the His65 ligand (Chart 8).[227]

The affinity of the CBS heme for CO (5-fold) and NO• (2-fold) is increased in the presence of AdoMet.[223] Interestingly, deletion of the heme domain reverses the sensitivity of CBS to AdoMet, leading to a 1.5-fold decrease in activity.[212] The heme ligand mutants, C52A/S, exhibit a similar magnitude of inhibition in the presence of AdoMet.[229] The influence of the C-terminal domain on the heme redox potential (discussed above) and the effect of AdoMet on the affinity of the heme ligands, CO, and NO• hint at very long-range communication between the N- and C-terminal domains, which are >50 Å apart in the structure of AdoMet-bound CBS.[195]

Insights into how changes in the heme domain are communicated over an ~20 Å distance to the active site have emerged from fluorescence and resonance Raman studies.[230] The ketoenamine tautomer of PLP is key to reactivity since it facilitates the nucleophilic attack by the substrate amino group to form the external aldimine and subsequently stabilizes the carbanion following α-proton abstraction. Changes in the heme ligand environment (e.g., CO binding or heat treatment which displaces the Cys52 ligand)[231] shift the PLP equilibrium from the ketoenamine to the enolimine tautomer, in which the proton relocates to the exocyclic oxygen at the C3 atom on the PLP ring. The salt bridge between Cys52 and Arg266 is postulated to be critical for stabilizing the active ketoenamine tautomer.[230] Arg266 resides at one end of an α-helix. At the other end of the same α-helix are two conserved electrostatic interactions between Thr257 and Thr260 and the phosphate group of PLP (Figure 3). Loss of the Cys52-Arg266 salt bridge either via ligand exchange or in the pathogenic R266M mutant, stabilizes the inactive enolimine tautomer.[230] The conservative

R226K mutation leads to lengthening of the ferric Fe–S bond and perturbations in the PLP electronic spectrum.[232] The allosteric communication between the heme and PLP sites is bidirectional since the pathogenic T257M mutation promotes loss of the Cys52 ligand in the ferrous state and a concomitant shift to the inactive enolimine tautomer.[233]

4.2.2. AdoMet-Dependent Allosteric Regulation of CBS—The C-terminal regulatory domain imparts both intrasteric and allosteric effects and is responsible for the propensity of the full-length protein to aggregate. Binding of AdoMet increases k_{cat} ~2-fold from 2.8 to 5.2 s^{-1}, while deletion of the entire domain increases k_{cat} 5-fold to 10 s^{-1} (all values calculated per monomer at 37 °C). The structures of human CBS with and without AdoMet provide molecular insights into the autoinhibitory effect of the C-terminal domain and its alleviation by AdoMet (Figure 2).[194,195] While the catalytic cores in the two structures are virtually identical, the C-terminal domain undergoes a substantial rearrangement. In the absence of AdoMet, the C-terminal domain of each subunit sits on the catalytic core of the adjacent subunit, impeding access to the active site. A combination of hydrophobic interactions between residues in the CBS2 motif (Ile537, Leu540, and Ala544) and the catalytic core (Ile166, Val189, Val206, Leu210, and Ile214) and hydrogen bonding interactions between residues in the CBS1 motif (Thr460, Asn463, Ser466, and Tyr484) and a loop at the active site entrance (Glu201, Asn194, Arg196, and Asp198) lock in this conformation. AdoMet binds in a cleft between the CBS1 and CBS2 domains, which is solvent exposed and is stabilized via hydrophobic interactions and a network of hydrogen bonds. Binding of AdoMet leads to a major structural rearrangement in which the C-terminal domains uncross and dimerize in a head-to-tail fashion on top of the catalytic domain with which all interactions are broken. A flexible linker between the catalytic core and the C-terminal domain (spanning residues 381–411) is critical for mediating the AdoMet-induced conformational change, which leads to unobstructed access to the active site. The structure of human CBS with AdoMet is very similar to that of full-length *Drosophila* CBS, which is hyperactive in its basal state but does not bind AdoMet.[196]

A number of pathogenic mutations in the C-terminal domain (P422L, P427L, I435T, D444N, S466L, and L540Q) render the protein more active than wild-type CBS but insensitive to further activation by AdoMet,[234–236] begging the question as to why they are disease causing. Curiously, a subset of pathogenic mutations in the catalytic core of CBS (A114V, A158V, V168M, A226T, R224H, T262M, I278T, A331V, and T353M) are functionally suppressed by deleting the C-terminal domain (i.e., the last 145 residues)[237] or selecting for mutations in this domain that suppress the most common patient mutation in CBS, I278T.[238] The suppressor mutants are unresponsive to AdoMet suggesting that the mutations stabilize the activated conformation even in the absence of the allosteric ligand.

4.2.3. Regulation of CBS by Covalent Modifications—CBS is regulated by at least three types of covalent modifications: (i) sumoylation, (ii) glutathionylation, and (iii) phosphorylation. CBS is a target of modification by the small ubiquitin-like modifier-1 protein (SUMO-I). A number of proteins belonging to the sumoylation machinery were identified as potential interacting partners of human CBS from a yeast two-hybrid screen and included Pc2, PIAS1, PIAS3, Ubc9, and RanBPM.[186] Of these, Ubc9 is an E2

conjugating enzyme, while PIAS1, PIAS3, and Pc2 are E3 SUMO ligases, which confer target specificity and reaction efficiency. Under in vitro conditions, Pc2 enhances CBS sumoylation, which is correlated with a 70% decrease in activity.[239]

The C-terminal regulatory domain is required for the interaction between CBS and the other sumoylation machinery proteins noted above although the modification itself appears to occur in the catalytic core. Mutation of Lys211, embedded in a canonical ΨKXE sumoylation motif and exposed to solvent, leads to loss of sumoylation in vitro, suggesting that this lysine might be tagged by SUMO1. Sumoylation of CBS is correlated with its nuclear localization and can be visualized in cells and in tissue when care is taken to deactivate desumoylases.[186] Interestingly, in porcine brain, sumoylated CBS appears to be the dominant form of the protein. The physiological significance of CBS sumoylation is presently unknown. It could serve to translocate CBS to the nucleus under conditions of stress (e.g., hydrogen peroxide, heat shock, heavy metals, or ethanol treatment) that result in a global increase in sumoylation,[240–242] leading to a local increase in H_2S and/or GSH synthesis assuming that CSE, which is sumoylated in vitro,[239] also relocates under these conditions.

Glutathionylation of CBS is observed under both in vitro conditions and in cultured cells challenged with H_2O_2.[243] This modification leads to a 2–3-fold increase in CBS activity and occurs at Cys346, which resides in the catalytic core near the dimer interface and is not particularly surface exposed. Glutathionylation of CBS renders the protein insensitive to further activation by AdoMet. Cys346 resides in a loop between two α-helices, which are involved in the interface between the catalytic core and the linker region in the (AdoMet-induced) activated conformation of CBS. Hence, modification at Cys346 might stabilize the activated conformation of CBS even in the absence of AdoMet. The functional significance of glutathionylation appears to be to up-regulate transsulfuration flux under oxidizing conditions, which deplete GSH pools, leading to greater synthesis of cysteine. The transsulfuration pathway is known to be an important feeder for cysteine, the limiting reagent for GSH synthesis.[244,245] Glutathionylation of CBS, which is transiently increased in cells in response to oxidative stress, accounts for the increased flux of sulfur through the transsulfuration pathway under these conditions.

In the urothelium, CBS is reportedly phosphorylated at Ser227 and Ser525 in a cGMP/protein kinase G-dependent reaction.[246] Phosphorylation was triggered with 8-bromo-cGMP, a stable analogue of cGMP, which caused an ~2-fold increase in H_2S production in urothelial cell lysates. H_2S production was, however, tested in the presence of a high concentration of cysteine, which is a more effective substrate for CSE than for CBS, both of which are present in the urothelial cells. It was concluded that Ser227 rather than Ser525 is important for the phosphorylation-induced increase in CBS activity based on the responses of transfected cell lines harboring the S227A or S525A mutations.[246] While S525A CBS expressing cells exhibited increased H_2S production when treated with 8-bromo cGMP, S227A CBS expressing cells showed very low H_2S synthesis, which was not responsive to 8-bromo cGMP. It should be noted, however, that the S227A mutant itself showed very low activity indicating that the mutant is catalytically compromised even in the absence of

phosphorylation. A physiological role for H_2S synthesis in bladder relaxation has been proposed.[247]

4.3. γ-Cystathionase (CSE)

CSE is the second enzyme in the transsulfuration pathway and is also dependent on the PLP cofactor, for catalysis.[181,182] It catalyzes the γ-elimination of cystathionine to give cysteine, α-ketobutyrate, and ammonia (Chart 9).[248] Cysteine synthesis via the transsulfuration pathway is a quantitatively significant source of this amino acid, supplying ~50% of the cysteine present in the hepatic GSH pool.[245] Like CBS, CSE exhibits substantial substrate promiscuity and catalyzes a complex array of H_2S generating reactions involving chemistry at both the β-and γ-carbons of the substrate.[249] In addition, CSE catalyzes both Cys-SSH and homocysteine persulfide (Hcy-SSH) synthesis from cystine and homocystine, respectively.[165,226] Mutations in CSE lead to cystathionuria, an autosomal recessive disorder that is generally benign.[250,251] In contrast to CBS, very few pathogenic mutations have been reported in CSE.[251,252]

A significant difference between CBS and CSE is the ability of the latter to form a Schiff base with either cysteine or homocysteine bound to PLP, leading to chemical transformations at either the β- or γ-carbon of the substrate. This renders CSE-catalyzed H_2S synthesis responsive to homocysteine concentrations and H_2S production is predicted to increase between 20- and 200-fold in homocystinuria.[249] This explains the clinical observation that homolanthionine (the condensation product of 2 mol of homocysteine) is present in urine of homocystinuric patients with CBS deficiency[253] and emphasizes an underappreciated role for CSE in homocysteine management. Under V_{max} conditions, the highest k_{cat} for H_2S generation is for the γ-replacement reaction of homocysteine by a second mole of the same substrate. This is followed by the γ-elimination of H_2S from homocysteine or by the β-replacement of 1 mol of cysteine by another. In addition to H_2S, these reactions produce the novel sulfur metabolites, homolanthionine and lanthionine (Chart 9). At physiologically relevant concentrations of substrates, the β-elimination of cysteine is predicted to be the major H_2S-producing reaction catalyzed by CSE.[249]

The early part of the CSE-catalyzed reactions proceeds through the same steps as the CBS reaction (Chart 9) leading up to the carbanion intermediate. Thereafter, a second deprotonation at the β-carbon sets up the subsequent γ-elimination of H_2S and formation of the β–γ unsaturated imine intermediate I, which is fully conjugated and can suffer one of two fates (Chart 10). Intermediate I can continue down the γ-elimination path, which involves protonation at the γ-carbon followed by imine hydrolysis to give an eneamino acid. Tautomerization of the eneamino acid to the keto acid (α-ketobutyrate) appears to be enzyme catalyzed as revealed by the stereochemical analysis of the α-ketobutyrate formed by γ-elimination of homoserine. In the γ-replacement path, a second amino acid (e.g., homocysteine or cysteine) adds to the electrophilic γ-carbon in intermediate I forming a condensation product. Following α-carbon protonation and Schiff base exchange with the active site lysine (Lys212 in human CSE), the resting internal aldimine is reformed.

4.3.1. Relative Efficacy of H_2S versus Cys-SSH or Hcy-SSH Synthesis by CSE—Cys-SSH and homocysteine-persulfide (Hcy-SSH) are formed by the CSE-catalyzed β-elimination of cystine and γ-elimination of homocystine, respectively (Chart 9).[165,226] The kinetic parameters for CSE-catalyzed Cys-SSH formation are k_{cat} = 0.21 s^{-1} and k_{cat}/K_m = 1.75 × 10^3 M^{-1} s^{-1} at pH 7.4 and 37 °C.[226] Due to the insolubility of homocystine, the kinetic parameters for Hcy-SSH synthesis were determined at pH 8.5 and 37 °C and reported to be k_{cat} = 1.5 s^{-1} and k_{cat}/K_m = 221 M^{-1} s^{-1}. The activity of CSE at pH 7.4 is ~11-fold lower than at pH 8.5. At physiologically relevant concentrations of substrate, Hcy-SSH synthesis by CSE is predicted to be negligible. H_2S synthesis is estimated to represent ~98.7% and Cys-SSH only 1.3% of CSE activity. However, a note of caution here is important. The intracellular concentration of cystine is low and not well determined. Allowing for a 25-fold higher hepatic cystine concentration (i.e., 5 μM) than previously reported (i.e., 0.2 μM),[165] Cys-SSH and H_2S synthesis are estimated to represent 33% and 66%, respectively of total CSE activity. CSE rather than CBS is predicted to be the major contributor of hepatic Cys-SSH synthesis at physiological concentrations of cystine, due to the higher protein levels of CSE versus CBS in this tissue.[254] The kinetic analysis of H_2S versus Cys-SSH synthesis suggests that, under conditions that lead to increased intracellular cystine levels (e.g., oxidizing conditions), Cys-SSH formation could be elevated.

4.3.2. Structural Organization of CSE—The structures of human CSE with (Figure 4) and without the PLP cofactor and with the suicide inactivator, propargylglycine (PPG) have been reported.[255] The protein is a homotetramer (45 kDa monomers) and comprises two domains: a larger PLP domain (residues 9–263) and smaller C-terminal domain (264–401). The PLP is anchored via a Schiff base linkage to Lys212 and Asp187 is involved in an electrostatic interaction with the pyridinium nitrogen (Figure 5A). Tyr114 engages in a π-stacking interaction with the pyridinium ring. Residues contributed from the adjacent subunit also interact with the PLP. Reactions at the γ-carbon require a two-base mechanism (Chart 10); Tyr114 and Lys212 could serve this role.[256] On the other hand, reactions at the β-carbon as in the synthesis of H_2S from cysteine, involve a single base, i.e., Lys212. Consistent with this model, mutation of Tyr114 to phenylalanine not only fails to inhibit but, in fact, enhances H_2S synthesis from cysteine 3.6-fold compared to wild-type CSE.[257] Unfortunately the canonical cystathionine cleavage activity of this mutant was not reported.

A number of other active site residues are also highly conserved in CSE including Tyr60, Arg62, Thr189, and Arg375. Replacement of any of these residues with alanine leads to loss of H_2S synthesis activity with the exception of the E339A mutant, which exhibits a 3-fold enhancement in the catalytic efficiency of H_2S synthesis from cysteine.[257] Based on a structure-based sequence alignment analysis, the residue corresponding to Glu339 in human CSE was predicted to be an important determinant of reaction specificity, i.e., for β- versus γ-elimination.[256] Hydrophobic residues at this position are found in enzymes that catalyze β-elimination reactions as in plant and bacterial cystathionine β-lyases. In human CSE the hydrophobic E339Y substitution increased the catalytic efficiency of H_2S synthesis 7-fold.[257]

Remarkably, the structure of inactivated CSE revealed that the PPG is not bound to PLP; instead, its Cγ is covalently linked to Tyr114 through a vinyl ether linkage (Figure 5B). In

fact, the PPG is rotated 180° away from the PLP site, and its amino and carboxyl groups are involved in hydrogen bonding interactions with Arg62 (donated by an adjacent monomer), Glu339, and Arg119. In contrast, the PPG-bound structures of the *Trichomonas vaginalis* methionine γ-lyase (PDB: 1E5E) and the *E. coli* CsdB (PDB: 1I29),[258] which catalyzes cysteine desulfuration and selenocysteine deselenation, respectively, show that the inhibitor is linked via a Schiff base to the PLP. In methionine γ-lyase, the Cγ of PPG is covalently linked to a tyrosine residue that is homologous to Tyr114 in human CSE. No additional covalent linkages are seen between PPG and CsdB, which is reversibly inhibited by PPG in contrast to irreversible inhibition of CSE and methionine γ-lyase.

4.3.3. Regulation of CSE—CSE levels are markedly reduced in malignant lymphoid cells, which exhibit cysteine auxotrophy.[259] Since CSE deficiency can be clinically benign, it has been the subject of limited mechanistic and epidemiological scrutiny, and we understand little about how this enzyme is regulated in comparison to CBS. CSE has two CXXC motifs of which one, Cys_{307}-X-X-Cys_{310}, is relatively surface exposed. The second motif, Cys_{252}-X-X-Cys_{255}, is more buried and proximal to the dimer–dimer interface. The potential role of these CXXC motifs in allosteric regulation via redox changes or metal coordination is not known.

Protein kinase G-dependent phosphorylation of CSE at Ser377 has been reported to inhibit H_2S production in the carotid body.[260] However, Ser377 is completely buried and it is unclear how this residue can be phosphorylated or how the insertion of a phosphate group in the protein's interior is stabilized. H_2S synthesis by CSE reportedly increased in the presence of calcium/calmodulin,[12] although other laboratories have not been able to reproduce this observation.[261] Sumoylation of human CSE has been reported in vitro[239] but the physiological relevance of this modification remains to be assessed.

4.4. Regulation of H_2S Synthesis by the Transsulfuration Pathway

The multitude of reactions catalyzed by CBS and CSE[165,190,226,249] begs the question as to how the trans-sulfuration pathway responds to cellular demands for cysteine versus H_2S synthesis. At one level, this pathway might be controlled by gene expression, i.e., by the predominance or complete absence of one of the transsulfuration enzymes in some cells. For instance, if CBS expression is turned off, then cystathionine will not be synthesized in that cell type and therefore unavailable as a substrate for CSE (extracellular cystathionine levels are very low). Under these conditions, only the H_2S synthesis reactions of CSE will be catalyzed. On another level, substrate levels control the dominant flux (i.e., serine versus cysteine for CBS and cysteine/homocysteine versus cystathionine for CSE). Finally, allosteric regulation by ligands whose concentrations change transiently in response to stimuli could regulate the dominant metabolic track that CBS and CSE operate on.

All three strategies are involved in regulating flux through the transsulfuration pathway and in triggering metabolic track switching in response to cellular needs.[262] Binding of ligands, e.g., CO or NO• to the heme sensor in CBS, can flip the operating preference of the transsulfuration pathway from cysteine to H_2S synthesis (Figure 6).[262] Thus, despite the similar catalytic efficiencies for serine (2650 M^{-1} s^{-1}) and cysteine (2882 M^{-1} s^{-1}), CBS

preferentially synthesizes cystathionine (from serine) over H_2S (from cysteine) under basal conditions due to the higher cellular concentration of serine (~1–2 mM) than cysteine (~50–100 μM). The major product of CBS, i.e., cystathionine, is a more efficient substrate for CSE (8200 M^{-1} s^{-1}) than is cysteine (270 M^{-1} s^{-1}) or homocysteine (350 M^{-1} s^{-1}).[249] Hence, under basal conditions or upon AdoMet activation of CBS, the predominant flux in the transsulfuration pathway is toward cysteine synthesis (Figure 6, left). In contrast, under conditions that trigger H_2S-signaling such as endoplasmic reticulum stress,[263] CBS is inhibited by CO,[217] a product of heme oxygenase-1 that is induced under these conditions.[264] Furthermore, AdoMet exacerbates CO inhibition of CBS.[223] In the absence of competition from cystathionine, CSE preferentially uses cysteine (which is ~100-fold more abundant than homocysteine) to produce H_2S (Figure 6, right). The track-switching model has important implications for sulfur metabolism. For instance, it predicts that H_2S homeostasis will be dysregulated in CBS deficiency-induced hyperhomocysteinemia and suggests that H_2S-dependent signaling cascades are perturbed in complex diseases like cardiovascular, neurodegenerative, neoplastic, and metabolic diseases where compromised endoplasmic reticulum function is a significant factor.[265] Finally, there is growing evidence for crosstalk between $NO^{\bullet}$, CO, and H_2S signaling pathways,[262,266–268] but the molecular mechanisms underlying this interconnectedness are far from understood. The transsulfuration pathway represents a platform for the interplay between them via a heme sensor embedded in CBS.

4.5. Mercaptopyruvate Sulfur Transferase

MST is a sulfurtransferase that is found in the cytoplasm and in the mitochondrion.[189,269] The specific activity of MST is reported to be 3-fold higher in mitochondria than in the cytosol in rat liver.[189] MST catalyzes the transfer of the sulfur atom from 3-mercaptopyruvate, which is derived from cysteine via the action of cysteine aminotransferase (CAT, identical to aspartate aminotransferase), a PLP enzyme that utilizes α-ketoglutarate as a cosubstrate (Chart 11). In the first half reaction, sulfur transfer from mercaptopyruvate to an active site cysteine residue (Cys248 in the human MST sequence) results in a stable Cys-SSH intermediate and formation of pyruvate. In the second half reaction, the outer sulfur from the Cys-SSH intermediate is transferred to a nucleophilic acceptor, which can be a small molecule thiol or the protein, thioredoxin. H_2S is subsequently liberated from the sulfur acceptor (Chart 11B).[270,271]

Alternatively, the sulfur transfer can occur to cyanide, generating thiocyanate.[272] Based on the k_{cat}/K_m parameters for sulfur transfer from mercaptopyruvate, the following order for decreasing catalytic efficiency has been reported for various biologically relevant acceptors: thioredoxin $\gg$ cyanide $\approx$ dihydrolipoic acid > cysteine > homocysteine > GSH.[271] Dithiothreitol and mercaptoethanol can serve as surrogate acceptors in vitro. In nature, MST variants fused to thioredoxin are found[273,274] suggesting that thioredoxin is the physiological sulfur acceptor for MST.[275] In principle, other proteins could serve as sulfur acceptors by interacting directly with MST; however, the identities of such protein acceptors if they exist, are not known.

An alternative route for 3-mercaptopyruvate synthesis is via the oxidation of D-cysteine by the FAD-dependent peroxisomal enzyme, D-amino acid oxidase (Chart 11C), which was first inferred from studies on cyanide detoxification by rat hepatocytes.[276] H_2S production from D-cysteine is repressed by indole 2-carboxylate, an inhibitor of D-amino acid oxidase.[277] While the highest MST levels are seen in liver, large intestine and kidney, the highest D-amino acid oxidase levels are seen in kidney and cerebellum. H_2S production from D-cysteine is apparently significantly higher than from L-cysteine in kidney and in cerebellum.[277] However, a cellular source for D-cysteine is not known.

MST belongs to the rhodanese superfamily and comprises two domains: an N-terminal domain extending from residues 1–138 and a C-terminal domain extending from residues 165–285 (Figure 7A). A long linker (residues 139–164) connects the two domains. The active site is located in a cleft between the two domains with each contributing residues to it. The structure of human MST has been captured with the persulfide intermediate (Cys248-SSH) and pyruvate (Figure 7B).[271] A second structure was solved with an apparently unproductive complex in which the 3-mercaptopyruvate substrate forms a mixed disulfide with Cys248.[271] Mutation of the active site cysteine to serine in rat MST leads to complete loss of activity.[278]

Two conserved arginine residues, Arg188 and Arg197, which were known from mutagenesis studies to be important for substrate orientation,[278] form ionic and hydrogen-bonding interactions with the carboxylate group of the substrate and product (Figure 7B). Arg197 additionally forms a hydrogen bond with the carbonyl group of the substrate/product. A Ser-His-Asp catalytic triad, first noted in the *Leishmania* MST crystal structure,[279] is also present in human MST (Ser250-His74-Asp63). The N-terminal domain contributes Asp63 and His74 to the triad. The Cys248 residue is predominantly deprotonated, acoording to a pK_a of 7.2.[271] The reaction catalyzed by MST is proposed to involve attack by the thiolate of Cys248 on the sulfur of 3-mercaptopyruvate resulting in the formation of pyruvate and a persulfide (Cys-SSH). This product complex has been captured crystallographically (Figure 7B,C).[271] The outer sulfur of the persulfide, most likely in the anionic Cys-SS^- state, is surrounded by an hexapeptide loop and forms hydrogen bonds or other types of polar interactions with the four backbone amides of Gly249, Ser250, Val252 and Thr253 and with the hydroxyl of the latter. The role of the Ser250 hydroxyl in the catalytic triad might be to interact with the carbonyl group of mercaptopyruvate and facilitate catalysis by polarizing the C═O bond.[279] An additional proposal, based on a QM/MM study, suggests that Ser250 is involved in the deprotonation of the 3-mercaptopyruvate substrate thiol and in the stabilization of the transient enolate oxyanion.[280] However, mutation of the corresponding serine to alanine or lysine in rat MST decreases k_{cat}/K_m by a modest ~4–10-fold, suggesting a relatively minor contribution of this residue to catalysis.[278] The mechanism of sulfur transfer is proposed to consist of a stepwise process consisting of deprotonation of the 3-mercaptopyruvate thiol, sulfur atom transfer to the Cys248 thiolate to form nascent persulfenate and pyruvate enolate anions, and protonation of the enolate to the corresponding pyruvate enol, which tautomerizes to the keto form.[280] The calculated activation barrier for this process is ~67 kJ mol^{-1}. In contrast, an alternative process of SH transfer that does not require the initial deprotonation of the 3-mercaptopyruvate thiol has a much higher calculated activation energy barrier, 180 kJ mol^{-1}.[280] The electrostatic

repulsion between the thiolates of the substrate and of Cys248 during the sulfur atom transfer is proposed to be reduced by interactions of the sulfur with the surrounding amide and hydroxyl groups. Release of pyruvate followed by attack of the thiol acceptor on Cys-SSH moves the sulfane sulfur out of the MST active site, regenerating the resting enzyme (Chart 11). The attack by the thiolate acceptor on the outer sulfur of the persulfide would be favored by the specific geometry of the active site and by the increase in electrophilicity of the outer sulfur caused by hydrogen bonding to the amide and hydroxyl groups of the surrounding loop.[280]

4.5.1. Regulation of MST—Our understanding of how CAT/MST-dependent H_2S synthesis is regulated is very limited. The active site cysteine in MST is sensitive to oxidation and could potentially be involved in redox regulation of the enzyme.[275] Reversible inhibition of rat MST by treatment with stoichiometric quantities of hydrogen peroxide or tetrathionate and rescue of the resulting cysteine sulfenate by reductants such as dithiothreitol or thioredoxin has been reported.[275] It is not known whether the active site cysteine residue is also susceptible to overoxidation, which would lead to irreversible inactivation.

A role for redox regulation of rat MST via formation of an intersubunit disulfide bond has been reported. Of the three surface-exposed cysteines in rat CST, two (Cys154 and Cys263) form an intersubunit linkage under oxidizing conditions.[275,281] Reduction of the disulfide bond by thioredoxin increases MST activity 4.6-fold. These cysteines are not conserved in the human protein, which is only observed to exist as a monomer.[271]

Calcium (0–2.9 μM) reportedly inhibits CAT/MST-dependent H_2S production in mouse retinal lysate.[282] The inhibitory effect of calcium appears to be on CAT rather than MST since H_2S production from 3-mercaptopyruvate was unaffected by the presence of calcium. The mechanisms by which calcium regulates CAT remain to be elucidated.

4.6. Inhibitors of H_2S Biogenesis

The paucity of specific inhibitors of H_2S-producing enzymes has limited advancements in the field and led to the indiscriminate use of nonspecific PLP enzyme inhibitors such as aminooxyacetic acid and hydroxylamine to “target” H_2S production.[181] Alternatively, aspartate, the preferred substrate for CAT/AAT, has been used to indirectly inhibit MST-dependent H_2S production. Historically, the acetylenic substrate analog, propargylglycine, was the first mechanism-based inactivator designed to target CSE.[283] The structure of human CSE revealed that propargylglycine is covalently linked to Tyr114 in the active site but is not attached to the PLP via a Schiff base.[255] Propargylglycine exhibits low bioavailability and is typically used at high (1–10 mM) concentrations in cell culture experiments. It also exhibits off-target activity with alanine aminotransferase,[284] limiting its utility.

An assessment of the commonly used generic inhibitors confirmed a lack of selectivity for CBS versus CSE with three compounds: hydroxylamine, aminooxyacetic acid, and trifluoroalanine.[285] In contrast, two compounds showed selectivity for CSE. Of these, β-cyano-L-alanine (IC_{50} = 14 μM for human CSE[285]), a plant-derived neurotoxin, is known to

act as a suicide inhibitor of PLP enzymes, which abstract a proton from the β-carbon of substrates, e.g., alanine aminotransferase.[286,287] Injection of β-cyano-L-alanine induces convulsions and rigidity and leads to cystathionuria in rat, indicating CSE inhibition in vivo.[288] Aminoethoyxvinylglycine (reported IC_{50} = 1 μM[285] and K_i = 10.5 μM[289] for human CSE) is a known inhibitor of ethylene synthesis by the plant enzyme, 1-aminocyclopropane-1-carboxylate synthase[290] and of bacterial cystathionine β-lyase.[291] It is likely to be a more useful reagent in cell culture experiments although information on its bioavailability and toxicity in cell culture and in whole animals is limited. Aminoethoxyvinyl glycine is a slow-binding but reversible inhibitor of cystathionine β-lyase.[291]

More recent efforts to address the gap in selective targeting of H_2S-generating enzymes have involved high throughput screening[292–294] and rational mechanism-based inhibitor design.[295] In one study, CBS inhibitors were designed to mimic the product, cystathionine but the α-amino group that forms a Schiff base, was substituted by the heteroatomic functional groups: $–NHNH_2$, $–ONH_2$, and –NHOH to form a hydrazone, oxime, and nitrone linkage, respectively, with the PLP.[295] The inhibitors showed modest potency against CBS, but their activity against CSE, which also binds cystathionine, was not tested. A high throughput assay of a library of 1900 compounds yielded a O-polymethoxylated flavone, tangeritin, and 1,4-napthaquinone, exhibiting modest IC_{50} values and are unlikely to be useful inhibitors for cell culture studies.[293] A second high throughput screen of 6491 compounds yielded mostly large flavonoids as CBS inhibitors with a subset showing selectivity against CSE although selectivity against MST was not evaluated. These compounds are unlikely to selectively inhibit CBS in the cell.[294] A third screen identified benserazide, a known DOPA decarboxylase inhibitor used for managing Parkinson's disease, as a CBS inhibitor with modest selectivity against CSE and MST.[292]

5. ENZYMATIC H_2S OXIDATION

The toxicity of H_2S is associated with its inhibition of cytochrome c oxidase (half maximal inhibition occurs at ~0.3 μM in cell extracts and ~20 μM in intact cells).[296] Steady-state H_2S concentrations are maintained at low levels (6–80 nM)[159,179] except in aorta, where the concentration is reportedly ~20–200-fold higher.[178] Hence, cells have strategies for avoiding H_2S build-up. One such strategy involves the canonical H_2S oxidation pathway, which exists in the mitochondrion and converts H_2S to thiosulfate and sulfate,[297] with the product distribution being tissue specific.[298–300] Alternatively, H_2S can be oxidized by globins to thiosulfate and protein-bound hydropolysulfides.[301,302] Much less is known about the enzymology of H_2S oxidation compared to its biogenesis, and in this section, the structures and functions of the human proteins in the mitochondrial H_2S oxidation pathway are discussed, while globins that have H_2S oxidation capacity are covered in section 6.

5.1. Mitochondrial H_2S Oxidation Pathway

The eight-electron oxidation of H_2S to sulfate starts in the mitochondrial matrix and is completed in the intermitochondrial membrane space where sulfite oxidase resides (Figure 8).

The first enzyme in the pathway is sulfide quinone oxidoreductase (SQR), which catalyzes a two-electron oxidation of H_2S to persulfide and reduces coenzyme Q (CoQ). The latter enters the electron transfer chain at the level of complex III, thus connecting H_2S oxidation to ATP and reactive oxygen species formation.[303,304] Beyond this step, there is controversy regarding how the pathway is wired. Depending on whether the persulfide acceptor from SQR is GSH or sulfite, glutathione persulfide (GSSH) or thiosulfate results. GSSH synthesis by SQR would set up a competition between its utilization by persulfide dioxygenase (PDO also referred to as ETHE1), the product of the *ethe1* gene, and by rhodanese (Figure 8A). Alternatively, if thiosulfate is the product of SQR, it would first have to undergo a sulfur transfer reaction catalyzed by rhodanese to form GSSH, which would then be oxidized to sulfite by PDO (Figure 8B). Sulfite is eventually oxidized to sulfate via sulfite oxidase.

5.2. Sulfide Quinone Oxidoreductase

SQR is a member of the flavin disulfide reductase superfamily, which catalyzes pyrimidine nucleotide-dependent reduction of substrates.[305] Like other family members, SQR houses two redox centers, an active site disulfide and a noncovalent FAD cofactor that relays electrons from H_2S to CoQ. Human SQR is a dimeric[306] membrane-anchored protein with a globular domain that faces the mitochondrial matrix. The structure of a mammalian SQR is not yet available, but structures of SQR from *Acidianus ambivalens*[307] (Figure 9) and other bacteria[308,309] provide insights into its likely active site architecture.

SQR is a combination of a sulfurtransferase that generates an active site Cys-SSH intermediate and an oxidoreductase, which oxidizes H_2S as it reduces CoQ with FAD serving as an intermediate electron carrier (Chart 12). The sulfane sulfur from Cys-SSH is transferred to an acceptor, which can be GSH, sulfite, cyanide, or a second equivalent of H_2S.[297,310,311] As discussed in more detail below, the identity of the acceptor under physiological conditions is a subject of controversy. It is noteworthy that the bacterial SQRs do not require sulfur acceptors; instead, they form polysulfide or cyclooctasulfur products. In fact, a trisulfide intermediate is seen in the *A. ambivalens* SQR structure (Figure 9B).[307] Also unlike some bacterial SQRs, the FAD in human SQR is bound noncovalently.[310] It exhibits maxima at 385 and 450 nm and a promiment shoulder at 473 nm. The two-electron redox potential of the bound FAD is −123 ± 7 mV.[306]

The detailed mechanism of SQR is complex and involves a two-step sulfur transfer and a multistep electron transfer through the protein (Chart 13).[306,310,311] The initial step involves nucleophilic attack of H_2S on the active site disulfide (presumably formed between Cys301 and Cys379 in human SQR) and leads to the formation of Cys379-SSH and Cys201-S^- on the *re* face of FAD. At this step, the formation of an unusually strong charge transfer complex is observed, which exhibits a maximum at 673 nm and extends out to 900 nm.[306] The bimolecular rate constant for the formation of the H_2S-dependent charge transfer species is 3.4×10^5 M^{-1} s^{-1} at pH 7.4 and 4 °C.[306] In the presence of CoQ, the rate constant for the formation of the charge transfer complex increases 2.9-fold indicating that the reaction occurs more efficiently in a ternary complex.

A charge transfer complex is also formed in the presence of sulfite, which presumably adds to the disulfide bond forming a sulfocysteine intermediate (Cys379-SSO_3^{2-}). However, the

bimolecular rate constant for sulfite addition is only 1×10^2 M^{-1} s^{-1} at pH 7.4 and 4 °C, which is 3000-fold lower than the k_{on} for H_2S and is unlikely to be significant except perhaps under pathological conditions when sulfite concentrations are elevated.

A variety of small molecules can accept the sulfane sulfur from the Cys-SSH intermediate in SQR, exhibiting a range of catalytic efficiencies (k_{cat}/K_M): sulfite (1.7×10^6 M^{-1} s^{-1}), cyanide (5.1×10^5 M^{-1} s^{-1}, pH 8.5), H_2S (2.3×10^5 M^{-1} s^{-1}), and GSH (5.1×10^3 M^{-1} s^{-1}) at pH 7.4 and 25 °C unless noted otherwise.[310,311] Cysteine and homocysteine can also serve as sulfane sulfur acceptors and exhibit catalytic efficiencies that are similar to GSH.[311]

The controversy regarding the physiological sulfur acceptor (Figure 8) originated from the reported inability of GSH to support SQR activity,[310] which has since been shown to be incorrect.[311] While GSH is abundant (1–10 mM depending on the cell type), sulfite, which is reactive, is present at low steady-state concentrations. A recent study reported that the intracellular sulfite concentration in rat liver is 9.2 μM based on HPLC analysis of tissue lysates, albeit without mass spectrometric or any other experimental validation of the identity of the compound that comigrated with authentic sulfite.[312] Based on the k_{cat}/K_M values discussed above, the estimated apparent k_{cat} at 10 μM sulfite is 16 versus 36 s^{-1} at 7 mM GSH, as previously predicted by kinetic simulations.[311] In addition to the high probability that tissue sulfite concentrations were not determined accurately,[312] the use of sulfite as the primary sulfane sulfur acceptor by SQR runs counter to logic for the following reasons. First, it would appear unlikely that if the SQR active site evolved to use a small molecule like sulfite as a substrate, that it could just coincidentally bind the tripeptide substrate, GSH, too. The crystal structure of human SQR should provide needed insights into this debate. Second, the dependence of the first step in a H_2S oxidation pathway on sulfite, a six-electron oxidized product of the pathway (Figure 8B), would appear to be organizationally illogical and was described as “convoluted” even by its proponents.[310] Third, thiosulfate is a poor substrate for rhodanese for GSSH synthesis,[311] which is required for continued oxidation since GSSH is the only known substrate for PDO. The only other known thiosulfate sulfurtransferase that catalyzes the conversion of thiosulfate to GSSH is located in the cytoplasm[313] and its involvement in the mitochondrial H_2S oxidation pathway would require the unlikely translocation of the reactive GSSH intermediate across compartments. For these reasons, it appears likely that the flow of sulfur through the H_2S oxidation pathway is $HS^- \rightarrow GSSH \rightarrow SO_3^{2-} \rightarrow SO_4^{2-} + S_2O_3^{2-}$ as shown in Figure 8A.

5.3. Persulfide Dioxygenase

PDO is a nonheme mononuclear iron-containing mitochondrial matrix protein, which belongs to the metallo β-lactamase superfamily family and has a subunit molecular mass of 28 kDa.[314] It catalyzes an oxygen-dependent oxidation of GSSH giving sulfite and GSH (eq 20).[297,315,316]

$$GSSH + O_2 + H_2O \rightarrow GSH + SO_3^{2-} + 2H^+ \quad (20)$$

As isolated, the iron is predominantly in the ferrous oxidation state[317] and is coordinated by a 2His-1Asp facial triad.[318,319] Mutations in PDO lead to ethylmalonic encephalopathy, which is inherited as an autosomal recessive disease and is associated with severe neurological and gastrointestinal clinical presentations.[315,320,321] Thiosulfate and H_2S accumulate in PDO deficiency, and intriguingly, a tissue-specific reduction in cytochrome c levels is seen in muscle and brain.[315,322,323]

In solution, human PDO behaves as a mixture of monomer and dimer[316,319] and, like the *Arabidopsis thaliana* and bacterial enzymes,[318,324] crystallizes as a dimer.[319] The structure of human PDO reveals an $\alpha\beta\beta\alpha$ fold typical of metallo β-lactamase family members (Figure 10A).

His79, His135, and Asp154 coordinate iron together with three water molecules, completing an octahedral coordination. A deep channel exists that leads to the active site and is predicted to be where the GSSH substrate binds. In fact, the interactions between the product, GSH, and the active site residues are visible in the *Pseudomonas putida* PDO structure where the sulfur of GSH is within 2.5 Å of the iron (Figure 10B).[324] GSH binding displaces a single water ligand. Interestingly, Cys247, located near the surface, is oxidized to cysteine sulfinate in the structures of human and *A. thaliana* PDO.[318,319] It is not known whether this oxidative modification is autocatalytic and whether it has mechanistic/regulatory import or is silent.[319]

Both GSSH and coenzyme A persulfide serve as substrates; the specific activity of PDO is, however, ~50-fold higher with GSSH than with coenzyme A persulfide. The k_{cat}/K_M with GSSH is 1.4×10^5 M^{-1} s^{-1} at pH 7.4, 22 °C. There has been limited interrogation of the reaction mechanism of PDO. In analogy with related dioxygenases such as cysteine dioxygenase, a mechanism has been proposed in which binding of GSSH displaces one or more water molecules, simultaneously creating the binding site for O_2 (Chart 14, [1–2]).[316,319] The crystal structure of the *P. putida* PDO with bound GSH[324] and the structure of human PDO in which GSSH has been modeled,[319] show monodentate coordination by the sulfur atom. This is distinct from the bidentate coordination seen in cysteine dioxygenase in which the amine and sulfhydryl groups of cysteine serve as ligands to iron.[325] In the mechanism proposed for PDO,[316,319] binding of GSSH and of O_2 leads to an Fe^{III}-superoxo intermediate (Chart 14, [3]) that is in resonance with an Fe^{II}-superoxo species in which the sulfane sulfur ligand has a partial cation character [4]. Recombination of the sulfane sulfur radical cation and the Fe^{II}-superoxo species leads to a cyclic peroxo intermediate [5]. Following O–O bond cleavage, a reactive metal bound oxygen and a sulfoxy cation [6] are formed. Alternatively, cleavage of the Fe–O bond and transfer of the activated oxygen to the sulfoxy sulfur cation gives [7]. Rearrangement of either [6] or [7] gives [8] (Chart 14), which following hydrolysis, yields sulfite.

Two patient mutations in PDO, T1521 and D196N, have been characterized biochemically.[316] Both mutations affect the iron content of PDO, decrease its thermal stability, and have smaller effects on either the K_m for GSSH and/or on k_{cat}. The mutated residues are distal from the active site and the decrease in thermal stability (by 10–15 °C) is likely to be the major biochemical penalty leading to disease.

5.4. Rhodanese

Rhodanese is a sulfurtransferase found in the mitochondrial matrix. Historically, rhodanese was thought to have a role in cyanide detoxification since it can convert thiosulfate and cyanide to thiocyanate (Chart 15A).[326] More recently, its role in the mitochondrial H_2S oxidation pathway has been demonstrated where it preferentially catalyzes thiosulfate synthesis versus utilization (Chart 15, B vs C).[297,311] Elevated rhodanese expression is correlated with lower adiposity and knockout of the rhodanese gene in mouse leads to markedly increased diabetes.[327] Other phenotypic and metabolic expressions of rhodanese deficiency have not yet been described.

Rhodanese, like MST, belongs to the sulfurtransferase superfamily, characterized by a "rhodanese" domain fold with an α/β topology named after this protein, which is present in a single copy, in tandem repeats or fused with other proteins in members of this family.[328,329] Human rhodanese is a monomeric protein with a molecular mass of 33 kDa.[330] Two polymorphic variants of rhodanese have been described, which lead to E102D and P285A substitutions.[331] The Glu102 residue is located at the entrance to the active site pocket and is ~19 Å away from the catalytic cysteine, Cys257. Pro285 is surface exposed and ~17 Å away from the active site. Interestingly, both variants exhibit greater thermal stability than wild-type rhodanese.[330]

The structure of bovine liver rhodanese[332] serves as a useful model for the human protein with which it shares 89% sequence identity (Figure 11). The structure comprises two globular domains of approximately equal length and an active site that is housed in a cleft between the two domains. The C-terminal domain provides the catalytic cysteine and a mixture of hydrophilic and hydrophobic residues wall in the active site. The reaction mechanism of rhodanese involves an active site Cys-SSH intermediate from which the sulfane sulfur is transferred to an acceptor. In the bovine rhodanese structure, the Cys-SSH intermediate is stabilized by hydrogen bonds from the hydroxyl group of Thr252 and the backbone amides of Arg248, Lys249, and Val251.[332] The catalytic triad present in MST is absent in rhodanese. This coincides with its preferential substrates being predominantly deprotonated at physiological pH.[280]

Like MST, the reaction catalyzed by rhodanese involves two sulfur transfer reactions: from the sulfur donor to the active site cysteine and from Cys-SSH to the sulfur acceptor (Chart 15). The various sulfur transfer reactions catalyzed by wild-type rhodanese and its polymorphic variants have been characterized.[311,330] Human rhodanese preferentially catalyzes sulfur transfer in the direction of GSSH $\rightarrow$ $S_2O_3^{2-}$ ($k_{cat}/K_{m(sulfite)}$ = 6.5 × 10^6 M^{-1} s^{-1} at pH 7.4, 37 °C) versus in the reverse direction, $S_2O_3^{2-}$ $\rightarrow$ GSSH ($k_{cat}/K_{m(GSH)}$ = 0.03 × 10^3 M^{-1} s^{-1} at pH 7.4, 37 °C). Based on these values, rhodanese exhibits an estimated 217 000-fold discrimination against utilization of thiosulfate versus GSSH as a sulfur donor. The K_m values for GSSH (450 μM) and sulfite (60 μM) in the GSSH $\rightarrow$ $S_2O_3^{2-}$ sulfurtransfer reaction are lower than the K_m values for the substrates, thiosulfate (340 μM) and GSH (21 mM), in the $S_2O_3^{2-}$ $\rightarrow$ GSSH direction. Like wild-type rhodanese, the polymorphic variants also exhibit a marked preference for making rather than utilizing thiosulfate and exhibit comparable catalytic efficiencies for this reaction ($k_{cat}/K_{m(sulfite)}$ = 1.5–4.2 × 10^3 M^{-1} s^{-1} at pH 7.4, 37 °C).[330]

Interestingly, cysteine and homocysteine can replace GSH as sulfur acceptors in the $S_2O_3^{2-}$ → GSSH sulfur transfer reaction with catalytic efficiencies ($k_{cat}/K_{m(Hcy\ or\ Cys)} \approx 0.4 \times 10^3$ M^{-1} s^{-1} at pH 7.4, 37 °C) that are ~13-fold higher than with GSH.[311] However, the concentration of these amino acids is low in most tissues, and their high K_m values (~21 mM each) make them unlikely substrates for the reverse reaction under physiological conditions compared to GSH. In some tissues like kidney, which has high cysteine,[333] or under pathological conditions like homocystinuria, which is characterized by elevated homocysteine,[193] these sulfur containing amino acids might become relevant substrates, albeit in the less favorable reverse sulfur transfer reaction from thiosulfate.

The thiosulfate:cyanide transfer kinetics of wild-type rhodanese are characterized by relatively low catalytic efficiency ($k_{cat}/K_{m(KCN)} = 31 \times 10^3$ M^{-1} s^{-1} at pH 7.4, 25 °C) and high K_m for cyanide (29 mM) making a role for rhodanese in cyanide detoxification unlikely. Interestingly, the E102D mutant shows higher efficiency ($k_{cat}/K_{m(KCN)} = 534 \times 10^3$ M^{-1} s^{-1}) while the P285A mutant shows similar efficiency (48×10^3 M^{-1} s^{-1}) as the wild-type protein in the cyanide detoxification assay.

5.5. Sulfite Oxidase

The nearly ubiquitous presence and conserved architecture of sulfite oxidases is consistent with the evolutionarily ancient role of this protein in protecting against sulfite-induced damage.[334] Sulfite oxidase is a molybdenum containing protein, which catalyzes the two-electron oxidation of sulfite to sulfate in which water serves as the oxygen source (eq 21).

$$SO_3^{2-} + H_2O \rightarrow SO_4^{2-} + 2H^+ + 2e^- \quad (21)$$

In humans, sulfite oxidase is a soluble enzyme found in the mitochondrial intermembrane space. Electrons from the sulfite oxidation reaction are passed via a heme cofactor found in vertebrate sulfite oxidases to cytochrome c and from there to complex IV. The important role of sulfite oxidase in detoxifying sulfite is borne out by its presence in the peroxisomal compartment in plant cells where it functions to remove toxic sulfite derived from atmospheric sulfur dioxide or from catabolism of sulfur containing amino acids, rather than a role in sulfur assimilation in the chloroplast.[335] Sulfite oxidase deficiency is an autosomal recessive disorder that presents with severe neonatal neurological problems.[336] It can result from defects in the synthesis of the molybdopterin cofactor or from mutations in the gene encoding sulfite oxidase itself.

Sulfite oxidase is a homodimer with a subunit molecular mass of 52 kDa and contains a heme b cofactor housed in the N-terminal domain that is connected via a flexible linker to the central molybdopterin-binding domain, which in turn is followed by the C-terminal dimerization domain. The structure of chicken sulfite oxidase[337] (Figure 12) serves as a useful model for the human protein with which it shares 68% sequence identity. The 5-coordinate molybdenum center has square pyramidal geometry (Chart 16A). Of the three sulfur ligands, two are derived from the dithiolene group of the molybdopterin cofactor, while the third is donated by Cys207 (human sequence numbering). The remaining

coordination sites are occupied by equatorial and apical oxo ligands. The substrate-binding pocket in chicken sulfite oxidase comprises Arg138, Arg190, and Arg450 in addition to Tyr322 and Trp204. A pathogenic mutation in a patient with severe sulfite oxidase deficiency has been mapped to Arg160, which corresponds to Arg138 in the chicken sequence.[338]

The catalytic cycle of sulfite oxidase comprises reductive and oxidative half reactions. Sulfite binds transiently to an equatorial oxo/hydroxyl ligand and reduces the molybdenum center to Mo^{IV} (Chart 16A). Sulfite is released as sulfate following hydrolysis. The $k_{cat}/K_{m(sulfite)}$ is 4.7×10^6 M^{-1} s^{-1} at pH 7.5 and 25 °C.[339] In the oxidative cycle, sequential one-electron transfers occur from Mo^{IV} to the exogenous electron acceptor, i.e. heme iron in cytochrome c, via the heme b cofactor in sulfite oxidase (Chart 16B). The catalytic mechanism of sulfite oxidase has been extensively characterized by spectroscopic and rapid reaction kinetic methods combined with mutagenesis studies and has been reviewed recently.[334]

6. CHEMICAL BIOLOGY OF H_2S

Notwithstanding the growing body of evidence for the biological roles of H_2S, the gap between the physiological effects of H_2S and its mechanism of action remains large. Based on chemical principles, H_2S reactivity can be categorized into three reaction groups: (i) binding to and/or redox reactions with metal centers, (ii) cross-talk with and scavenging of reactive oxygen (ROS) and reactive nitrogen species (RNS), and (iii) oxidative modification of protein cysteines to form the corresponding persulfides (Figure 13).[340–342] In this section, we provide an overview of the reactions grouped in (i) and (ii) while protein persulfidation is discussed in section 7.

6.1. Interaction of H_2S with Metal Centers

Different possilbilites exist for the interaction between H_2S and a metal center. First, H_2S (or HS^-) can coordinate the metal ion. Second, H_2S can reduce the metal center, concomitantly forming $HS^{\bullet}$ and other downstream sulfur oxidation products. Third, H_2S can modify heme porphyrins covalently.

The first described biological effect of H_2S identified in 1929 by Keilin was its toxicity, which was ascribed to inhibition of respiration by targeting cytochrome c oxidase (CcO).[343] The reaction with H_2S was later used to stabilize cytochrome c oxidase for its spectral characterization.[344,345] CcO is the final acceptor in the mitochondrial electron transport chain, which uses electrons delivered by cytochrome c to reduce oxygen to water.[346] It contains two copper centers (Cu_A and Cu_B) and two heme iron centers (a and a_3).[347–349] Oxygen binds to ferrous heme a_3. $NO^{\bullet}$ and CO also inhibit the enzyme reversibly.[350–352] Inhibition of CcO by H_2S is almost as strong as with CN^-, with K_i of ~0.2 μM,[353] and it is noncompetitive with respect to both cytochrome c and oxygen. The work of Nicholls and colleagues was instrumental in pointing out that, in addition to inhibiting CcO, H_2S might also serve as a substrate/electron donor.[353–356] They observed that the initial product of H_2S/CcO (aa_3) interaction is not an inhibited form of the enzyme and that >1 mol of sulfide/mol CcO was required for full inhibition.[355] Binding of H_2S to catalytically active

CcO (k_{on} = 1.5 × 10^4 M^{-1} s^{-1}, k_{off} = 6 × 10^{-4} s^{-1}, and K_D = 4 × 10^{-8} M^{-1}) is much tighter than the binding of ligands such as azide or fluoride (Chart 17).

A generalized mechanism has been proposed to explain the interaction of H_2S with CcO.[356,357] At low levels (1:1 ratio of H_2S:CcO), H_2S reduces ferric heme a_3 with concomitant oxidation to $HS^{\bullet}$. The reduction of this heme iron by H_2S is thermodynamically unfavorable, and it is likely that $HS^{\bullet}$ removal, e.g., by reaction with HS^- to form $H_2S_2^{\bullet -}$ (eq 9), pulls the reduction in the forward direction. Heme iron reduction promotes oxygen binding and reduction, explaining why low concentrations of H_2S stimulate respiration.[355,358] Alternatively, $HS^{\bullet}$ can react with oxygen to form $HSOO^{\bullet}$ (eq 10) further contributing to oxygen consumption. At moderate concentrations (2–3 fold excess of H_2S), H_2S coordinates to the Cu_B center forming a stable Cu–SH_2 complex as documented by EPR. It is likely that HS^- reduces Cu_B^{II} first and then coordinates to Cu_B^{I} forming a stable complex that is difficult to reoxidize. In the presence of a large excess of H_2S, HS^- binds to ferric heme a_3, in a process that is likely aided by a conformational change caused by HS^- binding to Cu_B^{I} (Chart 17).

Using a synthetic CcO model system, a similar behavior was observed, i.e., that at low H_2S concentration, the ferric iron center was reduced but stable H_2S binding was not observed.[359] They also noted that cytochrome c can be reduced at low H_2S concentrations, thus injecting more reducing equivalents into the electron transfer chain and stimulating oxygen consumption (Chart 17).[359] Second order rate constants for H_2S-induced cytochrome c reduction observed under aerobic (81 ± 5 M^{-1} s^{-1}) and anaerobic (480 ± 2 M^{-1} s^{-1}) conditions differed ~6-fold at 25 °C.[97]

Another well-documented reaction of H_2S is its reaction with hemoglobin (Hb) and myoglobin (Mb), known since the 19th Century,[360–362] when a green compound was reported to form upon treatment of oxy-Hb or oxy-Mb with H_2S.[363] Although H_2S poisoning resulting in sulfhemoglobinemia is rare, misuse of sulfadrugs (sulfonamides) can lead to “green blood”.[364] Sulfhemoglobin (λ_{max} ~ 618 nm), results from covalent addition of sulfur to a double bond in one of the pyrrole rings[365–369] leading to the formation of a chlorin type heme (Chart 18A).[370] This covalent modification results in significant delocalization of π electron density away from the iron, reducing its affinity for O_2 (~2500-fold in Mb and ~135-fold in Hb).[369] Mb can be recovered by treating sulfmyoglobin with azide or cyanide, which probably react with the sulfur inserted in the pyrrole ring.[371]

Despite extensive studies, the actual mechanism of sulfheme formation is still unclear. It is postulated to involve the formation of an oxoferryl [Fe^{IV}═O $Por^{\bullet}$+] or [Fe^{IV}═O] intermediate (Chart 18B).[372] Sulfmyoglobin is formed stoichiometrically in the reaction between H_2S and metmyoglobin peroxide.[371,373] Sulfcatalase is formed in the reaction between compound II catalase and H_2S.[371] H_2S inhibits the heme in catalase in two ways: by irreversibly modifying the porphyrin and by reversibly ligating to the iron.[371] Like catalase, lactoperoxidase compound II reacts with H_2S to form sulflactoperoxidase.[374] Studies on myeloperoxidase, a hemeprotein that produces hypochlorous acid and other oxidants for killing pathogens,[375] indicate that H_2S is a potent inhibitor (IC_{50} = 1 μM). H_2S exhibits high bimolecular rate constants for reactions with compound I (1.1 × 10^6 M^{-1} s^{-1})

and compound II (2×10^5 M^{-1} s^{-1}).[376] Surprisingly, the reaction of H_2S with Fe^{III}, Fe^{II}, compound I, or compound II resulted in the formation of a ferrous–H_2S complex.

The activity of soluble guanylate cyclase (sGC) can also be modulated by H_2S. Essential for $NO^{\bullet}$ sensing, ferric sGC is reduced by HS^-, which in turn facilitates $NO^{\bullet}$ binding and activation of cyclic guanosine monophosphate synthesis.[377]

6.1.1. Catalytic H_2S Oxidation by Methemoglobin, Myoglobin, and Neuroglobin

—The ability of free hemin to oxidize H_2S to thiosulfate was also known for a long time.[378] In fact, the design of a H_2S sensor is based on its affinity for ferricmyoglobin (Fe^{III}–Mb or metmyoglobin).[379] These observations presaged the discovery of catalytic H_2S oxidation by methemoglobin (Fe^{III}–Hb)[301] and Fe^{III}–Mb[302] to a mixture of thiosulfate and iron-bound hydropolysulfides (Chart 19). Red blood cells lack mitochondria and, therefore, do not have the canonical H_2S oxidation pathway. Yet, these cells have MST and, therefore, the capacity to make H_2S[301,380] raising the question as to whether alternative mechanisms exist for disposing H_2S in these and other cells. The search for an answer to this question resulted in the discovery of catalytic H_2S oxidation by globins containing iron in the ferric oxidation state, as described below.

Binding of H_2S to Fe^{III}–Hb or Fe^{III}-Mb to give the corresponding HS^-–Fe^{III} species (Chart 19, [1]) is readily monitored by a shift in the Soret maximum from 405 → 423 nm in Hb[301] and from 409 →428 nm in Mb.[302] A concomitant resolution of the α/β bands at 577 and 541 nm in Hb and 578 and 545 nm in Mb is observed. The bimolecular rate constant for H_2S binding to Fe^{III}–Hb is 3.2×10^3 M^{-1} s^{-1}, the k_{off} is 0.05 s^{-1} and K_D is 17 μM at pH 7.4, 37 °C. The corresponding values for Mb are $k_{on} = 1.6 \times 10^4$ M^{-1} s^{-1}, $k_{off} = 1.6$ s^{-1}, and $K_D = 96$ μM. The K_D values represent upper limits since the rate constant for H_2S binding to Fe^{III}–Hb and Fe^{III}–Mb increases with decreasing pH and only ~20% of the dissolved sulfide exists as H_2S at pH 7.4, where the measurements were made. Binding of H_2S to sperm whale Fe^{III}–Mb has also been reported ($K_D = 18.5$ μM at pH 7.5 and 20 °C).[381]

Binding of H_2S to Fe^{III}–Hb results in the conversion of a high-spin $g = 5.83$ signal to a low-spin rhombic signal with g values of 2.51, 2.25, and 1.86.[301] Similar changes are observed with Fe^{III}–Mb, which converts from a high-spin $g = 5.92$ signal to a low-spin $g = 2.57$, 2.27, and 1.85 signal.[302] Signal integration reveals less than stoichiometric spin concentration associated with the low-spin species indicating the presence of spin silent (diamagnetic and/or an integer spin species) intermediate(s) even at the earliest time point at which the spectra were recorded following H_2S addition. Computational modeling suggested that the electronic structure of the S = $^5/_2$ species can be described as a resonance hybrid of high-spin Fe^{III}-SH^- and high-spin Fe^{II}–$^{\bullet}SH$. However, this model is 116 kJ/mol higher in energy than the S = $^1/_2$ model. Therefore, the initial intermediate is best described as Fe^{III}–SH^- with probably a small contribution of the $HS^{\bullet}$ coordinated structure.

The HS^-–Fe^{III} species has been characterized by multiple approaches. These include resonance Raman spectroscopy and X-ray absorption spectroscopy, which reveal the initial formation of a 6-coordinate low-spin ferric species. The resonance Raman spectrum reveals the subsequent formation of high-spin ferrous species, albeit it is unclear whether the signal

represents one or more likely, multiple intermediates. Coordination of H_2S to Mb was observed by ultrahigh resolution ESI time-of-flight cryo-MS under anaerobic conditions even when H_2S was in excess. Additional evidence for the initially formed ferric sulfide species comes from the X-ray structure of H_2S treated with hemoglobin solved at 1.8 Å resolution (Figure 14A).[382] The structure shows extra density above the iron on the distal side of the heme, which was assigned as sulfide based on the sulfur anomalous difference map. The Fe–S distance is 2.2 Å in both the α and β-subunits of hemoglobin and the HS^-–Fe^{III} intermediate is stabilized via hydrogen bonding to a histidine. Interestingly, a second sulfide was captured at the surface of the α-subunit, at the mouth of the PHE path, previously proposed to serve as an entry/exit channel for iron ligands.

Bound, H_2S probably exists in equilibrium with [Fe^{II}–$HS^{\bullet}$] which could react with another HS^- to form $H_2S_2^{\bullet-}$. Coordinated $H_2S_2^{\bullet-}$ could react further with HS^- and oxygen leading to the propagation of hydropolysulfide chain coordinated to Fe^{2+} or to formation of thiosulfate (Chart 19). In principle, the ferrous heme-bound $HS^{\bullet}$ radical could also react with O_2 to form $HSO_2^{\bullet}$ (see section 2).

Under anaerobic conditions, binding of 1 equivalent of H_2S to ferric iron is observed. However, under aerobic conditions, net consumption of H_2S is seen with formation of thiosulfate and hydropolysulfides, which remain iron bound. In the proposed mechanism, the second intermediate is an iron-bound hydrodisulfide (Chart 19, [2]), which has been observed by cryo-MS on Fe^{III}–Mb samples treated with Na_2S. Exposure of Fe^{III}–Hb to Na_2S_2 results in a shift in the Soret peak from 405 to 421 nm and in the appearance of α/β peaks at 575 and 543 nm, which is similar to the spectrum of HS^-–Fe^{III}.[382] Under aerobic conditions, thiosulfate is formed from Na_2S_2 in the presence of Fe^{III}–Hb.

Since the intracellular milieu is reducing, the fate of the iron-bound hydropolysulfides in the presence of physiologically relevant reductants is a pertinent issue. In the presence of GSH, the iron-bound hydropolysulfides are unstable, and GSSH, GSSG, and H_2S products are observed.[382] If formed, hydropolysulfides generated via globin-dependent oxidation are unlikely to be stable in the cell and would be converted to GSSH or other persulfides.

The catalytic nature of H_2S oxidation by Hb and Mb at the expense of oxygen is evident from the stoichiometric excess of products formed over heme iron concentration. Furthermore, exposure of sulfide-treated Fe^{III}–Hb to NADPH/flavin oxidoreductases led to the formation of O_2–Fe^{II}-Hb with a shift in the Soret peak from 423 to 415 nm. Collectively, these results establish that (i) Fe^{III}–Hb and Fe^{III}–Mb can catalyze multiple rounds of sulfide oxidation, and (ii) the O_2-liganded globin can be reformed in the presence of reductases like methemoglobin reductase.

Unlike Hb and Mb in which the distal heme site is available for binding exogenous ligands, the heme in neuroglobin has bis-histidine coordination.[383] The function of neuroglobin, which is highly expressed in neuronal tissues and in some metabolically active tissues, is not known.[384] Despite the coordinately saturated iron site, ferrous neuroglobin can bind O_2, CO and $NO^{\bullet}$.[385–388] The presence of the distal histidine ligand does in fact mute the reactivity of ferric neuroglobin (Fe^{III}–Nb) toward H_2S and leads to slow reduction to the ferrous state and

to inefficient formation of thiosulfate and hydropolysulfides.[389] In the presence of sulfide, the Soret peak of Fe^{III}–Nb shifts from 412 to 415 nm and the α/β bands are broad and centered at 540 nm with a 575 nm shoulder. It is unclear what this spectral change represents, but it is likely to be a mixture of species as also suggested by EPR and resonance Raman spectroscopy. The EXAFS data do not show evidence for an iron–sulfur bond in sulfide-treated neuroglobin, indicating that the sulfide oxidation products are formed even in the absence of direct coordination to iron. The k_{on} for the interaction of sulfide with Fe^{III}–Nb is 13.8 M^{-1} s^{-1} at pH 7.4 and 25 °C, which is significantly smaller than the values for Fe^{III}–Hb and Fe^{III}–Mb. The k_{off} and K_D for the interaction of sulfide with Fe^{III}–Nb are 5 × 10^{-3} s^{-1} and 370 μM, respectively. As expected, the H64A mutation of the distal histidine residue allows direct binding of sulfide as confirmed by EXAFS analysis, increases the rate constant for sulfide binding 4000-fold, and supports active oxidation of sulfide to thiosulfate and protein bound hydropolysulfides. A rich array of oxidation products were identified with the H64A mutant using cryo-MS including hydropolysulfides with 2–6 sulfur atoms and variously oxygenated derivatives in addition to thiosulfate and sulfate.[389]

Collectively, the studies on the globins reveal the potential for ferric-iron dependent sulfide oxidation chemistry, whose relative importance in the cell awaits evaluation. An open ligation site promotes sulfide coordination and oxidation chemistry, and in its absence, iron reduction is supported. The relatively low steady-state concentration of H_2S likely reduces the prevalence of reactions between sulfide and heme or nonheme iron (or other metalloproteins) except in special cases like red blood cells where Fe^{III}–Hb represents 1–3% of total hemoglobin, whose concentration is high (~5 mM).

6.1.2. Binding and Transport of H_2S by Globins—Specialized hemoglobins that transport H_2S are found in organisms that are adapted to life in sulfide-rich environments. The best-studied example of such a Hb is from the clam, *Lucina pectinata* (Figure 14B),[381,390–403] which lives in H_2S-rich waters. The monomeric *L. pectinata* Hb hemoglobin I (HbI) transports H_2S to symbiotic bacteria, which assimilate it and provide the host with a source of organic sulfur. HbI exhibits a high association constant (k_{on} = 2.3 × 10^5 M^{-1} s^{-1}) and an unusually low dissociation constant (k_{off} = 0.22 × 10^{-3} s^{-1}) for H_2S,[390] which suggests the stabilization of distal sulfide ligand by the active site.[391,395,396,398,400,401] In human Hb, a histidine residue hydrogen bonds with the iron-bound sulfide. The corresponding residue in HbI is a glutamine, which has a flexible side chain. Mutation of the glutamine residue in HbI to valine precludes heme reduction, while mutation to histidine promotes formation of sulfhemoglobin. Another difference from human Hb, is the presence of phenylalanines in HbI that form a hydrophobic pocket around the sulfide.[401] It is unclear whether H_2S release occurs via slow dissociation or by heme iron reduction. Introduction of positively charged substituents on the porphyrin ring changes the reactivity of metal porphyrins from simple binding of H_2S to catalytic oxidation of H_2S.[404] Hence, at low concentrations, H_2S release could be due to its dissociation from the heme iron, while at high concentrations, heme reduction and H_2S/hydropolysulfide delivery might predominate.[405]

Another sulfide-adapted organism, the giant tubeworm, *Riftia pachyptila*, lives in deep-sea hydrothermal vents in symbiotic relationship with sulfide-oxidizing bacteria that need both

H_2S and O_2.[406–408] The *Riftia* hemoglobins are large proteins with a molecular mass of ~3500 kDa (Figure 14C). Binding of H_2S and O_2 occurs at separate sites. While O_2 binds at the heme iron site, it is unclear where H_2S binds. The protein contains 12 Zn^{2+} ions, which have been suggested as potential sites for H_2S binding.[408]

6.1.3. Interaction of H_2S with Zn^{II}-Containing Proteins—The interaction of H_2S with Zn^{II}-containing proteins is poorly studied. It is reported that H_2S represses androgen receptor transactivation by targeting the second zinc-finger module.[409] Phosphodiesterase 5, a Zn^{II}-containing enzyme, is inhibited by nanomolar H_2S concentrations.[410] Zinc–hydrogensulfido complexes are not easy to prepare and isolate and require bulky apolar ligands.[411] The synthesis of a stable zinc hydrogensulfido complex with the tris(2-pyridylmethyl)amine ligand has been reported.[412] H_2S was released from the complex in acidic medium or transferred to a zinc center with higher affinity via intermediate formation of a μ-sulfido dinuclear species. The ability of Zn^{II} to coordinate HS^- was reported to depend on the ability of the HS^- ligand to form hydrogen bonds.[413] Chemical modifications on the ligand that precluded hydrogen bonding with HS^- resulted in decomposition of the complex and ZnS precipitation. This study highlighted the importance of the second coordination sphere in stabilizing the Zn-HS^- adduct, suggesting that the protein environment could do the same.

6.2. Interaction of H_2S with ROS and Other Biologically Relevant Oxidants

Being at the lowest oxidation state of −2, the sulfur in H_2S can only undergo oxidation. Oxidation leads to sulfate (SO_4^{2-}), sulfite (SO_3^{2-}), thiosulfate ($S_2O_3^{2-}$), persulfides (RSS^-), organic (RSS_nSR) and inorganic (HSS_nSR) polysulfides, and elemental sulfur (S_n). The direct reaction of H_2S with O_2 is thermodynamically disfavored (see section 2).[63,414] Given the high one-electron reduction potential ($E^{\circ\prime}(HS^\bullet, 2H^+/H_2S)$ = +0.91–0.94),[64,65] only relatively strong one-electron oxidants can oxidize H_2S to $HS^\bullet$, with further reaction of $HS^\bullet$ providing an additional driving force. Indeed, several biologically relevant oxidants can support the one-electron oxidation of H_2S, such as hydroxyl radical,[415,416] carbonate radical,[65] nitrogen dioxide,[61] and myeloperoxidase oxoferryl compounds I and II;[376] the rate constants of these reactions are shown in Table 2. The list of one-electron oxidants that can oxidize H_2S can probably be extended to peroxyl and phenoxyl radicals as well as to other metal centers (see section 6.1). The superoxide radical can also oxidize H_2S.[97] The apparent rate constants at pH 7.4 vary depending on the oxidant and are similar to those reported for cysteine and GSH.[61] Mixtures of polysulfides and polysulfide radical anions ($S_2^{\bullet-}$ and $S_3^{\bullet-}$) are observed in reaction mixture containing superoxide and H_2S in DMSO.[97]

The initial oxidation product of H_2S is the sulfyil radical ($HS^\bullet$). $HS^\bullet$ is an oxidizing free radical capable of reacting with electron donors including ascorbate and GSH. Importantly, the one-electron oxidation of H_2S can unleash oxygen-dependent free radical chain reactions amplifying the initial oxidative event.[61,65] Although the reaction of $HS^\bullet$ with a second $HS^\bullet$ to form HSSH has a high rate constant ($(6–9) \times 10^9\ M^{-1}\ s^{-1}$, eq 7),[65] this reaction is unlikely to occur in most contexts because of its dependence on the square of $HS^\bullet$ concentration. Alternatively, $HS^\bullet$ can react with O_2 to form $SO_2^{\bullet-}$ ($(5–7) \times 10^9\ M^{-1}\ s^{-1}$, eq 10),[65] a reducing radical which in turn can react with O_2 forming $O_2^{\bullet-}$. $HS^\bullet$ can also react

reversibly with HS^- forming $HSSH^{\bullet-}$ (forward and reverse rate constants, 5.4×10^9 M^{-1} s^{-1} and 5.3×10^5 s^{-1});[65] the latter can also react with O_2 forming $O_2^{\bullet-}$ (eq 11 and 12).[65,97,415] Superoxide radical ($O_2^{\bullet-}$) can dismutate, spontaneously or enzymatically, to O_2 and H_2O_2[414]

The rate constants for reaction of H_2S with two-electron oxidants (Table 2) are also comparable to those of low molecular weight thiols.[61] The reaction with hydroperoxides (ROOH) initially forms HSOH, which can react with a second HS^- to form HSSH.[61,73] In the case of hydrogen peroxide, the final products depend on the initial ratio of hydrogen peroxide to H_2S and consist mainly of polysulfides, elemental sulfur, and, in the presence of excess oxidant, sulfate.[73,417] By analogy to thiols, the reaction with hypochlorous acid is likely to form HSCl that quickly hydrolyzes to HSOH.[418]

The reaction of peroxynitrite with H_2S is more complex than its reaction with thiols and generates novel products.[61,419,420] The decay of peroxynitrite in the presence of H_2S is first order in peroxynitrite and first order in H_2S; the second order rate constant is 6.7×10^3 M^{-1} s^{-1} (pH 7.4, 37 °C).[420] The pH-dependence is bell-shaped, consistent with HS^- and ONOOH being the reacting species. Computational modeling suggests that the reaction starts with the nucleophilic substitution of HS^- on ONOOH to give HSOH and NO_2^- as initial products. The reaction then proceeds to the formation of “yellow” products that absorb at 408 nm.[419] The increase in absorbance at 408 nm occurs with a lag phase, consistent with the formation of intermediates that precede formation of the yellow products.[420] Free radical scavengers or nitrite had no effect on the amount of yellow product formed, but the yield increased when peroxynitrite was in excess. Thus, it was proposed that the reaction of HSSH with peroxynitrite leads to formation of the yellow products, and indeed, mixtures of HSSH and peroxynitrite in acetonitrile yielded products with similar absorbance spectra.[420] Based on mass spectrometric and computational studies, it was proposed that at least one of the yellow products is $HSNO_2$ or its isomer HSONO. In addition to the direct reaction of peroxynitrous acid with HS^-, the free radicals derived from peroxynitrite (nitrogen dioxide, hydroxyl and carbonate radical) can also react with H_2S.[61]

The probability of H_2S acting as a direct scavenger of oxidants in biological systems depends on kinetic factors, i.e., on the products of the rate constants times H_2S concentration. While the reactions of H_2S with some oxidants display relatively high rate constants, comparable to those of LMW thiols, the tissue concentrations of H_2S (submicromolar, see section 3.5) are very low, i.e., several orders of magnitude lower than those of other reductants (e.g., millimolar for some thiols). Thus, it can be concluded that the direct reaction of H_2S with oxidants would not be fast enough in biological contexts to support a significant scavenging role. Furthermore, H_2S would not be able to compete with thiols for one- and two-electron oxidants, unless high local concentrations H_2S were reached as, for example, with bolus administration of exogenous H_2S. In conclusion the biological “antioxidant” effects ascribed to H_2S are unlikely to be due to direct scavenging of oxidants by H_2S but rather to indirect effects on enzymes, transporters, and/or other targets in signaling pathways.

6.3. Reaction of H_2S with $NO^•$ and Its Metabolites

$NO^•$ has important signaling roles in mammals including blood pressure regulation,[423,424] immune defense,[425,426] and neurotransmission.[427–429] Most of the "classical" effects of $NO^•$, such as vasodilation or neuro-modulation, are mediated by coordination of $NO^•$ to the heme iron in sGC, which activates the enzyme to generate cyclic guanosine monophosphate (cGMP), a powerful second messenger.[430,431] But not all of the actions of $NO^•$ proceed via cGMP signaling (Chart 20). $NO^•$ can also lead to an oxidative posttranslational modification of cysteine called *S*-nitrosation.[432–436] How *S*-nitrosothiols are formed in the cells is still a matter of debate.[436–438] $NO^•$ can also undergo one-electron reduction to form nitroxyl (HNO, IUPAC name: hydridooxidonitrogen, azanone, nitrosylhydride),[439–442] a powerful vasodilator.[267,439,442] $NO^•$ is oxidized to nitrite and nitrate. Nitrite is now recognized as an important metabolite that can be reduced to $NO^•$.[443–445] Finally, peroxynitrite and its protonated form (ONOOH) can be generated in a diffusion controlled reaction between $NO^•$ and $O_2^{•-}$ ($\sim 1 \times 10^{10}$ M^{-1} s^{-1}).[446–448]

H_2S interferes with $NO^•$ signaling, either by reacting with $NO^•$ or its downstream metabolites[267,419,420,449–453] or by modulating $NO^•$ production[268,454,455] and cGMP levels.[266,377,410] The first report on H_2S-induced vasodilatory effects demonstrated its synergy with $NO^•$.[7] Inhibition of endothelial NO synthase (eNOS) leads to abrogation of H_2S-induced vasodilation,[7,266,267] while deletion of CSE prevented the vasodilatory effects of acetylcholine and $NO^•$.[266] In addition, the cardioprotective effects of H_2S were abolished in $eNOS^{-/-}$ mice.[268] Different mechanisms have been proposed for this crosstalk that are covered in section 10. In this section, we focus on the chemical aspects of the direct reactions between $NO^•$ (and its metabolites) and H_2S.

6.3.1. Direct Reaction between $NO^•$ and H_2S—Studies on the direct reaction between $NO^•$ and H_2S date back to the 19th and early 20th century. The reaction of gaseous $NO^•$ and H_2S was reported to form, among other products, nitrous oxide (N_2O) and elemental sulfur.[456–461] Formation of N_2O was difficult to explain as a single step process. N_2O is a product of HNO dimerization[439–442] so HNO formation could be the actual intermediate step.[461]

It has been suggested that $NO^•$ and H_2S can form HNO in vivo.[451,452] The combination of H_2S and $NO^•$ donors was observed to have the same effects in murine heart as the application of the HNO donor, Angeli's salt.[452] Indeed, when the reaction between H_2S and $NO^•$ was studied at pH 7.4 under anaerobic conditions, the rate of HNO formation was first order on both $NO^•$ and H_2S 267. The combination of $NO^•$ and H_2S (2 μM each) yielded a peak HNO concentration of ~0.5 μM, similar to the effects of 1 mM Angeli's salt. Intracellular HNO production, detected by an HNO fluorescence sensor was also shown to depend on both $NO^•$ and H_2S.[267]

Direct one-electron transfer from HS^- to $NO^•$ to give HNO and $S^{•-}$ (eq 22) is thermodynamically unfavorable ($\Delta G^{0\prime} = +102$ kJ/mol).[64] An alternative mechanism is

$$NO^• + HS^- \rightarrow HNO + S^{•-} \quad (22)$$

the formation of $HSNO^{\bullet -}$ (eq 23), which is similar to the reaction

$$NO^{\bullet} + HS^{-} \rightarrow HSNO^{\bullet -} \quad (23)$$

reported between $NO^{\bullet}$ and aromatic and "pseudoaromatic" alcohols such as tyrosine, hydroquinone, and ascorbic acid.[462] $HSNO^{\bullet -}$ is a powerful reducing agent ($RSNO^{\bullet -}$/RSNO, $E < -1$ V)[463] that can initiate a cascade of reactions, leading to N_2O and S_n formation (eqs 24–28).

$$HS^{-} + NO^{\bullet} \rightarrow HSNO^{\bullet -} \quad (24)$$

$$HSNO^{\bullet -} + NO^{\bullet} + H^{+} \rightarrow HSNO + HNO \quad (25)$$

$$HSNO + HS^{-} \rightarrow HNO + HS_2^{-} \quad (26)$$

$$HS_2^{-} + H^{+} \rightarrow H_2S + \frac{1}{n}s_n \quad (27)$$

$$2HNO \rightarrow N_2O + H_2O \quad (28)$$

Endogenous HNO production would be critically dependent on $NO^{\bullet}$ and H_2S being produced in close proximity since both can engage in competing reactions with other molecules (Figure 15A). The transient receptor potential channel A1 (TRPA1), a biological sensor that regulates HNO-induced release of the powerful vasodilator calcitonin gene related peptide, colocalizes with CBS[267] and nNOS,[464] potentially forming a functional unit for HNO formation and its action.[267,465] Studies with an HNO-responsive two-photon ratiometric fluorescence imaging probe confirmed that endogenous HNO generation is dependent on endogenous H_2S and $NO^{\bullet}$ formation in cells and brain tissues.[466]

6.3.2. Reaction of H_2S with S-Nitrosothiols and Metal-Nitrosyls—Formation of a new *S*-nitrosothiol, HSNO (IUPAC name: nitrososulfane or (hydridosulfanido)oxidonitrogen), in the reaction of H_2S with *S*-nitrosothiols (or other nitrosocontaining species) was first proposed in 2006.[467,468] HSNO was known as a product of *cis*-HNSO photolysis in argon matrices, where it has been studied computationally and by IR spectroscopy.[469–472] The crystal structure of the bis-(triphenylphosphine)iminium SNO salt ($PNP^{+}SNO^{-}$) was reported,[473] but a detailed study in aqueous solution was missing.

Using pulse radiolysis to generate $HS^{\bullet}$ and $NO^{\bullet}$, formation of a species with the spectral characteristics ($\lambda_{max} \approx 330$ nm) of an *S*-nitrosothiol was observed (Chart 21).[449] The species was short-lived with a half-life of ~12 μs[449] yielding an estimate of ~10^7 M^{-1} s^{-1} for the rate constant for the reaction of HSNO with sulfide anion (eq 26).[64]

HSNO was also detected in reactions of H_2S with "NO^+" carriers: acidified nitrite,[449] N_2O_3,[474] metal nitrosyls,[450,475–477] and *S*-nitrosothiols.[449,453] For example, in the reaction with acidified nitrite, a brown-red intermediate was formed prior to the solution turning milky white. ESI-TOF MS analysis of the acidic and neutralized solution of the brown-red intermediate revealed the parent ion mass and isotopic pattern expected for HSNO.[449]

Reaction of thiosemicarbazide with $NO^{\bullet}$ results in HSNO formation under physiological conditions; thiosemicarbazides are therefore proposed to serve as a tool capable of transforming intracellular $NO^{\bullet}$ into HSNO.[478]

In the reaction of H_2S with N_2O_3 (eq 29), the facile formation of stable HSNO was demonstrated by Fourier-transform microwave spectroscopy.[474]

$$N_2O_3 + H_2S \rightarrow HSNO + HNO_2 \quad (29)$$

Generation of HNO and N_2O (eq 26 and 28) was confirmed when ^{18}O labeled N_2O_3 was reacted with excess of H_2S.[474] HSNO formation from N_2O_3 and H_2S could be important for intracellular RSNO generation. Formation of N_2O_3 is deemed to be kinetically improbable due to the low intracellular concentration of NO• compared to O_2.[437] However, N_2O_3 could be formed in the lipid bilayers where $NO^{\bullet}$ and O_2 accumulate.[437] H_2S can also accumulate in lipid bilayers based on its partition coefficient[57] creating conditions that might be conducive for HSNO formation (Figure 15B). Reaction of HSNO with thiols (Chart 21 and Figure 15C) can result in transnitrosation. HSNO can act as an "NO^+" carrier from one protein to another and across the cell membrane (Figure 15C). This idea is supported by the ability of H_2S to promote nitrosation of BSA outside a dialysis bag containing nitrosated BSA but also nitrosation of hemoglobin in the red blood cells from extracellular nitrosated BSA.[449] NaHS treatment during cardiac ischemia was reported to increase tissue *S*-nitrosation[479] possibly via HSNO formation which would then act as transnitrosating agent.

Using a combination of spectroscopic approaches and ESI-TOF MS to study the trans-nitrosation reaction between *S*-nitrosoglutathione and H_2S, HSNO was detected within 30 min.[449] Greater than equimolar H_2S concentration promoted N_2O and hydroxylamine formation via intermediate HNO generation (eqs 26, 28, and 30).

$$HNO + 2HS^- + H^+ \rightarrow NH_2OH + HS_2^- \quad (30)$$

An unexplained observation made during the transnitrosation reaction between GSNO and H_2S was that the solution turned yellow ($\lambda_{max} = 412$ nm).[449,480] MS analysis of the RSNO/H_2S reaction mixture identified, among other products, $SSNO^-$ which was suggested

to be a stable yellow product.[481] $SSNO^-$ formation from RSNO and H_2S was proposed to occur via eqs 31–33.[453,480,481]

$$RSNO + HS^- \rightarrow SNO^- + RSH \quad (31)$$

$$SNO^- + HS^- \rightarrow HS_2^- + HNO \quad (32)$$

$$HS_2^- + \text{“}NO^+\text{”}(RSNO \text{ or } HSNO) \rightleftharpoons SSNO^- + RSH(\text{or } H_2S) \quad (33)$$

Whether $SSNO^-$ is stable enough to mediate biological effects has been the subject of debate. Crystalline PNP^+SSNO^- synthesized by a published method[473] has been used to chemically characterize $SSNO^-$.[69] Crystalline $SSNO^-$ and $SSNO^-$ dissolved in organic solvent are air and water sensitive.[69,473] The reduction potential of $SSNO^-$ was determined to be −0.21 V versus NHE, which is within the range of physiological reductants like glutathione with which it reacted readily.[69] Furthermore, $SSNO^-$ decomposed rapidly in the presence of H_2S and cyanide forming SNO^-.[69,482] $^{15}N/^{14}N$ NMR and cryo-ESI TOF MS analyses confirmed the formation of SNO^-/HSNO in the reaction of $SSNO^-$ with HS^- and CN^- (eqs 34 and 35).[482]

$$SS^{15}NO^- + HS^- \rightarrow S^{15}NO^- + HS_2^- \quad (34)$$

$$SS^{15}NO^- + C^{14}N^- \rightarrow SC^{14}N^- + S^{15}NO^- \quad (35)$$

A role for $SSNO^-$ in signaling is doubtful based on kinetic grounds (the apparent rate constant for its formation estimated from published data[481] is 10^{-14} M^{-1} s^{-1}) as well.[64] Considering the very low concentrations of HS^- (section 3.5) and RSNO[436,437] and the very high concentrations of thiol, the reaction of SNO^- with HS^- (eq 32) in a cellular millieu seems unlikely. Furthermore, HS_2^-, which is intrinsically unstable and readily reduced by thiols, is unlikely to persist long enough or to react specifically with “NO^+” to form $SSNO^-$ (eq 33). Even if formed, $SSNO^-$ would readily react with thiols to form HSNO.[482] In summary, HSNO remains the chemically most plausible nitrosating agent that can react with cysteines (Chart 21 and Figure 15) and engage in transnitrosation reactions.[482,483]

6.3.3. Metal-Catalyzed Reaction between Nitrite and Sulfide—Although nitrite and H_2S do not react directly at pH 7.4,[97] $NO^\bullet$ generation has been reported in cells treated with these two reagents.[450] Intracellular HNO generation which was localized to mitochondria was observed when cells were treated with 100 μM nitrite and sulfide but not in cells

depleted of mitochondria.[450] This result implicated a role for mitochondrial proteins in catalyzing the reaction between nitrite and H_2S. To understand the possible role of heme iron in the reaction mechanism for HNO generation from nitrite and sulfide, a water-soluble iron–porphyrin was used as a model system.[450] Initial binding of nitrite to ferric heme and subsequent oxygen atom transfer[484,485] to H_2S to give HSOH was the predominant reaction observed when nitrite was in excess. The $[Fe^{II}(NO)] \leftrightarrow [Fe^{III}(NO^-)]$ complex then slowly released HNO.[450,485] When sulfide was in excess, it reduced ferric to ferrous heme so that the classic nitrite reductase activity of Fe^{II} heme was observed. The formed $[Fe^{III}(NO)] \leftrightarrow [Fe^{II}(NO^+)]$ reacted with HS^- to form an $[Fe^{II}(HSNO)]$ complex (Chart 22).[450] These results support the feasibility of H_2S reacting with metal-nitrosyls to form *S*-nitrosothiols via HSNO, which represents an alternative mechanism for the physiological generation of HNO.

Another metalloprotein, a molibdopterin-containing xanthine oxidase, was reported to catalyze H_2S-stimulated nitrite reduction in endothelial cells and in mice injected with Na_2S. However, the mechanism of this reaction was not elucidated.[486]

7. PROTEIN PERSULFIDATION

Protein persulfidation, an oxidative posttranslation modification of cysteines, represents a mechanism by which H_2S signals. This modification is also referred to in the literature as "sulfhydration",[19] which implies "hydration" and is inaccurate. Instead, the process involves "sulfuration", i.e., the addition of a sulfur atom.[64,487] The term "persulfuration" has been also used, but the term "persulfidation" has been gaining wide acceptance and is used here. Other ways to describe RSSH are hydropersulfide, or hydrodisulfide, or as a disulfane derivative (e.g., CH_3SSH is methyldisulfane[64]). A less ambiguous name for RSSH is hydridodisulfide. In this review, the term "persulfide" is used to designate $RSSH/RSS^-$.

Contrary to the chemically incorrect claim that H_2S can directly modify cysteine residues to form persulfides, the reaction between H_2S and thiols (eq 36) requires an oxidant.[64,181]

$$RSH + HS^- \rightarrow RSS^- + 2H^+ + 2e^- \quad E^{\circ\prime} = +0.18\ V \qquad (36)$$

Due to their instability and greater reactivity than thiols, working with persulfides is challenging. In the following subsections, progress on developing methods to study persulfides and our current understanding of their reactivity are discussed.

7.1. Model Systems to Study Protein Persulfidation

Persulfides are relatively unstable in aqueous solution and are typically synthesized immediately before use. Several model systems have been used to study persulfide chemistry. These models are grouped in two categories: (i) low molecular weight (LMW) persulfides and (ii) protein persulfide models.

7.1.1. LMW Persulfide Models—Several LMW persulfides have been reported that are either synthesized in situ or have been characterized following purification. A synthetic method for persulfides dates back to 1954 when alkyl- and arylpersulfides were prepared

from sulfenyl chloride and thiols.[488] The resulting acyldisulfide was hydrolyzed by HCl to give persulfide (Chart 23A, [I]). Persulfides can also be prepared from methoxycarbonyl disulfides, which would undergo alkoxide-induced displacement of the RSS^- anion (Chart 23A, [II]).[489] Alternatively acyl disulfides can be synthesized in the reaction of dialkyl thiosulfones with thioacid (Chart 23A, [III]).[490] In fact, the acidic hydrolysis of acyl disulfides has become a general synthetic strategy for the preparation of small molecule persulfides like ethyl-, t-butyl-, benzyl-, diphenylmethyl-, trityl-, adamantyl-, and penicillamine-derived persulfide (Chart 23B).[488,491–500] The hydrophobic LMW persulfides need to be handled in organic solvents and are consequently protonated,[494,495] which reduces their nucleophilicity. In contrast, persulfides are deprotonated and more reactive at physiological pH (see section 6.2).

A water-soluble penicillamine-derived LMW persulfide has been prepared.[501] The synthetic protocol involved acylprotected disulfides and gave high yields (Chart 24). At pH 2.7, <5% degradation of the acyl-protected disulfide of penicillamine was observed after 120 min at room temperature, allowing relatively stable stock solutions to be prepared. When placed in buffers with pH >6 the disulfide underwent *S*- to *N*-methoxycarbonyl transfer, generating *N*-methoxycarbonyl penicillamine persulfide, a persulfide related to a commonly used *S*-nitrosothiol (Chart 24).

LMW persulfides can be generated in situ in aqueous solution by mixing disulfides (such as cystine or GSSG) with H_2S in equimolar ratio (Chart 25A).[60,502–505] As this is an equilibrium process, the reaction mixture contains unreacted disulfides and H_2S in addition to the persulfide. Alternatively, persulfides can be prepared in situ by CBS- or CSE-catalyzed conversion of cystine or homocystine to the corresponding persulfides.[165,226] Cysteine persulfide and homocysteine persulfide are formed via α,β or α,γ elimination reactions, respectively (Chart 25B; for details see section 3). The LMW persulfide, GSSH, can also be formed in situ. Rhodanese in the presence of thiosulfate[313,330] (or *p*-toluenethiosulfonate)[506,507] and glutathione forms GSSH (Chart 25C) while SQR forms GSSH via sulfurtransfer from H_2S to GSH (Figure 8).[311] Another route for preparing GSSH is to reduce the trisulfide (GSSSG) with glutathione reductase and NADPH (Chart 25D).[165,508]

7.1.2. Protein Persulfide Models—A commonly used strategy for preparing protein persulfides is the reaction of activated disulfides with equimolar H_2S. For example, a protein with one reactive cysteine is first treated with Ellman's reagent, 5,5′-dithiobis(2-nitrobenzoate) (DTNB), to form a mixed disulfide.[60,505,509] The thionitrobenzoate anion (TNB) is a good leaving group, and in the next step the protein–TNB mixed disulfide is reacted with an equimolar concentration of H_2S to generate the protein persulfide (Figure 16A).[60,509] The concomitant release of TNB, which has a strong absorbance at 412 nm,[510] provides a simple method for quantifying the reaction yield. Persulfides of papain,[505,509] glutathione peroxidase 3,[509] and human serum albumin[60] have been prepared using this approach.

The reaction of sulfenic acid with H_2S (for details see section 8.2) can also be used to prepare protein persulfides.[511] The primary obstacle with this approach is that sulfenic acid

modifications on proteins are generally unstable. An exception is the sulfenic acid derivative of serum albumin, which is relatively stable[512,513] and has been exploited to generate the corresponding persulfide (Figure 16B).[60,511]

A less specific approach for protein persulfidation involves mixing the protein with H_2S and an oxidant, such as HOCl, or mixing the protein with polysulfide salts (Figure 16C).[514] Uncontrolled protein poly thiolation is an inevitable outcome of this approach (see section 8.3), and the use of these methods is discouraged.

Alternatively, a protein thiolate can be reacted with 9-fluorenylmethyl disulfide to form a mixed disulfide which is then exposed to alkaline pH to promote hydrolysis generating the protein persulfide (Figure 16D).[515] However, the alkaline conditions could lead to protein denaturation.

7.2. Persulfide Reactivity

Persulfides have characteristics in common with thiols, disulfides, polysulfides, hydroperoxides, and sulfenic acids. The chemistry of persulfides is very rich, and persulfides are very versatile molecules that are being assigned roles of increasing importance in biology.

The crystal structure of tritylpersulfide shows an S–S bond length of 2.0396 Å, which fits well with the S–S bond length observed in crystals of inorganic polysulfides. The CSSH dihedral angle is 82.2°,[494] which is close to the CSSC dihedral angle of 83° seen in unstrained disulfides.[516] The crystal structures of some proteins involved in sulfur metabolism have been obtained with cysteine residues modified to persulfides, e.g., the structures of bovine rhodanese[332,517] and of human MST.[271] In addition, the crystal structures of some proteins that contain free cysteine persulfide bound as a ligand have been obtained.[518,519]

In alkaline solutions, persulfides show an absorption maximum at 335–340 nm[494,495,501,502] and a relatively low absorption coefficient (~310 M^{-1} cm^{-1}).[31] The IR spectra of alkyl and aryl persulfides show a weak S–H stretch at ~2500 cm^{-1} (Table 3), which is shifted to lower wavenumbers than thiols (~2570 cm^{-1}), consistent with the presence of a stronger S–H bond in thiols.[494,495,520] Similar shifts are observed in the Raman spectra, with the additional presence of a band in the 200–500 cm^{-1} region due to the S–S bond. ^{1}H NMR spectra of persulfides in organic solvents show shifts in the S–H proton relative to the corresponding thiols. For example, the S–H proton shows an ~0.4 ppm upfield shift in tritylpersulfide and an ~1.2 ppm downfield shift in benzenepersulfide and adamantylpersulfide (Table 3).[494,495]

7.2.1. Persulfide Acidity—Protonated persulfides can ionize to form the corresponding anionic persulfides (eq 37).

$$RSSH \rightleftharpoons RSS^- + H^+ \quad (37)$$

In agreement with the weaker S–H bond in persulfides than in thiols, the acidity of persulfides is predicted to be higher. There are very few reported experimental measurements of persulfide pK_a. From the pH dependence of the rate of hydrogen atom transfer from 2-[(3-aminopropyl)amino]ethane persulfide to a carbon-centered free radical, the pK_a of the persulfide was estimtated to be 6.2 ± 0.1 in comparison to a pK_a of 7.6 ± 0.1 for the corresponding thiol.[489] A computational study estimated that the pK_a of cysteine persulfide (4.3) is ~4 units lower than of cysteine thiol (8.29).[60] The available data suggests that at physiological pH, RSS^- will predominate over RSSH and that the $[RSS^-]/[RSSH]$ ratio can be ~10^4-fold higher than the corresponding $[RS^-]/[RSH]$. The acidity of persulfides and thiols on proteins will be modulated by their microenvironment, i.e., by the presence of functional groups.

7.2.2. Persulfide Nucleophilicity—Ionized persulfides (RSS^-) are nucleophilic. Although both sulfurs in the ionized and in the protonated species have lone pairs of electrons, the outer or terminal sulfur in RSS^- is the more nucleophilic center (eq 38).

$$RSS^- + E^+ \rightarrow RSSE \quad (38)$$

Basicity and nucleophilicity are generally correlated, and the stronger the base, the greater the nucleophilicity.[521] Since the pK_a of persulfides is significantly lower than that of the corresponding thiol,[60] persulfide would be expected to be less nucleophilic. However, the presence of a vicinal sulfur atom with lone electron pairs increases the nucleophilicity of the terminal sulfur atom via the alpha effect.[522,523] Examples of the alpha effect enhancing nucleophilicity include HOO^- relative to HO^- and NH_2NH_2 and NH_2OH relative to NH_3.[521] As noted previously, nucleophilicity is a kinetic concept and needs to be evaluated from the rate constants for the relevant reactions. A comparison between the reactivity of the persulfide versus thiol in human serum albumin toward 4,4′-dithiodipyridine provided a quantitative estimate of the magnitude of the alpha effect.[60] The pH-independent rate constant for the reaction of the albumin persulfide with 4,4′-dithiodipyridine was 3-fold greater than for the thiolate. At pH 7.4, the persulfide is estimated to be fully ionized while the thiol is only partially ionized (the pK_a of the single thiol is 8.1).[60] Thus, the observed rate constant at pH 7.4 was 20-fold greater for persulfide than for the thiol.[60]

Computational evaluations of the HOMO energies are consistent with a higher nucleophilicity of persulfides than thiols. In one estimate, the energy of the HOMO of methylpersulfide was ~29 kJ mol^{-1} higher than that of methylthiolate.[103] In another estimate, the HOMO of cysteine persulfide was 51 kJ mol^{-1} higher than that of cysteine thiolate and, in addition, cysteine persulfide had lower chemical hardness than cysteine thiolate.[60]

The nucleophilicity of persulfides is evident from their reactivity toward thiol alkylating agents such as 1-chloro-2,4-dinitrobenzene,[499] iodoacetamide,[505,509,515] *N*-ethylmaleimide,[505,509,515] methyl acrylate,[515] monobromobimane,[165,515] benzyl bromide,[515] 2-methylsulfonyl benzothiazol,[135,511,515,524] and methylmethanethiosulfonate[509] (Chart 26A). In contrast to thiols, which form thioeters with these reagents, persulfides form disulfides,

which can be reduced to the corresponding thiols with reductants such as dithiothreitol. Interestingly, 9-fluorenylmethyl-based thioester models of LMW persulfide reacted with methylsulfonyl benzothiazol to give a trisulfide due to the reactivity of the initial benzothiazol disulfide derivative,[515] which was not the case for other LMW persulfides or for protein (bovine serum albumin and glutathione peroxidase-3) persulfides.[135,511,524] The nucleophilicity of persulfides is also revealed by their reaction with disulfides such as 5,5′-dithiobis(2-nitrobenzoic acid),[60,509] *N*-acetylcysteine piridyldisulfide,[509] and 4,4′-dithiodipyridine,[60] to form trisulfides and other products (Chart 26B).

Persulfides also react with electrophiles such as 8-nitroguanosine 3′,5′-cyclic monophosphate (8-nitro-cGMP) giving HS-cGMP,[165,501] with methylmercury[525] (Chart 26C) and, as described in the following sections, with one- and two-electron oxidants. In summary, persulfides are better nucleophiles than thiols because of the greater availability of RSS^- versus RS^- at neutral pH and higher intrinsic reactivity due to the alpha effect.

7.2.3. Reaction of Persulfides with Two-Electron Oxidants—Another manifestation of the nucleophilicity of the persulfides is their reactivity with two-electron oxidants. For example, the apparent rate constant of the reaction of albumin persulfide with peroxynitrite ($1.2 \times 10^4\ M^{-1}\ s^{-1}$ at 20 °C) is 4-fold higher than of the corresponding thiol ($2.7 \times 10^3\ M^{-1}\ s^{-1}$).[60] By analogy with thiols, the immediate product of the reaction between a persulfide and a hydroperoxide is likely to be an unstable perthiosulfenic acid (RSSOH), which undergoes further reactions forming polysulfides (RS_nR and RS_n^-) and, in the presence of excess oxidant, perthiosulfinic and perthiosulfonic acids ($RSSO_2H$ and $RSSO_3H$). The latter have been detected as oxidation products of papain, albumin, and glutathione peroxidase.[60,509,511] Importantly, in contrast to the thiol-derived sulfinic and sulfonic acids (RSO_2H and RSO_3H), which are generally considered to be irreversible oxidation products, the corresponding persulfide derivatives $RSSO_2H$ and $RSSO_3H$ can be reduced back to thiol by common reductants.[135,340] Higher recovery of thiols after exposure of persulfides versus thiols to hydrogen peroxide (or HNO) followed by dithiothreitol treatment was demonstrated.[526]

The higher reactivity of persulfides to oxidants and the recovery of thiols following reduction of the resulting oxidation products, support the proposal that persulfides can serve a protective functions for protein thiols (Chart 27).[135,340,341,527]

7.2.4. Reaction or Persulfides with One-Electron Oxidants—Persulfides are excellent one-electron reductants and are in fact better than thiols or H_2S.[528] This is consistent with the lower energy of dissociation of the S–H bond (293 kJ mol^{-1}) in comparison to thiols and H_2S (385 kJ mol^{-1}).[529] It is also consistent with the one-electron reduction potential of persulfides ($E^{\circ\prime}(RSS^{\bullet}/RSS^-) = 0.68$ V), which is lower than those of the corresponding thiol, ($E^{\circ\prime}(RS^{\bullet}, H^+/RSH) = 0.96$ V) and of H_2S ($E^{\circ\prime}(S^{\bullet-}, H^+/HS^-) = 0.91$ V),[64] respectively. Thus, persulfides can be oxidized by weaker oxidants than thiols or H_2S, and $RSS^{\bullet}$ is less oxidizing than $RS^{\bullet}$ or $HS^{\bullet}$.

Depending on the nature of the one-electron oxidant ($A_1^{\bullet}$ or $A_2^{\bullet}$ in eqs 39 and 40, e.g., carbon centered radical or peroxyl $CCl_3OO^{\bullet}$ radicals, respectively) the persulfide can react

through a hydrogen atom or electron transfer mechanism, which affects the pH dependence of the process.[528]

$$RSSH + A_1^{\bullet} \rightarrow RSS^{\bullet} + A_1H \quad (39)$$

$$RSS^{-} + A_2^{\bullet} \rightarrow RSS^{\bullet} + A_2^{-} \quad (40)$$

Exposure of aralkyl persulfides to ferric salts under organic solvents led to the formation of tetrasulfide and ferrous ion, showing that persulfides can be oxidized by ferric ions (eqs 41 and 42).[530]

$$RSSH + Fe^{3+} \rightarrow RSS^{\bullet} + H^{+} + Fe^{2+} \quad (41)$$

$$2RSS^{\bullet} \rightarrow RSSSSR \quad (42)$$

Importantly, persulfides were unable to oxidize ferrous salts.[530] This contrasts with the behavior of hydrogen peroxide and alkyl hydroperoxides, which oxidize ferrous to ferric ion with concomitant formation of a hydroxyl radical via the Fenton reaction (eq 43).

$$H_2O_2 + Fe^{2+} \rightarrow HO^{-} + HO^{\bullet} + Fe^{3+} \quad (43)$$

Persulfides can reduce ferricyanide,[531] ferric cytochrome c,[501,505,532] and metmyoglobin.[531] In addition, persulfides have been proposed to react with carbon centered radicals,[489] peroxyl radicals,[528,533] and the nitroxide TEMPOL,[531] yielding the perthiyl radical. All of these reactions appear to be faster with persulfides than with thiols. For example, the rate constant for the reaction of 2-[(3-aminopropyl)amino]ethane persulfide and the carbon-centered α-hydroxyalkyl radical derived from isopropanol is 2.4×10^9 M^{-1} s^{-1}, which is 1 order of magnitude higher than the corresponding reaction of the thiol.[489]

Penicillamine-derived persulfide reduces ferric cytochrome c quantitatively in contrast to penicillamine and glutathione, which do not show significant reduction.[501] However, this reaction is thermodynamically uphill given the mismatch in redox potentials between the persulfide (+0.68 V) and cytochrome c ($E^{\circ\prime}$(cyt c^{3+}/cyt c^{2+}) = +0.26 V).[64] Persulfides react directly with oxygen, albeit slowly (k < 0.3–0.4 M^{-1} s^{-1}).[103] This reaction also faces thermodynamic and kinetic barriers due to a mismatch in the redox potentials and the triplet state of oxygen and reveals the intrinsically higher reactivity of persulfides with respect to thiols and H_2S. A likely explanation for why each of these unfavorable reactions occurs is that the perthiyl radical product is efficiently removed via recombination forming tetrasulfide (eq 44). Perthiyl radicals decay predominantly through second order processes

with rate constants of 1–6 × 10^9 M^{-1} s^{-1}.[528,533,534] The resulting RSSSSR can decompose to give RSSR and S_2 (eq 45).

$$2RSS^{\bullet} \rightarrow RSSSSR \quad (44)$$

$$RSSSSR \rightarrow RSSR + S_2 \quad (45)$$

Perthiyl radicals have been characterized by pulse radiolysis, flash photolysis, and EPR spectroscopy.[528] The unpaired electron in perthiyl radicals is delocalized between the two sulfur atoms. The resonance stabilization energy of perthiyl radicals relative to thiyl radicals is estimated in 8.8 kJ mol^{-1}.[489,528] This inherent stability of perthiyl radicals contributes to the efficiency of persulfides as reductants.

In addition to the radical recombination reaction to form tetrasulfides, perthiyl radicals can also act as oxidants, but the rate constants of these reactions are smaller than those of thiyl radicals.[528] For example, the rate constant for hydrogen atom abstraction by the perthiyl radical from a polyunsaturated fatty acid is 1.2 × 10^6 M^{-1} s^{-1}, 1 order of magnitude lower than the corresponding reaction of a thiyl radical, 1.4 × 10^7 M^{-1} s^{-1}. The rate constant for the reaction of a perthiyl radical with ascorbate is (1–6) × 10^6 M^{-1} s^{-1}, which is 1 order of magnitude smaller than that of the thiyl radical.[528]

Perthiyl radicals reportedly react with oxygen with a second order rate constant of 5 × 10^6 M^{-1} s^{-1} initially forming an $RSSOO^{\bullet}$ species and ultimately forming inorganic sulfate.[534] However, recent studies have not confirmed this experimentally, and computational studies suggest that the reaction of perthiyl radicals with oxygen is thermodynamically uphill.[531,533] In contrast, thiyl radical reacts reversibly with oxygen forming thioperoxyl radicals ($RSOO^{\bullet}$) with forward and reverse rate constants of ~10^9 M^{-1} s^{-1} and ~10^5 s^{-1}, respectively,[535,536] a reaction that contributes to oxidative damage via chain propagation.

A perthiyl radical can react with RSS^- to form $RSSSSR^{\bullet -}$, which is unstable,[537] has not been detected directly, and reacts with oxygen to form $O_2^{\bullet -}$ and the more stable RSSSSR (eqs 46 and 47). Analogously, $RSS^{\bullet}$ can react with RS^- to form $RSSSR^{\bullet -}$.[528]

$$RSS^- + RSS^{\bullet} \rightarrow RSSSSR^{\bullet -} \quad (46)$$

$$RSSSSR^{\bullet -} + O_2 \rightarrow RSSSSR + O_2^{\bullet -} \quad (47)$$

In contrast to thiyl radicals that react with $NO^{\bullet}$ very rapidly forming nitrosothiols,[538] perthiyl radicals do not appear to react with $NO^{\bullet}$. The apparent lack of reactivity has been attributed to the relatively high stability of the radicals and to the weakness of the N–S bond

in RSSNO. Accordingly, attempts to prepare RSSNO failed with immediate $NO^{\bullet}$ generation from the reaction mixture.[531,539]

In summary, persulfides are excellent one-electron reductants, which can be explained by their ease of oxidation, by the high relative stability of the perthiyl radical, and by the rapid radical recombination, which facilitates product removal.

7.2.5. Electrophilicity—Persulfides are relatively weak electrophiles. The reactions of persulfides in the protonated state with a general nucleophile Nu^-, are shown in eqs 48 and 49. When the inner sulfur is the site of nucleophilic attack, H_2S is released. When the outer sulfur is the site of attack sulfur transfer to the nucleophile occurs with elimination of the thiol.

$$RSSH + Nu^- \rightarrow RSNu + HS^- \quad (48)$$

$$RSSH + Nu^- \rightarrow RSH + NuS^- \quad (49)$$

Persulfides can react with cyanide,[540] thiolates,[501,509,540] sulfite,[540] phosphines,[496] and amines.[541] Thiols and H_2S are formed as reaction products, together with S_n and polysulfides. In organic solvents, cyanide, amines, hydroxide, and halides react as bases rather than as nucleophiles, abstracting a proton from RSSH and promoting its decay.[103,495,541,542]

Computational modeling of the lowest unoccupied molecular orbital (LUMO) of methylpersulfide (CH_3SSH) shows that attack at either sulfur atom is possible, while the electrostatic potential surface analysis shows a slight preference for attack on the outer sulfur.[103]

Steric hindrance is a critical factor that can bias nucleophilic attack toward the outer sulfur, while unhindered persulfides can be attacked on the inner sulfur releasing H_2S.[495,543] The importance of steric hindrance has been documented by comparing the base-promoted decay of trityl- and adamantylpersulfides versus benzylpersulfide. In the former cases, thiol and S_n were the reaction products, while polysulfides (RSSnSR) and H_2S were formed with the more accessible benzylpersulfide.[494,495]

Another factor that critically influences the site of attack is the acidity of the leaving group. H_2S has a pK_a of 6.98, while thiols have higher pK_a values (8.29 and 8.94 for cysteine and glutathione, respectively, 25 °C).[544] It is therefore expected that nucleophiles will attack cysteine persulfides at the inner sulfur releasing the sulfide anion (HS^-), which is the better leaving group. With protein persulfides, geometric considerations around the persulfide also determine the electrophilicity of the two sulfur atoms. For example, in MST, attack on the outer sulfur is favored by steric and inductive effects, which are governed by active site residues that also render the persulfide highly electrophilic.[280]

Persulfides can also react with substituted phosphines (R_3P) in a process that is reminiscent of hydroperoxides. The major products formed are phosphine sulfide ($R_3P{=}S$) and thiol.[496] Analysis of the reaction products provided evidence that, while the attack can occur at either sulfur atom, attack at the outer sulfur predominates, particularly when the persulfide is sterically hindered.[545] Phosphines have been used to detect persulfides in biological samples (see section 7.3.2).

The reaction of persulfides with cyanide to give thiols and thiocyanate (eq 50) deserves mention.

$$RSSH + CN^- \rightarrow RSH + SCN^- \quad (50)$$

This reaction can be used for the detection of persulfides (see section 7.3.2) since thiocyanate can react with ferric ions forming a red complex that absorbs at 460 nm and can be quantified spectrophotometrically (eq 51).[31]

$$SCN^- + Fe^{3+} \rightarrow FeSCN^{2+}(\text{colored}) \quad (51)$$

The reaction of persulfides with cyanide is favored at pH 7.4 relative to pH 10, suggesting that RSSH is the reactive species.[103] From a mechanistic standpoint, cyanide has been postulated to react with the RS(S)H tautomer of persulfide.[546] However, computational modeling of the reaction of methylpersulfide (CH_3SSH) with cyanide in a polar medium predicted a linear transition state with an ~50 kJ mol^{-1} activation free energy barrier, which is compatible with a nucleophilic displacement mechanism. While the activation free energy barrier for the nucleophilic attack on the inner sulfur was 3 kJ mol^{-1} lower than the attack on the outer sulfur, the free energy change for the reaction was higher by 96 kJ mol^{-1}, indicating that the reaction on the outer sulfur is thermodynamically favored.[103] MST and rhodanese catalyze transfer of the outer sulfur from their active site cysteine persulfides to cyanide and to other acceptors (thiols, sulfite). In addition, thiols, which are present at millimolar concentrations inside cells,[547] are likely to react with LMW persulfides.

Reaction with a thiol at the inner sulfur can give rise to disulfide and H_2S (eq 52).

$$RSSH + R'S^- \rightleftharpoons RSSR' + HS^- \quad (52)$$

Penicillamine-derived persulfide reacts with glutathione to generate H_2S,[501] while glutathione peroxidase-3 persulfide formed a mixed disulfide between the protein and the thiol in the reactions with glutathione and *N*-acetyl cysteine.[509] The general reaction described in eq 52 provides a mechanism for H_2S generation from persulfide (see section 8.9).

Reaction at the outer sulfur with a LMW or protein thiol results in trans-persulfidation (eq 53). This reaction is relevant for some proteins involved in iron–sulfur cluster formation and

H_2S biosynthesis and oxidation. The role of trans-persulfidation in protein persulfide formation and signaling, and in enzyme-catalyzed depersulfidation is discussed in section 8.

$$RSSH + R'S^- \rightleftharpoons RS^- + R'SSh \quad (53)$$

7.2.6. Spontaneous Decay of Persulfides—Persulfides are unstable in aqueous solution, which poses challenges for their characterization. For example, real-time MS analysis of penicillamine-derived persulfide showed that it decays with a half-life of 2.7 min at 23 °C;[135] somewhat higher values have been reported for the decay of CysSSH (35 min at 37 °C).[226] The decay represents a disproportionation reaction involving two molecules of persulfide (eqs 54–56),[542] which is consistent with the sulfur atoms possessing both electrophilic and nucleophilic character. The importance of RSSH ionization is evidenced by the dependence of the decay rate of persulfides in organic solvents on the strength of the added base.[494] Acidic conditions also appear to favor decay.[495,499]

$$RSSH + RSS^- \rightleftharpoons RSSS^- + RSH \quad (54)$$

$$RSSSH \rightarrow RSH + S_2 \quad (55)$$

$$RSSH + RSS^- \rightleftharpoons RSSSR + HS^- \quad (56)$$

The decay products vary depending on the site of the original attack. Persulfides with bulky substituents react preferentially at the outer sulfur yielding thiol and elemental sulfur (eqs 54 and 55), while those with small substitutents react at the inner sulfur yielding polysulfanes and H_2S (eq 56).[226,494,495,501] Attack at the inner sulfur is also favored by the release of HS^-, which is a better leaving group than RS^- as discussed previously. Cysteine persulfide predominantly decays via the reaction shown in eq 56,[226] and a similar behavior has been reported for the penicillamine-derived persulfide.[501]

In addition to disproportionation, persulfides can undergo thermal or light-induced homolysis of the S–S bond giving the corresponding $RS^\bullet$ and $HS^\bullet$ radicals.[548] This behavior is expected from the S–S bond energies of HS-SH (276 kJ mol^{-1}) and CH_3S-SCH_3 (309 kJ mol^{-1}).[529] Homolysis of persulfides is very slow and is unlikely to contribute to their decay at room temperature and under moderate light.[548]

7.3. Methods for Detecting Persulfidated Cysteines

Spectrophotometric analysis of protein persulfides is of limited utility as they absorb between 335 and 340 nm and have a weak extinction coefficient (~300 M^{-1} s^{-1}).[31,549] The IR spectra of thiols and persulfides are similar. However, a band in the 200–500 cm^{-1} region due to the S–S bond is characteristic of persulfides (Table 3).[491–494] With a few exceptions

(Figure 17A) these spectroscopic methods have limited applicability for detecting protein persulfides in complex mixtures.

The major challenge in developing labeling methods is to discriminate between the reactivity of persulfides and thiols, disulfides, sulfenic acids, and polysulfides. Consequently, not too many reliable methods are currently available. The available methods for intracellular persulfide detection can be grouped into two categories: (i) methods for protein persulfide labeling (which rely on the nucleophilic nature of the outer sulfur) and (ii) methods for sulfane sulfur detection (which rely on the electrophilic nature of the persulfide).

7.3.1. Methods for Protein Persulfide Labeling—Due to their greater nucleophilicity, persulfides react faster with commonly used thiol blocking electrophiles than the corresponding thiols[60] and yield distinct products. Thus, alkylation of thiols yields thioethers while disulfides are formed from persulfides.[509] Several methods exploit these characteristics of persulfides for their detection.

A spectroscopic method for the indirect detection of protein persulfides relies on the reaction of protein persulfides with 1-fluoro-2,4-dinitrobenzene to form mixed disulfides.[550] Subsequent treatment with 1,4-dithiothreitol (DTT) releases 2,4-dinitrobenzenethiol with a characteristic absorbance at 408 nm under alkaline (1 M NaOH) conditions. Using an extinction coefficient of 13 800 M^{-1} cm^{-1} for 2,4-dinitrobenzenethiol, the protein persulfide concentration can be estimated (Figure 17B).[550]

MS can be used to directly detect the presence of persulfides in proteins.[19] However, the mass increase due to the addition of one sulfur atom ($\Delta m/z$ = 31.97207) is very similar to that caused by the addition of two oxygen atoms ($\Delta m/z$ = 31.98984) and can only be distinguished in small peptides but not whole proteins.[19] The relative instability of persulfides further limits their direct detection by MS analysis. To circumvent these problems, persulfidated proteins can be blocked with agents such as *N*-ethylmaleimide or iodoacetamide (Figure 17C) and then analyzed by MS.[505,509] This treatment stabilizes the persulfide modification, and the detection of a $\Delta m/z$ of 32 with respect to the nonpersulfidated peptide, confirmed by daughter ions, provides strong evidence for the presence of persulfide.

In principle, treatment of cells with $H_2{}^{35}S$ followed by Western blot analysis and radioactivity measurement can provide a semiquantitive estimate of protein persulfidation levels. However, the inavailability of $H_2{}^{35}S$ and the instability of persulfides limit this approach.

The modified biotin switch method first used for proteomic analysis of persulfides[19] was based on the premise that, unlike thiols, persulfides would not react with the electrophilic thiol-blocking reagent, *S*-methylmethanethiosulfonate (MMTS). The strategy involved initial blocking of thiols with MMTS followed by persulfides labeling with *N*-[6-(biotinamido)hexyl]–3′-(2′-pyridyldithio)propionamide (biotin-HPDP; Figure 18A). One problem with this method is that MMTS treatment induced intra- and intermolecular protein

disulfides.[551] However, the more important flaw with the modified biotin swtich approach for persulfide proteome mapping is that MMTS and its analogue *S*-4-bromobenzyl methanethiosulfonate react readily with protein persulfides.[509] Unfortunately, despite these limitations the modified biotin switch method continues to be used and has been shown to illustrate decreased labeling in CSE[19,552–554] and CBS[555,556] knockout cell lines and tissues and increased labeling in response to H_2S treatment. In some cases, cysteines identified as persulfidated targets have been validated by mutagenesis.[552,554,557] A plausible explanation for how some persulfides might become labeled by the modified biotin-switch assay is that persulfides react with MMTS faster than free thiols[509] and the resulting RS–S–S–Me reacts with residual free thiols regenerating free thiols at sites that carried the persulfide modification originally. The newly formed thiol is subsequently labeled by biotin-HPDP or by fluorescently tagged maleimides (Figure 18B). Given the chemical issues in its design and the resulting misrepresentation of the persulfide proteome, the use of the modified biotin switch method is discouraged.

A second method for persulfide detection involves blocking free thiols and persulfides with Cy5-maleimide and subsequently reducing the R–S–S–maleimideCy5 adduct (Figure 19),[552] which results in the loss fluorescence. The loss of red fluoresecence is detected following separation of proteins by gel electrophoresis. While relatively simple, the limitation of this method is that it is based on the absence of a signal associated with persulfides rather than on a positive signal, which can be coupled to MS for proteomic analysis. Furthermore, since maleimides are known to react with amines, extensive labeling can give high backgrounds obscuring changes in signal intensity when persulfides are present at low concentrations.

A method that allows trapping of persulfidated proteins and subsequent MS analysis[60] is the basis of the biotin thiol assay (BTA).[558] Biotin maleimide[60] (or maleimide-PEG_2-biotin)[558] is initially used to react with thiols and persulfides (Figure 20). Proteins are then trypsinized, and thiol- and persulfide-tagged biotinylated peptides are immobilized on streptavidin beads. Persulfidated peptides are reduced and peptides are eluted from the beads and derivatized with iodoacetamide for subsequent MS analysis. The use of heavy (deuterated) and light iodoacetamide allows for quantitative analysis.[558] Using the BTA method >800 proteins have been identified as persulfidation targets.[558] Modifications of this method referred to as qPerS-SID[559] and ProPerDP[514] have been reported in which biotinylated iodoacetamide is used instead of biotin maleimide and (tris(2-carboxyethyl)phosphine) instead of DTT.

One difference between the ProPerDP and BTA method is that in the former intact proteins rather than peptides are eluted from the streptavidin beads (Figure 21). Immobilization of intact proteins on streptavidin beads is, however, not recommended since it leads to an underestimation of persulfide targets. For example, a protein containing three cysteine residues (e.g., GAPDH) of which only one is persulfidated will be eluted with a lower yield as binding can occur via any of the cysteine sites. This could explain the relatively low number of protein persulfidation targets identified by the ProPerDP method (Figure 21).[514]

Combining the persulfide labeling qPerS-SID approach with the SILAC (stable isotope labeling with amino acid in culture) method allows for quanititative persulfide proteomics analysis[559] (Figure 22). However, the selectivity of the qPerS-SID and similar methods

would be improved by optimizing the initial blocking conditions. As described for the BTA method,[558] limiting the concentration of the blocking reagent and the duration of labeling, decreases background labeling and identification of false positives (e.g., due to the reactivity of sulfenic acids with IA-biotin[560]). A potential limitation of persulfide tagging methods is that the reduction step also reduces disulfide bonds that were originally present within and across proteins. These disulfide-containing peptides/proteins will, however, only be released from streptavidin beads if they contain a biotin-tagged persulfide but not a biotin-tagged thiol (Figure 20B). In the former case, the identity of the cysteine that was the site of persulfidation will not be revealed by the MS/MS analysis. However, disulfides are not common in intracellular proteins, and the interference by disulfide-containing peptides/proteins in persulfide identification is expected to be low.

A related approach that was used to detect tyrosine phosphatase 1B (PTP1B) persulfidation[561] used iodoacetamide to initially block free thiols and persulfidated cysteines, followed by reduction and capture of the newly exposed cysteine thiol with biotinylated iodoacetamide. Although potentially useful to identify potential persulfidation sites on purified proteins, DTT treatment also reduces other oxidative cysteine modifications that might exist on the protein (e.g., nitrosothiol and sulfenic acid) confounding the result.

In another approach, thiols and persulfides are blocked with a maleimide derivative with a peptide arm (MalP).[562] The persulfidated protein is then detected directly in gel upon loss of the succinimide-peptide moiety (the product of maleimide reaction with a sulfhydryl) upon cleavage of the S–S bond by DTT. The size of the MalP derivative was optimized to cause a detectable shift in protein migration by denaturing polyacrylamide gel electrophoresis.[562] The best results were obtained with a 16-mer of MalP (MalP16:1.95 kDa; Figure 23). This method is useful for monitoring persulfidation changes in a known target but not for proteome wide analysis.

An alternative tag-switch strategy for identifying protein persulfides is based on the premise that the disulfide bonds resulting from alkylation of protein persulfides with an appropriate thiol blocking reagent show enhanced reactivity to nucleophiles than protein disulfides in which the electrophilicity of the two sulfur atoms is similar (Figure 24).[135,511,524] Therefore, it is possible to introduce a tag-switching reagent (containing both the nucleophile and a reporting molecule) to label only the persulfide products. It should be noted that thiol products are thioethers, which are not expected to react with the nucleophile. Typical thiol-blocking reagents such as maleimides and iodoacetamides are not suited for the tagswitch technology. However, a reagent that gives a mixed aromatic disulfide linkage when reacting with persulfides provides the differential reactivity criteria for the tag-switch technology. In the first step, MSBT or its more water-soluble analogue (benzothiazole-2-sulfonyl)-acetic acid (MSBT-A)[563] is used to block thiols and persulfides. In the next step, a biotinylated derivative of methyl cyanoacetate serves as a nucleophile to label the inner sulfur atom of the benzothiazole-blocked persulfide. The selectivity of this method was demonstrated by the reactivity of persulfidated but not glutathionylated, sulfenylated or unmodified bovine serum albumin, which contains intramolecular disulfides in addition to a reactive cysteine.[511,524] The sensitivity of this method has been increased with two new cyanoacetic acid derivatives containing the fluorescent BODIPY moiety (CN-BOT) or the Cy3-dye (CN-Cy3;

Figure 24B). These probes allow detection of persulfidated proteins by fluorescence confocal microscopy or in gels.[135] The reactivity of sulfenic acids with cyanoacetic acid-derivatives is a potential concern and this can be prevented by blocking sulfenic acids with dimedone prior to the reaction with MSBT,[511,524] although no difference in detected persulfide levels was observed between dimedone pretreated and untreated samples.[511,524] The concern that highly reactive protein disulfides would cross-react with cyanoacetic acid-derivatives is overcome by the denaturing conditions of the assay in which the different protein benzothiazole derivatives would be expected to show similar reactivity. The method has been successfully used for mining of the persulfidation proteome in *Arabidopsis thaliana*, identifying >2000 persulfidated protein targets (5% of the entire *Arabidopsis* proteome).[564]

7.3.2. Methods for Sulfane Sulfur Detection—The simplest way to detect the total sulfane sulfur pool is by reducing the sample with DTT (Figure 25),[100,101] which releases H_2S. The latter can then be detected by one of several methods as discussed in section 3. However, this method can detect sulfurs from iron sulfur clusters, in addition to inorganic polysulfides and thiosulfates.[565]

Cold cyanolysis is widely used to detect sulfane sulfur (Figure 25).[31,60,566,567] In this method, the cyanide anion attacks the sulfur–sulfur bond[103,546] in persulfides, polysulfides (RSS_nR), and aryl thiosulfonates (pH 8.5–10, 10 °C to room temperature). The resulting thiocyanate is converted to ferric thiocyanate and measured by its characteristic absorbance at 460 nm. When the reaction is performed at higher temperatures (referred to as “hot cyanolysis”), sulfane sufur from thrithionate ($^-O_3SS_nSO_3^-$) and thiosulfate ($^-SSO_3^-$) can be detected as well.[31] The reactivity of sulfane sufur toward cyanolysis decreases in the following order: persulfide > polysulfide > thiosulfonate > polythionate = thiosulfate > elemental sulfur.

Fluorescent probes have been developed to visualize and quantify sulfane sufur (Figure 25) in cells. The first such probes described were SSP1 and SSP2 (Chart 28A).[568] Sulfane sufur reacts with a nucleophilic thiol in the nonfluorescent SSP1/SSP2 probe to form a persulfide intermediate, which in turn reacts with an electrophilic ester group leading to spontaneous cyclization and release of the fluorophore (Chart 28B). Negligible basal fluorescence is seen in cells treated with SSP1 or SSP2 indicating that they are either inefficient at detecting protein and/or LMW persulfides or that the concentrations of these compounds are very low.

Electrophilic probes like DSPI-3, which initially reacts with inorganic polysulfides and releases the fluorophore upon internal cyclization, have been reported.[569–571] (Chart 29). While DSPI-3 reacts readily with thiols as well, the subsequent intramolecular cyclization leading to generation of a fluorescent signal does not occur (Chart 29A). However, if the thiol adduct were to react further with polysulfides, fluorophore release would occur.[569] The reaction of protein persulfides or LMW persulfides with DSP probes has not been tested. Optimization of this class of probes for greater selectivity for polysulfide has been reported together with the development of a FRET probe, which detects both H_2S and polysulfides (Chart 29C).[571]

A ratiometric near-IR fluorescence probe (Cy-Dise) for cysteine persulfide based on a selenium–sulfur exchange reaction has been reported (Chart 30A).[572] The method exploits the lower pK_a and greater nucleophilicity of cysteine persulfide compared to cysteine thiol. It is unclear however how this probe is selective for cysteine persulfide versus cysteine thiols with low pK_as, other persulfides, or inorganic polysulfides. The same limitation is also true with a persulfide probe that combines nucleophile-induced xanthene fluorescence quenching with coumarin as a FRET donor (Chart 30B).[573]

Isotope dilution MS is a reliable method for quantifying total sulfane sulfur pool[574] and is based on their known reactivity with triphenylphosphines (Figure 25). This method relies on the use of ^{13}C isotope-labeled triarylphosphine sulfide as an internal standard spiked into the biological sample treated with triarylphosphine. From the ratio of the MS signal intensities of the internal standard and triarylphosphine sulfide, an estimate of the total sulfane concentration is obtained (Chart 31).[574]

8. CELLULAR MECHANISMS OF PERSULFIDE FORMATION AND REMOVAL

An initial estimate based on the modified biotin tag switch assay was that up to 25% of all proteins are persulfidated.[19] The BTA method identified 834 persulfidated proteins in a pancreatic beta cell line,[558] representing ~5% of the proteome. The cyanoacetate-based tag-switch method confirmed that ~5% of the entire plant proteome is persulfidated.[564] Significantly lower steady-state protein persulfide levels were reported in HEK293 cells (0.15% of the proteome) and in murine liver (1.2% of the proteome) using the ProPerDP method.[514] Unexpectedly high concentrations of LMW persulfides (150 μM GSSH in brain and 1–4 μM cysteine persulfide in different mouse tissues) were reported in an MS study.[165] The isotope-dilution MS method yielded estimates of sulfane sulfur levels in murine plasma and erythrocytes of 4.7–13.1 and 2.3–3.7 nmol/g protein, respectively, and higher values in other organs: 57.0 (liver), 150.9 (kidney), 46.0 (brain), 61.8 (heart), 56.1 (spleen), and 20.8 (lung) nmol/g tissue.[574] Extrapolating from these values, this study suggests that the sulfane sulfur concentration in plasma and tissues is in the low micromolar range. In the next section, routes for persulfide formation and removal are described.

8.1. Reaction between H_2S and Disulfides

Early reports indicated that cystine and other LMW and protein disulfides react at alkaline pH with sodium sulfide. The product absorbed at 320–350 nm, was unstable, reacted with cyanide, and was assigned as persulfide (eq 57).[502,575,576]

$$HS^- + RSSR' \rightleftharpoons RSSH + R'S^- \quad (57)$$

Thermochemical calculations and computational modeling of the reaction with cystine suggest that the formation of the RSSH and RS^- products is uphill by +56.1 kJ mol^{-1}, but that fast equilibration to RSS^- and RSH due to the lower pK_a of the persulfide drives the reaction in the forward direction. The reaction is also driven by further reactions of the unstable persulfide product.[60,64]

The reactions of H_2S with typical LMW disulfides are slow.[60,179,503–505] For example, the rate constant for the reaction of H_2S with cystine at pH 7.4 and 25 °C is 0.6 M^{-1} s^{-1}.[60] The reaction of H_2S with GSSG is also slow and reversible and leads to GSSH and a mixture of products.[504,505] Nevertheless, the protein environment can accelerate the reaction. For example, in SQR, the reaction of H_2S with an active site disulfide is accelerated by ~10^6-fold with respect to free cystine.[306,310,311]

Reaction of H_2S with typical disulfides is slower than the analogous reaction of RSH (the thiol–disulfide exchange reactions), probably due to the lack of inductive/field or solvation effects attributed to the adjacent methylene group in thiolates.[60] The logarithm of the pH-independent rate constant for the reaction of HS^- with disulfides decreases linearly with a slope of −0.75 as the pK_a of the thiol that constitutes the disulfide increases, consistent with acidic thiols being better leaving groups. Computational modeling predicts a linear transition state as expected for a concerted S_N2 mechanism.[60] The influence of the thiol pK_a on kinetics supports the prediction that proteins that contain disulfides formed with acidic thiols are better targets for H_2S. In asymmetrical disulfides (RSSR′) as found in proteins the more acidic thiol can be expected to be the leaving group although steric constraints would also influence which sulfur was attacked.

In the cytosol, the concentration of LMW and protein disulfides is very low.[547,577,578] Hence, the direct reaction between H_2S and disulfides could be more relevant in compartments such as the endoplasmic reticulum and under oxidizing conditions.[511]

8.2. Reaction between H_2S and Sulfenic Acids

Sulfenic acids (RSOH) are usually formed by reaction of a thiol with a hydroperoxide or with hypochlorous acid.[579] The sulfur in sulfenic acid is a weak nucleophile and also a soft electrophile.[580–582] Sulfenic acids are typically unstable and decay mainly by reaction with thiols forming disulfides.[581,582] In addition sulfenic acids can react with H_2S (eq 58).

$$HS^- + RSOH \rightarrow RSSH + OH^- \quad (58)$$

The formation of persulfide in this reaction was confirmed using the sulfenic acid formed on Cys34 of human albumin.[60,511] This sulfenic acid is located in a cleft with no neighboring thiols. The second-order rate constant for this reaction is 270 M^{-1} s^{-1} at pH 7.4 and 25 °C.[60] The pH-independent rate constant with H_2S is ~4-fold higher than with the corresponding thiol[60] and suggests that steric constraints influence the effective access of the nucleophile.

Intracellular persulfide levels increase when cells are treated with H_2O_2, suggesting the relevance of sulfenic acid for priming the persulfide modification on proteins. Persulfide levels in H_2O_2-treated cells were decreased by inhibiting CBS and CSE.[60] Since H_2O_2 can also promote disulfide formation in cells, the effect of diamide, which only supports disufide formation, was compared to the effect of H_2O_2. However, diamide had the opposite effect, leading to lower persulfide levels, which is consistent with the kinetic data that the reaction between disulfides and H_2S is slow and therefore unlikely to be physiologically significant

except in special cases.[135] Under conditions of endoplasmic reticulum stress,[558] which leads to enhanced ROS production,[583] increased persulfidation was observed.

Sulfenic acid can be further oxidized to sulfinic acid (RSO_2H) and sulfonic acid (RSO_3H)[580] which are typically irreversible modifications.[584–587] As discussed previously in section 7.2.4, reaction of H_2S with protein sulfenic acids to form persulfides could protect against overoxidation and irreversible protein damage. Namely, oxidation of persulfidated residues would result in the formation of $RSSO_2H$ and $RSSO_3H$, which could be reduced back to thiols in the cell.

8.3. Reaction between H_2S and *S*-Nitrosothiols as a Source of Persulfides

S-Nitrosothiols represent another post-translational modification of cysteine residues important for the regulation of protein function,[432–437] as discussed in section 6.3. When reacting with thiols, *S*-nitrosothiols usually undergo trans-nitrosation, a reaction that is largely thermoneutral (eq 59).[437]

$$RSNO + R'S^- \rightleftharpoons RS^- + R'SNO \quad (59)$$

An alternative thiol-assisted decomposition of *S*-nitrosothiols has been proposed in which disulfide and HNO are formed as products.[588,589]

$$RSNO + RSH \rightarrow RSSR + HNO \quad (60)$$

Consistent with this mechanism, an increase in protein *S*-glutathionylation is seen in cells treated with GSNO.[590] However, since this reaction is thermodynamically unfavorable (~ +30 kJ/mol), it would be relevant only if it were coupled to product removal.[64,449]

The expected product for the reaction of H_2S with RSNO is HSNO.[449,453] Formation of HNO and a protein persulfide (eq 61) is thermodynamically unfavored (+26 kJ/mol),[64] although the protein microenvironment could facilitate this reaction.

$$RSNO + HS^- \rightarrow RSS^- + HNO \quad (61)$$

The dichotomous reactivity of RSNO with nucleophiles can be explained by the unusual electronic structure of the —SNO group.[591] The resonance representations of RSNO include the standard Lewis structure with a single S—N bond, a zwitterionic structure with an S═N double bond ($RS^+{=}N{-}O^-$) and an ionic structure I ($RS^{-}\cdots NO^+$) (Figure 26A). Direct interaction with charged and polar residues in the protein microenvironment could affect the electronic structure of the —SNO group by increasing the electrophilicity of the S atom and therefore its susceptibility to nucleophilic attack (eq 61) or by weakening the S—N bond and increasing the electrophilicity of the N atom thereby promoting transnitrosation (eq 59).[592] In addition, external electric fields created by the protein environment could influence

the electronic structure of RSNOs so as to favor thiolation (or persulfidation in case of the reaction with HS^-) over trans-nitrosation reaction (Figure 26B).[592,593]

S-Nitrosation and persulfidation might differentially regulate protein function.[594] In one study, the persulfide and *S*-nitrosothiol proteomes reportedly exhibited a 36% overlap.[558] Further work is needed to delineate the effects of these modifications on proteins function.

8.4. Role of Polysulfides in Protein Persulfidation

Inorganic polysulfides (HSS_nS^-) and polysulfanes (HSS_nSH) are sulfane sulfur compounds and prone to nucleophilic attack by thiolates. The high abundance of contaminating inorganic polysulfides in H_2S solutions (particularly when NaHS is the source) and their chemical reactivity have led to their contributing to the numerous effects originally ascribed to H_2S. For instance, at nanomolar concentrations, polysulfides activate TRPA1[595] while H_2S at micromolar concentrations fails to do so.[267,595] Similarly, polysulfide contaminants in an NaHS-derived solution led to disulfide bond formation in the lipid phosphatase and tensin homologue (PTEN),[596] by attack of a proximal cysteine on the initially polythiolated cysteine (Chart 32A). Inorganic polysulfides also contain negatively charged terminal sulfurs that could react with electrophiles. Polysulfides or H_2S solutions containing traces of Fe^{3+} or Cu^{2+}, which stimulate polysulfide formation, were shown to reduce disulfide bonds in human immunoglobulins.[97] Hence, an additional caution with the use of H_2S solutions containing polysulfide contaminants is that they can react with disulfide bonds forming RSH and $RSnS^-$ (Chart 32B).

While much emphasis has recently been placed on the potential role of inorganic polysulfides as signaling molecules that are responsible for the effects of H_2S,[597,598] it is unclear and unlikely that they serve this role under physiological conditions. Polysulfides are charged and full protonation is almost impossible under physiological conditions, making diffusion across membranes very slow. Considering the very low steady state levels of H_2S and its tightly regulated oxidation (see sections 3.5 and 5), it is difficult to envision that stochastic oxidation could result in significant amounts of inorganic polysulfides. Polysulfides are unstable and can be readily reduced so it is additionally unclear how they endure reducing intracellular environement. Finally, to serve in signaling, synthesis of polysulfide (which represents a family of catenated sulfur compounds of variable length) should be tightly regulated and their action on targets should be exerted with specificity. To date, none of these criteria are met by polysulfides. An enzymatic reaction in mammals that leads to regulated polysulfide synthesis is not known. Instead, polysulfide synthesis appears to be stochasticity controlled by the concentration of oxygen and metals on the one hand and protein thiols/disulfides on the other.

The reported production of polysulfides (H_2S_2 and H_2S_3) from 3-mercaptopyruvate by MST[599] was problematic for the following reasons. Polysulfide formation from 3-mercaptopyruvate was observed when the reaction was run in the absence of a sulfur acceptor. Under these conditions, the K_M for 3-mercaptopyruvate was reportedly 4.5 mM, although substrate inhibition led to complete loss of enzyme activity above 2 mM concentration.[271] Furthermore, the K_M value obtained in the H_2S_3 synthesis assay is at least 10-fold higher than the K_M for 3-mercaptopyruvate (20—350 μM) in the presence of

acceptors, which leads to H_2S synthesis. Therefore, conditions supporting polysulfide synthesis by MST are unlikely to exist in the cell since MST exhibits a low K_M (2.5 μM) for its physiological acceptor, thioredoxin.[271]

The chemical characteristics of inorganic polysulfides and polysulfanes make them unlikely to be signaling molecules as well.[600,601] The equilibrium between elemental sulfur and aqueous polysulfide at 25 °C was studied either by adding acid to polysulfide solutions until the sulfur precipitated, or by dissolving elemental sulfur in aqueous polysulfide solution until an equilibrium was established. The ratio between the S_n and HS^- species was strongly dependent on the alkalinity of the solution.

$$S_n + HS^- + OH^- \rightleftharpoons {S_{n+1}}^{2-} + H_2O \quad (62)$$

Since the polysulfide dianions of different chain-lengths are in an equilibrium (eq 63) that is rapidly established, it is not possible to reliably separate polysulfide species by ion chromatography.[603]

$$S_mS^{2-} + HS^- + OH^- \rightleftharpoons S_xS^{2-} + S_yS^{2-} + H_2O \quad (63)$$
$$m = x + y$$

The pK_as were studied using solutions of pure salts of S_2^{2-} to S_5^{2-} and a special streaming apparatus, which mixed polysulfides with HCl and allowed determination of the pH within 10^{-2} s.[604] The short mixing time averted decomposition of the protonated polysulfide into sulfur and monosulfide. Only the pentasulfide did not equilibrate as multiple species upon acidification, which allowed precise determination of its pK_a. The shorter polysulfides disproportionated within the mixing time of the experiment.[604] S_2^{2-} and S_3^{2-} could not be detected in an aqueous solution of potassium trisulfide which equilibrated to 18% HS^-, 62% S_4^{2-}, and 20% S_5^{2-}.[604] In fact, other groups have confirmed that HS_2^- and S_3^{2-} do not exist at detectable concentrations in neutral solutions.[49,605–609] Tetra-sulfide dianion is the predominant species until a pH of 10–11. However, even tetrasulfides disproportionate to give the pentasulfide (eq 64),[605,606,608,609] although this reaction is slow.

$$4{S_4}^{2-} + H_2O \rightarrow OH^- + SH^- + 3{S_5}^{2-} \quad (64)$$

Polysulfanes can be prepared by rapid acidification of crude sodium sulfane (Na_2S_n) to produce raw sulfane (H_2S_n). H_2S_3 (as a side product) and H_2S_2 can be collected by fractional distillation of raw sulfane at room temperature and at −80 °C, respectively.[69,70] Sulfanes are liquids that are miscible with carbon disulfide, benzene, tetrachloromethane, and dry diethyl ether. H_2S_2 and H_2S_3 are colorless/pale yellow, but the higher sulfanes are more yellow.[69,70] Using ^{1}H NMR, the existence of sulfanes with up to 35 sulfur atoms was demonstrated.[610] Exposure of pure sulfanes to air/humidity caused immediate decomposition. In the cases of H_2S_2 and H_2S_3 the decomposition is explosive.[69]

$$8H_2S_2(1) \rightarrow 8H_2S(g) + S_8(s) \quad (65)$$

The pK_a values of H_2S_2 are pK_1 5.0 and pK_2 9.7. The pK_a values of H_2S_3 are pK_1 4.2 and pK_2 7.5. In fact, ab initio MO calculations confirm that the acidity of sulfanes increases with the number of sulfur atoms in the molecule.[611]

Instability of aqueous polysulfide solutions (particularly S_2^{2-} to S_4^{2-}) is also due to their rapid autoxidation in air at temperatures between 23 and 40 °C forming thiosulfate and elemental sulfur (eq 66).[612] No other sulfur containing species are detected in these reactions.

$$S_{2+x}{}^{2-} + 3/2O_2 \rightarrow S_2O_3{}^{2-} + x/8S_8 \quad (66)$$

Polysulfides can also react with sulfite in neutral solution to give thiosulfate and HS^- (eq 67).[613]

$$S_4{}^{2-} + HSO_3{}^- \rightarrow 3S_2O_3{}^{2-} + HS^- + 2H^+ \quad (67)$$

Studies in which inorganic polysulfides are trapped as organic polysulfanes (e.g., with monobromobimane) in order to establish their intracellular formation need to be viewed with caution. Organic polysulfanes (RSSnSR) are also unstable; even pure substances tend to decompose by equilibration with other chain lengths and by formation of elemental sulfur. These reactions are accelerated by light and heat, and by the presence of nucleophiles.[614] Due to the intrinsic instability of inorganic and organic polysulfanes and polysulfides neither standards nor products used in this methodological approach are stable.

Based on all these chemical characteristics, it is very difficult to envision a biological setting that is conducive to the regulated production of polysullfides or their utilization in signaling in mammalian systems. However, polysulfides with the caveats of their instability noted above might have some pharmacological potential.

8.5. Persulfide Formation via Radical Reactions

Strong one-electron oxidants can react with H_2S and RSH forming $HS^\bullet$ and $RS^\bullet$, respectively. Rapid free radical recombination between $HS^\bullet$ and $RS^\bullet$ would lead to persulfide formation (eq 68), although this is highly likely to be an insignificant source of persulfides in cells due to the low concentration of the free radicals.

$$HS^\bullet + RS^\bullet \rightarrow RSSH \quad (68)$$

An alternative and more likely, radical pathway for RSSH formation is via the reaction of $HS^{\bullet}$ with RS^{-} or, conversely, $RS^{\bullet}$ with HS^{-}, to form the radical anion, $RSSH^{\bullet -}$. The latter can react with oxygen forming RSSH and $O_2^{\bullet -}$ (eqs 69–71).

$$HS^{\bullet} + RS^{-} \rightarrow RSSH^{\bullet -} \quad (69)$$

$$RS^{\bullet} + HS^{-} \rightarrow RSSH^{\bullet -} \quad (70)$$

$$RSSH^{\bullet -} + O_2 \rightarrow RSSH + O_2^{\bullet -} \quad (71)$$

The potential importance of free radical reactions in persulfide synthesis was demonstrated by increased protein persufidation in cell lysates treated with metal ions (Fe^{3+} or Cu^{2+}) and H_2S.[511] Similarly, persulfidation of BSA was strongly induced by treatment with H_2S and a water-soluble heme iron.[511] The reactivity of H_2S and RSH with metal ions under aerobic conditions should serve as a caution for handling cell lysates, which could contain higher free metal ion concentrations and in the presence of H_2S could lead to an artifactual increases in persulfidation.

H_2S can react with the oxidized form of several metalloproteins like cytochrome c[97,505] (see section 5.1) leading to their reduction and formation of $HS^{\bullet}$. It is possible that, under conditions of increased H_2S production or decreased oxidation (e.g., during hypoxia),[615] ferric cytochrome c is reduced while H_2S is oxidized to $HS^{\bullet}$ leading to increased protein persulfidation in mitochondria. The role of metalloprotein-assisted $HS^{\bullet}$ generation in protein persulfidation remains to be investigated.

The chemistry of polysulfides is closely related to that of the radical monoanions $S_x^{\bullet -}$ (eqs 72 and 73) in that they are in equilibrium with each other.

$$S_4^{2-} \rightleftharpoons 2S_2^{\bullet -} \quad (72)$$

$$S_6^{2-} \rightleftharpoons 2S_3^{\bullet -} \quad (73)$$

In solution these radicals are formed by homolytic dissociation of the polysulfide anions, a process that is enhanced in solvents of lower polarity than water and/or by higher temperatures.[600,616] In aqueous solutions at room temperature, the reactions given in eqs 72 and 73 are shifted to the left. However, if the solutions are very dilute, then radical anions could be more abundant. The radical anions would be reactive toward thiols leading to protein polythiolation and $O_2^{\bullet -}$ formation (eqs 74 and 75).

$$S_x^{\bullet -} + RSH \rightarrow RSS_xH^{\bullet -} \quad (74)$$

$$RSS_xH^{\bullet -} + O_2 \rightarrow O_2^{\bullet -} + RSS_x^{-} + H^+ \quad (75)$$

8.6. Reaction between Thiols and Activated Organic Disulfides and Polysulfides

Organosulfur compounds in garlic can react with thiols and serve as a source of persulfides and H_2S. Allicin (diallyl thiosulfinate) is synthesized from alliin after release of alliinase when garlic is crushed. Allicin is rapidly metabolized in aqueous solution to diallyl sulfide, diallyl disulfide, diallyl trisulfide, and ajoene (Chart 33A).[105,110,111,617]

GSH reacts with the active principles in garlic leading to H_2S release.[618] These reactions are facilitated by allyl substituents and by increasing numbers of sulfur atoms. A similar structure–activity correlation has been reported for the cancer-preventative effects of garlic-derived organic polysulfides.[619] In addition to H_2S, LMW persulfides are also formed in the reaction of GSH with organic disulfides and polysulfides resulting from nucleophilic substitution at the α-carbon, yielding S-allyl-glutathione and allyl persulfide (Chart 33B).[618] The latter reacts with GSH releasing H_2S and allyl-glutathione disulfide, which in turn is an additional target for nucleophilic substitution leading to GSSH formation. Diallyltrisulfide and higher order diallylpolysulfides react in a similar manner and have the additional possibility of undergoing a direct nucleophilic attack by GSH at the sulfane sulfur.[618] In addition to GSH, other thiolates in cells can engage in similar chemical reactions with garlic-derived allyl sulfides.

8.7. Elimination Reactions of Disulfides

Disulfides degrade under alkaline conditions giving rise to a variety of products. Base-promoted elimination of disulfides leads to the formation of the corresponding persulfide and dehydroalanine derivative (Chart 34).[576,620,621]

Elimination reactions of disufide substrates (cysteine and homocystine) are catalyzed by CBS and CSE forming the corresponding persulfides[165,226,622–624] At physiologically relevant substrate concentrations, the contributions of CBS and CSE to Cys-SSH generation is low and homocysteine persulfide synthesis by CSE is negligible (see sections 4.1.3 and 4.3.1).[226] However, under pathological conditions that lead to cystine accumulation, Cys-SSH synthesis by CSE might become a contributing factor to persulfide synthesis.

8.8. Sulfur Transfer Reactions

Sulfurtransferases react with their substrates forming a persulfide intermediate from which the sulfane sulfur is transferred to an acceptor. In addition to MST, rhodanese and SQR that are directly involved in H_2S synthesis or clearance (sections 4 and 5), the cysteine desulfurases catalyze sulfur transfer reactions needed in biosynthetic pathways e.g. synthesis of iron sulfur clusters[625–636] and thionucleosides.[629,633,634,636] While some

sulfurtransferases (e.g cysteine desulfurase) utilize the PLP cofactor, others do not (e.g., MST). These enzyme promote the formation of a Cys-SSH in the active site and can, in principle, transfer the sulfane sulfur to a thiol on a target protein or to a LMW thiol. The role of these enzymes in catalyzing protein persulfidation remains to be determined.

8.9. Reaction between Thiols and Persulfides (Transpersulfidation)

As discussed in section 7.2, nucleophilic attack by thiolates on persulfides occurs predominantly on the inner sulfur with formation of disulfide and release of H_2S (eq 52). This chemistry has been documented with LMW persulfides and with protein persulfide models.[494,501,509] However, proteins such as the sulfurtransferases modulate the reactivity of persulfides such that the outer sulfur is transferred and H_2S is not released (see section 5.2). Very high levels of LMW persulfides in cells, tissue and circulation (50–100 μM) have been reported[165] leading to the suggestion that Cys-SSH and/or GSSH are major biologically relevant transpersulfidating reagents.[527] However, high concentrations of reactive persulfides and especially in an oxidizing compartment like blood are unlikely. Cys-SSH and GSSH have been proposed to be major biologically relevant transpersulfidating reagents that can even be transported across the membrane.[165,637] However, the low tissue levels of sulfane sulfur compounds[32,574] and the fact that their reaction with thiolates, which are abundant in cells, favor H_2S release, argue against this possibility.

The transfer of the terminal sulfur from a persulfide to a thiolate, constitutes a transpersulfidation reaction, and has been documented in several proteins. Sulfur-containing cofactors and modified thionucleosides, as well as iron–sulfur clusters obtain their sulfur atom via transpersulfidation reactions.[636,638] It is likely that steric factors, the acidity of the parent thiol and the protein microenvironment determine the predominance of thiolate attack on the outer versus the inner sulfur of the persulfide.

The reaction mechanism of transpersulfidation by the LMW persulfides (eq 53) has been proposed to involve the tautomeric thiosulfoxide species (Chart 35) as the sulfur donor.[33,34,546] The S═S bond in thiosulfoxides can be considered to be either a double[639] or "semipolar"[640] bond depending on the electronegativity of substituents. Nevertheless, computational studies reveal that, although the thiosulfoxide is only 5 kJ/mol less stable than the corresponding persulfide, the energy barrier for tautomerization is very high, i.e., >100 kJ/mol.[641] Hence, LMW thiosulfoxides appear to be unlikely donors in uncatalyzed cellular transpersulfidation reactions.

Transpersulfidation can, however, occur in the active site of certain enzymes. A computational analysis of the sulfurtransfer reaction[280] based on cystal structure of human MST[271] suggests that the persulfide anion is the sulfur donor to the thiolate acceptor, in a reaction that is facilitated by the increase in electrophilicity of the outer sulfur through multiple hydrogen bonding interactions. Therefore, the active site geometry and electronics favor transfer of the terminal sulfur, i.e. transpersulfidation to either LMW or a protein thiol (Figure 7).

MST transfers the sulfane sulfur to sulfite forming thiosulfate, albeit very inefficiently.[642] Treatement of red blood cells with the MST substrate, 3-mercaptopyruvate, reportedly

inhibited many glycolytic enzymes including hexokinase, phosphofructokinase, pyruvate kinase, glucose-6-phosphate dehydrogenase and 6 phosphogluconate dehydrogenase.[643] Transpersulfidation of the sulfane sulfur from MST to those enzymes was suggested but not established as the mechanism of inhibition.[643] An increase of persulfidation was reported in cells treated with D-cysteine,[135] a source of 3-mercaptopyruvate via D-amino acid oxidase.[277] The cryo-EM structure of complex I isolated from *Yarrowia lipolytica* indicates the presence of an additional subunit, which was identified to be an accessory sulfurtransferase subunit. This rhodanese/MST-like subunit was capable of using 3-mercaptopyruvate as a substrate and, in the presence of thiols, released H_2S. The role of this sulfurtransferase subunit on the structure and function of complex I remains to be elucidated.[644]

There are limited examples of rhodanese-catalyzed sulfur transfer to protein acceptors. Although a role for rhodanese in iron sulfur biogenesis had been previously proposed,[645–649] it has since been shown to not be involved in this process. Rhodanese catalyzed sulfur transfer from thiosulfate to malate dehydrogenase as monitored by ^{35}S radiolabel transfer and led to an almost 2-fold increase in activity. Hence, persulfidation could regulate energy metabolism via the citric acid cycle.[650] In the presence of thiosulfate, bovine rhodanese restored the activity of partially inactivated NADH dehydrogenase, a subunit of complex I.[651]

Rhodanese has been identified as a candidate obesity-resistance gene with increased expression in adipocytes being correlated with leaness.[327] Overexpression of rhodanese in adipocytes protected mice from diet-induced obesity and insulin-resistant diabetes and rhodanese-deficient mice showed aggravated development of diabetes.[327] An earlier study had correlated low rhodanese expression with increased whole cell ROS and mitochondrial $O_2^{\bullet-}$ levels and higher mortality in hemodialysis patients.[652] The link between these observations and changes in intracellular persulfide levels and whether rhodanese in fact catalyzes protein persulfidation, remains to be elucidated.

The rhodanese homology domain has been identified in ~500 proteins in the three major evolutionary phyla. In the human genome, there are 47 examples of rhodanese-domain containing proteins.[328] Cdc25 phosphatase, an activator of cell division kinases during the cell cycle, is an example of rhodanese domain-containing protein. The crystal structure of the catalytic domain of human Cdc25A reveals a small α/β domain with a rhodanese domain fold.[653] It is not known, however, whether the signaling role of Cdc25 involves transpersulfidation. Other proteins that have a rhodanese domain and form an active site Cys-SSH are adenylyltransferase and the MOCS3 sulfurtransferase.[654,655] The roles of these proteins in catalyzing transpersulfidation chemistry are, however, likely to be restricted to the specific pathways in which they are involved e.g. molybdopterin biosynthesis.

8.10. Depersulfidation

Signaling via protein persulfidation requires the existence of cellular mechanisms for removal of the persulfide modification and inactivation of the signal. Thioredoxin (Trx) is a 12 kDa disulfide oxidoreductase, which serves as a redox partner for a wide variety of client proteins.[656–659] In humans, Trx1 is present in the cytosol and the nucleus while Trx2 is present in mitochondria. Trx contain two cysteines (Figure 27A) in an active site CXXC

motif.[656] The pK_a values of the nucleophilic cysteine is between 6 and 7 and for the resolving cysteine is between 8 and 9.[660–662] Reduction of a client protein disulfide starts with the attack of the nucleophilic cysteine to form an intermolecular mixed disulfide, followed by subsequent attack of the resolving cysteine on the mixed disulfide to form the fully oxidized Trx. The two-electron reduction potential of the disulfide/dithiol couple in thioredoxin is −284 mV at pH 7.0 and 25 °C.[656,663] The recognition between Trx and its client proteins is postulated to be entropically driven.[664] Oxidized Trx is reduced by the FAD-containing selenoprotein, thioredoxin reductase (TrxR1). Three isoforms of this protein exist in mammals: cytosolic TrxR1, mitochondrial TrxR2 and TrxR3 present only in testis. TrxR uses NADPH as a source of electrons (Figure 27B). Excellent reviews on the Trx/TrxR system have been published.[656–659]

As discussed in Section 4.5, the Trx/TrxR is involved in the sulfur transfer reaction catalyzed by MST,[270,271,273] and formation of thioredoxin persulfide was demonstrated with the *Trichomonas vaginalis* MST.[274] Trx is ~200-fold more efficient at reducing the Cys-SSH in PTP1B than DTT.[561] Addition of Trx to cell lysate resulted in H_2S generation, while the treatment of cells with auranofin, a TrxR inhibitor, increased total intracellular persulfidation levels.[135] Trx reduced penicillamine-derived HSA persulfide and Cys-SSH.[135] The first order rate constant for the reaction of Trx with Cys-SSH was estimated to be 4.5×10^3 M^{-1} s^{-1} at 23 °C and pH 7.4, which is almost 10-fold higher than with Cys-SS-Cys. A similar rate constant was observed with HSA-SSH (4.1×10^3 M^{-1} s^{-1}).[135] The Trx/TrxR/NADPH system exhibited Michaelis–Menten-like kinetic behavior. These results are consistent with an important role for the Trx/TrxR system in protein depersulfidation.[135,514] The involvement of a related protein, TRP14 (thioredoxin-related protein of 14 kDa),[665] was demonstrated by its silencing, which resulted in increased persulfide levels.[514] TRP14 might be important as a depersulfidase particularly under conditions of oxidative stress when Trx is tied up with the peroxiredoxin system.[514]

Depersulfidation by Trx can occur via one of two mechanisms: (i) transfer of the outer sulfur from the persulfide to the nucleophilic cysteine of Trx leading to the transient formation of Trx-SSH which is subsequently resolved forming H_2S and oxidized Trx and (ii) a nucleophilic attack on the inner sulfur of the persulfide with elimination of H_2S and formation of a mixed Trx-client disulfide complex, which is resolved (Figure 27C).[135] While the formation of mixed disulfides is part of the disulfide reductase activity of Trx, the mechanism of the depersulfidase activity remains to be established.

Increased Trx levels are associated with diseases such as rheumatoid arthritis, hepatitis C and HIV-1 infections.[666–668] HIV-1 patients with high viral load have increased levels of circulating Trx.[666,667] An inverse correlation was seen between total plasma sulfane sulfur levels and viral load in HIV-1 patients. Indirectly, this result is consistent with a role for the Trx system in depersulfidation in vivo.[135]

The glutaredoxin system (GSH/glutathione reductase (GR)/glutaredoxin (Grx)) could also be involved in catalyzing depersulfidation in vivo (Chart 36).[514] GR activity has been reported in cytoplasm and in organelles (ER, lysosome, mitochondria and nucleus). GR

regulates cellular redox status by maintaining low levels of GSSG and is important in protecting cells from oxidative stress.[669–671]

The Grx system efficiently reduced polysulfides and BSA-SSH in vitro. In murine hepatocytes with the double knockout (TrxR1/GR null), increased persulfidation was observed.[514] GR null cells, however, showed no difference in persulfidation levels compared to controls.[514] Since the in vitro assay requires addition of GSH, the observed polysulfide and protein persulfide reduction could have resulted from their direct reduction by GSH.

Beside Grx, the Trx fold is also found in several other classes of enzymes, such as Dsb (disulfide bond formation protein) proteins, glutathione *S*-transferase, and protein disulfide isomerase (PDI) families.[656] Further systematic studies should unravel the potential role, if any, of these enzymes in protein depersulfidation.

9. PERSULFIDATION IN ACTION

As a growing list of persulfidated proteins is being identified, the stage is being set for making the connection between these targets and the molecular mechanisms of H_2S action. In this section, we provide an overview of protein targets and downstream signaling pathways that are affected by H_2S-induced persulfidation with the caution that, in many systems, the persulfidation target has not been rigorously established and correlated with functional effects.

9.1. Persulfidation of K_{ATP} Channels

Although CSE knockout mice exhibit hypertension,[12] which is consistent with a role for H_2S as an endogenous regulator of blood pressure,[7,672] subsequent studies have revealed that this effect is mediated via cross-talk with $NO^{\bullet}$,[266,267,451,673] an established vasodilator. Glibenclamide, a selective potassium ATP channel (K_{ATP}) blocker, partially inhibits the vasodilatory effects of H_2S.[672] Persulfidation of Cys43 on the Kir6.1 subunit of the K_{ATP} channel in smooth muscle cells prevents its association with ATP and promotes binding to phosphathidylinositol-4,5-bisphosphate,[553] which leads to channel opening, to K^+ influx, and, subsequently, to smooth muscle cell relaxation.

9.2. Persulfidation of Keap-1, p66Shc, and RAGE

A major mechanism for upregulating antioxidant enzymes involves activation of the antioxidant response element (ARE) by the oxidative-stress sensor protein Kelch-like ECH-associated protein 1 (Keap1) and the transcription factor nuclear factor (erythroid-derived 2)-like 2 (Nrf-2).[674–676] Normally, Keap1 binds to the Neh2 domain of Nrf-2 and sequesters it in the cytoplasm, where it is targeted for proteosomal degradation. Electrophilic agents such as sulforaphane can modify Keap1, promoting Nrf-2 nuclear accumulation and ARE activation.[674,676] A widely accepted model for the nuclear accumulation of Nrf-2 invokes modification of critical cysteines on Keap-1 resulting in a conformational change, which induces dissociation of the Keap1–Nrf-2 complex leading to nuclear translocation of Nrf-2 (Figure 28).[674–676]

The cardioprotective effects of H_2S, particularly in ischemia-reperfusion injury, depend on the nuclear translocation of Nrf-2 and activation of antioxidant defense enzymes.[677,678] One group has reported that Keap-1 is persulfidated at Cys151 (identified using the modified biotin-switch assay) when cells are exposed to H_2S,[554] (Figure 28). In contrast, a second study has reported the formation of a disulfide bond between Cys226 and Cys613 in Keap1 in H_2S-treated cells.[679] Surprisingly, the same study reported that Cys226 and Cys613 were also persulfidated, which is not expected if persulfidation involves attack of the initially formed disulfide by H_2S.[679] Alternatively, persulfidation could occur by reaction of H_2S with the sulfenic acid derivative of each cysteine. Activation of the Keap1-Nrf-2 signaling cascade resulted in the upregulation of enzymes involved in H_2S metabolism, CBS, CSE, and SQR.[679]

An alternative mechanism proposed for regulating intracellular ROS production involves persulfidation of the p66Shc protein.[680] The p66Shc protein is a member of the ShcA family with which it shares three functionally identical domains: the C-terminal Src homology 2 domain (SH2), the central collagen homology domain (CH1), and the N-terminal phosphotyrosine-binding domain (PTB).[681] When cells are exposed to oxidative stress caused by exposure to UV light or to H_2O_2, p66Shc is activated by phosphorylation at Ser36. Activated p66Shc is then dephosphorylated and translocated to the mitochondrion, where it binds to cytochrome c and assists in the electron transport process.[681] p66Shc$^{-/-}$ mice show a 30% increase in lifespan.[681] Persulfidation of p66Shc at Cys59 inhibits its interaction with PKC$_{\beta II}$ and attenuates H_2O_2-induced p66Shc phosphorylation, a critical step in p66Shc-mediated mitochondrial ROS generation.[680] H_2S is known to protect against oxidative stress, which cannot readily be explained by a direct antioxidant role (see section 2). Inhibition of mitochondrial ROS production via persulfidation of p66Shc[680] and upregulation of antioxidant defense enzymes via Keap1-Nrf-2 signaling[554,679] provide a mechanistic basis for the protective effects of H_2S.

Persulfidation of RAGE (receptor for AGE: advanced glycation end products) at Cys259 and Cys301 by H_2S treatment or CBS overexpression attenuates cell death and senescence caused by both AGE and β-amyloid[682] AGE are glycated proteins and lipids observed in diabetic patients.[683] Dimeric RAGE is processed in the ER and delivered to the cell membrane. Persulfidated RAGE monomers are less stable, which disrupts their translocation from the ER to the plasma membrane and leads to increased protection against cell death and senescence.[682]

9.3. Persulfidation and ER Stress

ER stress induces a major transcriptional, translational, and metabolic reprogramming in cells and is associated with the development of many diseases, ranging from metabolic dysfunction to neurodegeneration.[684] ATF4, a master transcriptional regulator, is induced during the ER stress response and upregulates CSE[263] and the cysteine transporter, Slc7a11.[558] Persuflidation of a number of protein targets is increased during ER stress and is correlated with reprogramming of energy metabolism toward increased glycolytic flux in pancreatic beta cells (Figure 29).[558]

The ER-stress response also leads to persulfidation of the protein tyrosine phosphatase (PTP) family of enzymes.[561] PTPs are cysteine hydrolases and are sensitive to oxidation.[685] PTP-1B is a members of this class of enzymes that is located on the cytoplasmic face of the ER and plays an important role in ER stress signaling.[686] Persulfidation of Cys215 in PTP-1B leads to the loss of enzymatic activity and, consequently, to increased phosphorylation and activation of PERK,[561] which results in global inhibition of protein translation (Figure 29). ER stress conditions induce ROS production, which could promote protein sulfenylation and potentiate subsequent persulfidation.

9.4. H_2S Effects on GAPDH

GAPDH is an important glycolytic enzyme and exhibits high reactivity toward H_2O_2, which oxidizes the nucleophilic Cys152 residue in the active site, inactivating the enzyme. The redox sensitivity of GAPDH is important for metablic adaptation to increased intracellular H_2O_2[687] levels. *S*-Nitrosation of the catalytic Cys152 abolishes GAPDH activity and promotes its binding to the E3-ubiquitin-ligase, Siah1.[688] The latter possesses a nuclear localization tag and leads to nuclear accumulation of GAPDH. Stabilization of Siah1 by GAPDH promotes degradation of nuclear proteins and leads to apoptosis.[688] Persulfidation of GAPDH reportedly also promotes Siah1 binding although the modification site was not rigorously determined.[556]

Besides the active site Cys152 residue, human GAPDH has two other cysteines, Cys156 and Cys247. Due to its high abundance, GAPDH is a commonly identified target in proteomic searches including persulfide proteomic data sets.[19,558] While some studies have reported activation of GAPDH in response to persulfidation,[19,558] the connection between persulfidation of Cys152 and GAPDH activity has not been rigorously established. Cys152 functions as a nucleophile in the reaction cycle, and given the inhibitory effect of S-nitrosation of Cys152 on activity, it would appear a priori that persulfidation of GAPDH would also be inhibitory. Consistent with this prediction, persulfidation of purified GAPDH at Cys152 was shown to inhibit activity.[689] A caveat of this study is that persulfidation induced by NaHS or polysulfides was observed at Cys156 and Cys247 in wild-type enzyme but not at Cys152 although modification at these other two sites did not affect enzyme activity. Cys152 was persulfidated only when Cys156 was mutated to serine, and while the mutation did not affect the activity of unmodified enzyme, activity was inhibited upon persulfidation at Cys152.[689]

9.5. Persulfidation of NFkB

Nuclear factor κB (NF-κB) is an antiapoptotic transcription factor. Under basal conditions, it is sequestered in the cytosol via interaction with the inhibitor, IκBα.[690] During inflammation, cells produce tumor necrosis factor α (TNF-α), which can potentially lead to cell death.[691] H_2S is known to protect against inflammation, but the underlying mechanism is not known.[692] The discovery that NF-κB is persulfdiated at Cys38 in the p65 subunit suggests a potential mechanism of H_2S action.[552] Persulfidation was suggested to promote binding of NF-κB to the coactivator ribosomal protein S3, increasing its binding to promoters of antiapoptotic genes, including CSE (Figure 30). An opposing mechanism was however suggested by the report that H_2S suppresses oxidized low-density lipoprotein-

induced macrophage inflammation by inhibiting NF-κB.[693] Persulfidation of Cys38 was suggested to lead to cytoplasmic retention of NF-κB, inhibiting its DNA binding activity.

9.6. MEK1/PARP-1 Activation and DNA Damage Repair

DNA damage stimulates a complex and highly concerted DNA damage repair response, which includes binding of poly(ADP- ribose)ation polymerases (PARPs) to DNA strand breaks and catalysis of poly(ADP-ribose)ation. Poly(ADP-ribose)ation attracts other DNA damage repair proteins.[694] The MEK/ERK signaling cascade plays an important role in activating PARPs.[695] Persulfidation of Cys341 in MEK1 reportedly facilitates the translocation of phosphorylated ERK1/2 into the nucleus, where it activates PARP-1 and increases the DNA damage repair yield.[557]

9.7. Persulfidation of Parkin

Mutations in parkin, an E3 ubiquitin ligase, are associated with the etiology of Parkinson's disease, which is caused by the death of dopamine-generating cells in the substantia nigra.[696,697] Parkin contains reactive cysteine residues that are susceptible to oxidative modifications. For example, *S*-nitrosation of parkin inhibits its activity.[698] Parkin can be persulfidated at Cys59, Cys95, and Cys182.[594] The activity of parkin is reportedly increased upon persulfidation and is correlated with the rescue of neurons from cell death by removal of damaged proteins (Figure 31). A decrease in parkin persulfidation has been reported in brain from Parkinson's disease patients, while *S*-nitrosation is increased in the same samples.[594] If substantiated, the activity of parkin would appear to be differentially regulated by modifications at the same cysteine residues and H_2S donors could have therapeutic potential in the early treatment of Parkinson's disease.

Parkin is also a regulator of mitophagy, which leads to the removal of damaged mitochondria, particularly during ischemia-reperfusion injury.[699] The pharmacological potential of H_2S in preventing ischemia-reperfusion injury,[677,678] might be mediated in part by the persulfidation of parkin.

9.8. Persulfidation of the TRP Channels

CBS-deficient patients exhibit a variety of phenotypes, including osteoporosis,[700] which is characterized by a low bone density and increased risk of fracture. Bone marrow mesenchymal stem cells are nonhematopoietic multipotent stem cells responsible for bone formation and balancing osteoclast-mediated bone resorption to maintain bone mineral density. H_2S donors reportedly protect MC3T3-E1 osteoblasts against H_2O_2-induced oxidative damage, although the mechanism of this effect is not known.[701] CBS deficiency reportedly resulted in aberrant intracellular Ca^{2+} influx due to reduced persulfidation of multiple TRP channels.[555] Decreased Ca^{2+} influx downregulates PKC/Erk-mediated Wnt/β-catenin signaling, which is important for controlling osteogenic differentiation of bone marrow mesenchymal stem cells that are postulated to produce H_2S to regulate their self-renewal and osteogenic differentiation.[555]

9.9. Persulfidation Targets Revealed by Proteomic Approaches

Early studies on xanthine oxidase and aldehyde oxidase, which are molybdopterin containing enzymes, reported that they are regulated by persulfidation. However, the location of the persulfide was not established, and based on later structural and spectroscopic studies, the labile sulfur was found to be a sulfide ligand to molybdenum rather than persulfide.[702] Early studies on Cu,ZnSOD reported the presence of an absorbance peak at 325 nm[703] that was assigned to persulfidation at Cys111.[704] Persulfidation blocked copper-induced protein aggregation but did not affect SOD activity.[705] In addition to being modified by persulfidation at Cys111, two SOD monomers can be covalently linked via a polysulfane bridge (up to 5 sulfur atoms) between their Cys111 residues.[706]

Persulfide proteome analysis in response to increased endogenous H_2S levels due to ER stress[558] or exogenous treatment with GYY4137 and polysulfides[559] has identified many persulfidated proteins. Under ER stress conditions, a total of 827 proteins were identified[558] of which 178 overlapped with the much smaller 208 persulfidated protein data set reported in the GYY4137 treatment study.[559] Enrichment of persulfidated proteins involved in translation, glycolysis, and the TCA cycle was reported in both studies in addition to the heat shock proteins Hsp70 and Hsp90 proteins and proteins involved in actin remodeling (actin, actinin, cofilin, and actin-related proteins),[558,559] Actin and Hsp70 and Hsp90 were also identified previously in studies that yielded very limited persulfide target identification.[19,165,511] Significant overlap was observed between persulfidation, sulfenylation, *S*-nitrosation and glutathionylation targets.[558,559] Although no consensus sequence motif could be identified around persulfidated cysteines, there was some enrichment of the location of target cysteines at the N-termini of alpha helices.[558]

10. PHYSIOLOGICAL AND PHARMACOLOGICAL EFFECTS OF H_2S

The past two decades have witnessed an increasing interest in understanding the physiological and pharmacological effects of H_2S and its donors. However, with the recent development of analytical tools for H_2S detection (see section 3.4), it has become clear that the actual endogenous values of H_2S are quite low (see section 3.5), while the vast majority of physiological experiments were performed with supra-physiological amounts of H_2S. Therefore, in this section, we provide an overview of processes relevant to human biology that are regulated by endogenous H_2S or are responsive to the pharmacological treatment of H_2S or its donors. Microbial[707–713] and plant[714–722] sulfur metabolism and the physiological roles of H_2S in these systems are not covered.

10.1. H_2S and the Nervous System

H_2S affects hippocampal long-term potentiation by acting on *N*-methyl-D-aspartate (NMDA)-type glutamate receptors albeit only when applied together with weak tetanic stimulation at active but not quiescent synapses.[6] Under these conditions, H_2S facilitated NMDA receptor-mediated currents by activating adenylyl cyclase and the downstream cyclic adenosine mono-phosphate (cAMP)/protein kinase A (PKA) cascades.[723] Although persulfidation of the NMDA receptor has been implicated, it has not been demonstrated.

Several ion channels have been identified as potential targets of H_2S.[724–736] H2S increases intracellular Ca^{2+} levels and subsequent Ca^{2+} waves in primary astrocyte cultures and hippocampal slices from rats.[724] Similar results were obtained with microglial cells and with a neuroblastoma cell line.[725,726] Furthermore, H_2S affected intracellular acidification in a concentration-dependent manner in primary cultured microglia and astrocytes by regulating the activities of the Cl^-/HCO_3^- exchanger and Na^+/H^+ exchanger.[727]

H_2S is postulated to have both pro- and antinociceptive effects in the peripheral nervous system.[728–736] Colonic luminal administration of NaHS caused nociceptive behavior manifested as abdominal allodynia/hyperalgesia in mice, which was abolished by a T-type channel blocker.[728] NaHS-induced nociception also caused reversible T-type Ca^{2+} channel-dependent hyperalgesia in the rat spinal cord and peripheral tisssues.[730,731] These results suggest that sensitization/activation of T-type Ca^{2+} channels might be involved[728,731] although TRP channels have also been suggested to mediate pronociceptive effects of H_2S in rodent models.[732–734] In contrast, subcutaneous injection of millimolar H_2S solutions did not cause pain in humans.[267] The antinociceptive effects of H_2S have been linked to activation of K_{ATP} channels.[129,735,737] However, most of these effects were caused at high, rather than pharmacological, doses of H_2S.

As a pharmacological agent, H_2S can improve disease outcomes in different pathological settings (Figure 32). For example, neuronal cell death caused by peroxynitrite was significantly attenuated by H_2S treatment.[738] Neuronal injury induced by H_2O_2 in primary cultured rat astrocytes impaired glutamate uptake, whereas treatment with H_2S exerted a neuroprotective effect by increasing glutamate uptake.[739] Pharmacological H_2S treatment has also shown some promise for treating Parkinson's disease as discussed in section 9.7.[594]

H_2S levels are reported to be substantially reduced in brain of Alzheimer's disease patients as compared to healthy individuals.[740,741] In a rat model of Alzheimer's disease, pretreatment with NaHS improved learning and memory deficits.[742] Treatment of PC12 cell line with H_2S inhibited expression of BACE-1 (beta-site amyloid precursor protein cleaving enzyme-1) mRNA and protein, a major β-secretase involved in amyloid beta ($A\beta$) production.[743] The PI3K/Akt signaling pathway is reportedly involved in the H_2S-induced decrease in BACE-1 expression and $A\beta$ release. H_2S treatment of SH-SY5Y cells suppressed $A\beta$ formation probably by inhibition of amyloid precursor protein glycosylation and γ-secretase activities.[744] These studies suggest that the H_2S might exerts its effects on different steps involved in $A\beta$ generation (Figure 32).[743,744]

H_2S production is reported to be markedly decreased in Huntington's disease.[745,746] Mutant huntingtin protein inhibits Sp1, a transcriptional activator of CSE, leading to decreased protein expression and consequently, H_2S production (Figure 32).[746] H_2S showed beneficial effects for spinocerebellar ataxia type 3 (SCA3), a neurodegenerative disease caused by polyQ repeats in ataxin-3, which leads to protein aggregation and subsequent neuronal dysfunction and death.[747] In a *Drosophila* model of SCA3, CSE overexpression or treatment with thiosulfate reduced levels of oxidized proteins, inhibited the immune response and prevented SCA3-associated tissue degeneration. These beneficial effects were correlated with an increase in persulfidation levels.[747]

10.2. H_2S and the Cardiovascular System

H_2S exerts multiple effects in the cardiovascular system including attenuating myocardial ischemia reperfusion injury, promoting angiogenesis, relaxing smooth muscle cells, and regulating blood pressure.[748–752] CSE is believed to be the primary H_2S producing enzyme in the cardiovascular system. It is expressed in vascular endothelial cells, smooth muscle cells, and cardiomyocytes.[12,672,753]

Relaxation of rat aortic tissue in vitro was one of the first described effects of H_2S in the cardiovascular system and occurred in synergy with $NO^{\bullet}$.[7] Intravenous application of H_2S decreased blood pressure in rats, which was suppressed by glibenclamide, a K_{ATP} channel blocker.[672,754–756] Exposure of isolated vascular smooth muscle cells to H_2S increased K_{ATP} currents. A vasodilatory role for endogenously synthesized H_2S appeared to be supported by the observation that CSE knockout mice develop age-related hypertension.[12] However, a contradictory result was reported by a second group, which found no changes in blood pressure in CSE knockout mice.[757] H_2S has been described as an endothelium-derived hyperpolarizing factor (Figure 33),[756] acting primarily via activation of the K_{ATP} channel, which can be persulfidated at Cys43 in the pore-forming Kir 6.1 subunit[553] (see section 9.1). However, the mechanism by which Cys43 is persulfidated and whether H_2S acts alone as an endothelium-derived hyperpolarizing factor are unclear.

There is growing evidence that the vasodilatory effects of H_2S are intricately linked to $NO^{\bullet}$ signaling pathways.[7,266–268,465,758] For instance, the K_{ATP} channel-based vasodilatory effect of H_2S is attenuated in the absence of $NO^{\bullet}$,[672,754] and inhibition of eNOS abrogated H_2S-induced vasorelaxation.[7,266,267] Furthermore, HNO, a product of the reaction between H_2S and $NO^{\bullet}$, activates TRPA1.[267] Stimulation of the calcitonin gene-related receptor on smooth muscle cells activates adenylate cyclase, which then generates cAMP, a powerful secondary messenger responsible for vasodilation (Figure 33).[267]

Regulation of cGMP levels appears to be an important mechanism by which H_2S potentiates the effects of $NO^{\bullet}$ particularly in the context of angiogenesis.[266,410,758,759] H_2S inhibits the phosphodiesterase[410,758,759] slowing cGMP degradation and increasing its half-life. Furthermore, binding of H_2S to soluble guanylate cyclase leads to reduction of the heme iron to the ferrous state, which binds $NO^{\bullet}$377 (Figure 33). H_2S also regulates eNOS activity and expression. Phosphorylation of eNOS increases its enzymatic activity and is enhanced in cells and blood vessels treated with H_2S apparently via persulfidation at Cys443[266,268,454] (Figure 33). Persulfidation increases eNOS activity and its ability to be phosphorylated, while also preventing the inhibitory *S*-nitrosation modification at the same cysteine residue.[454] Surprisingly, H_2S inhibits neuronal NOS and inducible NOS by directly binding to the iron heme center but does not inhibit purified eNOS.

Circulating H_2S levels in patients with chronic heart disease or heart failure are significantly reduced compared to age-matched controls.[760] The pharmacological potential of H_2S has been demonstrated in a myocardial ischemia/reperfusion injury model[677,678,750] where H_2S administration at the time of reperfusion reduced infarct size by 72%.[750] The protective effect of H_2S was linked to preservation of mitochondrial function, reduction of cardiomyocyte apoptosis, anti-inflammatory responses, and antioxidant effects.[750] Heart

Nrf-2 and phosphorylated Akt levels were significantly higher in H_2S treated mice suggesting that antioxidant gene expression was increased.[677] Upregulation of the antiapoptotic Blc-2 protein and down-regulation of the pro-apoptotic factors Bax and caspase 2 were seen after H_2S treatment.[761] These effects could be regulated by persulfidation of Keap1 as described in section 9.2.

Binding of vascular endothelial growth factor (VEGF) to its receptor increases CSE expression via intermediate production of H_2O_2 as a signaling molecule.[762] H_2S production stimulates the Akt pathway, resulting in eNOS phosphorylation and higher $NO^{\bullet}$ levels. The VEGF receptor might be a direct target of H_2S, which reportedly reduces the Cys1045−Cys1024 disulfide bond and disrupts the active conformation of the receptor.[763]

Antiatherosclerotic properties of H_2S have been reported.[764,765] CSE knockout mice fed an atherogenic diet developed atherosclerotic lesions and exhibited a different plasma lipid profile than wild-type mice.[765] Expression of the adhesion molecule ICAM-1, which is important for the development of atherosclerotic lesions, was significantly elevated in aorta of CSE knockout mice on an atherogenic diet.[764] Additionally, NFκB expression was elevated in smooth muscle cells isolated from CSE knockout mice.[764]

10.3. H_2S and Inflammation

H_2S reportedly elicits proinflammatory and anti-inflammatory effects in various models of inflammation.[766] H_2S had a proinflammatory effect on acute pancreatitis and associated lung injury and treatment with the CSE inhibitor, D,L-propargylglycine, significantly decreased pancreatic and lung injury.[767] The proinflammatory effect of H_2S was diminished in CSE knockout mice in which acute pancreatitis and associated lung injury was induced.[768] Furthermore, in an ischemia reperfusion injury model, a reduced inflammatory response was observed in kidneys of CSE knockout mice.[769] A proinflammatory response to H_2S has also been reported in several models of sepsis,[770–772] and H_2S levels are increased in patients with septic shock.[692]

An anti-inflammatory effect of H_2S has been reported in subjects with intestinal ischemic damage and ethanol-induced gastritis.[773–775] CSE expression is decreased in the gastric mucosa by nonsteroidal anti-inflammatory drugs[776–778] and NaHS treatment decreased expression of TNF-α, intercellular adhesion molecule 1 (ICAM-1), and lymphocyte-associated antigen-1.[776,777] H_2S synthesis is markedly increased in colon ulcers, and it promotes the rapid restoration of the epithelial barrier integrity and the repair of the damaged tissue.[779] The slow releasing H_2S donor GYY4137 also exerts an anti-inflammatory effect[121,780] by inhibiting NFkB activity. Persulfidation of the p65 subunit of NFkB is proposed to increase its interaction with the ribosomal protein S3 and to upregulate several antiapoptotic genes (see section 9.5).[552]

10.4. H_2S and the Respiratory System

H_2S treatment reportedly attenuates bleomycin-induced pulmonary fibrosis in rats.[781] H_2S treatment suppressed the migration, proliferation, and myofibroblast trans-differentiation of a human lung fibroblast cell line. The inhibitory effects of H_2S were correlated with a decrease in ERK phosphorylation.[782,783] Transforming growth factor β1 (TGF-β1) is a

master regulator of fibrosis, and its inhibition by H_2S resulted in decreased vimentin expression and increased E-cadherin levels.[784] A bronchodilatory effect of H_2S was ascribed to inhibition of Ca^{2+} release from the ER.[785] H_2S treatment induced relaxation of mouse tracheal smooth muscle cells by activating the calcium-activated potassium channel.[786] Furthermore, H_2S reportedly plays a role in the pathology and treatment of chronic obstructive pulmonary disease.[787]

10.5. H_2S and the Renal System

H_2S appears to play an important role in the onset and progression of renal diseases. Plasma H_2S levels are lower in patients with diabetic versus nondiabetic nephropathy undergoing chronic hemodialysis.[788] CBS and CSE expression is downregulated in experimental models of diabetes.[789,790]

An intrarenal infusion of NaHS increased blood flow, glomerular filtration rate, and urinary sodium and potassium excretion in rats.[791,792] H_2S inhibited the $Na^+/K^+/2Cl^-$ cotransporter and Na^+/K^+/ATPase activity in proximal kidney tubule epithelial cells[792] and decreased cAMP levels in different renal cell types.[793,794] H_2S also decreased renin production in rat kidney.[794] CSE overexpression increased endogenous H_2S production and suppressed isoproterenol-induced renin release.[794] However, the underlying mechanism by which H_2S regulates renin release is unclear.

Conflicting results on the effects of H_2S on kidney ischemia/reperfusion injury have been reported.[769,795] Increased damage and mortality after renal ischemia/reperfusion was reported in CSE knockout mice, and H_2S treatment protected mice from ischemia-induced renal injury and decreased mortality.[795] A second study using a different strain of CSE knockout mice failed to observe a significant difference between wild-type and knockout animals exposed to kidney ischemia/reperfusion.[769]

10.6. H_2S and the Liver

All H_2S-producing enzymes are expressed in the liver, which plays an important role in glucose and lipid homeostasis, xenobiotic metabolism, and antioxidant defense.[796–799] H_2S is suggested to be an important modulator of hepatic micro-circulation.[800] H_2S donors such as diallyl trisulfide attenuate ethanol-induced liver injury in mice and increase the activity of mitochondrial antioxidant enzymes.[801] The hepatoprotective effects of H_2S donors were correlated with Nrf2 translocation and increased expression of antioxidant genes, which is regulated by Keap1 persulfidation (see section 9.2).[554,679]

10.7. H_2S and the Gut

Some gut microbes use sulfate as a terminal electron acceptor for respiration and produce H_2S using the dissimilatory sulfite reductase enzyme complex.[710,712] *Desulfovibrio* is the predominant sulfate reducing bacterium in the human intestine, while *Desulfobacter*, *Desulfomonas*, *Desulfobulbus*, and *Desulfotomaculum* are found at lower levels.[802] Very high H_2S (up to 1000 ppm) has been reported in the rat cecum,[803] and 0.2−30 ppm of H_2S has been reported in human flatus.[804] It is estimated that approximately half of the fecal H_2S is produced by gut microbes with the remainder being derived from host metabolism.[805] An

imbalance in the number or composition of gut microbes is associated with various diseases.[712] Sulfate reducing bacteria are resistant to a broad spectrum of antibiotics, and repeated use of these drugs might favor a bloom of these bacteria.[806] An increase in the number of sulfate reducers has been observed in patients with ulcerative colitis, inflammatory bowel disease and Crohn's disease,[807] periodontitis,[808] pouchitis,[804] and irritable bowel syndrome.[809] Probiotic and prebiotic treatments reduce the numbers of *Desulfovibrio* bacteria[810,811] and the levels of proinflammatory cytokines IFN-γ, TNF-α, and IL-1β.[811]

10.8. H_2S and the Reproductive System

CBS and CSE are expressed in the human *corpus cavernosum*, the muscular trabeculae, and smooth muscle components of the penile artery.[812,813] The administration of CSE inhibitors into corpus cavernosum impaired the normal intracavernosal pressure response to cavernous nerve electrostimulation suggesting a possible role for H_2S in penile tissue smooth muscle relaxation.[814,815] NaHS treatment induced relaxation of rabbit[815] and human[812] corpus cavernosum strips in a concentration-dependent manner. An H_2S-donating derivative of sildenafil has been developed for potential use in treating erectile dysfunction.[816]

H_2S also exerts effects on male and female fertility.[817–823] Expression of H_2S-producing enzymes and H_2S synthesis have been reported in uterus, vagina, and placenta.[818–821] NaHS was shown to reversibly attenuate the contractile response of isolated rat uterus and delay parturition[824–827] and mediate spontaneous contractions of the human oviduct.[823]

10.9. H_2S and Oxygen Sensing and Hibernation

Exposure to low concentrations of H_2S (80 ppm) induced a suspended animation-like state in mice, by decreasing metabolic rate and core body temperature.[13] The H_2S-induced depression of the metabolic rate observed in mice could be beneficial in patients with major trauma or cardiac arrest.[828]

Hypoxia increases H_2S production in carotid bodies of rat and mice.[829] In CSE knockout mice and wild-type rats treated with a CSE inhibitor, the hypoxic sensitivity of carotid bodies is markedly impaired. CO reportedly abolished CSE activity and reduced H_2S generation in rat carotid bodies via protein kinase G-dependent phosphorylation of CSE.[829,830] In hypoxia, CO levels and CSE phosphorylation decrease, leading to increased H_2S production (Figure 34).[260]

The stimulatory effect of H_2S on carotid body sensory activity is completely abolished by cadmium chloride, a nonselective inhibitor of voltage-activated Ca^{2+} channels.[829,831] H_2S treatment and hypoxia induced an increase in intracellular Ca^{2+} concentrations in rat glomus cells. Inhibition of H_2S production prevented carotid body activation and hypertension in rodents exposed to intermittent hypoxia, which is a model for obstructive and central sleep apnea.

Treatment of *Caenorhabditis elegans* with H_2S increased thermotolerance and longevity at higher temperatures.[832] Several proteins were associated with these effects including hypoxia-inducible factor-1 and SKN-1, a homologue of mammalian Nrf-2. Furthermore, knockout of the MST ortholog reduced lifespan in *C. elegans*,[833] and the effect was rescued

by GYY4137. H_2S and ROS are postulated to play important roles in extending lifespan in *C. elegans*.[156] Decreased expression of CBS significantly reduced the lifespan of germline-deficient *C. elegans* mutants compared to the wild type strain.[156] The role of protein persulfidation in lifespan extension has not been examined.

10.10. H_2S and Cancer

The roles of H_2S in cancer development and progression are still controversial. Some of the biological effects of H_2S that might be relevant to cancer biology include stimulation of angiogenesis, regulation of intracellular signaling and cell death, and cellular bioenergetics.[834–836] Many of the effects exhibit a biphasic dose−response curve; low concentrations of H_2S are cytoprotective and high concentrations are cytotoxic.[835–839]

Overexpression of CBS at protein and mRNA levels has been reported in primary epithelial ovarian cancer tissue[840–842] and in several breast cancer cell lines.[843–845] However, CBS expression is reportedly suppressed in gastric and colorectal cancers, glioma, and hepatocellular carcinoma.[846–848] Additional studies are needed to elucidate the roles of CBS in cancer development and progression. Similar contradictory observations have been reported for CSE, which was shown to be both up- and down-regulated in several cancer types.[849–853] The pro-carcinogenic effects of H_2S also contradict studies using H_2S donors, which show anticarcinogenic effects.[837–839,854] A deeper understanding of whether and how H_2S plays a role in cancer etiology and progression is needed.

11. CONCLUSIONS

While an increasing number of signaling roles and physiological effects are being attributed to H_2S, our understanding of the underlying mechanisms lags far behind. Significant barriers that have thwarted progress in the field include the technical challenges of working with a redox active and volatile molecule whose salts are often contaminated with polysulfides, which can be more reactive than H_2S itself. The scarcity of sensitive, rigorous, and readily available methods for quantifying H_2S or persulfides poses additional challenges. The identities of the preferred targets for H_2S and of its downstream signaling intermediates are not yet completely understood. While persulfide proteomic analyses are beginning to reveal a rich trove of protein targets, the functional validation of how persulfidation affects individual proteins and metabolic flux has been challenging, since quantitative methods for introducing the persulfidation modification and stabilizing it under assay conditions are not readily available. Solving this methodological problem would lead to insights into how H_2S signals and could identify important therapeutic targets. It would also lead to the resolution of the many contradictory effects of H_2S that have been reported with purified proteins, at the cellular and organismal levels.

The contributions of the enzymes in H_2S-producing and H_2S-oxidizing pathways in controlling H_2S levels and the conditions that permit spiking of H_2S from low nanomolar steady-state concentrations to levels which trigger signaling are other important gaps in the field. Furthermore, the relative contributions of the three H_2S-producing enzymes in different tissues are largely unknown. The development of selective inhibitors for CBS, CSE, MST, and SQR in particular will be very useful as molecular reagents together with

gene editing technology for dissecting the roles of these enzymes in H_2S homeostasis. Expanding the tool set for selective and ratiometric fluorescence visualization of protein persulfidation will facilitate elucidation of the spatiotemporal changes that occur during H_2S signaling.

The field of H_2S biology would benefit greatly by being strongly grounded in chemical studies on H_2S and persulfide formation and decay kinetics and reactivity, to provide a more rigorours framework for understanding the potential roles of persulfidation in cell signaling. Proteomic studies suggest significant overlap between persulfidation and other oxidative cysteine modifications. Teasing apart why modifications like *S*-nitrosation, glutathionylation, and sulfenylation or persulfidation target the same cysteines in some proteins will provide important insights into cross-talk between oxidative cysteine-based signaling pathways.

Regulation of persulfidation is another area that is poorly understood. Are catalysts involved, and if so, what are their identities? Enzyme-catalyzed trans-persulfidation reactions are expected to be important both for adding and removing the persulfide modification, and an understanding of how each process is regulated and how target specificity is achieved is critical for elucidating H_2S-based signaling. The relative newness of the H_2S chemical biology field and the large fundamental gaps in our understanding combine to portend an exciting future.

Acknowledgments

M.R.F. and J.Z. acknowledge support from ATIP Avenir grant and Investments for the future “Programme IdEx Bordeaux” (ANR-10-IDEX-03-02). B.A. is supported by grants from Comisión Sectorial de Investigación Científica (CSIC), Universidad de la República, Uruguay. R.B. acknowledges support from NIH (HL58984 and GM112455). We are grateful to Dr. Ernesto Cuevasanta and Emilia Kouroussis for their assistance.

Biographies

Milos R. Filipovic received his undergraduate and postgraduate training in biochemistry (University of Belgrade). After his postdoc at Friedrich-Alexander University Erlangen-Nuremberg, where he also worked as a group leader for a few years, he moved to Institut de Biochimie et Génétique Cellulaires (IBGC, CNRS UMR5095) at the University of Bordeaux, as Idex Junior Chair and ATIP-Avenir awardee to lead the “Signaling by gasotransmitters” group. He is interested in redox signaling, in general, and in developing new tools to dissect molecular mechanisms by which different gasotransmitters signal in the human body, in particular.

Jasmina Zivanovic studied biology at the University of Belgrade where she also obtained her Ph.D. (in endocrinology). She is a postdoc researcher at IBGC CNRS UMR5095 in the “Signaling by gasotransmitters” group. Her research focus is on developing new tools for persulfide labelling to address the changes of persulfidation in ageing and ageing-related diseases.

Beatriz Alvarez is Associate Professor of Enzymology at the School of Sciences, University of the Republic, Montevideo, Uruguay. She received her M.Sc. and Ph.D. in Chemistry

degrees from the University of the Republic. Her interests span the areas of redox biochemistry, kinetics and enzymology, especially in relation to biological thiols and hydrogen sulfide.

Ruma Banerjee was raised as a peripatetic army brat changing ten schools before graduating. She received her formal training in plant science (B.S. and M.S., University of Delhi), biochemistry (Ph.D., Rensselaer Polytechnic Institute, NY), and biophysics (postdoc, University of Michigan). She is currently the Vincent Massey Collegiate Professor and Associate Chair of Biological Chemistry at the University of Michigan Medical School. Her interests range from B_{12} trafficking and metalloenzymology to hydrogen sulfide homeostasis and signaling. She is an Associate Editor for Chemical Reviews and for the Journal of Biological Chemistry.

References

1. Parker ET, Cleaves HJ, Dworkin JP, Glavin DP, Callahan M, Aubrey A, Lazcano A, Bada JL. Primordial Synthesis of Amines and Amino Acids in a 1958 Miller H2S-Rich Spark Discharge Experiment. Proc Natl Acad Sci U S A. 2011; 108:5526–5531. [PubMed: 21422282]
2. Patel BH, Percivalle C, Ritson DJ, Duffy CD, Sutherland JD. Common Origins of RNA, Protein and Lipid Precursors in a Cyanosulfidic Protometabolism. Nat Chem. 2015; 7:301–307. [PubMed: 25803468]
3. Winogradsky S. Ueber Schwefelbakterien. Bot Zeitung. 1887; 45:489–507. 513–523, 529–539, 545–559, 569–576, 585–594.
4. Ramazzini, B. Baptiftam Conzattum; Padua: 1713. De Morbis Artificum Diatriba.
5. Scheele, CW. Chemische Abhandlung von der Luft und dem Feuer (Chemical treatise on air and fire). Magnus Swederus; Upsala, Sweden: 1777.
6. Abe K, Kimura H. The Possible Role of Hydrogen Sulfide as an Endogenous Neuromodulator. J Neurosci. 1996; 16:1066–1071. [PubMed: 8558235]
7. Hosoki R, Matsuki N, Kimura H. The Possible Role of Hydrogen Sulfide as an Endogenous Smooth Muscle Relaxant in Synergy with Nitric Oxide. Biochem Biophys Res Commun. 1997; 237:527–531. [PubMed: 9299397]
8. Grigorian RM, Vasilenko FD, Akulova RF, Timoshenko MA. The Effect of Hydrogen Sulfide Baths on the Peripheral Blood Circulation after Reconstructive Operations on the Major Arteries on the Extremities. Sov Med. 1963; 26:46–51.
9. Lavrov VP. The Effect of Matsesta Hydrogen Sulfide Baths on the Status of the Myocardium and Coronary Arteries in Experimental Atherosclerosis. Vopr Kurortol Fizioter Lech Fiz Kult. 1968; 33:313–316. [PubMed: 5736797]
10. Bocconi G. The Biological Actions of Sulfurated Waters. Minerva Ecol Idroclimatol Fis Sanit. 1976; 16:105–116. [PubMed: 1053101]
11. Kruszyna H, Kruszyna R, Smith RP. Cyanide and Sulfide Interact with Nitrogenous Compounds to Influence the Relaxation of Various Smooth Muscles. Exp Biol Med. 1985; 179:44–49.
12. Yang G, Wu L, Jiang B, Yang W, Qi J, Cao K, Meng Q, Mustafa AK, Mu W, Zhang S, et al. H2S as a Physiologic Vasorelaxant: Hypertension in Mice with Deletion of Cystathionine -Lyase. Science. 2008; 322:587–590. [PubMed: 18948540]
13. Blackstone E. H2S Induces a Suspended Animation-Like State in Mice. Science. 2005; 308:518–518. [PubMed: 15845845]
14. Asfar P, Calzia E, Radermacher P. Is Pharmacological, H2S-Induced “Suspended Animation” Feasible in the ICU? Crit Care. 2014; 18:215. [PubMed: 25028804]
15. Szabó C. Hydrogen Sulphide and Its Therapeutic Potential. Nat Rev Drug Discovery. 2007; 6:917–935. [PubMed: 17948022]

16. Li L, Rose P, Moore PK. Hydrogen Sulfide and Cell Signaling. Annu Rev Pharmacol Toxicol. 2011; 51:169–187. [PubMed: 21210746]
17. Wang R. Physiological Implications of Hydrogen Sulfide: A Whiff Exploration That Blossomed. Physiol Rev. 2012; 92:791–896. [PubMed: 22535897]
18. Mustafa AK, Gadalla MM, Snyder SH. Signaling by Gasotransmitters. Sci Signaling. 2009; 2:re2–re2.
19. Mustafa AK, Gadalla MM, Sen N, Kim S, Mu W, Gazi SK, Barrow RK, Yang G, Wang R, Snyder SH. H2S Signals Through Protein S-Sulfhydration. Sci Signaling. 2009; 2:ra72–ra72.
20. Paul BD, Snyder SH. H2S Signalling through Protein Sulfhydration and beyond. Nat Rev Mol Cell Biol. 2012; 13:499–507. [PubMed: 22781905]
21. Carroll JJ, Mather AE. The Solubility of Hydrogen Sulphide in Water from 0 to 90°C and Pressures to 1 MPa. Geochim Cosmochim Acta. 1989; 53:1163–1170.
22. Iliuta MC, Larachi F. Solubility of Total Reduced Sulfurs (Hydrogen Sulfide, Methyl Mercaptan, Dimethyl Sulfide, and Dimethyl Disulfide) in Liquids. J Chem Eng Data. 2007; 52:2–19.
23. De Bruyn WJ, Swartz E, Hu JH, Shorter JA, Davidovits P, Worsnop DR, Zahniser MS, Kolb CE. Henry's Law Solubilities and Śetchenow Coefficients for Biogenic Reduced Sulfur Species Obtained from Gas-Liquid Uptake Measurements. J Geophys Res. 1995; 100:7245–7251.
24. Evans CL. The Toxicity of Hydrogen Sulphide and Other Sulphides. Q J Exp Physiol Cogn Med Sci. 1967; 52:231–248. [PubMed: 5182405]
25. Yant WP. Hydrogen Sulphide in Industry-Occurrence, Effects, and Treatment. Am J Public Health Nations Health. 1930; 20:598–608. [PubMed: 18013029]
26. Elkins, HB. The Chemistry of Industrial Toxicology. John Wiley & Sons; New York: 1950.
27. Beauchamp RO, Bus JS, Popp JA, Boreiko CJ, Andjelkovich DA, Leber P. A Critical Review of the Literature on Hydrogen Sulfide Toxicity. CRC Crit Rev Toxicol. 1984; 13:25–97.
28. Ahlborg G. Hydrogen Sulfide Poisoning in Shale Oil Industry. AMA Arch Ind Hyg Occup Med. 1951; 3:247–266. [PubMed: 14810252]
29. Haggard HW. The Toxicity of Hydrogen Sulphide. J Ind Hyg Toxicol. 1925; 7:113–121.
30. Poda GA. Hydrogen Sulfide Can Be Handled Safely. Arch Environ Health. 1966; 12:795–800. [PubMed: 5938584]
31. Wood JL. Sulfane Sulfur. Methods Enzymol. 1987; 143:25–29. [PubMed: 3657542]
32. Ubuka T. Assay Methods and Biological Roles of Labile Sulfur in Animal Tissues. J Chromatogr B: Anal Technol Biomed Life Sci. 2002; 781:227–249.
33. Toohey JI. Sulfur Signaling: Is the Agent Sulfide or Sulfane? Anal Biochem. 2011; 413:1–7. [PubMed: 21303647]
34. Toohey J, Cooper A. Thiosulfoxide (Sulfane) Sulfur: New Chemistry and New Regulatory Roles in Biology. Molecules. 2014; 19:12789–12813. [PubMed: 25153879]
35. Rickard D, Luther GW. Chemistry of Iron Sulfides. Chem Rev. 2007; 107:514–562. [PubMed: 17261073]
36. Trindle C. Molecular Structure and Bonding, the Qualitative Molecular Orbital Approach (Gimarc, M.). J Chem Educ. 1979; 56:A352.
37. Rickard D, Luther GW. Kinetics of Pyrite Formation by the H2S Oxidation of Iron (II) Monosulfide in Aqueous Solutions between 25 and 125°C: The Mechanism. Geochim Cosmochim Acta. 1997; 61:135–147.
38. Drzaic, PS., Marks, J., Brauman, JI. Gas Phase Ion Chemistry. Bowers, MT., editor. Vol. 3. Elsevier; Amsterdam, The Netherlands: 1984.
39. Radzig, AA., Smirnov, BM. Reference Data on Atoms, Molecules, and Ions. Vol. 31. Springer; Berlin: 1985. Springer Series in Chemical Physics
40. McDaniel DH, Evans WG. Strong Hydrogen Bonds. III. Hydrogen Sulfide-Hydrosulfide Anion Interactions. Inorg Chem. 1966; 5:2180–2181.
41. Drozdov AP, Eremets MI, Troyan IA, Ksenofontov V, Shylin SI. Conventional Superconductivity at 203 K at High Pressures in the Sulfur Hydride System. Nature. 2015; 525:73–76. [PubMed: 26280333]

42. Fathe K, Holt JS, Oxley SP, Pursell CJ. Infrared Spectroscopy of Solid Hydrogen Sulfide and Deuterium Sulfide. J Phys Chem A. 2006; 110:10793–10798. [PubMed: 16970373]
43. Millero FJ. The Thermodynamics and Kinetics of the Hydrogen Sulfide System in Natural Waters. Mar Chem. 1986; 18:121–147.
44. Fogg, PGT., Young, CL., Clever, HL., Boozer, EL., Hayduk, W. Hydrogen Sulfide, Deuterium Sulfide and Hydrogen Selenide. Pergamon Press; Oxford, U.K: 1988.
45. Konopik N, Leberl O. Colorimetric pH Determination in the Range 10 to 15. IV. The Second Dissociation Constant of Hydrogen Sulphide. Monatsh Chem. 1949; 80:781–787.
46. Kubli H. Die Dissoziation von Schwefelwas-Serstoff. Helv Chim Acta. 1946; 29:1962–1973.
47. Ellis AJ, Golding RM. Spectrophotometric Determination of the Acid Dissociation Constants of Hydrogen Sulphide. J Chem Soc. 1959; 127
48. Knox J. Zur Kenntnis Der Ionengbildung Des Schwefels Und Der Komplexionen Des Quecksilber. Z Elektrochem Angew Phys Chem. 1906; 12:477–481.
49. Maronny G. Constantes de Dissociation de L'hydrogène Sulfuré. Electrochim Acta. 1959; 1:58–69.
50. Ellis AJ, Giggenbach W. Hydrogen Sulphide Ionization and Sulphur Hydrolysis in High Temperature Solution. Geochim Cosmochim Acta. 1971; 35:247–260.
51. Giggenbach W. Optical Spectra of Highly Alkaline Sulfide Solutions and the Second Dissociation Constant of Hydrogen Sulfide. Inorg Chem. 1971; 10:1333–1338.
52. Meyer B, Ward K, Koshlap K, Peter L. Second Dissociation Constant of Hydrogen Sulfide. Inorg Chem. 1983; 22:2345–2346.
53. Licht S, Manassen J. The Second Dissociation Constant of Hydrogen Sulfide. J Electrochem Soc. 1987; 134:918–921.
54. Myers RJ. The New Low Value for the Second Dissociation Constant for H2S: Its History, Its Best Value, and Its Impact on the Teaching of Sulfide Equilibria. J Chem Educ. 1986; 63:687.
55. Schoonen MAA, Barnes HL. An Approximation of the Second Dissociation Constant for H2S. Geochim Cosmochim Acta. 1988; 52:649–654.
56. Guenther EA, Johnson KS, Coale KH. Direct Ultraviolet Spectrophotometric Determination of Total Sulfide and Iodide in Natural Waters. Anal Chem. 2001; 73:3481–3487. [PubMed: 11476251]
57. Cuevasanta E, Denicola A, Alvarez B, Möller MN. Solubility and Permeation of Hydrogen Sulfide in Lipid Membranes. PLoS One. 2012; 7:e34562. [PubMed: 22509322]
58. Mathai JC, Missner A, Kugler P, Saparov SM, Zeidel ML, Lee JK, Pohl P. No Facilitator Required for Membrane Transport of Hydrogen Sulfide. Proc Natl Acad Sci U S A. 2009; 106:16633–16638. [PubMed: 19805349]
59. Riahi S, Rowley CN. Why Can Hydrogen Sulfide Permeate Cell Membranes? J Am Chem Soc. 2014; 136:15111–15113. [PubMed: 25323018]
60. Cuevasanta E, Lange M, Bonanata J, Coitiño EL, Ferrer-Sueta G, Filipovic MR, Alvarez B. Reaction of Hydrogen Sulfide with Disulfide and Sulfenic Acid to Form the Strongly Nucleophilic Persulfide. J Biol Chem. 2015; 290:26866–26880. [PubMed: 26269587]
61. Carballal S, Trujillo M, Cuevasanta E, Bartesaghi S, Möller MN, Folkes LK, García-Bereguiaín MA, Gutiérrez-Merino C, Wardman P, Denicola A, et al. Reactivity of Hydrogen Sulfide with Peroxynitrite and Other Oxidants of Biological Interest. Free Radic Biol Med. 2011; 50:196–205. [PubMed: 21034811]
62. Trujillo M, Alvarez B, Radi R. One- and Two-Electron Oxidation of Thiols: Mechanisms, Kinetics and Biological Fates. Free Radical Res. 2016; 50:150–171. [PubMed: 26329537]
63. Armstrong DA, Huie RE, Koppenol WH, Lymar SV, Merényi G, Neta P, Ruscic B, Stanbury DM, Steenken S, Wardman P. Standard Electrode Potentials Involving Radicals in Aqueous Solution: Inorganic Radicals (IUPAC Technical Report). Pure Appl Chem. 2015; 87:1139–1150.
64. Koppenol WH, Bounds PL. Signaling by Sulfur-Containing Molecules. Quantitative Aspects. Arch Biochem Biophys. 2017; 617:3–8. [PubMed: 27670814]

65. Das TN, Huie RE, Neta P, Padmaja S. Reduction Potential of the Sulfhydryl Radical: Pulse Radiolysis and Laser Flash Photolysis Studies of the Formation and Reactions of ·SH and HSSH· - in Aqueous Solutions. J Phys Chem A. 1999; 103:5221–5226.
66. Darwent BD. Bond Dissociation Energies in Simple Molecules. National Standard Reference Data System, National Bureau of Standards. 1970:1–58.
67. Wood PM. The Potential Diagram for Oxygen at pH 7. Biochem J. 1988; 253:287–289. [PubMed: 2844170]
68. Karmann W, Meissner G, Henglein A. Pulsradiolyse Des Schwefelwasserstoffs in Wäßriger Lösung. Z Naturforsch, B: J Chem Sci. 1967; 22:273–282.
69. Wedmann R, Zahl A, Shubina TE, Dürr M, Heinemann FW, Bugenhagen BEC, Burger P, Ivanovic-Burmazovic I, Filipovic MR. Does Perthionitrite (SSNO–) Account for Sustained Bioactivity of NO? A (Bio)chemical Characterization. Inorg Chem. 2015; 54:9367–9380. [PubMed: 26111441]
70. Feher, F. Handbook of Preparative Inorganic Chemistry. Academic Press; New York: 1963. Sulfur, Selenium, Tellurium; p. 341-456.
71. Zhu J, Petit K, Colson AO, DeBolt S, Sevilla MD. Reactions of Sulfhydryl and Sulfide Radicals with Oxygen, Hydrogen Sulfide, Hydrosulfide, and Sulfide: Formation of SO2-, HSSH-, HSS.2- and HSS. J Phys Chem. 1991; 95:3676–3681.
72. Hoffmann MR, Lim BC. Kinetics and Mechanism of the Oxidation of Sulfide by Oxygen: Catalysis by Homogeneous Metal-Phthalocyanine Complexes. Environ Sci Technol. 1979; 13:1406–1414.
73. Hoffmann MR. Kinetics and Mechanism of Oxidation of Hydrogen Sulfide by Hydrogen Peroxide in Acidic Solution. Environ Sci Technol. 1977; 11:61–66.
74. O'Brien DJ, Birkner FB. Kinetics of Oxygenation of Reduced Sulfur Species in Aqueous Solution. Environ Sci Technol. 1977; 11:1114–1120.
75. Kotronarou A, Hoffmann MR. Catalytic Autoxidation of Hydrogen Sulfide in Wastewater. Environ Sci Technol. 1991; 25:1153–1160.
76. Zhang J-Z, Millero FJ. The Products from the Oxidation of H2S in Seawater. Geochim Cosmochim Acta. 1993; 57:1705–1718.
77. Sun J, Stanbury DM. Trace Metal-Ion Catalysis of Oxidation of Aqueous Hydrogen Sulfide by Outer-Sphere Oxidants. Inorg Chim Acta. 2002; 336:39–45.
78. Panda SK, Andersson JT, Schrader W. Characterization of Supercomplex Crude Oil Mixtures: What Is Really in There? Angew Chem, Int Ed. 2009; 48:1788–1791.
79. Holleman, AF., Wiberg, E. Lehrbuch Der Anorganischen Chemie. Walter de Gruyter & Co; Berlin: 1995.
80. Kotronarou A, Mills G, Hoffmann MR. Oxidation of Hydrogen Sulfide in Aqueous Solution by Ultrasonic Irradiation. Environ Sci Technol. 1992; 26:2420–2428.
81. Poulton SW, Krom MD, Rijn JV, Raiswell R. The Use of Hydrous Iron (III) Oxides for the Removal of Hydrogen Sulphide in Aqueous Systems. Water Res. 2002; 36:825–834. [PubMed: 11848352]
82. Ruhland B, Helmut F. Stripping of Sulfide-Containing Liquids, Especially from Leather or Petrochemical Industries, with Carbon Dioxide-Containing Gas Involves Recycling of Hydrogen Sulfide-Containing Off-Gas. DE 10204654A1. 2003
83. Hardison LC. Removal of Hydrogen Sulfide from Sour Water without Loss of Heavy Metal. US 5292440A. 1992
84. Piché S, Larachi F. Hydrosulfide Oxidation Pathways in Oxic Solutions Containing iron(III) Chelates. Environ Sci Technol. 2007; 41:1206–1211. [PubMed: 17593720]
85. Martell AE, Motekaitis RJ, Chen D, Hancock RD, McManus D. Selection of New Fe(III)/Fe(II) Chelating Agents as Catalysts for the Oxidation of Hydrogen Sulfide to Sulfur by Air. Can J Chem. 1996; 74:1872–1879.
86. Hughes MN, Centelles MN, Moore KP. Making and Working with Hydrogen Sulfide. Free Radic Biol Med. 2009; 47:1346–1353. [PubMed: 19770036]
87. Steudel R, Eckert B. Solid Sulfur Allotropes Sulfur Allotropes. Top Curr Chem. 2003; 230:1–80.
88. Steudel R. Liquid Sulfur Liquid Sulfur. Top Curr Chem. 2003; 230:81–116.

89. Steudel R. Aqueous Sulfur Sols. Top Curr Chem. 2003; 230:153–166.
90. Tebbe FN, Wasserman E, Peet WG, Vatvars A, Hayman AC. Composition of Elemental Sulfur in Solution: Equilibrium of S6, S7 and S8 at Ambient Temperatures. J Am Chem Soc. 1982; 104:4971–4972.
91. Hojo M, Sawyer DT. Hydroxide-Induced Reduction of Elemental Sulfur (S8) to Trisulfur Anion Radical ($S_3^{\bullet -}$). Inorg Chem. 1989; 28:1201–1202.
92. Bartlett PD, Meguerian G. Reactions of Elemental Sulfur. I. The Uncatalyzed Reaction of Sulfur with Triarylphosphines 1. J Am Chem Soc. 1956; 78:3710–3715.
93. Piery M, Bonnamour S, De Milhaud M. Dégagement d'Hydrogène Sulfure Par Le Voies Respiratoires Après Injections Intraveineuse De Soufre Colloïdal. Compt Rend Soc Biol. 1924; (91):679–720.
94. Bernheim F, Bernheim MLC. The Action of Colloidal Sulfur on Liver Oxidations. J Biol Chem. 1932; 96:331–339.
95. Searcy DG, Lee SH. Sulfur Reduction by Human Erythrocytes. J Exp Zool. 1998; 282:310–322. [PubMed: 9755482]
96. Clinical Trials. Gov Identifier: NCT01989208.
97. Wedmann R, Bertlein S, Macinkovic I, Böltz S, Miljkovic JL, Muñoz LE, Herrmann M, Filipovic MR. Working with "H2S": Facts and Apparent Artifacts. Nitric Oxide. 2014; 41:85–96. [PubMed: 24932545]
98. Hartle MD, Pluth MD. A Practical Guide to Working with H2S at the Interface of Chemistry and Biology. Chem Soc Rev. 2016; 45:6108–6117. [PubMed: 27167579]
99. Brauer, G. Handbook of Preparative Inorganic Chemistry. 2nd. Academic Press; New York: p. 1963
100. Greiner R, Pálinkás Z, Bäsell K, Becher D, Antelmann H, Nagy P, Dick TP. Polysulfides Link H2S to Protein Thiol Oxidation. Antioxid Redox Signal. 2013; 19:1749–1765. [PubMed: 23646934]
101. Nagy P, Pálinkás Z, Nagy A, Budai B, Tóth I, Vasas A. Chemical Aspects of Hydrogen Sulfide Measurements in Physiological Samples. Biochim Biophys Acta, Gen Subj. 2014; 1840:876–891.
102. Hartle MD, Meininger DJ, Zakharov LN, Tonzetich ZJ, Pluth MD. NBu_4SH Provides a Convenient Source of HS–Soluble in Organic Solution for H_2S and Anion-Binding Research. Dalt Trans. 2015; 44:19782–19785.
103. Saund SS, Sosa V, Henriquez S, Nguyen QNN, Bianco CL, Soeda S, Millikin R, White C, Le H, Ono K, et al. The Chemical Biology of Hydropersulfides (RSSH): Chemical Stability, Reactivity and Redox Roles. Arch Biochem Biophys. 2015; 588:15–24. [PubMed: 26519887]
104. Bełtowski J. Hydrogen Sulfide in Pharmacology and Medicine – An Update. Pharmacol Rep. 2015; 67:647–658. [PubMed: 25933982]
105. Kashfi K, Olson KR. Biology and Therapeutic Potential of Hydrogen Sulfide and Hydrogen Sulfide-Releasing Chimeras. Biochem Pharmacol. 2013; 85:689–703. [PubMed: 23103569]
106. Zhao Y, Biggs TD, Xian M. Hydrogen Sulfide (H2S) Releasing Agents: Chemistry and Biological Applications. Chem Commun. 2014; 50:11788–11805.
107. Wallace JL, Wang R. Hydrogen Sulfide-Based Therapeutics: Exploiting a Unique but Ubiquitous Gasotransmitter. Nat Rev Drug Discovery. 2015; 14:329–345. [PubMed: 25849904]
108. Whiteman M, Perry A, Zhou Z, Bucci M, Papapetropoulos A, Cirino G, Wood ME. Phosphinodithioate and Phosphoramidodithioate Hydrogen Sulfide Donors. Handb Exp Pharmacol. 2015; 230:337–363. [PubMed: 26162843]
109. Zhao Y, Pacheco A, Xian M. Medicinal Chemistry: Insights into the Development of Novel H2S Donors. Handb Exp Pharmacol. 2015; 230:365–388. [PubMed: 26162844]
110. Pluth M, Bailey T, Hammers M, Hartle M, Henthorn H, Steiger A. Natural Products Containing Hydrogen Sulfide Releasing Moieties. Synlett. 2015; 26:2633–2643.
111. Yagdi E, Cerella C, Dicato M, Diederich M. Garlic-Derived Natural Polysulfanes as Hydrogen Sulfide Donors: Friend or Foe? Food Chem Toxicol. 2016; 95:219–233. [PubMed: 27430419]

112. Zhao Y, Wang H, Xian M. Cysteine-Activated Hydrogen Sulfide (H2S) Donors. J Am Chem Soc. 2011; 133:15–17. [PubMed: 21142018]
113. Zhao Y, Bhushan S, Yang C, Otsuka H, Stein JD, Pacheco A, Peng B, Devarie-Baez NO, Aguilar HC, Lefer DJ, et al. Controllable Hydrogen Sulfide Donors and Their Activity against Myocardial Ischemia-Reperfusion Injury. ACS Chem Biol. 2013; 8:1283–1290. [PubMed: 23547844]
114. Roger T, Raynaud F, Bouillaud F, Ransy C, Simonet S, Crespo C, Bourguignon M-P, Villeneuve N, Vilaine J-P, Artaud I, et al. New Biologically Active Hydrogen Sulfide Donors. ChemBioChem. 2013; 14:2268–2271. [PubMed: 24115650]
115. Martelli A, Testai L, Citi V, Marino A, Pugliesi I, Barresi E, Nesi G, Rapposelli S, Taliani S, Da Settimo F, et al. Arylthioamides as H_2S Donors: L -Cysteine-Activated Releasing Properties and Vascular Effects in Vitro and in Vivo. ACS Med Chem Lett. 2013; 4:904–908. [PubMed: 24900583]
116. Foster JC, Powell CR, Radzinski SC, Matson JB. S-Aroylthiooximes: A Facile Route to Hydrogen Sulfide Releasing Compounds with Structure-Dependent Release Kinetics. Org Lett. 2014; 16:1558–1561. [PubMed: 24575729]
117. Carter JM, Qian Y, Foster JC, Matson JB. Peptide-Based Hydrogen Sulphide-Releasing Gels. Chem Commun (Cambridge, U K). 2015; 51:13131–13134.
118. Ozturk T, Ertas E, Mert O. Use of Lawesson's Reagent in Organic Syntheses. Chem Rev. 2007; 107:5210–5278. [PubMed: 17867708]
119. Wallace JL, Vong L, McKnight W, Dicay M, Martin GR. Endogenous and Exogenous Hydrogen Sulfide Promotes Resolution of Colitis in Rats. Gastroenterology. 2009; 137:569. [PubMed: 19375422]
120. Li L, Whiteman M, Guan YY, Neo KL, Cheng Y, Lee SW, Zhao Y, Baskar R, Tan C-H, Moore PK. Characterization of a Novel, Water-Soluble Hydrogen Sulfide-Releasing Molecule (GYY4137): New Insights Into the Biology of Hydrogen Sulfide. Circulation. 2008; 117:2351–2360. [PubMed: 18443240]
121. Li L, Salto-Tellez M, Tan C-H, Whiteman M, Moore PK. GYY4137, a Novel Hydrogen Sulfide-Releasing Molecule, Protects against Endotoxic Shock in the Rat. Free Radic Biol Med. 2009; 47:103–113. [PubMed: 19375498]
122. Li L, Fox B, Keeble J, Salto-Tellez M, Winyard PG, Wood ME, Moore PK, Whiteman M. The Complex Effects of the Slow-Releasing Hydrogen Sulfide Donor GYY4137 in a Model of Acute Joint Inflammation and in Human Cartilage Cells. J Cell Mol Med. 2013; 17:365–376. [PubMed: 23356870]
123. Liu Z, Han Y, Li L, Lu H, Meng G, Li X, Shirhan M, Peh MT, Xie L, Zhou S, et al. The Hydrogen Sulfide Donor, GYY4137, Exhibits Anti-Atherosclerotic Activity in High Fat Fed Apolipoprotein E −/− Mice. Br J Pharmacol. 2013; 169:1795–1809. [PubMed: 23713790]
124. Park C-M, Zhao Y, Zhu Z, Pacheco A, Peng B, Devarie-Baez NO, Bagdon P, Zhang H, Xian M. Synthesis and Evaluation of Phosphorodithioate-Based Hydrogen Sulfide Donors. Mol BioSyst. 2013; 9:2430. [PubMed: 23917226]
125. Alexander BE, Coles SJ, Fox BC, Khan TF, Maliszewski J, Perry A, Pitak MB, Whiteman M, Wood ME, et al. Investigating the Generation of Hydrogen Sulfide from the Phosphonamidodithioate Slow-Release Donor GYY4137. MedChem-Comm. 2015; 6:1649–1655.
126. Kang J, Li Z, Organ CL, Park C-M, Yang C, Pacheco A, Wang D, Lefer DJ, Xian M. pH-Controlled Hydrogen Sulfide Release for Myocardial Ischemia-Reperfusion Injury. J Am Chem Soc. 2016; 138:6336–6339. [PubMed: 27172143]
127. Caliendo G, Cirino G, Santagada V, Wallace JL. Synthesis and Biological Effects of Hydrogen Sulfide (H_2S): Development of H_2S-Releasing Drugs as Pharmaceuticals. J Med Chem. 2010; 53:6275–6286. [PubMed: 20462257]
128. Wallace JL, Caliendo G, Santagada V, Cirino G. Markedly Reduced Toxicity of a Hydrogen Sulphide-Releasing Derivative of Naproxen (ATB-346). Br J Pharmacol. 2010; 159:1236–1246. [PubMed: 20128814]

129. Distrutti E. 5-Amino-2-Hydroxybenzoic Acid 4-(5-Thioxo-5H-[1,2]dithiol-3yl)-Phenyl Ester (ATB-429), a Hydrogen Sulfide-Releasing Derivative of Mesalamine, Exerts Antinociceptive Effects in a Model of Postinflammatory Hypersensitivity. J Pharmacol Exp Ther. 2006; 319:447–458. [PubMed: 16855178]
130. Vannini F, MacKessack-Leitch AC, Eschbach EK, Chattopadhyay M, Kodela R, Kashfi K. Synthesis and Anti-Cancer Potential of the Positional Isomers of NOSH-Aspirin (NBS-1120) a Dual Nitric Oxide and Hydrogen Sulfide Releasing Hybrid. Bioorg Med Chem Lett. 2015; 25:4677–4682. [PubMed: 26323873]
131. Lougiakis N, Papapetropoulos A, Gikas E, Toumpas S, Efentakis P, Wedmann R, Zoga A, Zhou Z, Iliodromitis EK, Skaltsounis A-L, et al. Synthesis and Pharmacological Evaluation of Novel Adenine–Hydrogen Sulfide Slow Release Hybrids Designed as Multitarget Cardioprotective Agents. J Med Chem. 2016; 59:1776–1790. [PubMed: 26809888]
132. Le Trionnaire S, Perry A, Szczesny B, Szabo C, Winyard PG, Whatmore JL, Wood ME, Whiteman M. The Synthesis and Functional Evaluation of a Mitochondria-Targeted Hydrogen Sulfide Donor, (10-Oxo-10-(4-(3-Thioxo-3H-1,2-Dithiol-5-Yl)phenoxy)-decyl)triphenylphosphonium Bromide (AP39). MedChemComm. 2014; 5:728–736.
133. Gerő D, Torregrossa R, Perry A, Waters A, Le-Trionnaire S, Whatmore JL, Wood M, Whiteman M. The Novel Mitochondria-Targeted Hydrogen Sulfide (H2S) Donors AP123 and AP39 Protect against Hyperglycemic Injury in Microvascular Endothelial Cells in Vitro. Pharmacol Res. 2016; 113:186–198. [PubMed: 27565382]
134. Ahmad A, Olah G, Szczesny B, Wood ME, Whiteman M, Szabo C. AP39, A Mitochondrially Targeted Hydrogen Sulfide Donor, Exerts Protective Effects in Renal Epithelial Cells Subjected to Oxidative Stress in Vitro and in Acute Renal Injury in Vivo. Shock. 2016; 45:88–97. [PubMed: 26513708]
135. Wedmann R, Onderka C, Wei S, Szijártó IA, Miljkovic JL, Mitrovic A, Lange M, Savitsky S, Yadav PK, Torregrossa R, et al. Improved Tag-Switch Method Reveals That Thioredoxin Acts as Depersulfidase and Controls the Intracellular Levels of Protein Persulfidation. Chem Sci. 2016; 7:3414–3426. [PubMed: 27170841]
136. Clinical Trials. Gov Identifiers: NCT01926444.
137. Devarie-Baez NO, Bagdon PE, Peng B, Zhao Y, Park C-M, Xian M. Light-Induced Hydrogen Sulfide Release from “Caged” Gem -Dithiols. Org Lett. 2013; 15:2786–2789. [PubMed: 23697786]
138. Zhou Z, von Wantoch Rekowski M, Coletta C, Szabo C, Bucci M, Cirino G, Topouzis S, Papapetropoulos A, Giannis A. Thioglycine and L-Thiovaline: Biologically Active H2S-Donors. Bioorg Med Chem. 2012; 20:2675–2678. [PubMed: 22436388]
139. Steiger AK, Pardue S, Kevil CG, Pluth MD. Self-Immolative Thiocarbamates Provide Access to Triggered H2S Donors and Analyte Replacement Fluorescent Probes. J Am Chem Soc. 2016; 138:7256–7259. [PubMed: 27218691]
140. Powell CR, Foster JC, Okyere B, Theus MH, Matson JB. Therapeutic Delivery of H2S via COS: Small Molecule and Polymeric Donors with Benign Byproducts. J Am Chem Soc. 2016; 138:13477–13480. [PubMed: 27715026]
141. Zhao Y, Bolton SG, Pluth MD. Light-Activated COS/H2S Donation from Photocaged Thiocarbamates. Org Lett. 2017; 19:2278–2281. [PubMed: 28414240]
142. Zhao Y, Pluth MD. Hydrogen Sulfide Donors Activated by Reactive Oxygen Species. Angew Chem, Int Ed. 2016; 55:14638–14642.
143. Xu S, Yang C-T, Meng F-H, Pacheco A, Chen L, Xian M. Ammonium Tetrathiomolybdate as a Water-Soluble and Slow-Release Hydrogen Sulfide Donor. Bioorg Med Chem Lett. 2016; 26:1585–1588. [PubMed: 26898812]
144. Dyson A, Dal-Pizzol F, Sabbatini G, Lach AB, Galfo F, dos Santos Cardoso J, Pescador Mendonça B, Hargreaves I, Bollen Pinto B, Bromage DI, et al. Ammonium Tetrathiomolybdate Following Ischemia/reperfusion Injury: Chemistry, Pharmacology, and Impact of a New Class of Sulfide Donor in Preclinical Injury Models. PLOS Med. 2017; 14:e1002310. [PubMed: 28678794]

145. Zuman P, Szafranski W. Ultraviolet Spectra of Hydroxide, Alkoxide, and Hydrogen Sulfide Anions. Anal Chem. 1976; 48:2162–2163.

146. Kubán V, Dasgupta PK, Marx JN. Nitroprusside and Methylene Blue Methods for Silicone Membrane Differentiated Flow Injection Determination of Sulfide in Water and Wastewater. Anal Chem. 1992; 64:36–43. [PubMed: 1736678]

147. Lawrence NS, Davis J, Jiang L, Jones TGJ, Davies SN, Compton RG. The Electrochemical Analog of the Methylene Blue Reaction: A Novel Amperometric Approach to the Detection of Hydrogen Sulfide. Electroanalysis. 2000; 12:1453–1460.

148. Fischer E. Bildung von Methylenblau Als Reaktion Auf Schwefelwasserstoff. Ber Dtsch Chem Ges. 1883; 16:2234–2236.

149. Fogo JK, Popowsky M. Spectrophotometric Determination of Hydrogen Sulfide. Anal Chem. 1949; 21:732–734.

150. Siegel LM. A Direct Microdetermination for Sulfide. Anal Biochem. 1965; 11:126–132. [PubMed: 14328633]

151. Haddad PR, Heckenberg AL. Trace Determination of Sulfide by Reversed-Phase Ion-Interaction Chromatography Using Pre-Column Derivatization. J Chromatogr. 1988; 447:415–420. [PubMed: 3225287]

152. Small JM, Hintelmann H. Methylene Blue Derivatization Then LC–MS Analysis for Measurement of Trace Levels of Sulfide in Aquatic Samples. Anal Bioanal Chem. 2007; 387:2881–2886. [PubMed: 17323053]

153. Olson KR. A Practical Look at the Chemistry and Biology of Hydrogen Sulfide. Antioxid Redox Signal. 2012; 17:32–44. [PubMed: 22074253]

154. Chen X, Jhee K-H, Kruger WD. Production of the Neuromodulator H_2S by Cystathionine β-Synthase via the Condensation of Cysteine and Homocysteine. J Biol Chem. 2004; 279:52082–52086. [PubMed: 15520012]

155. Hine C, Harputlugil E, Zhang Y, Ruckenstuhl C, Lee BC, Brace L, Longchamp A, Treviño-Villarreal JH, Mejia P, Ozaki CK, et al. Endogenous Hydrogen Sulfide Production Is Essential for Dietary Restriction Benefits. Cell. 2015; 160:132–144. [PubMed: 25542313]

156. Wei Y, Kenyon C. Roles for ROS and Hydrogen Sulfide in the Longevity Response to Germline Loss in Caenorhabditis Elegans. Proc Natl Acad Sci U S A. 2016; 113:E2832–E2841. [PubMed: 27140632]

157. Doeller JE, Isbell TS, Benavides G, Koenitzer J, Patel H, Patel RP, Lancaster JR, Darley-Usmar VM, Kraus DW. Polarographic Measurement of Hydrogen Sulfide Production and Consumption by Mammalian Tissues. Anal Biochem. 2005; 341:40–51. [PubMed: 15866526]

158. Xu T, Scafa N, Xu L-P, Zhou S, Abdullah Al-Ghanem K, Mahboob S, Fugetsu B, Zhang X. Electrochemical Hydrogen Sulfide Biosensors. Analyst. 2016; 141:1185–1195. [PubMed: 26806283]

159. Furne J, Saeed A, Levitt MD. Whole Tissue Hydrogen Sulfide Concentrations Are Orders of Magnitude Lower than Presently Accepted Values. Am J Physiol Regul Integr Comp Physiol. 2008; 295:R1479–R1485. [PubMed: 18799635]

160. Vitvitsky V, Banerjee R. H2S Analysis in Biological Samples Using Gas Chromatography with Sulfur Chemiluminescence Detection. Methods Enzymol. 2015; 554:111–123. [PubMed: 25725519]

161. Kosower NS, Kosower EM, Newton GL, Ranney HM. Bimane Fluorescent Labels: Labeling of Normal Human Red Cells under Physiological Conditions. Proc Natl Acad Sci U S A. 1979; 76:3382–3386. [PubMed: 291011]

162. Wintner EA, Deckwerth TL, Langston W, Bengtsson A, Leviten D, Hill P, Insko MA, Dumpit R, VandenEkart E, Toombs CF, et al. A Monobromobimane-Based Assay to Measure the Pharmacokinetic Profile of Reactive Sulphide Species in Blood. Br J Pharmacol. 2010; 160:941–957. [PubMed: 20590590]

163. Shen X, Pattillo CB, Pardue S, Bir SC, Wang R, Kevil CG. Measurement of Plasma Hydrogen Sulfide in Vivo and in Vitro. Free Radic Biol Med. 2011; 50:1021–1031. [PubMed: 21276849]

164. Shen X, Peter EA, Bir S, Wang R, Kevil CG. Analytical Measurement of Discrete Hydrogen Sulfide Pools in Biological Specimens. Free Radic Biol Med. 2012; 52:2276–2283. [PubMed: 22561703]
165. Ida T, Sawa T, Ihara H, Tsuchiya Y, Watanabe Y, Kumagai Y, Suematsu M, Motohashi H, Fujii S, Matsunaga T, et al. Reactive Cysteine Persulfides and S-Polythiolation Regulate Oxidative Stress and Redox Signaling. Proc Natl Acad Sci U S A. 2014; 111:7606–7611. [PubMed: 24733942]
166. Lin VS, Chen W, Xian M, Chang CJ. Chemical Probes for Molecular Imaging and Detection of Hydrogen Sulfide and Reactive Sulfur Species in Biological Systems. Chem Soc Rev. 2015; 44:4596–4618. [PubMed: 25474627]
167. Takano Y, Shimamoto K, Hanaoka K. Chemical Tools for the Study of Hydrogen Sulfide (H2S) and Sulfane Sulfur and Their Applications to Biological Studies. J Clin Biochem Nutr. 2016; 58:7–15. [PubMed: 26798192]
168. Feng W, Dymock BW. Fluorescent Probes for H2S Detection and Quantification. Handb Exp Pharmacol. 2015; 230:291–323. [PubMed: 26162841]
169. Lippert AR, New EJ, Chang CJ. Reaction-Based Fluorescent Probes for Selective Imaging of Hydrogen Sulfide in Living Cells. J Am Chem Soc. 2011; 133:10078–10080. [PubMed: 21671682]
170. Peng H, Cheng Y, Dai C, King AL, Predmore BL, Lefer DJ, Wang B. A Fluorescent Probe for Fast and Quantitative Detection of Hydrogen Sulfide in Blood. Angew Chem, Int Ed. 2011; 50:9672–9675.
171. Montoya LA, Pluth MD. Selective Turn-on Fluorescent Probes for Imaging Hydrogen Sulfide in Living Cells. Chem Commun. 2012; 48:4767.
172. Qian Y, Karpus J, Kabil O, Zhang S-Y, Zhu H-L, Banerjee R, Zhao J, He C. Selective Fluorescent Probes for Live-Cell Monitoring of Sulphide. Nat Commun. 2011; 2:495. [PubMed: 21988911]
173. Liu C, Pan J, Li S, Zhao Y, Wu LY, Berkman CE, Whorton AR, Xian M. Capture and Visualization of Hydrogen Sulfide by a Fluorescent Probe. Angew Chem, Int Ed. 2011; 50:10327–10329.
174. Sasakura K, Hanaoka K, Shibuya N, Mikami Y, Kimura Y, Komatsu T, Ueno T, Terai T, Kimura H, Nagano T. Development of a Highly Selective Fluorescence Probe for Hydrogen Sulfide. J Am Chem Soc. 2011; 133:18003–18005. [PubMed: 21999237]
175. Olson KR, DeLeon ER, Liu F. Controversies and Conundrums in Hydrogen Sulfide Biology. Nitric Oxide. 2014; 41:11–26. [PubMed: 24928561]
176. Olson KR. Is Hydrogen Sulfide a Circulating “gasotransmitter” in Vertebrate Blood? Biochim Biophys Acta, Bioenerg. 2009; 1787:856–863.
177. Whitfield NL, Kreimier EL, Verdial FC, Skovgaard N, Olson KR. Reappraisal of H2S/sulfide Concentration in Vertebrate Blood and Its Potential Significance in Ischemic Preconditioning and Vascular Signaling. Am J Physiol Regul Integr Comp Physiol. 2008; 294:R1930–R1937. [PubMed: 18417642]
178. Levitt MD, Abdel-Rehim MS, Furne J. Free and Acid-Labile Hydrogen Sulfide Concentrations in Mouse Tissues: Anomalously High Free Hydrogen Sulfide in Aortic Tissue. Antioxid Redox Signal. 2011; 15:373–378. [PubMed: 20812866]
179. Vitvitsky V, Kabil O, Banerjee R. High Turnover Rates for Hydrogen Sulfide Allow for Rapid Regulation of Its Tissue Concentrations. Antioxid Redox Signal. 2012; 17:22–31. [PubMed: 22229551]
180. Linden DR, Sha L, Mazzone A, Stoltz GJ, Bernard CE, Furne JK, Levitt MD, Farrugia G, Szurszewski JH. Production of the Gaseous Signal Molecule Hydrogen Sulfide in Mouse Tissues. J Neurochem. 2008; 106:1577–1585. [PubMed: 18513201]
181. Kabil O, Banerjee R. Redox Biochemistry of Hydrogen Sulfide. J Biol Chem. 2010; 285:21903–21907. [PubMed: 20448039]
182. Singh S, Banerjee R. PLP-Dependent H2S Biogenesis. Biochim Biophys Acta, Proteins Proteomics. 2011; 1814:1518–1527.
183. Kabil O, Banerjee R. Enzymology of H2S Biogenesis, Decay and Signaling. Antioxid Redox Signal. 2014; 20:770–782. [PubMed: 23600844]

184. Kabil O, Motl N, Banerjee R. H2S and Its Role in Redox Signaling. Biochim Biophys Acta, Proteins Proteomics. 2014; 1844:1355–1366.

185. Stipanuk MH, Beck PW. Characterization of the Enzymic Capacity for Cysteine Desulphhydration in Liver and Kidney of the Rat. Biochem J. 1982; 206:267–277. [PubMed: 7150244]

186. Kabil O, Zhou Y, Banerjee R. Human Cystathionine β-Synthase Is a Target for Sumoylation. Biochemistry. 2006; 45:13528–13536. [PubMed: 17087506]

187. Teng H, Wu B, Zhao K, Yang G, Wu L, Wang R. Oxygen-Sensitive Mitochondrial Accumulation of Cystathionine -Synthase Mediated by Lon Protease. Proc Natl Acad Sci U S A. 2013; 110:12679–12684. [PubMed: 23858469]

188. Fu M, Zhang W, Wu L, Yang G, Li H, Wang R. Hydrogen Sulfide (H2S) Metabolism in Mitochondria and Its Regulatory Role in Energy Production. Proc Natl Acad Sci U S A. 2012; 109:2943–2948. [PubMed: 22323590]

189. Nagahara N, Ito T, Kitamura H, Nishino T. Tissue and Subcellular Distribution of Mercaptopyruvate Sulfurtransferase in the Rat: Confocal Laser Fluorescence and Immunoelectron Microscopic Studies Combined with Biochemical Analysis. Histochem Cell Biol. 1998; 110:243–250. [PubMed: 9749958]

190. Singh S, Padovani D, Leslie RA, Chiku T, Banerjee R. Relative Contributions of Cystathionine β-Synthase and γ-Cystathio-nase to H2S Biogenesis via Alternative Trans-Sulfuration Reactions. J Biol Chem. 2009; 284:22457–22466. [PubMed: 19531479]

191. Mishanina TV, Libiad M, Banerjee R. Biogenesis of Reactive Sulfur Species for Signaling by Hydrogen Sulfide Oxidation Pathways. Nat Chem Biol. 2015; 11:457–464. [PubMed: 26083070]

192. Braunstein AE, Goryachenkova EV, Lac ND. Reactions Catalysed by Serine Sulfhydrase from Chicken Liver. Biochim Biophys Acta. 1969; 171:366–368. [PubMed: 5773443]

193. Mudd SH, Finkelstein JD, Irreverre F, Laster L. Homocystinuria: An Enzymatic Defect. Science. 1964; 143:1443–1445. [PubMed: 14107447]

194. Ereño-Orbea J, Majtan T, Oyenarte I, Kraus JP, Martínez-Cruz LA. Structural Basis of Regulation and Oligomerization of Human Cystathionine β-Synthase, the Central Enzyme of Transsulfuration. Proc Natl Acad Sci U S A. 2013; 110:E3790–E3799. [PubMed: 24043838]

195. Ereño-Orbea J, Majtan T, Oyenarte I, Kraus JP, Martínez-Cruz LA. Structural Insight into the Molecular Mechanism of Allosteric Activation of Human Cystathionine β-Synthase by S -Adenosylmethionine. Proc Natl Acad Sci U S A. 2014; 111:E3845–E3852. [PubMed: 25197074]

196. Koutmos M, Kabil O, Smith JL, Banerjee R. Structural Basis for Substrate Activation and Regulation by Cystathionine Beta-Synthase (CBS) Domains in Cystathionine Beta-Synthase. Proc Natl Acad Sci U S A. 2010; 107:20958–20963. [PubMed: 21081698]

197. Kery V, Bukovska G, Kraus JP. Transsulfuration Depends on Heme in Addition to Pyridoxal 5′-phosphate. Cystathionine Beta-Synthase Is a Heme Protein. J Biol Chem. 1994; 269:25283–25288. [PubMed: 7929220]

198. Alexander FW, Sandmeier E, Mehta PK, Christen P. Evolutionary Relationships among Pyridoxal-5′-phosphate-Dependent Enzymes. Regio-Specific Alpha, Beta and Gamma Families. Eur J Biochem. 1994; 219:953–960. [PubMed: 8112347]

199. Meier M. Structure of Human Cystathionine Beta-Synthase: A Unique Pyridoxal 5′-phosphate-Dependent Heme Protein. EMBO J. 2001; 20:3910–3916. [PubMed: 11483494]

200. Taoka S, Lepore BW, Kabil O, Ojha S, Ringe D, Banerjee R. Human Cystathionine Beta-Synthase Is a Heme Sensor Protein. Evidence That the Redox Sensor Is Heme and Not the Vicinal Cysteines in the CXXC Motif Seen in the Crystal Structure of the Truncated Enzyme. Biochemistry. 2002; 41:10454–10461. [PubMed: 12173932]

201. Bar-Or D, Rael LT, Thomas GW, Kraus JP. Inhibitory Effect of Copper on Cystathionine Beta-Synthase Activity: Protective Effect of an Analog of the Human Albumin N-Terminus. Protein Pept Lett. 2005; 12:271–273. [PubMed: 15777277]

202. Bateman A. The Structure of a Domain Common to Archaebacteria and the Homocystinuria Disease Protein. Trends Biochem Sci. 1997; 22:12–13.

203. Scott JW, Hawley SA, Green KA, Anis M, Stewart G, Scullion GA, Norman DG, Hardie DG. CBS Domains Form Energy-Sensing Modules Whose Binding of Adenosine Ligands Is Disrupted by Disease Mutations. J Clin Invest. 2004; 113:274–284. [PubMed: 14722619]
204. Finkelstein JD, Kyle WE, Martin JJ, Pick A-M. Activation of Cystathionine Synthase by Adenosylmethionine and Adenosylethionine. Biochem Biophys Res Commun. 1975; 66:81–87. [PubMed: 1164439]
205. Kabil H, Kabil O, Banerjee R, Harshman LG, Pletcher SD. Increased Transsulfuration Mediates Longevity and Dietary Restriction in Drosophila. Proc Natl Acad Sci U S A. 2011; 108:16831–16836. [PubMed: 21930912]
206. Kery V, Poneleit L, Kraus JP. Trypsin Cleavage of Human Cystathionine β-Synthase into an Evolutionarily Conserved Active Core: Structural and Functional Consequences. Arch Biochem Biophys. 1998; 355:222–232. [PubMed: 9675031]
207. Taoka S, Ohja S, Shan X, Kruger WD, Banerjee R. Evidence for Heme-Mediated Redox Regulation of Human Cystathionine Beta-Synthase Activity. J Biol Chem. 1998; 273:25179–25184. [PubMed: 9737978]
208. Kabil Ö, Toaka S, LoBrutto R, Shoemaker R, Banerjee R. Pyridoxal Phosphate Binding Sites Are Similar in Human Heme-Dependent and Yeast Heme-Independent Cystathionine β-Synthases. J Biol Chem. 2001; 276:19350–19355. [PubMed: 11278994]
209. Green EL, Taoka S, Banerjee R, Loehr TM. Resonance Raman Characterization of the Heme Cofactor in Cystathionine Beta-Synthase. Identification of the Fe-S(Cys) Vibration in the Six-Coordinate Low-Spin Heme. Biochemistry. 2001; 40:459–463. [PubMed: 11148040]
210. Taoka S, Green EL, Loehr TM, Banerjee R. Mercuric Chloride-Induced Spin or Ligation State Changes in Ferric or Ferrous Human Cystathionine Beta-Synthase Inhibit Enzyme Activity. J Inorg Biochem. 2001; 87:253–259. [PubMed: 11744063]
211. Jhee KH, McPhie P, Miles EW. Yeast Cystathionine Beta-Synthase Is a Pyridoxal Phosphate Enzyme But, Unlike the Human Enzyme, Is Not a Heme Protein. J Biol Chem. 2000; 275:11541–11544. [PubMed: 10766767]
212. Evande R, Ojha S, Banerjee R. Visualization of PLP-Bound Intermediates in Hemeless Variants of Human Cystathionine β-Synthase: Evidence That Lysine 119 Is a General Base. Arch Biochem Biophys. 2004; 427:188–196. [PubMed: 15196993]
213. Ojha S, Hwang J, Kabil O, Penner-Hahn JE, Banerjee R. Characterization of the Heme in Human Cystathionine Beta-Synthase by X-Ray Absorption and Electron Paramagnetic Resonance Spectros-copies. Biochemistry. 2000; 39:10542–10547. [PubMed: 10956045]
214. Singh S, Madzelan P, Banerjee R. Properties of an Unusual Heme Cofactor in PLP-Dependent Cystathionine β-Synthase. Nat Prod Rep. 2007; 24:631–639. [PubMed: 17534535]
215. Singh S, Madzelan P, Stasser J, Weeks CL, Becker D, Spiro TG, Penner-Hahn J, Banerjee R. Modulation of the Heme Electronic Structure and Cystathionine β-Synthase Activity by Second Coordination Sphere Ligands: The Role of Heme Ligand Switching in Redox Regulation. J Inorg Biochem. 2009; 103:689–697. [PubMed: 19232736]
216. Carballal S, Madzelan P, Zinola CF, Graña M, Radi R, Banerjee R, Alvarez B. Dioxygen Reactivity and Heme Redox Potential of Truncated Human Cystathionine β-Synthase. Biochemistry. 2008; 47:3194–3201. [PubMed: 18278872]
217. Taoka S, West M, Banerjee R. Characterization of the Heme and Pyridoxal Phosphate Cofactors of Human Cystathionine β-Synthase Reveals Nonequivalent Active Sites. Biochemistry. 1999; 38:2738–2744. [PubMed: 10052944]
218. Taoka S, Banerjee R. Characterization of NO Binding to Human Cystathionine Beta-Synthase: Possible Implications of the Effects of CO and NO Binding to the Human Enzyme. J Inorg Biochem. 2001; 87:245–251. [PubMed: 11744062]
219. Vadon-Le Goff S, Delaforge M, Boucher J-L, Janosik M, Kraus JP, Mansuy D. Coordination Chemistry of the Heme in Cystathionine β-Synthase: Formation of Iron(II)–Isonitrile Complexes. Biochem Biophys Res Commun. 2001; 283:487–492. [PubMed: 11327727]
220. Gherasim C, Yadav PK, Kabil O, Niu W-N, Banerjee R. Nitrite Reductase Activity and Inhibition of H2S Biogenesis by Human Cystathionine SS-Synthas. PLoS One. 2014; 9:e85544. [PubMed: 24416422]

221. Kabil O, Weeks CL, Carballal S, Gherasim C, Alvarez B, Spiro TG, Banerjee R. Reversible Heme-Dependent Regulation of Human Cystathionine β-Synthase by a Flavoprotein Oxidoreductase. Biochemistry. 2011; 50:8261–8263. [PubMed: 21875066]
222. Carballal S, Cuevasanta E, Yadav PK, Gherasim C, Ballou DP, Alvarez B, Banerjee R. Kinetics of Nitrite Reduction and Peroxynitrite Formation by Ferrous Heme in Human Cystathionine β-Synthase. J Biol Chem. 2016; 291:8004–8013. [PubMed: 26867575]
223. Vicente JB, Colaço HG, Sarti P, Leandro P, Giuffrè A. S-Adenosyl-L-Methionine Modulates CO and NO• Binding to the Human H2S-Generating Enzyme Cystathionine β-Synthase. J Biol Chem. 2016; 291:572–581. [PubMed: 26582199]
224. Yadav PK, Banerjee R. Detection of Reaction Intermediates during Human Cystathionine β-Synthase-Monitored Turnover and H2S Production. J Biol Chem. 2012; 287:43464–43471. [PubMed: 23124209]
225. Singh S, Ballou DP, Banerjee R. Pre-Steady-State Kinetic Analysis of Enzyme-Monitored Turnover during Cystathionine β-Synthase-Catalyzed H_2S Generation. Biochemistry. 2011; 50:419–425. [PubMed: 21141970]
226. Yadav PK, Martinov M, Vitvitsky V, Seravalli J, Wedmann R, Filipovic MR, Banerjee R. Biosynthesis and Reactivity of Cysteine Persulfides in Signaling. J Am Chem Soc. 2016; 138:289–299. [PubMed: 26667407]
227. Vicente JB, Colaço HG, Mendes MIS, Sarti P, Leandro P, Giuffrè A. $NO^{\bullet}$ Binds Human Cystathionine β-Synthase Quickly and Tightly. J Biol Chem. 2014; 289:8579–8587. [PubMed: 24515102]
228. Puranik M, Nielsen SB, Youn H, Hvitved AN, Bourassa JL, Case MA, Tengroth C, Balakrishnan G, Thorsteinsson MV, Groves JT, et al. Dynamics of Carbon Monoxide Binding to CooA. J Biol Chem. 2004; 279:21096–21108. [PubMed: 14990568]
229. Ojha S, Wu J, LoBrutto R, Banerjee R. Effects of Heme Ligand Mutations Including a Pathogenic Variant, H65R, on the Properties of Human Cystathionine Beta-Synthase. Biochemistry. 2002; 41:4649–4654. [PubMed: 11926827]
230. Weeks CL, Singh S, Madzelan P, Banerjee R, Spiro TG. Heme Regulation of Human Cystathionine β-Synthase Activity: Insights from Fluorescence and Raman Spectroscopy. J Am Chem Soc. 2009; 131:12809–12816. [PubMed: 19722721]
231. Pazicni S, Cherney MM, Lukat-Rodgers GS, Oliveriusová J, Rodgers KR, Kraus JP, Burstyn JN. The Heme of Cystathionine Beta-Synthase Likely Undergoes a Thermally Induced Redox-Mediated Ligand Switch. Biochemistry. 2005; 44:16785–16795. [PubMed: 16363792]
232. Smith AT, Su Y, Stevens DJ, Majtan T, Kraus JP, Burstyn JN. Effect of the Disease-Causing R266K Mutation on the Heme and PLP Environments of Human Cystathionine β-Synthase. Biochemistry. 2012; 51:6360–6370. [PubMed: 22738154]
233. Yadav PK, Xie P, Banerjee R. Allosteric Communication between the Pyridoxal 5′-Phosphate (PLP) and Heme Sites in the H2S Generator Human Cystathionine β-Synthase. J Biol Chem. 2012; 287:37611–37620. [PubMed: 22977242]
234. Evande R, Blom H, Boers GHJ, Banerjee R. Alleviation of Intrasteric Inhibition by the Pathogenic Activation Domain Mutation, D444N, in Human Cystathionine Beta-Synthase. Biochemistry. 2002; 41:11832–11837. [PubMed: 12269827]
235. Janosík M, Kery V, Gaustadnes M, Maclean KN, Kraus JP. Regulation of Human Cystathionine Beta-Synthase by S-Adenosyl-L-Methionine: Evidence for Two Catalytically Active Conformations Involving an Autoinhibitory Domain in the C-Terminal Region. Biochemistry. 2001; 40:10625–10633. [PubMed: 11524006]
236. Mendes MIS, Santos AS, Smith DEC, Lino PR, Colaço HG, de Almeida IT, Vicente JB, Salomons GS, Rivera I, Blom HJ, et al. Insights into the Regulatory Domain of Cystathionine Beta-Synthase: Characterization of Six Variant Proteins. Hum Mutat. 2014; 35:1195–1202. [PubMed: 25044645]
237. Shan X, Kruger WD. Correction of Disease-Causing CBS Mutations in Yeast. Nat Genet. 1998; 19:91–93. [PubMed: 9590298]

238. Shan X, Dunbrack RL, Christopher SA, Kruger WD. Mutations in the Regulatory Domain of Cystathionine Beta Synthase Can Functionally Suppress Patient-Derived Mutations in Cis. Hum Mol Genet. 2001; 10:635–643. [PubMed: 11230183]

239. Agrawal N, Banerjee R. Human Polycomb 2 Protein Is a SUMO E3 Ligase and Alleviates Substrate-Induced Inhibition of Cystathionine β-Synthase Sumoylation. PLoS One. 2008; 3:e4032. [PubMed: 19107218]

240. Kurepa J, Walker JM, Smalle J, Gosink MM, Davis SJ, Durham TL, Sung D-Y, Vierstra RD. The Small Ubiquitin-like Modifier (SUMO) Protein Modification System in Arabidopsis. J Biol Chem. 2003; 278:6862–6872. [PubMed: 12482876]

241. Hong Y, Rogers R, Matunis MJ, Mayhew CN, Goodson M, Park-Sarge O-K, Sarge KD. Regulation of Heat Shock Transcription Factor 1 by Stress-Induced SUMO-1 Modification. J Biol Chem. 2001; 276:40263–40267. [PubMed: 11514557]

242. Zhou W, Ryan JJ, Zhou H. Global Analyses of Sumoylated Proteins in Saccharomyces Cerevisiae. J Biol Chem. 2004; 279:32262–32268. [PubMed: 15166219]

243. Niu W-N, Yadav PK, Adamec J, Banerjee R. S-Glutathionylation Enhances Human Cystathionine β-Synthase Activity under Oxidative Stress Conditions. Antioxid Redox Signal. 2015; 22:350–361. [PubMed: 24893130]

244. Vitvitsky V, Thomas M, Ghorpade A, Gendelman HE, Banerjee R. A Functional Transsulfuration Pathway in the Brain Links to Glutathione Homeostasis. J Biol Chem. 2006; 281:35785–35793. [PubMed: 17005561]

245. Mosharov E, Cranford MR, Banerjee R. The Quantitatively Important Relationship between Homocysteine Metabolism and Glutathione Synthesis by the Transsulfuration Pathway and Its Regulation by Redox Changes. Biochemistry. 2000; 39:13005–13011. [PubMed: 11041866]

246. d'Emmanuele di Villa Bianca R, Mitidieri E, Esposito D, Donnarumm E, Russo A, Fusco F, Ianaro A, Mirone V, Cirino G, Russo G, et al. Human Cystathionine-β-Synthase Phosphorylation on Serine227 Modulates Hydrogen Sulfide Production in Human Urothelium. PLoS One. 2015; 10:e0136859. [PubMed: 26368121]

247. d'Emmanuele di Villa Bianca R, Mitidieri E, Fusco F, Russo A, Pagliara V, Tramontano T, Donnarumma E, Mirone V, Cirino G, Russo G, et al. Urothelium Muscarinic Activation Phosphorylates CBSSer227 via cGMP/PKG Pathway Causing Human Bladder Relaxation through H2S Production. Sci Rep. 2016; 6:31491. [PubMed: 27509878]

248. Zhu W, Lin A, Banerjee R. Kinetic Properties of Polymorphic Variants and Pathogenic Mutants in Human Cystathio-nine γ-Lyase. Biochemistry. 2008; 47:6226–6232. [PubMed: 18476726]

249. Chiku T, Padovani D, Zhu W, Singh S, Vitvitsky V, Banerjee R. H2S Biogenesis by Human Cystathionine Gamma-Lyase Leads to the Novel Sulfur Metabolites Lanthionine and Homolanthionine and Is Responsive to the Grade of Hyperhomocysteinemia. J Biol Chem. 2009; 284:11601–11612. [PubMed: 19261609]

250. Scott CR, Dassell SW, Clark SH, Chiang-Teng C, Swedberg KR. Cystathioninemia: A Benign Genetic Condition. J Pediatr. 1970; 76:571–577. [PubMed: 5420794]

251. Kraus JP, Hašek J, Kožich V, Collard R, Venezia S, Janošíková B, Wang J, Stabler SP, Allen RH, Jakobs C, et al. Cystathionine γ-Lyase: Clinical, Metabolic, Genetic, and Structural Studies. Mol Genet Metab. 2009; 97:250–259. [PubMed: 19428278]

252. Wang J, Hegele RA. Genomic Basis of Cystathioninuria (MIM 219500) Revealed by Multiple Mutations in Cystathionine Gamma-Lyase (CTH). Hum Genet. 2003; 112:404–408. [PubMed: 12574942]

253. Perry TL, Hansen S, MacDougall L. Homolanthionine Excretion in Homocystinuria. Science. 1966; 152:1750–1752. [PubMed: 5938411]

254. Kabil O, Vitvitsky V, Xie P, Banerjee R. The Quantitative Significance of the Transsulfuration Enzymes for H_2S Production in Murine Tissues. Antioxid Redox Signal. 2011; 15:363–372. [PubMed: 21254839]

255. Sun Q, Collins R, Huang S, Holmberg-Schiavone L, Anand GS, Tan C-H, Van-den-Berg S, Deng L-W, Moore PK, Karlberg T, et al. Structural Basis for the Inhibition Mechanism of Human Cystathionine γ-Lyase, an Enzyme Responsible for the Production of H2S. J Biol Chem. 2009; 284:3076–3085. [PubMed: 19019829]

256. Messerschmidt A, Worbs M, Steegborn C, Wahl MC, Huber R, Laber B, Clausen T. Determinants of Enzymatic Specificity in the Cys-Met-Metabolism PLP-Dependent Enzyme Family: Crystal Structure of Cystathionine γ-Lyase from Yeast and Intrafamiliar Structure Comparison. Biol Chem. 2003; 384:373–386. [PubMed: 12715888]

257. Huang S, Chua JH, Yew WS, Sivaraman J, Moore PK, Tan C-H, Deng L-W. Site-Directed Mutagenesis on Human Cystathionine-γ-Lyase Reveals Insights into the Modulation of H2S Production. J Mol Biol. 2010; 396:708–718. [PubMed: 19961860]

258. Mihara H, Fujii T, Kato S-i, Kurihara T, Hata Y, Esaki N. Structure of External Aldimine of Escherichia Coli CsdB, an IscS/Nifs Homolog: Implications for Its Specificity toward Selenocysteine. J Biochem. 2002; 131:679–685. [PubMed: 11983074]

259. Sturman JA, Beratis NG, Guarini L, Gaull GE. Transsulfuration by Human Long Term Lymphoid Lines. Normal and Cystathionase-Deficient Cells. J Biol Chem. 1980; 255:4763–4765. [PubMed: 7372609]

260. Yuan G, Vasavda C, Peng YJ, Makarenko VV, Raghuraman G, Nanduri J, Gadalla MM, Semenza GL, Kumar GK, Snyder SH, et al. Protein Kinase G-Regulated Production of H2S Governs Oxygen Sensing. Sci Signaling. 2015; 8:ra37–ra37.

261. Mikami Y, Shibuya N, Ogasawara Y, Kimura H. Hydrogen Sulfide Is Produced by Cystathionine γ-Lyase at the Steady-State Low Intracellular Ca2+ Concentrations. Biochem Biophys Res Commun. 2013; 431:131–135. [PubMed: 23313510]

262. Kabil O, Yadav V, Banerjee R. Heme-Dependent Metabolite Switching Regulates H2S Synthesis in Response to Endoplasmic Reticulum (ER) Stress. J Biol Chem. 2016; 291:16418–16423. [PubMed: 27365395]

263. Dickhout JG, Carlisle RE, Jerome DE, Mohammed-Ali Z, Jiang H, Yang G, Mani S, Garg SK, Banerjee R, Kaufman RJ, et al. Integrated Stress Response Modulates Cellular Redox State via Induction of Cystathionine γ-Lyase. J Biol Chem. 2012; 287:7603–7614. [PubMed: 22215680]

264. Liu X-M, Peyton KJ, Ensenat D, Wang H, Schafer AI, Alam J, Durante W. Endoplasmic Reticulum Stress Stimulates Heme Oxygenase-1 Gene Expression in Vascular Smooth Muscle. J Biol Chem. 2005; 280:872–877. [PubMed: 15546873]

265. Cao SS, Kaufman RJ. Endoplasmic Reticulum Stress and Oxidative Stress in Cell Fate Decision and Human Disease. Antioxid Redox Signal. 2014; 21:396–413. [PubMed: 24702237]

266. Coletta C, Papapetropoulos A, Erdelyi K, Olah G, Modis K, Panopoulos P, Asimakopoulou A, Gero D, Sharina I, Martin E, et al. Hydrogen Sulfide and Nitric Oxide Are Mutually Dependent in the Regulation of Angiogenesis and Endothelium-Dependent Vasorelaxation. Proc Natl Acad Sci U S A. 2012; 109:9161–9166. [PubMed: 22570497]

267. Eberhardt M, Dux M, Namer B, Miljkovic J, Cordasic N, Will C, Kichko TI, de la Roche J, Fischer M, Suárez SA, et al. H2S and NO Cooperatively Regulate Vascular Tone by Activating a Neuroendocrine HNO–TRPA1–CGRP Signalling Pathway. Nat Commun. 2014; 5:4381. [PubMed: 25023795]

268. King AL, Polhemus DJ, Bhushan S, Otsuka H, Kondo K, Nicholson CK, Bradley JM, Islam KN, Calvert JW, Tao Y-X, et al. Hydrogen Sulfide Cytoprotective Signaling Is Endothelial Nitric Oxide Synthase-Nitric Oxide Dependent. Proc Natl Acad Sci U S A. 2014; 111:3182–3187. [PubMed: 24516168]

269. Shibuya N, Tanaka M, Yoshida M, Ogasawara Y, Togawa T, Ishii K, Kimura H. 3-Mercaptopyruvate Sulfurtransferase Produces Hydrogen Sulfide and Bound Sulfane Sulfur in the Brain. Antioxid Redox Signal. 2009; 11:703–714. [PubMed: 18855522]

270. Mikami Y, Shibuya N, Kimura Y, Nagahara N, Ogasawara Y, Kimura H. Thioredoxin and Dihydrolipoic Acid Are Required for 3-Mercaptopyruvate Sulfurtransferase to Produce Hydrogen Sulfide. Biochem J. 2011; 439:479–485. [PubMed: 21732914]

271. Yadav PK, Yamada K, Chiku T, Koutmos M, Banerjee R. Structure and Kinetic Analysis of H2S Production by Human Mercaptopyruvate Sulfurtransferase. J Biol Chem. 2013; 288:20002–20013. [PubMed: 23698001]

272. Nagahara N, Ito T, Minami M. Mercaptopyruvate Sulfurtransferase as a Defense against Cyanide Toxication: Molecular Properties and Mode of Detoxification. Histol Histopathol. 1999; 14:1277–1286. [PubMed: 10506943]

273. Williams RAM, Kelly SM, Mottram JC, Coombs GH. 3-Mercaptopyruvate Sulfurtransferase of Leishmania Contains an Unusual C-Terminal Extension and Is Involved in Thioredoxin and Antioxidant Metabolism. J Biol Chem. 2003; 278:1480–1486. [PubMed: 12419809]

274. Westrop GD, Georg I, Coombs GH. The Mercaptopyruvate Sulfurtransferase of Trichomonas Vaginalis Links Cysteine Catabolism to the Production of Thioredoxin Persulfide. J Biol Chem. 2009; 284:33485–33494. [PubMed: 19762467]

275. Nagahara N, Katayama A. Post-Translational Regulation of Mercaptopyruvate Sulfurtransferase via a Low Redox Potential Cysteine-Sulfenate in the Maintenance of Redox Homeostasis. J Biol Chem. 2005; 280:34569–34576. [PubMed: 16107337]

276. Huang J, Niknahad H, Khan S, O'Brien PJ. Hepatocyte-Catalysed Detoxification of Cyanide by L- and D-Cysteine. Biochem Pharmacol. 1998; 55:1983–1990. [PubMed: 9714318]

277. Shibuya N, Koike S, Tanaka M, Ishigami-Yuasa M, Kimura Y, Ogasawara Y, Fukui K, Nagahara N, Kimura H. A Novel Pathway for the Production of Hydrogen Sulfide from D-Cysteine in Mammalian Cells. Nat Commun. 2013; 4:1366. [PubMed: 23340406]

278. Nagahara N, Nishino T. Role of Amino Acid Residues in the Active Site of Rat Liver Mercaptopyruvate Sulfurtransferase. CDNA Cloning, Overexpression, and Site-Directed Mutagenesis. J Biol Chem. 1996; 271:27395–27401. [PubMed: 8910318]

279. Alphey MS, Williams RAM, Mottram JC, Coombs GH, Hunter WN. The Crystal Structure of Leishmania Major 3-Mercaptopyruvate Sulfurtransferase. A Three-Domain Architecture with a Serine Protease-like Triad at the Active Site. J Biol Chem. 2003; 278:48219–48227. [PubMed: 12952945]

280. Huang G-T, Yu J-SK. Enzyme Catalysis That Paves the Way for S-Sulfhydration via Sulfur Atom Transfer. J Phys Chem B. 2016; 120:4608–4615. [PubMed: 27146345]

281. Nagahara N. Regulation of Mercaptopyruvate Sulfurtransfer-ase Activity Via Intrasubunit and Intersubunit Redox-Sensing Switches. Antioxid Redox Signal. 2013; 19:1792–1802. [PubMed: 23146073]

282. Mikami Y, Shibuya N, Kimura Y, Nagahara N, Yamada M, Kimura H. Hydrogen Sulfide Protects the Retina from Light-Induced Degeneration by the Modulation of Ca2+ Influx. J Biol Chem. 2011; 286:39379–39386. [PubMed: 21937432]

283. Abeles RH, Walsh CT, Acetylenic Enzyme Inactivators. Inactivation of Gamma-Cystathionase, in Vitro and in Vivo, by Propargylglycine. J Am Chem Soc. 1973; 95:6124–6125. [PubMed: 4733835]

284. Shinozijka S, Tanase S, Morino Y. Metabolic Consequences of Affinity Labeling of Cystathionase and Alanine Aminotransferase by L-Propargylglycine in Vivo. Eur J Biochem. 1982; 124:377–382. [PubMed: 7094918]

285. Asimakopoulou A, Panopoulos P, Chasapis CT, Coletta C, Zhou Z, Cirino G, Giannis A, Szabo C, Spyroulias GA, Papapetropoulos A. Selectivity of Commonly Used Pharmacological Inhibitors for Cystathionine β Synthase (CBS) and Cystathionine γ Lyase (CSE). Br J Pharmacol. 2013; 169:922–932. [PubMed: 23488457]

286. Alston TA, Porter DJT, Mela L, Bright HJ. Inactivation of Alanine Aminotransferase by the Neurotoxin β-Cyano-L-Alanine. Biochem Biophys Res Commun. 1980; 92:299–304. [PubMed: 7356461]

287. Pfeffer M, Ressler C. β-Cyanoalanine, an Inhibitor of Rat Liver Cystathionase. Biochem Pharmacol. 1967; 16:2299–2308. [PubMed: 6075392]

288. Ressler C, Nelson J, Pfeffer M. Metabolism of Beta-Cyanoalanine. Biochem Pharmacol. 1967; 16:2309–2319. [PubMed: 6075393]

289. Steegborn C, Clausen T, Sondermann P, Jacob U, Worbs M, Marinkovic S, Huber R, Wahl MC. Kinetics and Inhibition of Recombinant Human Cystathionine Gamma-Lyase. Toward the Rational Control of Transsulfuration. J Biol Chem. 1999; 274:12675–12684. [PubMed: 10212249]

290. Capitani G, McCarthy DL, Gut H, Grütter MG, Kirsch JF. Apple 1-Aminocyclopropane-1-Carboxylate Synthase in Complex with the Inhibitor L-Aminoethoxyvinylglycine. Evidence for a Ketimine Intermediate. J Biol Chem. 2002; 277:49735–49742. [PubMed: 12228256]

291. Clausen T, Huber R, Messerschmidt A, Pohlenz HD, Laber B. Slow-Binding Inhibition of Escherichia Coli Cystathionine Beta-Lyase by L-Aminoethoxyvinylglycine: A Kinetic and X-Ray Study. Biochemistry. 1997; 36:12633–12643. [PubMed: 9376370]
292. Druzhyna N, Szczesny B, Olah G, Mo´dis K, Asimakopoulou A, Pavlidou A, Szoleczky P, Gerö D, Yanagi K, Törö G, et al. Screening of a Composite Library of Clinically Used Drugs and Well-Characterized Pharmacological Compounds for Cystathionine β-Synthase Inhibition Identifies Benserazide as a Drug Potentially Suitable for Repurposing for the Experimental Therapy of Colon. Pharmacol Res. 2016; 113:18–37. [PubMed: 27521834]
293. Thorson MK, Majtan T, Kraus JP, Barrios AM. Identification of Cystathionine β-Synthase Inhibitors Using a Hydrogen Sulfide Selective Probe. Angew Chem, Int Ed. 2013; 52:4641–4644.
294. Niu W, Wu P, Chen F, Wang J, Shang X, Xu C. Discovery of Selective Cystathionine β-Synthase Inhibitors by High-Throughput Screening with a Fluorescent Thiol Probe. MedChem-Comm. 2017; 8:198–201.
295. McCune CD, Chan SJ, Beio ML, Shen W, Chung WJ, Szczesniak LM, Chai C, Koh SQ, Wong PT-H, Berkowitz DB. Zipped Synthesis" by Cross-Metathesis Provides a Cystathionine β-Synthase Inhibitor That Attenuates Cellular H_2S Levels and Reduces Neuronal Infarction in a Rat Ischemic Stroke Model. ACS Cent Sci. 2016; 2:242–252. [PubMed: 27163055]
296. Bouillaud F, Blachier F. Mitochondria and Sulfide: A Very Old Story of Poisoning, Feeding, and Signaling? Antioxid Redox Signal. 2011; 15:379–391. [PubMed: 21028947]
297. Hildebrandt TM, Grieshaber MK. Three Enzymatic Activities Catalyze the Oxidation of Sulfide to Thiosulfate in Mammalian and Invertebrate Mitochondria. FEBS J. 2008; 275:3352–3361. [PubMed: 18494801]
298. Bartholomew TC, Powell GM, Dodgson KS, Curtis CG. Oxidation of Sodium Sulphide by Rat Liver, Lungs and Kidney. Biochem Pharmacol. 1980; 29:2431–2437. [PubMed: 7426049]
299. Curtis CG, Bartholomew TC, Rose FA, Dodgson KS. Detoxication of Sodium 35 S-Sulphide in the Rat. Biochem Pharmacol. 1972; 21:2313–2321. [PubMed: 4647068]
300. Furne J, Springfield J, Koenig T, DeMaster E, Levitt MD. Oxidation of Hydrogen Sulfide and Methanethiol to Thiosulfate by Rat Tissues: A Specialized Function of the Colonic Mucosa. Biochem Pharmacol. 2001; 62:255–259. [PubMed: 11389886]
301. Vitvitsky V, Yadav PK, Kurthen A, Banerjee R. Sulfide Oxidation by a Noncanonical Pathway in Red Blood Cells Generates Thiosulfate and Polysulfides. J Biol Chem. 2015; 290:8310–8320. [PubMed: 25688092]
302. Bostelaar T, Vitvitsky V, Kumutima J, Lewis BE, Yadav PK, Brunold TC, Filipovic M, Lehnert N, Stemmler TL, Banerjee R. Hydrogen Sulfide Oxidation by Myoglobin. J Am Chem Soc. 2016; 138:8476–8488. [PubMed: 27310035]
303. Powell MA, Somero GN. Hydrogen Sulfide Oxidation Is Coupled to Oxidative Phosphorylation in Mitochondria of Solemya Reidi. Science. 1986; 233:563–566. [PubMed: 17820467]
304. Goubern M, Andriamihaja M, Nubel T, Blachier F, Bouillaud F. Sulfide, the First Inorganic Substrate for Human Cells. FASEB J. 2007; 21:1699–1706. [PubMed: 17314140]
305. Argyrou A, Blanchard JS. Flavoprotein Disulfide Reductases: Advances in Chemistry and Function. Prog Nucleic Acid Res Mol Biol. 2004; 78:89–142. [PubMed: 15210329]
306. Mishanina TV, Yadav PK, Ballou DP, Banerjee R. Transient Kinetic Analysis of Hydrogen Sulfide Oxidation Catalyzed by Human Sulfide Quinone Oxidoreductase. J Biol Chem. 2015; 290:25072–25080. [PubMed: 26318450]
307. Brito JA, Sousa FL, Stelter M, Bandeiras TM, Vonrhein C, Teixeira M, Pereira MM, Archer M. Structural and Functional Insights into Sulfide:quinone Oxidoreductase. Biochemistry. 2009; 48:5613–5622. [PubMed: 19438211]
308. Marcia M, Ermler U, Peng G, Michel H. The Structure of Aquifex Aeolicus Sulfide:quinone Oxidoreductase, a Basis to Understand Sulfide Detoxification and Respiration. Proc Natl Acad Sci U S A. 2009; 106:9625–9630. [PubMed: 19487671]
309. Cherney MM, Zhang Y, Solomonson M, Weiner JH, James MNG. Crystal Structure of Sulfide:Quinone Oxidoreductase from Acidithiobacillus Ferrooxidans: Insights into Sulfidotrophic Respiration and Detoxification. J Mol Biol. 2010; 398:292–305. [PubMed: 20303979]

310. Jackson MR, Melideo SL, Jorns MS. Human Sulfide:Quinone Oxidoreductase Catalyzes the First Step in Hydrogen Sulfide Metabolism and Produces a Sulfane Sulfur Metabolite. Biochemistry. 2012; 51:6804–6815. [PubMed: 22852582]

311. Libiad M, Yadav PK, Vitvitsky V, Martinov M, Banerjee R. Organization of the Human Mitochondrial Hydrogen Sulfide Oxidation Pathway. J Biol Chem. 2014; 289:30901–30910. [PubMed: 25225291]

312. Augustyn KDC, Jackson MR, Jorns MS. Use of Tissue Metabolite Analysis and Enzyme Kinetics To Discriminate between Alternate Pathways for Hydrogen Sulfide Metabolism. Biochemistry. 2017; 56:986–996. [PubMed: 28107627]

313. Melideo SL, Jackson MR, Jorns MS. Biosynthesis of a Central Intermediate in Hydrogen Sulfide Metabolism by a Novel Human Sulfurtransferase and Its Yeast Ortholog. Biochemistry. 2014; 53:4739–4753. [PubMed: 24981631]

314. Pettinati I, Brem J, Lee SY, McHugh PJ, Schofield CJ. The Chemical Biology of Human Metallo-β-Lactamase Fold Proteins. Trends Biochem Sci. 2016; 41:338–355. [PubMed: 26805042]

315. Tiranti V, Viscomi C, Hildebrandt T, Di Meo I, Mineri R, Tiveron C, D Levitt M, Prelle A, Fagiolari G, Rimoldi M, et al. Loss of ETHE1, a Mitochondrial Dioxygenase, Causes Fatal Sulfide Toxicity in Ethylmalonic Encephalopathy. Nat Med. 2009; 15:200–205. [PubMed: 19136963]

316. Kabil O, Banerjee R. Characterization of Patient Mutations in Human Persulfide Dioxygenase (ETHE1) Involved in H2S Catabo-lism. J Biol Chem. 2012; 287:44561–44567. [PubMed: 23144459]

317. Holdorf MM, Bennett B, Crowder MW, Makaroff CA. Spectroscopic Studies on Arabidopsis ETHE1, a Glyoxalase II-like Protein. J Inorg Biochem. 2008; 102:1825–1830. [PubMed: 18656261]

318. McCoy JG, Bingman CA, Bitto E, Holdorf MM, Makaroff CA, Phillips GN. Structure of an ETHE1-like Protein from Arabidopsis Thaliana. Acta Crystallogr, Sect D: Biol Crystallogr. 2006; 62:964–970. [PubMed: 16929096]

319. Pettinati I, Brem J, McDonough MA, Schofield CJ. Crystal Structure of Human Persulfide Dioxygenase: Structural Basis of Ethylmalonic Encephalopathy. Hum Mol Genet. 2015; 24:2458–2469. [PubMed: 25596185]

320. Tiranti V, D'Adamo P, Briem E, Ferrari G, Mineri R, Lamantea E, Mandel H, Balestri P, Garcia-Silva M-T, Vollmer B, et al. Ethylmalonic Encephalopathy Is Caused by Mutations in ETHE1, a Gene Encoding a Mitochondrial Matrix Protein. Am J Hum Genet. 2004; 74:239–252. [PubMed: 14732903]

321. Mineri R, Rimoldi M, Burlina AB, Koskull S, Perletti C, Heese B, von Dobeln U, Mereghetti P, Di Meo I, Invernizzi F, et al. Identification of New Mutations in the ETHE1 Gene in a Cohort of 14 Patients Presenting with Ethylmalonic Encephalopathy. J Med Genet. 2008; 45:473–478. [PubMed: 18593870]

322. García-Silva MT, Campos Y, Ribes A, Briones P, Cabello A, Borbujo JS, Arenas J, Garavaglia B. Encephalopathy, Petechiae, and Acrocyanosis with Ethylmalonic Aciduria Associated with Muscle Cytochrome c Oxidase Deficiency. J Pediatr. 1994; 125:843–844. [PubMed: 7965445]

323. Burlina A, Zacchello F, Dionisi-Vici C, Bertini E, Sabetta G, Bennet MJ, Hale DE, Schmidt-Sommerfeld E, Rinaldo P. New Clinical Phenotype of Branched-Chain Acyl-CoA Oxidation Defect. Lancet. 1991; 338:1522–1523.

324. Sattler SA, Wang X, Lewis KM, DeHan PJ, Park C-M, Xin Y, Liu H, Xian M, Xun L, Kang C. Characterizations of Two Bacterial Persulfide Dioxygenases of the Metallo-β-Lactamase Superfamily. J Biol Chem. 2015; 290:18914–18923. [PubMed: 26082492]

325. Driggers CM, Cooley RB, Sankaran B, Hirschberger LL, Stipanuk MH, Karplus PA. Cysteine Dioxygenase Structures from pH4 to 9: Consistent Cys-Persulfenate Formation at Intermediate pH and a Cys-Bound Enzyme at Higher pH. J Mol Biol. 2013; 425:3121–3136. [PubMed: 23747973]

326. Westley J. Rhodanese. Adv Enzymol Relat Areas Mol Biol. 2006; 39:327–368.

327. Morton NM, Beltram J, Carter RN, Michailidou Z, Gorjanc G, McFadden C, Barrios-Llerena ME, Rodriguez-Cuenca S, Gibbins MTG, Aird RE, et al. Genetic Identification of Thiosulfate

Sulfurtransferase as an Adipocyte-Expressed Antidiabetic Target in Mice Selected for Leanness. Nat Med. 2016; 22:771–779. [PubMed: 27270587]

328. Bordo D. The rhodanese/Cdc25 Phosphatase Superfamily: Sequence-Structure-Function Relations. EMBO Rep. 2002; 3:741–746. [PubMed: 12151332]
329. Cipollone R, Ascenzi P, Visca P. Common Themes and Variations in the Rhodanese Superfamily. IUBMB Life. 2007; 59:51–59. [PubMed: 17454295]
330. Libiad M, Sriraman A, Banerjee R. Polymorphic Variants of Human Rhodanese Exhibit Differences in Thermal Stability and Sulfur Transfer Kinetics. J Biol Chem. 2015; 290:23579–23588. [PubMed: 26269602]
331. Billaut-Laden I, Allorge D, Crunelle-Thibaut A, Rat E, Cauffiez C, Chevalier D, Houdret N, Lo-Guidice J-M, Broly F. Evidence for a Functional Genetic Polymorphism of the Human Thiosulfate Sulfurtransferase (Rhodanese), a Cyanide and H2S Detoxification Enzyme. Toxicology. 2006; 225:1–11. [PubMed: 16790311]
332. Ploegman JH, Drent G, Kalk KH, Hol WG. Structure of Bovine Liver Rhodanese. I. Structure Determination at 2.5 A Resolution and a Comparison of the Conformation and Sequence of Its Two Domains. J Mol Biol. 1978; 123:557–594. [PubMed: 691057]
333. Vitvitsky V, Dayal S, Stabler S, Zhou Y, Wang H, Lentz SR, Banerjee R. Perturbations in Homocysteine-Linked Redox Homeostasis in a Murine Model for Hyperhomocysteinemia. Am J Physiol Regul Integr Comp Physiol. 2004; 287:R39–R46. [PubMed: 15016621]
334. Kappler U, Enemark JH. Sulfite-Oxidizing Enzymes. J Biol Inorg Chem. 2015; 20:253–264. [PubMed: 25261289]
335. Nowak K, Luniak N, Witt C, Wüstefeld Y, Wachter A, Mendel RR, Hänsch R. Peroxisomal Localization of Sulfite Oxidase Separates It from Chloroplast-Based Sulfur Assimilation. Plant Cell Physiol. 2004; 45:1889–1894. [PubMed: 15653809]
336. Shih VE, Abroms IF, Johnson JL, Carney M, Mandell R, Robb RM, Cloherty JP, Rajagopalan KV. Sulfite Oxidase Deficiency. N Engl J Med. 1977; 297:1022–1028. [PubMed: 302914]
337. Kisker C, Schindelin H, Pacheco A, Wehbi WA, Garrett RM, Rajagopalan KV, Enemark JH, Rees DC. Molecular Basis of Sulfite Oxidase Deficiency from the Structure of Sulfite Oxidase. Cell. 1997; 91:973–983. [PubMed: 9428520]
338. Garrett RM, Johnson JL, Graf TN, Feigenbaum A, Rajagopalan KV. Human Sulfite Oxidase R160Q: Identification of the Mutation in a Sulfite Oxidase-Deficient Patient and Expression and Characterization of the Mutant Enzyme. Proc Natl Acad Sci U S A. 1998; 95:6394–6398. [PubMed: 9600976]
339. Wilson HL, Rajagopalan KV. The Role of Tyrosine 343 in Substrate Binding and Catalysis by Human Sulfite Oxidase. J Biol Chem. 2004; 279:15105–15113. [PubMed: 14729666]
340. Filipovic MR. Persulfidation (S-Sulfhydration) and H2S. Handb Exp Pharmacol. 2015; 230:29–59. [PubMed: 26162828]
341. Zivanovic J, Filipovic MR. Hydrogen Sulfide: Stench from the Past as a Mediator of the Future. Biochem (London). 2016; 38:12–17.
342. Li Q, Lancaster JR. Chemical Foundations of Hydrogen Sulfide Biology. Nitric Oxide. 2013; 35:21–34. [PubMed: 23850631]
343. Keilin D. Cytochrome and Respiratory Enzymes. Proc R Soc London, Ser B. 1929; 104:206–252.
344. Chance B, Schoener B. High and Low Energy States of Cytochromes. I. In Mitochondria. J Biol Chem. 1966; 241:4567–4573. [PubMed: 4162729]
345. Chance B, Lee CP, Schoener B. High and Low Energy States of Cytochromes. II. In Submitochondrial Particles. J Biol Chem. 1966; 241:4574–4576. [PubMed: 4162730]
346. Lehninger, AL., Nelson, DL., Cox, MM. Lehninger Principles of Biochemistry. Worth Publishers; New York: 2000.
347. Yoshikawa S, Shimada A. Reaction Mechanism of Cytochrome c Oxidase. Chem Rev. 2015; 115:1936–1989. [PubMed: 25603498]
348. Capaldi RA. Structure and Function of Cytochrome c Oxidase. Annu Rev Biochem. 1990; 59:569–596. [PubMed: 2165384]

349. Kaila VRI, Verkhovsky MI, Wikström M. Proton-Coupled Electron Transfer in Cytochrome Oxidase. Chem Rev. 2010; 110:7062–7081. [PubMed: 21053971]
350. Cooper CE, Brown GC. The Inhibition of Mitochondrial Cytochrome Oxidase by the Gases Carbon Monoxide, Nitric Oxide, Hydrogen Cyanide and Hydrogen Sulfide: Chemical Mechanism and Physiological Significance. J Bioenerg Biomembr. 2008; 40:533–539. [PubMed: 18839291]
351. Sarti P, Forte E, Mastronicola D, Giuffrè A, Arese M. Cytochrome c Oxidase and Nitric Oxide in Action: Molecular Mechanisms and Pathophysiological Implications. Biochim Biophys Acta, Bioenerg. 2012; 1817:610–619.
352. Cooper CE. Nitric Oxide and Cytochrome Oxidase: Substrate, Inhibitor or Effector? Trends Biochem Sci. 2002; 27:33–39. [PubMed: 11796222]
353. Nicholls P. Inhibition of Cytochrome c Oxidase by Sulphide. Biochem Soc Trans. 1975; 3:316–319. [PubMed: 165995]
354. Nicholls P. The Effect of Sulphide on Cytochrome aa3. Isosteric and Allosteric Shifts of the Reduced Alpha-Peak. Biochim Biophys Acta, Bioenerg. 1975; 396:24–35.
355. Nicholls P, Kim JK. Oxidation of Sulphide by Cytochrome aa3. Biochim Biophys Acta, Bioenerg. 1981; 637:312–320.
356. Nicholls P, Kim JK. Sulphide as an Inhibitor and Electron Donor for the Cytochrome c Oxidase System. Can J Biochem. 1982; 60:613–623. [PubMed: 6288202]
357. Hill BC, Woon TC, Nicholls P, Peterson J, Greenwood C, Thomson AJ. Interactions of Sulphide and Other Ligands with Cytochrome c Oxidase. An Electron-Paramagnetic-Resonance Study. Biochem J. 1984; 224:591–600. [PubMed: 6097224]
358. Koenitzer JR, Isbell TS, Patel HD, Benavides GA, Dickinson DA, Patel RP, Darley-usmar VM, Lancaster JR, Doeller JE, Kraus DW. Hydrogen Sulfide Mediates Vasoactivity in an O2 - Dependent Manner. Am J Physiol Hear Circ Physiol. 2006; 292:H1953–H1960.
359. Collman JP, Ghosh S, Dey A, Decreau RA. Using a Functional Enzyme Model to Understand the Chemistry behind Hydrogen Sulfide Induced Hibernation. Proc Natl Acad Sci U S A. 2009; 106:22090–22095. [PubMed: 20007376]
360. Araki T. Ueber Den Blutfarbstoff Und Seine Niiheren Umwanidlungsproducte. Ztschr f Phlysiol Chem. 1890; 14:405–416.
361. Lewisson. Zur Frage Uiber Ozon Im Blute. Virchow's Arch Bd. 1868; XXXVI:15.
362. Hoppe-Seyler F. Einwirkung Des Schwefelwasserstoffgases Auf Das Blut. Centr f d med Wissensch. 1863; 433:28.
363. Keilin D. On the Combination of Methaemoglobin with H_2S. Proc R Soc London, Ser B. 1933; 113:393–404.
364. Flexman AM, Del Vicario G, Schwarz SKW. Dark Green Blood in the Operating Theatre. Lancet. 2007; 369:1972. [PubMed: 17560450]
365. Berzofsky JA, Peisach J, Alben JO. Sulfheme Proteins. 3. Carboxysulfmyoglobin: The Relation between Electron Withdrawal from Iron and Ligand Binding. J Biol Chem. 1972; 247:3774–3782. [PubMed: 5033389]
366. Berzofsky JA, Peisach J, Blumberg WE. Sulfheme Proteins. I. Optical and Magnetic Properties of Sulfmyoglobin and Its Derivatives. J Biol Chem. 1971; 246:3367–3377. [PubMed: 4324899]
367. Berzofsky JA, Peisach J, Blumberg WE. Sulfheme Proteins. II. The Reversible Oxygenation of Ferrous Sulfmyoglobin. J Biol Chem. 1971; 246:7366–7372. [PubMed: 4331435]
368. Berzofsky JA, Peisach J, Horecker BL. Sulfheme Proteins. IV. The Stoichiometry of Sulfur Incorporation and the Isolation of Sulfhemin, the Prosthetic Group of Sulfmyoglobin. J Biol Chem. 1972; 247:3783–3791. [PubMed: 5033390]
369. Carrico RJ, Blumberg WE, Peisach J. The Reversible Binding of Oxygen to Sulfhemoglobin. J Biol Chem. 1978; 253:7212–7215. [PubMed: 29895]
370. Chatfield MJ, La Mar GN. 1H Nuclear Magnetic Resonance Study of the Prosthetic Group in Sulfhemoglobin. Arch Biochem Biophys. 1992; 295:289–296. [PubMed: 1316736]
371. Nicholls P. The Formation and Properties of Sulphmyoglobin and Sulphcatalase. Biochem J. 1961; 81:374–383. [PubMed: 14479446]

372. Ríos-González BB, Román-Morales EM, Pietri R, López-Garriga J. Hydrogen Sulfide Activation in Hemeproteins: The Sulfheme Scenario. J Inorg Biochem. 2014; 133:78–86. [PubMed: 24513534]

373. Libardi SH, Pindstrup H, Cardoso DR, Skibsted LH. Reduction of Ferrylmyoglobin by Hydrogen Sulfide. Kinetics in Relation to Meat Greening. J Agric Food Chem. 2013; 61:2883–2888. [PubMed: 23425699]

374. Nakamura S, Nakamura M, Yamazaki I, Morrison M. Reactions of Ferryl Lactoperoxidase (Compound II) with Sulfide and Sulfhydryl Compounds. J Biol Chem. 1984; 259:7080–7085. [PubMed: 6725282]

375. Nussbaum C, Klinke A, Adam M, Baldus S, Sperandio M. yeloperoxidase: A Leukocyte-Derived Protagonist of Inflammation and Cardiovascular Disease. Antioxid Redox Signal. 2013; 18:692–713. [PubMed: 22823200]

376. Pálinkás Z, Furtmüller PG, Nagy A, Jakopitsch C, Pirker KF, Magierowski M, Jasnos K, Wallace JL, Obinger C, Nagy P. Interactions of Hydrogen Sulfide with Myeloperoxidase. Br J Pharmacol. 2015; 172:1516–1532. [PubMed: 24824874]

377. Zhou Z, Martin E, Sharina I, Esposito I, Szabo C, Bucci M, Cirino G, Papapetropoulos A. Regulation of Soluble Guanylyl Cyclase Redox State by Hydrogen Sulfide. Pharmacol Res. 2016; 111:556–562. [PubMed: 27378567]

378. Sorbo B. On the Formation of Thiosulfate from Inorganic Sulfide by Liver Tissue and Heme Compounds. Biochim Biophys Acta. 1958; 27:324–329. [PubMed: 13522731]

379. Strianese M, De Martino F, Pellecchia C, Ruggiero G, D'Auria S. Myoglobin as a New Fluorescence Probe to Sense H2S. Protein Pept Lett. 2011; 18:282–286. [PubMed: 20858204]

380. Valentine WN, Frankenfeld JK. 3-Mercaptopyruvate Sulfurtransferase (EC 2.8.1.2): A Simple Assay Adapted to Human Blood Cells. Clin Chim Acta. 1974; 51:205–210. [PubMed: 4828222]

381. Kraus DW, Wittenberg JB, Lu JF, Peisach J. Hemoglobins of the Lucina Pectinata/bacteria Symbiosis. II. An Electron Paramagnetic Resonance and Optical Spectral Study of the Ferric Proteins. J Biol Chem. 1990; 265:16054–16059. [PubMed: 2168877]

382. Vitvitsky V, Yadav PK, An S, Seravalli J, Cho U-S, Banerjee R. Structural and Mechanistic Insights into Hemoglobin-Catalyzed Hydrogen Sulfide Oxidation and the Fate of Polysulfide Products. J Biol Chem. 2017; 292:5584–5592. [PubMed: 28213526]

383. Burmester T, Weich B, Reinhardt S, Hankeln T. A Vertebrate Globin Expressed in the Brain. Nature. 2000; 407:520–523. [PubMed: 11029004]

384. Burmester T, Hankeln T. What Is the Function of Neuroglobin? J Exp Biol. 2009; 212:1423–1428. [PubMed: 19411534]

385. Trent JT, Watts RA, Hargrove MS. Human Neuroglobin, a Hexacoordinate Hemoglobin That Reversibly Binds Oxygen. J Biol Chem. 2001; 276:30106–30110. [PubMed: 11429401]

386. Kriegl JM, Bhattacharyya AJ, Nienhaus K, Deng P, Minkow O, Nienhaus GU. Ligand Binding and Protein Dynamics in Neuroglobin. Proc Natl Acad Sci U S A. 2002; 99:7992–7997. [PubMed: 12048231]

387. Van Doorslaer S, Dewilde S, Kiger L, Nistor SV, Goovaerts E, Marden MC, Moens L. Nitric Oxide Binding Properties of Neuroglobin. J Biol Chem. 2003; 278:4919–4925. [PubMed: 12480932]

388. Nienhaus K, Kriegl JM, Nienhaus GU. Structural Dynamics in the Active Site of Murine Neuroglobin and Its Effects on Ligand Binding. J Biol Chem. 2004; 279:22944–22952. [PubMed: 15016813]

389. Ruetz M, Kumutima J, Lewis BE, Filipovic MR, Lehnert N, Stemmler TL, Banerjee R. A Distal Ligand Mutes the Interaction of Hydrogen Sulfide with Human Neuroglobin. J Biol Chem. 2017; 292:6512–6528. [PubMed: 28246171]

390. Kraus DW, Wittenberg JB. Hemoglobins of the Lucina Pectinata/bacteria Symbiosis. I. Molecular Properties, Kinetics and Equilibria of Reactions with Ligands. J Biol Chem. 1990; 265:16043–16053. [PubMed: 2398044]

391. Pietri R, Lewis A, León RG, Casabona G, Kiger L, Yeh S-R, Fernandez-Alberti S, Marden MC, Cadilla CL, López-Garriga J. Factors Controlling the Reactivity of Hydrogen Sulfide with Hemeproteins. Biochemistry. 2009; 48:4881–4894. [PubMed: 19368335]

392. Ramos-Alvarez C, Yoo B-K, Pietri R, Lamarre I, Martin J-L, López-Garriga J, Negrerie M. Reactivity and Dynamics of H2S, NO, and O2 Interacting with Hemoglobins from Lucina Pectinata. Biochemistry. 2013; 52:7007–7021. [PubMed: 24040745]

393. Díaz-Ayala R, Moya-Rodríguez A, Pietri R, Cadilla CL, López-Garriga J. Molecular Cloning and Characterization of a (Lys)6-Tagged Sulfide-Reactive Hemoglobin I from Lucina Pectinata. Mol Biotechnol. 2015; 57:1050–1062. [PubMed: 26482241]

394. Gavira JA, Camara-Artigas A, De Jesús-Bonilla W, López-Garriga J, Lewis A, Pietri R, Yeh S-R, Cadilla CL, García-Ruiz JM. Structure and Ligand Selection of Hemoglobin II from Lucina Pectinata. J Biol Chem. 2008; 283:9414–9423. [PubMed: 18203714]

395. Fernandez-Alberti S, Bacelo DE, Binning RC, Echave J, Chergui M, López-Garriga J. Sulfide-Binding Hemoglobins: Effects of Mutations on Active-Site Flexibility. Biophys J. 2006; 91:1698–1709. [PubMed: 16782787]

396. Silfa E, Almeida M, Cerda J, Wu S, López-Garriga J. Orientation of the Heme Vinyl Groups in the Hydrogen Sulfide-Binding Hemoglobin I from Lucina Pectinata. Biospectroscopy. 1998; 4:311–326. [PubMed: 9787907]

397. Cerda J, Echevarria Y, Morales E, López-Garriga J. Resonance Raman Studies of the Heme-Ligand Active Site of Hemoglobin I fromLucina Pectinata. Biospectroscopy. 1999; 5:289–301.

398. Nguyen BD, Zhao X, Vyas K, La Mar GN, Lile RA, Brucker EA, Phillips GN, Olson JS, Wittenberg JB. Solution and Crystal Structures of a Sperm Whale Myoglobin Triple Mutant That Mimics the Sulfide-Binding Hemoglobin from Lucina Pectinata. J Biol Chem. 1998; 273:9517–9526. [PubMed: 9545280]

399. Pietri R, Granell L, Cruz A, De Jesús W, Lewis A, León R, Cadilla CL, Garriga JL. Tyrosine B10 and Heme-Ligand Interactions of Lucina Pectinata Hemoglobin II: Control of Heme Reactivity. Biochim Biophys Acta, Proteins Proteomics. 2005; 1747:195–203.

400. Pietri R, León RG, Kiger L, Marden MC, Granell LB, Cadilla CL, López-Garriga J. Hemoglobin I from Lucina Pectinata: A Model for Distal Heme-Ligand Control. Biochim Biophys Acta, Proteins Proteomics. 2006; 1764:758–765.

401. Ramirez E, Cruz A, Rodriguez D, Uchima L, Pietri R, Santana A, López-Garriga J, López GE. Effects of Active Site Mutations in Haemoglobin I from Lucina Pectinata: A Molecular Dynamic Study. Mol Simul. 2008; 34:715–725. [PubMed: 19300529]

402. Román-Morales E, Pietri R, Ramos-Santana B, Vinogradov SN, Lewis-Ballester A, López-Garriga J. Structural Determinants for the Formation of Sulfhemeprotein Complexes. Biochem Biophys Res Commun. 2010; 400:489–492. [PubMed: 20732304]

403. Pietri R, Román-Morales E, López-Garriga J. Hydrogen Sulfide and Hemeproteins: Knowledge and Mysteries. Antioxid Redox Signal. 2011; 15:393–404. [PubMed: 21050142]

404. Filipovic MR, Ivanovic-Burmazovic I. Removal of Hydrogen Sulphide (H2S): Catalytic Oxidation of Sulphide Species. WO2012175630A1. 2012

405. Hartle MD, Prell JS, Pluth MD. Spectroscopic Investigations into the Binding of Hydrogen Sulfide to Synthetic Picket-Fence Porphyrins. Dalt Trans. 2016; 45:4843–4853.

406. Zal F, Leize E, Lallier FH, Toulmond A, Van Dorsselaer A, Childress JJ. S-Sulfohemoglobin and Disulfide Exchange: The Mechanisms of Sulfide Binding by Riftia Pachyptila Hemoglobins. Proc Natl Acad Sci U S A. 1998; 95:8997–9002. [PubMed: 9671793]

407. Bailly X, Vinogradov S. The Sulfide Binding Function of Annelid Hemoglobins: Relic of an Old Biosystem? J Inorg Biochem. 2005; 99:142–150. [PubMed: 15598498]

408. Flores JF, Fisher CR, Carney SL, Green BN, Freytag JK, Schaeffer SW, Royer WE. Sulfide Binding Is Mediated by Zinc Ions Discovered in the Crystal Structure of a Hydrothermal Vent Tubeworm Hemoglobin. Proc Natl Acad Sci U S A. 2005; 102:2713–2718. [PubMed: 15710902]

409. Zhao K, Li S, Wu L, Lai C, Yang G. Hydrogen Sulfide Represses Androgen Receptor Transactivation by Targeting at the Second Zinc Finger Module. J Biol Chem. 2014; 289:20824–20835. [PubMed: 24942741]

410. Bucci M, Papapetropoulos A, Vellecco V, Zhou Z, Pyriochou A, Roussos C, Roviezzo F, Brancaleone V, Cirino G. Hydrogen Sulfide Is an Endogenous Inhibitor of Phosphodiesterase Activity. Arterioscler Thromb Vasc Biol. 2010; 30:1998–2004. [PubMed: 20634473]

411. Galardon E, Tomas A, Selkti M, Roussel P, Artaud I. Synthesis, Characterization, and Reactivity of Alkyldisulfanido Zinc Complexes. Inorg Chem. 2009; 48:5921–5927. [PubMed: 19514736]

412. Galardon E, Tomas A, Roussel P, Artaud I. Synthesis, Stability, and Reactivity of [(TPA)Zn(SH)] + in Aqueous and Organic Solutions. Eur J Inorg Chem. 2011; 2011:3797–3801.

413. Hartle MD, Delgado M, Gilbertson JD, Pluth MD. Stabilization of a Zn(ii) Hydrosulfido Complex Utilizing a Hydrogen-Bond Accepting Ligand. Chem Commun (Cambridge, U K). 2016; 52:7680–7682.

414. Koppenol WH, Stanbury DM, Bounds PL. Electrode Potentials of Partially Reduced Oxygen Species, from Dioxygen to Water. Free Radic Biol Med. 2010; 49:317–322. [PubMed: 20406682]

415. Mills G, Schmidt KH, Matheson MS, Meisel D. Thermal and Photochemical Reactions of Sulfhydryl Radicals. Implications for Colloid Photocorrosion. J Phys Chem. 1987; 91:1590–1596.

416. Ross AB, Mallard WG, Helman WP, Buxton GV, Huie RT, Neta P. NDRL/NIST Solution Kinetics Database. 1998 version 3.

417. Rabai G, Orban M, Epstein IR. A Model for the pH-Regulated Oscillatory Reaction between Hydrogen Peroxide and Sulfide Ion. J Phys Chem. 1992; 96:5414–5419.

418. Nagy P, Winterbourn CC. Rapid Reaction of Hydrogen Sulfide with the Neutrophil Oxidant Hypochlorous Acid to Generate Polysulfides. Chem Res Toxicol. 2010; 23:1541–1543. [PubMed: 20845929]

419. Filipovic MR, Miljkovic J, Allgäuer A, Chaurio R, Shubina T, Herrmann M, Ivanovic-Burmazovic I. Biochemical Insight into Physiological Effects of H_2S: Reaction with Peroxynitrite and Formation of a New Nitric Oxide Donor, Sulfinyl Nitrite. Biochem J. 2012; 441:609–621. [PubMed: 21950347]

420. Cuevasanta E, Zeida A, Carballal S, Wedmann R, Morzan UN, Trujillo M, Radi R, Estrin DA, Filipovic MR, Alvarez B. Insights into the Mechanism of the Reaction between Hydrogen Sulfide and Peroxynitrite. Free Radic Biol Med. 2015; 80:93–100. [PubMed: 25555671]

421. Davies MJ, Hawkins CL, Pattison DI, Rees MD. Mammalian Heme Peroxidases: From Molecular Mechanisms to Health Implications. Antioxid Redox Signal. 2008; 10:1199–1234. [PubMed: 18331199]

422. Koppenol WH, Kissner R. Can O=NOOH Undergo Homolysis? Chem Res Toxicol. 1998; 11:87–90. [PubMed: 9511898]

423. Palmer RM, Ferrige AG, Moncada S. Nitric Oxide Release Accounts for the Biological Activity of Endothelium-Derived Relaxing Factor. Nature. 1987; 327:524–526. [PubMed: 3495737]

424. Palmer RM, Ashton DS, Moncada S. Vascular Endothelial Cells Synthesize Nitric Oxide from L-Arginine. Nature. 1988; 333:664–666. [PubMed: 3131684]

425. Bogdan C. Nitric Oxide and the Immune Response. Nat Immunol. 2001; 2:907–916. [PubMed: 11577346]

426. Bogdan C, Röllinghoff M, Diefenbach A. The Role of Nitric Oxide in Innate Immunity. Immunol Rev. 2000; 173:17–26. [PubMed: 10719664]

427. Gamper N, Ooi L. Redox and Nitric Oxide-Mediated Regulation of Sensory Neuron Ion Channel Function. Antioxid Redox Signal. 2015; 22:486–504. [PubMed: 24735331]

428. Santos AI, Martínez-Ruiz A, Araujó IM. S-Nitrosation and Neuronal Plasticity. Br J Pharmacol. 2015; 172:1468–1478. [PubMed: 24962517]

429. Nott A, Riccio A. Nitric Oxide-Mediated Epigenetic Mechanisms in Developing Neurons. Cell Cycle. 2009; 8:725–730. [PubMed: 19221483]

430. Friebe A, Koesling D. Regulation of Nitric Oxide-Sensitive Guanylyl Cyclase. Circ Res. 2003; 93:96–105. [PubMed: 12881475]

431. Moncada S, Palmer RM, Higgs EA. Nitric Oxide: Physiology, Pathophysiology, and Pharmacology. Pharmacol Rev. 1991; 43:109–142. [PubMed: 1852778]

432. Foster MW, Hess DT, Stamler JS. Protein S-Nitrosylation in Health and Disease: A Current Perspective. Trends Mol Med. 2009; 15:391–404. [PubMed: 19726230]

433. Hess DT, Stamler JS. Regulation by S-Nitrosylation of Protein Post-Translational Modification. J Biol Chem. 2012; 287:4411–4418. [PubMed: 22147701]

434. Seth D, Stamler JS. The SNO-Proteome: Causation and Classifications. Curr Opin Chem Biol. 2011; 15:129–136. [PubMed: 21087893]

435. Lima B, Forrester MT, Hess DT, Stamler JS. S-Nitrosylation in Cardiovascular Signaling. Circ Res. 2010; 106:633–646. [PubMed: 20203313]

436. Broniowska KA, Hogg N. The Chemical Biology of S-Nitrosothiols. Antioxid Redox Signal. 2012; 17:969–980. [PubMed: 22468855]

437. Lancaster JR. How Are Nitrosothiols Formed de Novo in Vivo? Arch Biochem Biophys. 2017; 617:137–144. [PubMed: 27794428]

438. Zhang Y, Hogg N. The Mechanism of Transmembrane S-Nitrosothiol Transport. Proc Natl Acad Sci U S A. 2004; 101:7891–7896. [PubMed: 15148403]

439. Miljkovic, JL., Filipovic, MR. HNO/Thiol Biology as a Therapeutic Target. Springer International Publishing; Berlin: 2016. p. 335-375.

440. Shafirovich V, Lymar SV. Nitroxyl and Its Anion in Aqueous Solutions: Spin States, Protic Equilibria, and Reactivities toward Oxygen and Nitric Oxide. Proc Natl Acad Sci U S A. 2002; 99:7340–7345. [PubMed: 12032284]

441. Bartberger MD, Liu W, Ford E, Miranda KM, Switzer C, Fukuto JM, Farmer PJ, Wink DA, Houk KN. The Reduction Potential of Nitric Oxide (NO) and Its Importance to NO Biochemistry. Proc Natl Acad Sci U S A. 2002; 99:10958–10963. [PubMed: 12177417]

442. Fukuto JM, Carrington SJ. HNO Signaling Mechanisms. Antioxid Redox Signal. 2011; 14:1649–1657. [PubMed: 21235348]

443. Gladwin MT, Schechter AN, Kim-Shapiro DB, Patel RP, Hogg N, Shiva S, Cannon RO, Kelm M, Wink DA, Espey MG, et al. The Emerging Biology of the Nitrite Anion. Nat Chem Biol. 2005; 1:308–314. [PubMed: 16408064]

444. Lundberg, JO., Weitzberg, E., Shiva, S., Gladwin, MT. Nitrite and Nitrate in Human Health and Disease. Humana Press; Totowa, NJ: 2011. The Nitrate–Nitrite–Nitric Oxide Pathway in Mammals; p. 21-48.

445. Lundberg JO, Weitzberg E, Gladwin MT. The Nitrate– nitrite–nitric Oxide Pathway in Physiology and Therapeutics. Nat Rev Drug Discovery. 2008; 7:156–167. [PubMed: 18167491]

446. Kissner R, Nauser T, Bugnon P, Lye PG, Koppenol WH. Formation and Properties of Peroxynitrite as Studied by Laser Flash Photolysis, High-Pressure Stopped-Flow Technique, and Pulse Radiolysis. Chem Res Toxicol. 1997; 10:1285–1292. [PubMed: 9403183]

447. Szabo´ C, Ischiropoulos H, Radi R. Peroxynitrite: Biochemistry, Pathophysiology and Development of Therapeutics. Nat Rev Drug Discovery. 2007; 6:662–680. [PubMed: 17667957]

448. Pacher P, Beckman JS, Liaudet L. Nitric Oxide and Peroxynitrite in Health and Disease. Physiol Rev. 2007; 87:315–424. [PubMed: 17237348]

449. Filipovic MR, Miljkovic JL, Nauser T, Royzen M, Klos K, Shubina T, Koppenol WH, Lippard SJ, Ivanović–Burmazović I. Chemical Characterization of the Smallest S-Nitrosothiol, HSNO; Cellular Cross-Talk of H2S and S-Nitrosothiols. J Am Chem Soc. 2012; 134:12016–12027. [PubMed: 22741609]

450. Miljkovic JL, Kenkel I, Ivanović–Burmazović I, Filipovic MR. Generation of HNO and HSNO from Nitrite by Heme-Iron-Catalyzed Metabolism with H_2S. Angew Chem, Int Ed. 2013; 52:12061–12064.

451. Yong Q-C, Hu L-F, Wang S, Huang D, Bian J-S. Hydrogen Sulfide Interacts with Nitric Oxide in the Heart: Possible Involvement of Nitroxyl. Cardiovasc Res. 2010; 88:482–491. [PubMed: 20660605]

452. Yong Q-C, Cheong JL, Hua F, Deng L-W, Khoo YM, Lee H-S, Perry A, Wood M, Whiteman M, Bian J-S. Regulation of Heart Function by Endogenous Gaseous Mediators-Crosstalk between Nitric Oxide and Hydrogen Sulfide. Antioxid Redox Signal. 2011; 14:2081–2091. [PubMed: 21194352]

453. Cortese-Krott MM, Fernandez BO, Santos JLT, Mergia E, Grman M, Nagy P, Kelm M, Butler A, Feelisch M. Nitrosopersulfide (SSNO(–)) Accounts for Sustained NO Bioactivity of S-Nitrosothiols Following Reaction with Sulfide. Redox Biol. 2014; 2:234–244. [PubMed: 24494198]

454. Altaany Z, Ju Y, Yang G, Wang R. The Coordination of S-Sulfhydration, S-Nitrosylation, and Phosphorylation of Endothelial Nitric Oxide Synthase by Hydrogen Sulfide. Sci Signaling. 2014; 7:ra87–ra87.

455. Heine CL, Schmidt R, Geckl K, Schrammel A, Gesslbauer B, Schmidt K, Mayer B, Gorren ACF. Selective Irreversible Inhibition of Neuronal and Inducible Nitric-Oxide Synthase in the Combined Presence of Hydrogen Sulfide and Nitric Oxide. J Biol Chem. 2015; 290:24932–24944. [PubMed: 26296888]

456. Berzelius, JJ. Traitè de Chimie. Oeuvres de Berzelius, JJ., editor. Paris: F. Didot frèrès; 1831.

457. LeConte MC. Action Des Hydracides Sur Les Acides Oxygénés. Ann Chim Phys. 1847:180–183.

458. Pierce JA. A Study of the Reaction between Nitric Oxide and Hydrogen Sulphide. J Phys Chem. 1928; 33:22–36.

459. Dunnicliff HB, Mohammad S, Kishen J. The Interaction between Nitric Oxide and Hydrogen Sulphide in the Presence of Water. J Phys Chem. 1930; 35:1721–1734.

460. Kurtenacker A, Löschner H. Über Die Einwirkung von Stickoxyd Auf Thiosulfat Und Sulfid. Zeitschrift för. Anorg und Allg Chemie. 1938; 238:335–349.

461. Kulik MD. Method for Removing Hydrogen Sulfide and Nitric Oxide from Gaseous Mixtures. US4314977A. 1982

462. Suarez SA, Neuman NI, Muñoz M, Álvarez L, Bikiel DE, Brondino CD, Ivanović-Burmazović I, Miljkovic JL, Filipovic MR, Martí MA, et al. Nitric Oxide Is Reduced to HNO by Proton-Coupled Nucleophilic Attack by Ascorbate, Tyrosine, and Other Alcohols. A New Route to HNO in Biological Media? J Am Chem Soc. 2015; 137:4720–4727. [PubMed: 25773518]

463. Arulsamy N, Bohle DS, Butt JA, Irvine GJ, Jordan PA, Sagan E. Interrelationships between Conformational Dynamics and the Redox Chemistry of S-Nitrosothiols. J Am Chem Soc. 1999; 121:7115–7123.

464. Poole DP, Pelayo JC, Cattaruzza F, Kuo Y, Gai G, Chiu JV, Bron R, Furness JB, Grady EF, Bunnett NW. Transient Receptor Potential Ankyrin 1 Is Expressed by Inhibitory Motoneurons of the Mouse Intestine. Gastroenterology. 2011; 141:565–575. [PubMed: 21689654]

465. Dux M, Will C, Vogler B, Filipovic MR, Messlinger K. Meningeal Blood Flow Is Controlled by H_2S-NO Crosstalk Activating a HNO-TRPA1-CGRP Signalling Pathway. Br J Pharmacol. 2016; 173:431–445. [PubMed: 25884403]

466. Zhou Y, Zhang X, Yang S, Li Y, Qing Z, Zheng J, Li J, Yang R. Ratiometric Visualization of NO/H2S Cross-Talk in Living Cells and Tissues Using a Nitroxyl-Responsive Two-Photon Fluorescence Probe. Anal Chem. 2017; 89:4587–4594. [PubMed: 28343380]

467. Whiteman M, Li L, Kostetski I, Chu SH, Siau JL, Bhatia M, Moore PK. Evidence for the Formation of a Novel Nitrosothiol from the Gaseous Mediators Nitric Oxide and Hydrogen Sulphide. Biochem Biophys Res Commun. 2006; 343:303–310. [PubMed: 16540095]

468. Ali MY, Ping CY, Mok Y-Y, Ling L, Whiteman M, Bhatia M, Moore PK. Regulation of Vascular Nitric Oxide in Vitro and in Vivo a New Role for Endogenous Hydrogen Sulphide? Br J Pharmacol. 2006; 149:625–634. [PubMed: 17016507]

469. Müller RP, Nonella M, Russegger P, Huber JR. UV-, VIS- and IR-Light-Induced Isomerization of HSNO in a Low-Temperature Matrix. Chem Phys. 1984; 87:351–361.

470. Tchir PO, Spratley RD. The Photolysis of Matrix Isolated Cis-Thinoylimide. 1. The Identification and Infrared Spectra of Cis-HOSN, HSNO and SNO. Can J Chem. 1975; 53:2318–2330.

471. Ivanova LV, Anton BJ, Timerghazin QK. On the Possible Biological Relevance of HSNO Isomers: A Computational Investigation. Phys Chem Chem Phys. 2014; 16:8476–8486. [PubMed: 24667901]

472. Timerghazin QK, Peslherbe GH, English AM. Structure and Stability of HSNO, the Simplest S-Nitrosothiol. Phys Chem Chem Phys. 2008; 10:1532–1539. [PubMed: 18327309]

473. Seel F, Kuhn R, Simon G, Wagner M. PNP-Perthionitrit Und PNP-Monothionitrit/PNP-Perthionitrite and PNP-M Onothionitrite. Z Naturforsch, B: J Chem Sci. 1985; 40:1607–1617.

474. Nava M, Martin-Drumel M-A, López CA, Crabtree KN, Womack CC, Nguyen TL, Thorwirth S, Cummins CC, Stanton JF, McCarthy MC. Spontaneous and Selective Formation of HSNO, a Crucial Intermediate Linking H_2S and Nitroso Chemistries. J Am Chem Soc. 2016; 138:11441–11444. [PubMed: 27540860]

475. Chatterjee D, Sarkar P, Oszajca M, van Eldik R. Formation of $[Ru^{III}(edta)(SNO)]^{2-}$ in Ru^{III}(edta)-Mediated S-Nitrosylation of Bisulfide Ion. Inorg Chem. 2016; 55:5037–5040. [PubMed: 27111693]

476. Quiroga SL, Almaraz AE, Amorebieta VT, Perissinotti LL, Olabe JA. Addition and Redox Reactivity of Hydrogen Sulfides (H_2S/HS^-) with Nitroprusside: New Chemistry of Nitrososulfide Ligands. Chem Eur J. 2011; 17:4145–4156. [PubMed: 21404343]

477. Filipovic MR, Eberhardt M, Prokopovic V, Mijuskovic A, Orescanin-Dusic Z, Reeh P, Ivanovic-Burmazovic I. Beyond H_2S and NO Interplay: Hydrogen Sulfide and Nitroprusside React Directly to Give Nitroxyl (HNO). A New Pharmacological Source of HNO. J Med Chem. 2013; 56:1499–1508. [PubMed: 23418783]

478. Islam ASM, Bhowmick R, Pal K, Katarkar A, Chaudhuri K, Ali MA. Smart Molecule for Selective Sensing of Nitric Oxide: Conversion of NO to HSNO Relevance of Biological HSNO Formation. Inorg Chem. 2017; 56:4324–4331. [PubMed: 28345897]

479. Sun J, Aponte AM, Menazza S, Gucek M, Steenbergen C, Murphy E. Additive Cardioprotection by Pharmacological Postconditioning with Hydrogen Sulfide and Nitric Oxide Donors in Mouse Heart: S-Sulfhydration vs. S-Nitrosylation. Cardiovasc Res. 2016; 110:96–106. [PubMed: 26907390]

480. Munro AP, Williams DLH. Reactivity of Sulfur Nucleophiles towards S-Nitrosothiols. J Chem Soc Perkin Trans2. 2000; 24:1794–1797.

481. Cortese-Krott MM, Kuhnle GGC, Dyson A, Fernandez BO, Grman M, DuMond JF, Barrow MP, McLeod G, Nakagawa H, Ondrias K, et al. Key Bioactive Reaction Products of the NO/H_2S Interaction Are S/N-Hybrid Species, Polysulfides, and Nitroxyl. Proc Natl Acad Sci U S A. 2015; 112:E4651–E4660. [PubMed: 26224837]

482. Wedmann R, Ivanovic-Burmazovic I, Filipovic MR. Nitrosopersulfide ($SSNO^-$) Decomposes in the Presence of Sulfide, Cyanide or Glutathione to Give $HSNO/SNO^-$: Consequences for the Assumed Role in Cell Signalling. Interface Focus. 2017; 7:20160139. [PubMed: 28382204]

483. Ivanovic-Burmazovic I. HNO Generation From NOradical Dot, Nitrite, Inorganic or Organic Nitrosyls, and Crosstalk With H_2S. Chemistry and Biology of Nitroxyl (HNO) Science direct. 2017:67–104.

484. Heinecke J, Ford PC. Formation of Cysteine Sulfenic Acid by Oxygen Atom Transfer from Nitrite. J Am Chem Soc. 2010; 132:9240–9243. [PubMed: 20565124]

485. Heinecke JL, Khin C, Pereira JCM, Suárez SA, Iretskii AV, Doctorovich F, Ford PC. Nitrite Reduction Mediated by Heme Models. Routes to NO and HNO? J Am Chem Soc. 2013; 135:4007–4017. [PubMed: 23421316]

486. Bir SC, Kolluru GK, McCarthy P, Shen X, Pardue S, Pattillo CB, Kevil CG. Hydrogen Sulfide Stimulates Ischemic Vascular Remodeling through Nitric Oxide Synthase and Nitrite Reduction Activity Regulating Hypoxia-Inducible Factor-1α and Vascular Endothelial Growth Factor-Dependent Angiogenesis. J Am Heart Assoc. 2012; 1:e004093–e004093. [PubMed: 23316304]

487. Toohey JI. The Conversion of H_2S to Sulfane Sulfur. Nat Rev Mol Cell Biol. 2012; 13:803–803. [PubMed: 23151660]

488. Böhme H, Zinner G. Über Darstellung Und Eigenschaften von Alkyl-Hydro-Polysulfiden. Justus Liebigs Ann Chem. 1954; 585:142–149.

489. Everett SA, Folkes LK, Wardman P, Asmus KD. Free-Radical Repair by a Novel Perthiol: Reversible Hydrogen Transfer and Perthiyl Radical Formation. Free Radical Res. 1994; 20:387–400. [PubMed: 8081454]

490. Park C-M, Weerasinghe L, Day JJ, Fukuto JM, Xian M. Persulfides: Current Knowledge and Challenges in Chemistry and Chemical Biology. Mol BioSyst. 2015; 11:1775–1785. [PubMed: 25969163]

491. Tsurugi J, Abe Y, Kawamura S. Synthesis of 2-Substituted Ethyl Hydrodisulfides. Bull Chem Soc Jpn. 1970; 43:1890–1892.

492. Tsurugi J, Nakabayashi T. Synthesis of Dibenzhydryl and Dibenzyl Penta- and Hexasulfides. J Org Chem. 1959; 24:807–810.

493. Nakabayashi T, Tsurugi J, Yabuta T. Organic Polysulfides. 1 IV. Synthesis of Bis(triphenylmethyl) Polysulfides. J Org Chem. 1964; 29:1236–1238.

494. Bailey TS, Pluth MD. Reactions of Isolated Persulfides Provide Insights into the Interplay between H_2S and Persulfide Reactivity. Free Radic Biol Med. 2015; 89:662–667. [PubMed: 26454077]

495. Bailey TS, Zakharov LN, Pluth MD. Understanding Hydrogen Sulfide Storage: Probing Conditions for Sulfide Release from Hydrodisulfides. J Am Chem Soc. 2014; 136:10573–10576. [PubMed: 25010540]

496. Tsurugi J, Nakabayashi T, Ishihara T. Aralkyl Hydro-disulfides. 1 III. The Reaction with Tertiary Phosphines. J Org Chem. 1965; 30:2707–2710.

497. Aycock DF, Jurch GR. Synthesis of Alkyl Trithioperesters (Alkyl Thiocarbonyl Disulfides). J Org Chem. 1979; 44:569–572.

498. Heimer NE, Field L. Biologically Oriented Organic Sulfur Chemistry. 23. A Hydrodisulfide from a Sulfonamide Derivative of Penicillamine. J Org Chem. 1984; 49:1446–1449.

499. Heimer NE, Field L, Neal RA. Biologically Oriented Organic Sulfur Chemistry. 21. Hydrodisulfide of a Penicillamine Derivative and Related Compounds. J Org Chem. 1981; 46:1374–1377.

500. Heimer NE, Field L, Waites JA. Organic Disulfides and Related Substances. 44. Preparation and Characterization of 1-Adamantyl Hydrodisulfide as a Stable Prototype of the Series. J Org Chem. 1985; 50:4164–4166.

501. Artaud I, Galardon E. A Persulfide Analogue of the Nitrosothiol SNAP: Formation, Characterization and Reactivity. ChemBioChem. 2014; 15:2361–2364. [PubMed: 25205314]

502. Rao GS, Gorin G. Reaction of Cystine with Sodium Sulfide in Sodium Hydroxide Solution. J Org Chem. 1959; 24:749–753.

503. Liu DK, Chang SG. Kinetic Study of the Reaction between Cystine and Sulfide in Alkaline Solutions. Can J Chem. 1987; 65:770–774.

504. Vasas A, Dóka É, Fábián I, Nagy P. Kinetic and Thermodynamic Studies on the Disulfide-Bond Reducing Potential of Hydrogen Sulfide. Nitric Oxide. 2015; 46:93–101. [PubMed: 25512332]

505. Francoleon NE, Carrington SJ, Fukuto JM. The Reaction of H(2)S with Oxidized Thiols: Generation of Persulfides and Implications to H(2)S Biology. Arch Biochem Biophys. 2011; 516:146–153. [PubMed: 22001739]

506. Mintel R, Westley J. The Rhodanese Reaction. Mechanism of Sulfur-Sulfur Bond Cleavage. J Biol Chem. 1966; 241:3381–3385. [PubMed: 5913127]

507. Villarejo M, Westley J. Mechanism of Rhodanese Catalysis of Thiosulfate-Lipoate Oxidation-Reduction. J Biol Chem. 1963; 238:4016–4020. [PubMed: 14086740]

508. Moutiez M, Aumercier M, Teissier E, Parmentier B, Tartar A, Sergheraert C. Reduction of a Trisulfide Derivative of Glutathione by Glutathione Reductase. Biochem Biophys Res Commun. 1994; 202:1380–1386. [PubMed: 8060317]

509. Pan J, Carroll KS. Persulfide Reactivity in the Detection of Protein S-Sulfhydration. ACS Chem Biol. 2013; 8:1110–1116. [PubMed: 23557648]

510. Ellman GL. Tissue Sulfhydryl Groups. Arch Biochem Biophys. 1959; 82:70–77. [PubMed: 13650640]

511. Zhang D, Macinkovic I, Devarie-Baez NO, Pan J, Park C-M, Carroll KS, Filipovic MR, Xian M. Detection of Protein S-Sulfhydration by a Tag-Switch Technique. Angew Chem, Int Ed. 2014; 53:575–581.

512. Turell L, Botti H, Carballal S, Ferrer-Sueta G, Souza JM, Durán R, Freeman BA, Radi R, Alvarez B. Reactivity of Sulfenic Acid in Human Serum Albumin. Biochemistry. 2008; 47:358–367. [PubMed: 18078330]

513. Alvarez B, Carballal S, Turell L, Radi R. Formation and Reactions of Sulfenic Acid in Human Serum Albumin. Methods Enzymol. 2010; 473:117–136. [PubMed: 20513474]

514. Dóka É, Pader I, Bíró A, Johansson K, Cheng Q, Ballagó K, Prigge JR, Pastor-Flores D, Dick TP, Schmidt EE, et al. A Novel Persulfide Detection Method Reveals Protein Persulfide- and Polysulfide-Reducing Functions of Thioredoxin and Glutathione Systems. Sci Adv. 2016; 2:e1500968. [PubMed: 26844296]

515. Park C-M, Johnson BA, Duan J, Park J-J, Day JJ, Gang D, Qian W-J, Xian M. 9-Fluorenylmethyl (Fm) Disulfides: Biomimetic Precursors for Persulfides. Org Lett. 2016; 18:904–907. [PubMed: 26870874]
516. Schmidt B, Ho L, Hogg PJ. Allosteric Disulfide Bonds. Biochemistry. 2006; 45:7429–7433. [PubMed: 16768438]
517. Ploegman JH, Drent G, Kalk KH, Hol WG. The Structure of Bovine Liver Rhodanese. II. The Active Site in the Sulfur-Substituted and the Sulfur-Free Enzyme. J Mol Biol. 1979; 127:149–162. [PubMed: 430559]
518. Souness RJ, Kleffmann T, Tchesnokov EP, Wilbanks SM, Jameson GB, Jameson GNL. Mechanistic Implications of Persulfenate and Persulfide Binding in the Active Site of Cysteine Dioxygenase. Biochemistry. 2013; 52:7606–7617. [PubMed: 24084026]
519. Clausen T, Kaiser JT, Steegborn C, Huber R, Kessler D. Crystal Structure of the Cystine C-S Lyase from Synechocystis: Stabilization of Cysteine Persulfide for FeS Cluster Biosynthesis. Proc Natl Acad Sci U S A. 2000; 97:3856–3861. [PubMed: 10760256]
520. Tsurugi J, Kawamura S, Horii T. Aryl Hydrodisulfides. J Org Chem. 1971; 36:3677–3680.
521. Anslyn, EV., Dougherty, DA. Modern Physical Chemistry. University Science Books; South Orange, NJ: 2006.
522. Jencks WP, Carriuolo J. Reactivity of Nucleophilic Reagents toward Esters. J Am Chem Soc. 1960; 82:1778–1786.
523. Edwards JO, Pearson RG. The Factors Determining Nucleophilic Reactivities. J Am Chem Soc. 1962; 84:16–24.
524. Park C-M, Macinkovic I, Filipovic MR, Xian M. Use of The “tag-Switch” method for the Detection of Protein S-Sulfhydration. Methods Enzymol. 2015; 555:39–56. [PubMed: 25747474]
525. Abiko Y, Yoshida E, Ishii I, Fukuto JM, Akaike T, Kumagai Y. Involvement of Reactive Persulfides in Biological Bismethylmercury Sulfide Formation. Chem Res Toxicol. 2015; 28:1301–1306. [PubMed: 25874357]
526. Millikin R, Bianco CL, White C, Saund SS, Henriquez S, Sosa V, Akaike T, Kumagai Y, Soeda S, Toscano JP, et al. The Chemical Biology of Protein Hydropersulfides: Studies of a Possible Protective Function of Biological Hydropersulfide Generation. Free Radic Biol Med. 2016; 97:136–147. [PubMed: 27242269]
527. Ono K, Akaike T, Sawa T, Kumagai Y, Wink DA, Tantillo DJ, Hobbs AJ, Nagy P, Xian M, Lin J, et al. Redox Chemistry and Chemical Biology of H_2S, Hydropersulfides, and Derived Species: Implications of Their Possible Biological Activity and Utility. Free Radic Biol Med. 2014; 77:82–94. [PubMed: 25229186]
528. Everett SA, Wardman P. Perthiols as Antioxidants: Radical-Scavenging and Prooxidative Mechanisms. Methods Enzymol. 1995; 251:55–69. [PubMed: 7651231]
529. Benson SW. Thermochemistry and Kinetics of Sulfur-Containing Molecules and Radicals. Chem Rev. 1978; 78:23–35.
530. Kawamura S, Abe Y, Tsurugi J. Aralkyl Hydrodisulfides. X. Reactions with Iron Salts. J Org Chem. 1969; 34:3633–3635.
531. Bianco CL, Chavez TA, Sosa V, Saund SS, Nguyen QNN, Tantillo DJ, Ichimura AS, Toscano JP, Fukuto JM. The Chemical Biology of the Persulfide (RSSH)/perthiyl (RSS•) Redox Couple and Possible Role in Biological Redox Signaling. Free Radic Biol Med. 2016; 101:20–31. [PubMed: 27677567]
532. Prütz WA. Catalytic Reduction of Fe(III)-Cytochrome-c Involving Stable Radiolysis Products Derived from Disulphides, Proteins and Thiols. Int J Radiat Biol. 1992; 61:593–602. [PubMed: 1349623]
533. Chauvin J-PR, Haidasz EA, Griesser M, Pratt DA. Polysulfide-1-Oxides React with Peroxyl Radicals as Quickly as Hindered Phenolic Antioxidants and Do so by a Surprising Concerted Homolytic Substitution. Chem Sci. 2016; 7:6347–6356. [PubMed: 28567247]
534. Everett SA, Schoeneich C, Stewart JH, Asmus KD. Perthiyl Radicals, Trisulfide Radical Ions, and Sulfate Formation: A Combined Photolysis and Radiolysis Study on Redox Processes with Organic Di- and Trisulfides. J Phys Chem. 1992; 96:306–314.

535. Quintiliani M, Badiello R, Tamba M, Esfandi A, Gorin G. Radiolysis of Glutathione in Oxygen-Containing Solutions of pH7. Int J Radiat Biol Relat Stud Phys, Chem Med. 1977; 32:195–202. [PubMed: 302250]

536. Tamba M, Simone G, Quintiliani M. Interactions of Thiyl Free Radicals with Oxygen: A Pulse Radiolysis Study. Int J Radiat Biol Relat Stud Phys, Chem Med. 1986; 50:595–600. [PubMed: 3489683]

537. Kende I, Pickering TL, Tobolsky AV. The Dissociation Energy of the Tetrasulfide Linkage. J Am Chem Soc. 1965; 87:5582–5586.

538. Madej E, Folkes LK, Wardman P, Czapski G, Goldstein S. Thiyl Radicals React with Nitric Oxide to Form S-Nitrosothiols with Rate Constants near the Diffusion-Controlled Limit. Free Radic Biol Med. 2008; 44:2013–2018. [PubMed: 18381080]

539. Bailey TS, Henthorn HA, Pluth MD. The Intersection of NO and H_2S: Persulfides Generate NO from Nitrite through Polysulfide Formation. Inorg Chem. 2016; 55:12618–12625. [PubMed: 27989184]

540. Kawamura S, Otsuji Y, Nakabayashi T, Kitao T, Tsurugi J. Aralkyl Hydrodisulfides. IV. The Reaction of Benzyl Hydrodisulfide with Several Nucleophiles. J Org Chem. 1965; 30:2711–2714.

541. Tsurugi J, Abe Y, Nakabayashi T, Kawamura S, Kitao T, Niwa M. Aralkyl Hydrodisulfides. XI. Reaction with Amines. J Org Chem. 1970; 35:3263–3266.

542. Kawamura S, Kitao T, Nakabayashi T, Horii T, Tsurugi J. Aralkyl Hydrodisulfides. VIII. Alkaline Decomposition and Its Competition with Nucleophiles. J Org Chem. 1968; 33:1179–1181.

543. Kawamura S, Nakabayashi T, Kitao T, Tsurugi J. Aralkyl Hydrodisulfides. VI. The Reaction of Benzhydryl Hydrosulfide with Several Neucleophiles. J Org Chem. 1966; 31:1985–1987.

544. Portillo-Ledesma S, Sardi F, Manta B, Tourn MV, Clippe A, Knoops B, Alvarez B, Coitiño EL, Ferrer-Sueta G. Deconstructing the Catalytic Efficiency of Peroxiredoxin-5 Peroxidatic Cysteine. Biochemistry. 2014; 53:6113–6125. [PubMed: 25184942]

545. Nakabayashi T, Kawamura S, Kitao T, Tsurugi J. Aralkyl Hydrodisulfides. 1 V. The Reaction of 35 S-Labeled Aralkyl Hydrodisulfides with Triphenylphosphine. J Org Chem. 1966; 31:861–864.

546. Toohey JI. Sulphane Sulphur in Biological Systems: A Possible Regulatory Role. Biochem J. 1989; 264:625–632. [PubMed: 2695062]

547. Hansen RE, Roth D, Winther JR. Quantifying the Global Cellular Thiol-Disulfide Status. Proc Natl Acad Sci U S A. 2009; 106:422–427. [PubMed: 19122143]

548. Nakabayashi T, Tsurugi J. Aralkyl Hydrodisulfides. II. The Thermal Decomposition of Benzhydryl Hydrodisulfide. J Org Chem. 1963; 28:813–816.

549. Cuevasanta E, Möller MN, Alvarez B. Biological Chemistry of Hydrogen Sulfide and Persulfides. Arch Biochem Biophys. 2017; 617:9–25. [PubMed: 27697462]

550. Sawahata T, Neal RA. Use of 1-Fluoro-2,4-Dinitrobenzene as a Probe for the Presence of Hydrodisulfide Groups in Proteins. Anal Biochem. 1982; 126:360–364. [PubMed: 6897606]

551. Karala A, Ruddock LW. Does S-Methyl Methanethiosulfonate Trap the Thiol-Disulfide State of Proteins? Antioxid Redox Signal. 2007; 9:527–531. [PubMed: 17280493]

552. Sen N, Paul BD, Gadalla MM, Mustafa AK, Sen T, Xu R, Kim S, Snyder SH. Hydrogen Sulfide-Linked Sulfhydration of NF-κB Mediates Its Antiapoptotic Actions. Mol Cell. 2012; 45:13–24. [PubMed: 22244329]

553. Mustafa AK, Sikka G, Gazi SK, Steppan J, Jung SM, Bhunia AK, Barodka VM, Gazi FK, Barrow RK, Wang R, et al. Hydrogen Sulfide as Endothelium-Derived Hyperpolarizing Factor Sulfhydrates Potassium Channels. Circ Res. 2011; 109:1259–1268. [PubMed: 21980127]

554. Yang G, Zhao K, Ju Y, Mani S, Cao Q, Puukila S, Khaper N, Wu L, Wang R. Hydrogen Sulfide Protects against Cellular Senescence via S-Sulfhydration of Keap1 and Activation of Nrf2. Antioxid Redox Signal. 2013; 18:1906–1919. [PubMed: 23176571]

555. Liu Y, Yang R, Liu X, Zhou Y, Qu C, Kikuiri T, Wang S, Zandi E, Du J, Ambudkar IS, et al. Hydrogen Sulfide Maintains Mesenchymal Stem Cell Function and Bone Homeostasis via Regulation of Ca(2+) Channel Sulfhydration. Cell Stem Cell. 2014; 15:66–78. [PubMed: 24726192]

556. Mir S, Sen T, Sen N. Cytokine-Induced GAPDH Sulfhydration Affects PSD95 Degradation and Memory. Mol Cell. 2014; 56:786–795. [PubMed: 25435139]

557. Zhao K, Ju Y, Li S, Al Tanny Z, Wang R, Yang G. S-Sulfhydration of MEK1 Leads to PARP-1 Activation and DNA Damage Repair. EMBO Rep. 2014; 15:792–800. [PubMed: 24778456]

558. Gao X-H, Krokowski D, Guan B-J, Bederman I, Majumder M, Parisien M, Diatchenko L, Kabil O, Willard B, Banerjee R, et al. Quantitative H_2S-Mediated Protein Sulfhydration Reveals Metabolic Reprogramming during the Integrated Stress Response. eLife. 2015; 4:e10067. [PubMed: 26595448]

559. Longen S, Richter F, Köhler Y, Wittig I, Beck K-F, Pfeilschifter J. Quantitative Persulfide Site Identification (qPerS-SID) Reveals Protein Targets of H_2S Releasing Donors in Mammalian Cells. Sci Rep. 2016; 6:29808. [PubMed: 27411966]

560. Reisz JA, Bechtold E, King SB, Poole LB, Furdui CM. Thiol-Blocking Electrophiles Interfere with Labeling and Detection of Protein Sulfenic Acids. FEBS J. 2013; 280:6150–6161. [PubMed: 24103186]

561. Krishnan N, Fu C, Pappin DJ, Tonks NK. H_2S-Induced Sulfhydration of the Phosphatase PTP1B and Its Role in the Endoplasmic Reticulum Stress Response. Sci Signaling. 2011; 4:ra86–ra86.

562. Parent A, Elduque X, Cornu D, Belot L, Le Caer J-P, Grandas A, Toledano MB, D'Autréaux B. Mammalian Frataxin Directly Enhances Sulfur Transfer of NFS1 Persulfide to Both ISCU and Free Thiols. Nat Commun. 2015; 6:5686. [PubMed: 25597503]

563. Zhang D, Devarie-Baez NO, Li Q, Lancaster JR, Xian M. Methylsulfonyl Benzothiazole (MSBT): A Selective Protein Thiol Blocking Reagent. Org Lett. 2012; 14:3396–3399. [PubMed: 22681565]

564. Aroca A, Benito JM, Gotor C, Romero LC. Persulfidation Proteome Reveals the Regulation of Protein Function by Hydrogen Sulfide in Diverse Biological Processes in Arabidopsis. J Exp Bot. 2017; 52:556–567.

565. Beinert H. Semi-Micro Methods for Analysis of Labile Sulfide and of Labile Sulfide plus Sulfane Sulfur in Unusually Stable Iron-Sulfur Proteins. Anal Biochem. 1983; 131:373–378. [PubMed: 6614472]

566. Catsimpoolas N, Wood JL. The Reaction of Cyanide with Bovine Serum Albumin. J Biol Chem. 1964; 239:4131–4137. [PubMed: 14247659]

567. Fletcher JC, Robson A. The Occurrence of Bis-(2-Amino-2-Carboxyethyl) Trisulphide in Hydrolysates of Wool and Other Proteins. Biochem J. 1963; 87:553–559. [PubMed: 16749017]

568. Chen W, Liu C, Peng B, Zhao Y, Pacheco A, Xian M. New Fluorescent Probes for Sulfane Sulfurs and the Application in Bioimaging. Chem Sci. 2013; 4:2892–2892. [PubMed: 23750317]

569. Liu C, Chen W, Shi W, Peng B, Zhao Y, Ma H, Xian M. Rational Design and Bioimaging Applications of Highly Selective Fluorescence Probes for Hydrogen Polysulfides. J Am Chem Soc. 2014; 136:7257–7260. [PubMed: 24809803]

570. Chen W, Rosser EW, Matsunaga T, Pacheco A, Akaike T, Xian M. The Development of Fluorescent Probes for Visualizing Intracellular Hydrogen Polysulfides. Angew Chem, Int Ed. 2015; 54:13961–13965.

571. Chen W, Pacheco A, Takano Y, Day JJ, Hanaoka K, Xian M. A Single Fluorescent Probe to Visualize Hydrogen Sulfide and Hydrogen Polysulfides with Different Fluorescence Signals. Angew Chem, Int Ed. 2016; 55:9993–9996.

572. Han X, Yu F, Song X, Chen L. Quantification of Cysteine Hydropersulfide with a Ratiometric near-Infrared Fluorescent Probe Based on Selenium–sulfur Exchange Reaction. Chem Sci. 2016; 7:5098–5107.

573. Kawagoe R, Takashima I, Uchinomiya S, Ojida A. Reversible Ratiometric Detection of Highly Reactive Hydropersulfides Using a FRET-Based Dual Emission Fluorescent Probe. Chem Sci. 2017; 8:1134–1140. [PubMed: 28451253]

574. Liu C, Zhang F, Munske G, Zhang H, Xian M. Isotope Dilution Mass Spectrometry for the Quantification of Sulfane Sulfurs. Free Radic Biol Med. 2014; 76:200–207. [PubMed: 25152234]

575. Andrews JC. The Optical Activity of Cysteine. J Biol Chem. 1926; 2:209–218.

576. Cavallini D, Federici G, Barboni E. Interaction of Proteins with Sulfide. Eur J Biochem. 1970; 14:169–174. [PubMed: 5447431]

577. Østergaard H, Tachibana C, Winther JR. Monitoring Disulfide Bond Formation in the Eukaryotic Cytosol. J Cell Biol. 2004; 166:337–345. [PubMed: 15277542]

578. Gutscher M, Pauleau A-L, Marty L, Brach T, Wabnitz GH, Samstag Y, Meyer AJ, Dick TP. Real-Time Imaging of the Intracellular Glutathione Redox Potential. Nat Methods. 2008; 5:553–559. [PubMed: 18469822]

579. Yang J, Gupta V, Carroll KS, Liebler DC. Site-Specific Mapping and Quantification of Protein S-Sulphenylation in Cells. Nat Commun. 2014; 5:4776. [PubMed: 25175731]

580. Paulsen CE, Carroll KS. Cysteine-Mediated Redox Signaling: Chemistry, Biology, and Tools for Discovery. Chem Rev. 2013; 113:4633–4679. [PubMed: 23514336]

581. Devarie-Baez NO, Silva López EI, Furdui CM. Biological Chemistry and Functionality of Protein Sulfenic Acids and Related Thiol Modifications. Free Radical Res. 2016; 50:172–194. [PubMed: 26340608]

582. Poole LB, Karplus PA, Claiborne A. Protein Sulfenic Acids in Redox Signaling. Annu Rev Pharmacol Toxicol. 2004; 44:325–347. [PubMed: 14744249]

583. Malhotra JD, Kaufman RJ. Endoplasmic Reticulum Stress and Oxidative Stress: A Vicious Cycle or a Double-Edged Sword? Antioxid Redox Signal. 2007; 9:2277–2293. [PubMed: 17979528]

584. Poynton RA, Hampton MB. Peroxiredoxins as Biomarkers of Oxidative Stress. Biochim Biophys Acta, Gen Subj. 2014; 1840:906–912.

585. Wood ZA, Poole LB, Karplus PA. Peroxiredoxin Evolution and the Regulation of Hydrogen Peroxide Signaling. Science. 2003; 300:650–653. [PubMed: 12714747]

586. Biteau B, Labarre J, Toledano MB. ATP-Dependent Reduction of Cysteine–sulphinic Acid by S. Cerevisiae Sulphiredoxin. Nature. 2003; 425:980–984. [PubMed: 14586471]

587. Woo HA, Chae HZ, Hwang SC, Yang K-S, Kang SW, Kim K, Rhee SG. Reversing the Inactivation of Peroxiredoxins Caused by Cysteine Sulfinic Acid Formation. Science. 2003; 300:653–656. [PubMed: 12714748]

588. Wong PS-Y, Hyun J, Fukuto JM, Shirota FN, DeMaster EG, Shoeman DW, Nagasawa HT. Reaction between S-Nitrosothiols and Thiols: Generation of Nitroxyl (HNO) and Subsequent Chemistry. Biochemistry. 1998; 37:5362–5371. [PubMed: 9548918]

589. Arnelle DR, Stamler JS. NO+, NO, and NO− Donation by S-Nitrosothiols: Implications for Regulation of Physiological Functions by S-Nitrosylation and Acceleration of Disulfide Formation. Arch Biochem Biophys. 1995; 318:279–285. [PubMed: 7733655]

590. Giustarini D, Milzani A, Aldini G, Carini M, Rossi R, Dalle-Donne I. S-Nitrosation versus S-Glutathionylation of Protein Sulfhydryl Groups by S-Nitrosoglutathione. Antioxid Redox Signal. 2005; 7:930–939. [PubMed: 15998248]

591. Talipov MR, Timerghazin QK. Protein Control of S-Nitrosothiol Reactivity: Interplay of Antagonistic Resonance Structures. J Phys Chem B. 2013; 117:1827–1837. [PubMed: 23316815]

592. Timerghazin QK, Talipov MR. Unprecedented External Electric Field Effects on S-Nitrosothiols: Possible Mechanism of Biological Regulation? J Phys Chem Lett. 2013; 4:1034–1038. [PubMed: 26291373]

593. Ivanova LV, Cibich D, Deye G, Talipov MR, Timerghazin QK. Modeling of S-Nitrosothiol-Thiol Reactions of Biological Significance: HNO Production by S-Thiolation Requires a Proton Shuttle and Stabilization of Polar Intermediates. ChemBioChem. 2017; 18:726–738. [PubMed: 28176426]

594. Vandiver MS, Paul BD, Xu R, Karuppagounder S, Rao F, Snowman AM, Seok Ko H, Il Lee Y, Dawson VL, Dawson TM, et al. Sulfhydration Mediates Neuroprotective Actions of Parkin. Nat Commun. 2013; 4:1626. [PubMed: 23535647]

595. Kimura Y, Mikami Y, Osumi K, Tsugane M, Oka J, Kimura H. Polysulfides Are Possible H_2S-Derived Signaling Molecules in Rat Brain. FASEB J. 2013; 27:2451–2457. [PubMed: 23413359]

596. Greiner R, Dick TP. Real-Time Assays for Monitoring the Influence of Sulfide and Sulfane Sulfur Species on Protein Thiol Redox States. Methods Enzymol. 2015; 555:57–77. [PubMed: 25747475]

597. Koike S, Ogasawara Y. Sulfur Atom in Its Bound State Is a Unique Element Involved in Physiological Functions in Mammals. Molecules. 2016; 21:1753.

598. Kimura H. Physiological Roles of Hydrogen Sulfide and Polysulfides. Handb Exp Pharmacol. 2015; 230:61–81. [PubMed: 26162829]

599. Kimura Y, Toyofuku Y, Koike S, Shibuya N, Nagahara N, Lefer D, Ogasawara Y, Kimura H. Identification of H2S3 and H_2S Produced by 3-Mercaptopyruvate Sulfurtransferase in the Brain. Sci Rep. 2015; 5:14774. [PubMed: 26437775]

600. Steudel, R. Inorganic Polysulfanes H2Sn with N > 1. In: Steudel, R., editor. Elemental Sulfur und Sulfur-Rich Compounds II. Springer; Berlin: 2003. p. 99-126.

601. Steudel, R. Inorganic Polysulfides Sn (2–) and Radical Anions S N (•–). In: Steudel, R., editor. Elemental Sulfur und Sulfur-Rich Compounds II. Springer; Berlin: 2003. p. 127-152.

602. Teder A, et al. The Equilibrium Between Elementary Sulfur and Aqueous Polysulfide Solutions. Acta Chem Scand. 1971; 25:1722–1728.

603. Steudel R, Holdt G, Göbel T. Ion-Pair Chromatographic Separation of Inorganic Sulphur Anions Including Polysulphide. J Chromatogr A. 1989; 475:442–446.

604. Schwarzenbach G, Fischer A. Acidität Der Sulfane Und Zusammensetzung Der Wässerigen Alkalipolysulfidlösungen. Helv Chim Acta. 1960; 43:1365–1390.

605. Fehér F, Baudler M. Beiträge Zur Chemie Des Schwefels, III. Mitteilung. Praparätive Darstellung Und Eigenschaften Des Wasser-stofftrisulfids. Z Anorg Chem. 1947; 254:251–254.

606. Feher F, Berthold HJ. Beitraege Zur Chemie Des Schwefels, XIII Mitteillung, Die Titrimetriche Bestimmung Reiner Alkalipolysulfide. Fresenius' Z Anal Chem. 1953; 138:245–249.

607. Kamyshny A, Goifman A, Rizkov D, Lev O. Kinetics of Disproportionation of Inorganic Polysulfides in Undersaturated Aqueous Solutions at Environmentally Relevant Conditions. Aquat Geochem. 2003; 9:291–304.

608. Cloke PL. The Geologic Role of polysulfides—Part I The Distribution of Ionic Species in Aqueous Sodium Polysulfide Solutions. Geochim Cosmochim Acta. 1963; 27:1265–1298.

609. Giggenbach W. Optical Spectra and Equilibrium Distribution of Polysulfide Ions in Aqueous Solution at 20.deg. Inorg Chem. 1972; 11:1201–1207.

610. Hahn J. Zusammensetzung von Rohsulfan, Nachweis Der Sulfane H2S9 Bis H2S35 Composition of Crude Sulfane Oil, Identification of the Sulfanes H2S9 to H2S35. Z Naturforsch, B: J Chem Sci. 1985; 40:263–272.

611. Otto AH, Steudel R. The Gas Phase Acidities of the Sulfanes H2Sn (N = 1–4). Eur J Inorg Chem. 1999; 1999:2057–2061.

612. Steudel R, Holdt G, Nagorka R. On the Autoxidation of Aqueous Sodium Polysulfide [1]. Z Naturforsch, B: J Chem Sci. 1986; 41:1519–1522.

613. Hanley, AV., Czech, FW. Analytical Chemistry of Sulfur and its Compounds, Part I. Karchmer, JH., editor. Wiley; New York: 1970. p. 285Chapter 5

614. Steudel R. The Chemistry of Organic Polysulfanes R–S(n)–R (N > 2). Chem Rev. 2002; 102:3905–3946. [PubMed: 12428982]

615. Arndt S, Baeza-Garza CD, Logan A, Rosa T, Wedmann R, Prime TA, Martin JL, Saeb-Parsy K, Krieg T, Filipovic MR, et al. Assessment of H_2S in Vivo Using the Newly Developed Mitochondria-Targeted Mass Spectrometry Probe MitoA. J Biol Chem. 2017; 292:7761–7773. [PubMed: 28320864]

616. Seel F, Guttler H-J, Simon G, Wieckowski A. Colored Sulfur Species in EPD-Solvents. Pure Appl Chem. 1977; 49:45–54.

617. Iciek M, Kwiecien´ I, Wlodek L. Biological Properties of Garlic and Garlic-Derived Organosulfur Compounds. Environ Mol Mutagen. 2009; 50:247–265. [PubMed: 19253339]

618. Benavides GA, Squadrito GL, Mills RW, Patel HD, Isbell TS, Patel RP, Darley-Usmar VM, Doeller JE, Kraus DW. Hydrogen Sulfide Mediates the Vasoactivity of Garlic. Proc Natl Acad Sci U S A. 2007; 104:17977–17982. [PubMed: 17951430]

619. Munday R, Munday JS, Munday CM. Comparative Effects of Mono-, Di-, Tri-, and Tetrasulfides Derived from Plants of the Allium Family: Redox Cycling in Vitro and Hemolytic Activity and Phase 2 Enzyme Induction in Vivo. Free Radic Biol Med. 2003; 34:1200–1211. [PubMed: 12706500]

620. Federici G, Duprè S, Matarese RM, Solinas SP, Cavallini D. Is the Alkaline Cleavage of Disulfide Bonds in Peptides an Alpha-Beta Elimination Reaction or a Hydrolysis? Int J Pept Protein Res. 1977; 10:185–189. [PubMed: 21142]

621. Florence TM. Degradation of Protein Disulphide Bonds in Dilute Alkali. Biochem J. 1980; 189:507–520. [PubMed: 7213343]

622. Cavallini D, Mondovi B, De Marco C, Sciosciasantoro A. Inhibitory Effect of Mercaptoethanol and Hypotaurine on the Desulfhydration of Cysteine by Cystathionase. Arch Biochem Biophys. 1962; 96:456–457. [PubMed: 13877467]

623. Flavin M. Microbial Transsulfuration: The Mechanism of an Enzymatic Disulfide Elimination Reaction. J Biol Chem. 1962; 237:768–777. [PubMed: 13893449]

624. Yamanishi T, Tuboi S. The Mechanism of the L-Cystine Cleavage Reaction Catalyzed by Rat Liver Gamma-Cystathionase. J Biochem. 1981; 89:1913–1921. [PubMed: 7287665]

625. Zheng L, White RH, Cash VL, Jack RF, Dean DR. Cysteine Desulfurase Activity Indicates a Role for NIFS in Metallocluster Biosynthesis. Proc Natl Acad Sci U S A. 1993; 90:2754–2758. [PubMed: 8464885]

626. Frazzon J, Fick JR, Dean DR. Biosynthesis of Iron-Sulphur Clusters Is a Complex and Highly Conserved Process. Biochem Soc Trans. 2002; 30:680–685. [PubMed: 12196163]

627. Yuvaniyama P, Agar JN, Cash VL, Johnson MK, Dean DR. NifS-Directed Assembly of a Transient [2Fe-2S] Cluster within the NifU Protein. Proc Natl Acad Sci U S A. 2000; 97:599–604. [PubMed: 10639125]

628. Zheng L, Dean DR. Catalytic Formation of a Nitrogenase Iron-Sulfur Cluster. J Biol Chem. 1994; 269:18723–18726. [PubMed: 8034623]

629. Flint DH. Escherichia Coli Contains a Protein That Is Homologous in Function and N-Terminal Sequence to the Protein Encoded by the nifS Gene of Azotobacter Vinelandii and That Can Participate in the Synthesis of the Fe-S Cluster of Dihydroxy-Acid Dehydratase. J Biol Chem. 1996; 271:16068–16074. [PubMed: 8663056]

630. Mihara H, Kurihara T, Yoshimura T, Soda K, Esaki N. Cysteine Sulfinate Desulfinase, a NIFS-like Protein of Escherichia Coli with Selenocysteine Lyase and Cysteine Desulfurase Activities. Gene Cloning, Purification, and Characterization of a Novel Pyridoxal Enzyme. J Biol Chem. 1997; 272:22417–22424. [PubMed: 9278392]

631. Mihara H, Maeda M, Fujii T, Kurihara T, Hata Y, Esaki N. A nifS-like Gene, csdB, Encodes an Escherichia Coli Counterpart of Mammalian Selenocysteine Lyase. Gene Cloning, Purification, Characterization and Preliminary X-Ray Crystallographic Studies. J Biol Chem. 1999; 274:14768–14772. [PubMed: 10329673]

632. Patzer SI, Hantke K. SufS Is a NifS-like Protein, and SufD Is Necessary for Stability of the [2Fe-2S] FhuF Protein in Escherichia Coli. J Bacteriol. 1999; 181:3307–3309. [PubMed: 10322040]

633. Lauhon CT, Kambampati R. The iscS Gene in Escherichia Coli Is Required for the Biosynthesis of 4-Thiouridine, Thiamin, and NAD. J Biol Chem. 2000; 275:20096–20103. [PubMed: 10781607]

634. Mihara H, Kato S, Lacourciere GM, Stadtman TC, Kennedy RAJD, Kurihara T, Tokumoto U, Takahashi Y, Esaki N. The iscS Gene Is Essential for the Biosynthesis of 2-Selenouridine in tRNA and the Selenocysteine-Containing Formate Dehydrogenase H. Proc Natl Acad Sci U S A. 2002; 99:6679–6683. [PubMed: 11997471]

635. Loiseau L, Ollagnier-de Choudens S, Lascoux D, Forest E, Fontecave M, Barras F. Analysis of the Heteromeric CsdA-CsdE Cysteine Desulfurase, Assisting Fe-S Cluster Biogenesis in Escherichia Coli. J Biol Chem. 2005; 280:26760–26769. [PubMed: 15901727]

636. Mueller EG. Trafficking in Persulfides: Delivering Sulfur in Biosynthetic Pathways. Nat Chem Biol. 2006; 2:185–194. [PubMed: 16547481]

637. Schaedler TA, Thornton JD, Kruse I, Schwarzländer M, Meyer AJ, van Veen HW, Balk J. A Conserved Mitochondrial ATP-Binding Cassette Transporter Exports Glutathione Polysulfide for Cytosolic Metal Cofactor Assembly. J Biol Chem. 2014; 289:23264–23274. [PubMed: 25006243]

638. Kessler D. Enzymatic Activation of Sulfur for Incorporation into Biomolecules in Prokaryotes. FEMS Microbiol Rev. 2006; 30:825–840. [PubMed: 17064282]

639. Kutney GW, Turnbull K. Compounds Containing the Sulfur-Sulfur Double Bond. Chem Rev. 1982; 82:333–357.

640. Kutzelnigg W. Chemical Bonding in Higher Main Group Elements. Angew Chem, Int Ed Engl. 1984; 23:272–295.

641. Steudel R, Drozdova Y, Miaskiewicz K, Hertwig RH, Koch W. How Unstable Are Thiosulfoxides? An Ab Initio MO Study of Various Disulfanes RSSR (R = H, Me, Pr, All), Their Branched Isomers R 2 SS, and the Related Transition States 1, 2. J Am Chem Soc. 1997; 119:1990–1996.

642. Sörbo B. Enzymic Transfer of Sulfur from Mercaptopyruvate to Sulfite or Sulfinates. Biochim Biophys Acta. 1957; 24:324–329. [PubMed: 13436433]

643. Valentine WN, Toohey JI, Paglia DE, Nakatani M, Brockway RA. Modification of Erythrocyte Enzyme Activities by Persulfides and Methanethiol: Possible Regulatory Role. Proc Natl Acad Sci U S A. 1987; 84:1394–1398. [PubMed: 3469673]

644. D'Imprima E, Mills DJ, Parey K, Brandt U, Kühlbrandt W, Zickermann V, Vonck J. Cryo-EM Structure of Respiratory Complex I Reveals a Link to Mitochondrial Sulfur Metabolism. Biochim Biophys Acta, Bioenerg. 2016; 1857:1935–1942.

645. Bonomi F, Pagani S, Cerletti P, Cannella C. Rhodanese-Mediated Sulfur Transfer to Succinate Dehydrogenase. Eur J Biochem. 1977; 72:17–24. [PubMed: 318999]

646. Pagani S, Bonomi F, Cerletti P. Sulfide Insertion into Spinach Ferredoxin by Rhodanese. Biochim Biophys Acta, Protein Struct Mol Enzymol. 1982; 700:154–164.

647. Bonomi F, Pagani S, Cerletti P. Insertion of Sulfide into Ferredoxins Catalyzed by Rhodanese. FEBS Lett. 1977; 84:149–152. [PubMed: 590515]

648. Tomati U, Matarese R, Federici G. Ferredoxin Activation by Rhodanese. Phytochemistry. 1974; 13:1703–1706.

649. Cerletti P. Seeking a Better Job for an under-Employed Enzyme: Rhodanese. Trends Biochem Sci. 1986; 11:369–372.

650. Agrò AF, Mavelli I, Cannella C, Federici G. Activation of Porcine Heart Mitochondrial Malate Dehydrogenase by Zero Valence Sulfur and Rhodanese. Biochem Biophys Res Commun. 1976; 68:553–560. [PubMed: 1252245]

651. Pagani S, Galante YM. Interaction of Rhodanese with Mitochondrial NADH Dehydrogenase. Biochim Biophys Acta, Protein Struct Mol Enzymol. 1983; 742:278–284.

652. Krueger K, Koch K, Jühling A, Tepel M, Scholze A. Low Expression of Thiosulfate Sulfurtransferase (Rhodanese) Predicts Mortality in Hemodialysis Patients. Clin Biochem. 2010; 43:95–101. [PubMed: 19695240]

653. Fauman EB, Cogswell JP, Lovejoy B, Rocque WJ, Holmes W, Montana VG, Piwnica-Worms H, Rink MJ, Saper MA. Crystal Structure of the Catalytic Domain of the Human Cell Cycle Control Phosphatase, Cdc25A. Cell. 1998; 93:617–625. [PubMed: 9604936]

654. Matthies A, Rajagopalan KV, Mendel RR, Leimkuhler S. Evidence for the Physiological Role of a Rhodanese-like Protein for the Biosynthesis of the Molybdenum Cofactor in Humans. Proc Natl Acad Sci U S A. 2004; 101:5946–5951. [PubMed: 15073332]

655. Matthies A, Nimtz M, Leimkühler S. Molybdenum Cofactor Biosynthesis in Humans: Identification of a Persulfide Group in the Rhodanese-like Domain of MOCS3 by Mass Spectrometry. Biochemistry. 2005; 44:7912–7920. [PubMed: 15910006]

656. Cheng Z, Zhang J, Ballou DP, Williams CH. Reactivity of Thioredoxin as a Protein Thiol-Disulfide Oxidoreductase. Chem Rev. 2011; 111:5768–5783. [PubMed: 21793530]

657. Lu J, Holmgren A. The Thioredoxin Antioxidant System. Free Radic Biol Med. 2014; 66:75–87. [PubMed: 23899494]

658. Buchanan BB, Holmgren A, Jacquot J-P, Scheibe R. Fifty Years in the Thioredoxin Field and a Bountiful Harvest. Biochim Biophys Acta, Gen Subj. 2012; 1820:1822–1829.

659. Lu J, Holmgren A. The Thioredoxin Superfamily in Oxidative Protein Folding. Antioxid Redox Signal. 2014; 21:457–470. [PubMed: 24483600]

660. Li H, Hanson C, Fuchs JA, Woodward C, Thomas GJ. Determination of the pKa Values of Active-Center Cysteines, Cysteines-32 and –35, in Escherichia Coli Thioredoxin by Raman Spectroscopy. Biochemistry. 1993; 32:5800–5808. [PubMed: 8099293]

661. Kallis GB, Holmgren A. Differential Reactivity of the Functional Sulfhydryl Groups of Cysteine-32 and Cysteine-35 Present in the Reduced Form of Thioredoxin from Escherichia Coli. J Biol Chem. 1980; 255:10261–10265. [PubMed: 7000775]

662. Jeng MF, Holmgren A, Dyson HJ. Proton Sharing between Cysteine Thiols in Escherichia Coli Thioredoxin: Implications for the Mechanism of Protein Disulfide Reduction. Biochemistry. 1995; 34:10101–10105. [PubMed: 7640264]

663. Lennon BW, Williams CH. Enzyme-Monitored Turnover of Escherichia Coli Thioredoxin Reductase: Insights for Catalysis. Biochemistry. 1996; 35:4704–4712. [PubMed: 8664260]

664. Palde PB, Carroll KS. A Universal Entropy-Driven Mechanism for Thioredoxin–target Recognition. Proc Natl Acad Sci U S A. 2015; 112:7960–7965. [PubMed: 26080424]

665. Jeong W, Yoon HW, Lee S-R, Rhee SG. Identification and Characterization of TRP14, a Thioredoxin-Related Protein of 14 kDa. New Insights into the Specificity of Thioredoxin Function. J Biol Chem. 2004; 279:3142–3150. [PubMed: 14607844]

666. Nakamura H, De Rosa S, Roederer M, Anderson MT, Dubs JG, Yodoi J, Holmgren A, Herzenberg LA, Herzenberg LA. Elevation of Plasma Thioredoxin Levels in HIV-Infected Individuals. Int Immunol. 1996; 8:603–611. [PubMed: 8671648]

667. Burke-Gaffney A, Callister MEJ, Nakamura H. Thioredoxin: Friend or Foe in Human Disease? Trends Pharmacol Sci. 2005; 26:398–404. [PubMed: 15990177]

668. Nakamura H, De Rosa SC, Yodoi J, Holmgren A, Ghezzi P, Herzenberg LA, Herzenberg LA. Chronic Elevation of Plasma Thioredoxin: Inhibition of Chemotaxis and Curtailment of Life Expectancy in AIDS. Proc Natl Acad Sci U S A. 2001; 98:2688–2693. [PubMed: 11226300]

669. Couto N, Wood J, Barber J. The Role of Glutathione Reductase and Related Enzymes on Cellular Redox Homoeostasis Network. Free Radic Biol Med. 2016; 95:27–42. [PubMed: 26923386]

670. Toledano MB, Delaunay-Moisan A, Outten CE, Igbaria A. Functions and Cellular Compartmentation of the Thioredoxin and Glutathione Pathways in Yeast. Antioxid Redox Signal. 2013; 18:1699–1711. [PubMed: 23198979]

671. Prast-Nielsen S, Huang H-H, Williams DL. Thioredoxin Glutathione Reductase: Its Role in Redox Biology and Potential as a Target for Drugs against Neglected Diseases. Biochim Biophys Acta, Gen Subj. 2011; 1810:1262–1271.

672. Zhao W, Zhang J, Lu Y, Wang R. The Vasorelaxant Effect of H(2)S as a Novel Endogenous Gaseous K(ATP) Channel Opener. EMBO J. 2001; 20:6008–6016. [PubMed: 11689441]

673. Wang R, Szabo C, Ichinose F, Ahmed A, Whiteman M, Papapetropoulos A. The Role of H_2S Bioavailability in Endothelial Dysfunction. Trends Pharmacol Sci. 2015; 36:568–578. [PubMed: 26071118]

674. Hybertson BM, Gao B, Bose SK, McCord JM. Oxidative Stress in Health and Disease: The Therapeutic Potential of Nrf2 Activation. Mol Aspects Med. 2011; 32:234–246. [PubMed: 22020111]

675. Kaspar JW, Niture SK, Jaiswal AK. Nrf2:INrf2 (Keap1) Signaling in Oxidative Stress. Free Radic Biol Med. 2009; 47:1304–1309. [PubMed: 19666107]

676. Wakabayashi N, Dinkova-Kostova AT, Holtzclaw WD, Kang M-I, Kobayashi A, Yamamoto M, Kensler TW, Talalay P. Protection against Electrophile and Oxidant Stress by Induction of the Phase 2 Response: Fate of Cysteines of the Keap1 Sensor Modified by Inducers. Proc Natl Acad Sci U S A. 2004; 101:2040–2045. [PubMed: 14764894]

677. Calvert JW, Elston M, Nicholson CK, Gundewar S, Jha S, Elrod JW, Ramachandran A, Lefer DJ. Genetic and Pharmacologic Hydrogen Sulfide Therapy Attenuates Ischemia-Induced Heart Failure in Mice. Circulation. 2010; 122:11–19. [PubMed: 20566952]

678. Calvert JW, Jha S, Gundewar S, Elrod JW, Ramachandran A, Pattillo CB, Kevil CG, Lefer DJ. Hydrogen Sulfide Mediates Cardioprotection through nrf2 Signaling. Circ Res. 2009; 105:365–374. [PubMed: 19608979]

679. Hourihan JM, Kenna JG, Hayes JD. The Gasotransmitter Hydrogen Sulfide Induces nrf2-Target Genes by Inactivating the keap1 Ubiquitin Ligase Substrate Adaptor through Formation of a

Disulfide Bond between Cys-226 and Cys-613. Antioxid Redox Signal. 2013; 19:465–481. [PubMed: 23145493]

680. Xie Z-Z, Shi M-M, Xie L, Wu Z-Y, Li G, Hua F, Bian J-S. Sulfhydration of p66Shc at Cysteine59 Mediates the Antioxidant Effect of Hydrogen Sulfide. Antioxid Redox Signal. 2014; 21:2531–2542. [PubMed: 24766279]
681. Giorgio M, Migliaccio E, Orsini F, Paolucci D, Moroni M, Contursi C, Pelliccia G, Luzi L, Minucci S, Marcaccio M, et al. Electron Transfer between Cytochrome c and p66Shc Generates Reactive Oxygen Species That Trigger Mitochondrial Apoptosis. Cell. 2005; 122:221–233. [PubMed: 16051147]
682. Zhou H, Ding L, Wu Z, Cao X, Zhang Q, Lin L, Bian J-S. Hydrogen Sulfide Reduces RAGE Toxicity through Inhibition of Its Dimer Formation. Free Radic Biol Med. 2017; 104:262–271. [PubMed: 28108276]
683. Ramasamy R, Yan SF, Schmidt AM. Receptor for AGE (RAGE): Signaling Mechanisms in the Pathogenesis of Diabetes and Its Complications. Ann N Y Acad Sci. 2011; 1243:88–102. [PubMed: 22211895]
684. Hetz C. The Unfolded Protein Response: Controlling Cell Fate Decisions under ER Stress and beyond. Nat Rev Mol Cell Biol. 2012; 13:89–102. [PubMed: 22251901]
685. Feldhammer M, Uetani N, Miranda-Saavedra D, Tremblay ML. PTP1B: a simple enzyme for a complex world. Crit Rev Biochem Mol Biol. 2013; 48:430–445. [PubMed: 23879520]
686. Paulsen CE, Truong TH, Garcia FJ, Homann A, Gupta V, Leonard SE, Carroll KS. Peroxide-Dependent Sulfenylation of the EGFR Catalytic Site Enhances Kinase Activity. Nat Chem Biol. 2011; 8:57–64. [PubMed: 22158416]
687. Peralta D, Bronowska AK, Morgan B, Dóka É, Van Laer K, Nagy P, Gräter F, Dick TP. A Proton Relay Enhances H2O2 Sensitivity of GAPDH to Facilitate Metabolic Adaptation. Nat Chem Biol. 2015; 11:156–163. [PubMed: 25580853]
688. Hara MR, Agrawal N, Kim SF, Cascio MB, Fujimuro M, Ozeki Y, Takahashi M, Cheah JH, Tankou SK, Hester LD, et al. S-Nitrosylated GAPDH Initiates Apoptotic Cell Death by Nuclear Translocation Following Siah1 Binding. Nat Cell Biol. 2005; 7:665–674. [PubMed: 15951807]
689. Jarosz AP, Wei W, Gauld JW, Auld J, Özcan F, Aslan M, Mutus B. Glyceraldehyde 3-Phosphate Dehydrogenase (GAPDH) Is Inactivated by S-Sulfuration in Vitro. Free Radic Biol Med. 2015; 89:512–521. [PubMed: 26453916]
690. Napetschnig J, Wu H. Molecular Basis of NF-κB Signaling. Annu Rev Biophys. 2013; 42:443–468. [PubMed: 23495970]
691. Aggarwal BB, Gupta SC, Kim JH. Historical Perspectives on Tumor Necrosis Factor and Its Superfamily: 25 Years Later, a Golden Journey. Blood. 2012; 119:651–665. [PubMed: 22053109]
692. Whiteman M, Winyard PG. Hydrogen Sulfide and Inflammation: The Good, the Bad, the Ugly and the Promising. Expert Rev Clin Pharmacol. 2011; 4:13–32. [PubMed: 22115346]
693. Du J, Huang Y, Yan H, Zhang Q, Zhao M, Zhu M, Liu J, Chen SX, Bu D, Tang C, et al. Hydrogen Sulfide Suppresses Oxidized Low-Density Lipoprotein (Ox-LDL)-Stimulated Monocyte Chemoattractant Protein 1 Generation from Macrophages via the Nuclear Factor B (NF-kB) Pathway. J Biol Chem. 2014; 289:9741–9753. [PubMed: 24550391]
694. D'Amours D, Desnoyers S, D'Silva I, Poirier GG. Poly(ADP-Ribosyl)ation Reactions in the Regulation of Nuclear Functions. Biochem J. 1999; 342:249–268. [PubMed: 10455009]
695. Cohen-Armon M, Visochek L, Rozensal D, Kalal A, Geistrikh I, Klein R, Bendetz-Nezer S, Yao Z, Seger R. DNA-Independent PARP-1 Activation by Phosphorylated ERK2 Increases Elk1 Activity: A Link to Histone Acetylation. Mol Cell. 2007; 25:297–308. [PubMed: 17244536]
696. Shulman JM, De Jager PL, Feany MB. Parkinson's Disease: Genetics and Pathogenesis. Annu Rev Pathol: Mech Dis. 2011; 6:193–222.
697. Moore DJ, West AB, Dawson VL, Dawson TM. Molecular Pathophysiology of Parkinson's Disease. Annu Rev Neurosci. 2005; 28:57–87. [PubMed: 16022590]
698. Chung KKK, Thomas B, Li X, Pletnikova O, Troncoso JC, Marsh L, Dawson VL, Dawson TM. S-Nitrosylation of Parkin Regulates Ubiquitination and Compromises Parkin's Protective Function. Science. 2004; 304:1328–1331. [PubMed: 15105460]

699. Scarffe LA, Stevens DA, Dawson VL, Dawson TM. Parkin and PINK1: Much More than Mitophagy. Trends Neurosci. 2014; 37:315–324. [PubMed: 24735649]

700. Herrmann M, Widmann T, Colaianni G, Colucci S, Zallone A, Herrmann W. Increased Osteoclast Activity in the Presence of Increased Homocysteine Concentrations. Clin Chem. 2005; 51:2348–2353. [PubMed: 16195358]

701. Xu Z-S, Wang X-Y, Xiao D-M, Hu L-F, Lu M, Wu Z-Y, Bian J-S. Hydrogen Sulfide Protects MC3T3-E1 Osteoblastic Cells against H2O2-Induced Oxidative Damage—implications for the Treatment of Osteoporosis. Free Radic Biol Med. 2011; 50:1314–1323. [PubMed: 21354302]

702. Gutteridge S, Tanner SJ, Bray RC. Comparison of the Molybdenum Centres of Native and Desulpho Xanthine Oxidase The Nature of the Cyanide-Labile Sulphur Atom and the Nature of the Proton-Accepting Group. Biochem J. 1978; 175:887–897. [PubMed: 217354]

703. Carrico RJ, Deutsch HF. Isolation of Human Hepatocuprein and Cerebrocuprein. Their Identity with Erythrocuprein. J Biol Chem. 1969; 244:6087–6093. [PubMed: 4310831]

704. de Beus MD, Chung J, Colón W. Modification of Cysteine 111 in Cu/Zn Superoxide Dismutase Results in Altered Spectroscopic and Biophysical Properties. Protein Sci. 2004; 13:1347–1355. [PubMed: 15096637]

705. Calabrese L, Federici G, Bannister WH, Bannister JV, Rotilio G, Finazzi-Agrò A. Labile Sulfur in Human Superoxide Dismutase. Eur J Biochem. 1975; 56:305–309. [PubMed: 1175624]

706. You Z, Cao X, Taylor AB, Hart PJ, Levine RL. Characterization of a Covalent Polysulfane Bridge in Copper–Zinc Superoxide Dismutase. Biochemistry. 2010; 49:1191–1198. [PubMed: 20052996]

707. Kelly DP, Shergill JK, Lu WP, Wood AP. Oxidative Metabolism of Inorganic Sulfur Compounds by Bacteria. Antonie van Leeuwenhoek. 1997; 71:95–107. [PubMed: 9049021]

708. Kellogg WW, Cadle RD, Allen ER, Lazrus AL, Martell EA. The Sulfur Cycle. Science. 1972; 175:587–596. [PubMed: 5009760]

709. Bang SW, Clark DS, Keasling JD. Engineering Hydrogen Sulfide Production and Cadmium Removal by Expression of the Thiosulfate Reductase Gene (phsABC) from Salmonella Enterica Serovar Typhimurium in Escherichia Coli. Appl Environ Microbiol. 2000; 66:3939–3944. [PubMed: 10966412]

710. Peck HD. Enzymatic Basis for Assimilatory and Dissimilatory Sulfate Reduction. J Bacteriol. 1961; 82:933–939. [PubMed: 14484818]

711. Carbonero F, Benefiel AC, Alizadeh-Ghamsari AH, Gaskins HR. Microbial Pathways in Colonic Sulfur Metabolism and Links with Health and Disease. Front Physiol. 2012; 3:448. [PubMed: 23226130]

712. Singh S, Lin H. Hydrogen Sulfide in Physiology and Diseases of the Digestive Tract. Microorganisms. 2015; 3:866–889. [PubMed: 27682122]

713. Shatalin K, Shatalina E, Mironov A, Nudler E. H_2S: A Universal Defense Against Antibiotics in Bacteria. Science. 2011; 334:986–990. [PubMed: 22096201]

714. Zhang H, Hu L-Y, Hu K-D, He Y-D, Wang S-H, Luo J-P. Hydrogen Sulfide Promotes Wheat Seed Germination and Alleviates Oxidative Damage against Copper Stress. J Integr Plant Biol. 2008; 50:1518–1529. [PubMed: 19093970]

715. Zhang H, Tang J, Liu X-P, Wang Y, Yu W, Peng W-Y, Fang F, Ma D-F, Wei Z-J, Hu L-Y. Hydrogen Sulfide Promotes Root Organogenesis in Ipomoea Batatas, Salix Matsudana and Glycine Max. J Integr Plant Biol. 2009; 51:1086–1094. [PubMed: 20021556]

716. Zhang H, Ye Y-K, Wang S-H, Luo J-P, Tang J, Ma D-F. Hydrogen Sulfide Counteracts Chlorophyll Loss in Sweetpotato Seedling Leaves and Alleviates Oxidative Damage against Osmotic Stress. Plant Growth Regul. 2009; 58:243–250.

717. Zhang H, Dou W, Jiang C-X, Wei Z-J, Liu J, Jones RL. Hydrogen Sulfide Stimulates β-Amylase Activity during Early Stages of Wheat Grain Germination. Plant Signaling Behav. 2010; 5:1031–1033.

718. Zhang H, Hu S-L, Zhang Z-J, Hu L-Y, Jiang C-X, Wei Z-J, Liu J, Wang H-L, Jiang S-T. Hydrogen Sulfide Acts as a Regulator of Flower Senescence in Plants. Postharvest Biol Technol. 2011; 60:251–257.

719. García-Mata C, Lamattina L. Hydrogen Sulphide, a Novel Gasotransmitter Involved in Guard Cell Signalling. New Phytol. 2010; 188:977–984. [PubMed: 20831717]

720. Jin Z, Xue S, Luo Y, Tian B, Fang H, Li H, Pei Y. Hydrogen Sulfide Interacting with Abscisic Acid in Stomatal Regulation Responses to Drought Stress in Arabidopsis. Plant Physiol Biochem. 2013; 62:41–46. [PubMed: 23178483]

721. Lisjak M, Srivastava N, Teklic T, Civale L, Lewandowski K, Wilson I, Wood ME, Whiteman M, Hancock JT. A Novel Hydrogen Sulfide Donor Causes Stomatal Opening and Reduces Nitric Oxide Accumulation. Plant Physiol Biochem. 2010; 48:931–935. [PubMed: 20970349]

722. Lisjak M, Teklić T, Wilson ID, Wood M, Whiteman M, Hancock JT. Hydrogen Sulfide Effects on Stomatal Apertures. Plant Signaling Behav. 2011; 6:1444–1446.

723. Kimura H. Hydrogen Sulfide Induces Cyclic AMP and Modulates the NMDA Receptor. Biochem Biophys Res Commun. 2000; 267:129–133. [PubMed: 10623586]

724. Nagai Y, Tsugane M, Oka J-I, Kimura H. Hydrogen Sulfide Induces Calcium Waves in Astrocytes. FASEB J. 2004; 18:557–559. [PubMed: 14734631]

725. Lee SW, Hu Y-S, Hu L-F, Lu Q, Dawe GS, Moore PK, Wong PT-H, Bian J-S. Hydrogen Sulphide Regulates Calcium Homeostasis in Microglial Cells. Glia. 2006; 54:116–124. [PubMed: 16718684]

726. Yong QC, Choo CH, Tan BH, Low C-M, Bian J-S. Effect of Hydrogen Sulfide on Intracellular Calcium Homeostasis in Neuronal Cells. Neurochem Int. 2010; 56:508–515. [PubMed: 20026367]

727. Lu M, Choo CH, Hu L-F, Tan BH, Hu G, Bian J-S. Hydrogen Sulfide Regulates Intracellular pH in Rat Primary Cultured Glia Cells. Neurosci Res. 2010; 66:92–98. [PubMed: 19818370]

728. Matsunami M, Tarui T, Mitani K, Nagasawa K, Fukushima O, Okubo K, Yoshida S, Takemura M, Kawabata A. Luminal Hydrogen Sulfide Plays a Pronociceptive Role in Mouse Colon. Gut. 2009; 58:751–761. [PubMed: 18852258]

729. Lee AT-H, Jitendrakumar Shah J, Li L, Cheng Y, Moore PK, Khanna S. A Nociceptive-Intensity-Dependent Role for Hydrogen Sulphide in the Formalin Model of Persistent Inflammatory Pain. Neuroscience. 2008; 152:89–96. [PubMed: 18248901]

730. Nelson MT, Woo J, Kang H-W, Vitko I, Barrett PQ, Perez-Reyes E, Lee J-H, Shin H-S, Todorovic SM. Reducing Agents Sensitize C-Type Nociceptors by Relieving High-Affinity Zinc Inhibition of T-Type Calcium Channels. J Neurosci. 2007; 27:8250–8260. [PubMed: 17670971]

731. Kawabata A, Ishiki T, Nagasawa K, Yoshida S, Maeda Y, Takahashi T, Sekiguchi F, Wada T, Ichida S, Nishikawa H. Hydrogen Sulfide as a Novel Nociceptive Messenger. Pain. 2007; 132:74–81. [PubMed: 17346888]

732. Andersson DA, Gentry C, Bevan S. TRPA1 Has a Key Role in the Somatic Pro-Nociceptive Actions of Hydrogen Sulfide. PLoS One. 2012; 7:e46917. [PubMed: 23071662]

733. Ogawa H, Takahashi K, Miura S, Imagawa T, Saito S, Tominaga M, Ohta T. H_2S Functions as a Nociceptive Messenger through Transient Receptor Potential Ankyrin 1 (TRPA1) Activation. Neuroscience. 2012; 218:335–343. [PubMed: 22641084]

734. Tsubota-Matsunami M, Noguchi Y, Okawa Y, Sekiguchi F, Kawabata A. Colonic Hydrogen Sulfide-Induced Visceral Pain and Referred Hyperalgesia Involve Activation of Both Ca(v)3.2 and TRPA1 Channels in Mice. J Pharmacol Sci. 2012; 119:293–296. [PubMed: 22785020]

735. Cunha TM, Dal-Secco D, Verri WA, Guerrero AT, Souza GR, Vieira SM, Lotufo CM, Neto AF, Ferreira SH, Cunha FQ. Dual Role of Hydrogen Sulfide in Mechanical Inflammatory Hypernociception. Eur J Pharmacol. 2008; 590:127–135. [PubMed: 18585702]

736. Sachs D, Cunha FQ, Ferreira SH. Peripheral Analgesic Blockade of Hypernociception: Activation of arginine/NO/cGMP/protein Kinase G/ATP-Sensitive K+ Channel Pathway. Proc Natl Acad Sci U S A. 2004; 101:3680–3685. [PubMed: 14990791]

737. Distrutti E, Sediari L, Mencarelli A, Renga B, Orlandi S, Antonelli E, Roviezzo F, Morelli A, Cirino G, Wallace JL, et al. Evidence That Hydrogen Sulfide Exerts Antinociceptive Effects in the Gastrointestinal Tract by Activating KATP Channels. J Pharmacol Exp Ther. 2005; 316:325–335. [PubMed: 16192316]

738. Whiteman M, Armstrong JS, Chu SH, Jia-Ling S, Wong B-S, Cheung NS, Halliwell B, Moore PK. The Novel Neuromodulator Hydrogen Sulfide: An Endogenous Peroxynitrite “Scavenger”? J Neurochem. 2004; 90:765–768. [PubMed: 15255956]

739. Lu M, Hu L-F, Hu G, Bian J-S. Hydrogen Sulfide Protects Astrocytes against H2O2-Induced Neural Injury via Enhancing Glutamate Uptake. Free Radic Biol Med. 2008; 45:1705–1713. [PubMed: 18848879]

740. Eto K, Asada T, Arima K, Makifuchi T, Kimura H. Brain Hydrogen Sulfide Is Severely Decreased in Alzheimer’s Disease. Biochem Biophys Res Commun. 2002; 293:1485–1488. [PubMed: 12054683]

741. Giuliani D, Ottani A, Zaffe D, Galantucci M, Strinati F, Lodi R, Guarini S. Hydrogen Sulfide Slows down Progression of Experimental Alzheimer’s Disease by Targeting Multiple Pathophysiological Mechanisms. Neurobiol Learn Mem. 2013; 104:82–91. [PubMed: 23726868]

742. Xuan A, Long D, Li J, Ji W, Zhang M, Hong L, Liu J. Hydrogen Sulfide Attenuates Spatial Memory Impairment and Hippocampal Neuroinflammation in β-Amyloid Rat Model of Alzheimer’s Disease. J Neuroinflammation. 2012; 9:202. [PubMed: 22898621]

743. Zhang H, Gao Y, Zhao F, Dai Z, Meng T, Tu S, Yan Y. Hydrogen Sulfide Reduces mRNA and Protein Levels of Beta-Site Amyloid Precursor Protein Cleaving Enzyme 1 in PC12 Cells. Neurochem Int. 2011; 58:169–175. [PubMed: 21095213]

744. Nagpure BV, Bian J-S. Hydrogen Sulfide Inhibits A2A Adenosine Receptor Agonist Induced β-Amyloid Production in SH-SY5Y Neuroblastoma Cells via a cAMP Dependent Pathway. PLoS One. 2014; 9:e88508. [PubMed: 24523906]

745. Paul BD, Sbodio JI, Xu R, Vandiver MS, Cha JY, Snowman AM, Snyder SH. Cystathionine γ-Lyase Deficiency Mediates Neurodegeneration in Huntington’s Disease. Nature. 2014; 509:96–100. [PubMed: 24670645]

746. Sbodio JI, Snyder SH, Paul BD. Transcriptional Control of Amino Acid Homeostasis Is Disrupted in Huntington’s Disease. Proc Natl Acad Sci U S A. 2016; 113:8843–8848. [PubMed: 27436896]

747. Snijder PM, Baratashvili M, Grzeschik NA, Leuvenink HGD, Kuijpers L, Huitema S, Schaap O, Giepmans BNG, Kuipers J, Miljkovic JL, et al. Overexpression of Cystathionine γ-Lyase Suppresses Detrimental Effects of Spinocerebellar Ataxia Type 3. Mol Med. 2015; 21:758.

748. Predmore BL, Lefer DJ. Development of Hydrogen Sulfide-Based Therapeutics for Cardiovascular Disease. J Cardiovasc Transl Res. 2010; 3:487–498. [PubMed: 20628909]

749. Elsey DJ, Fowkes RC, Baxter GF. Regulation of Cardiovascular Cell Function by Hydrogen Sulfide (H_2S). Cell Biochem Funct. 2010; 28:95–106. [PubMed: 20104507]

750. Elrod JW, Calvert JW, Morrison J, Doeller JE, Kraus DW, Tao L, Jiao X, Scalia R, Kiss L, Szabo C, et al. Hydrogen Sulfide Attenuates Myocardial Ischemia-Reperfusion Injury by Preservation of Mitochondrial Function. Proc Natl Acad Sci U S A. 2007; 104:15560–15565. [PubMed: 17878306]

751. Shen Y, Shen Z, Luo S, Guo W, Zhu YZ. The Cardioprotective Effects of Hydrogen Sulfide in Heart Diseases: From Molecular Mechanisms to Therapeutic Potential. Oxid Med Cell Longevity. 2015; 2015:1–13.

752. Szabó C, Papapetropoulos A. Hydrogen Sulphide and Angiogenesis: Mechanisms and Applications. Br J Pharmacol. 2011; 164:853–865. [PubMed: 21198548]

753. Zhu YZ, Wang ZJ, Ho P, Loke YY, Zhu YC, Huang SH, Tan CS, Whiteman M, Lu J, Moore PK. Hydrogen Sulfide and Its Possible Roles in Myocardial Ischemia in Experimental Rats. J Appl Physiol. 2006; 102:261–268. [PubMed: 17038495]

754. Zhao W, Wang R. H_2S-Induced Vasorelaxation and Underlying Cellular and Molecular Mechanisms. Am J Physiol -Hear Circ Physiol. 2002; 283:H474–H480.

755. Cheng Y, Ndisang JF, Tang G, Cao K, Wang R. Hydrogen Sulfide-Induced Relaxation of Resistance Mesenteric Artery Beds of Rats. Am J Physiol Hear Circ Physiol. 2004; 287:H2316–H2323.

756. Jiang B, Tang G, Cao K, Wu L, Wang R. Molecular Mechanism for H_2S-Induced Activation of K ATP Channels. Antioxid Redox Signal. 2010; 12:1167–1178. [PubMed: 19769462]

757. Ishii I, Akahoshi N, Yamada H, Nakano S, Izumi T, Suematsu M. Cystathionine Gamma-Lyase-Deficient Mice Require Dietary Cysteine to Protect against Acute Lethal Myopathy and Oxidative Injury. J Biol Chem. 2010; 285:26358–26368. [PubMed: 20566639]

758. Papapetropoulos A, Pyriochou A, Altaany Z, Yang G, Marazioti A, Zhou Z, Jeschke MG, Branski LK, Herndon DN, Wang R, et al. Hydrogen Sulfide Is an Endogenous Stimulator of Angiogenesis. Proc Natl Acad Sci U S A. 2009; 106:21972–21977. [PubMed: 19955410]

759. Bucci M, Papapetropoulos A, Vellecco V, Zhou Z, Zaid A, Giannogonas P, Cantalupo A, Dhayade S, Karalis KP, Wang R, et al. cGMP-Dependent Protein Kinase Contributes to Hydrogen Sulfide-Stimulated Vasorelaxation. PLoS One. 2012; 7:e53319. [PubMed: 23285278]

760. Kondo K, Bhushan S, King AL, Prabhu SD, Hamid T, Koenig S, Murohara T, Predmore BL, Gojon G, Wang R, et al. H_2S Protects against Pressure Overload-Induced Heart Failure via Upregulation of Endothelial Nitric Oxide Synthase. Circulation. 2013; 127:1116–1127. [PubMed: 23393010]

761. Wang X, Wang Q, Guo W, Zhu YZ. Hydrogen Sulfide Attenuates Cardiac Dysfunction in a Rat Model of Heart Failure: A Mechanism through Cardiac Mitochondrial Protection. Biosci Rep. 2011; 31:87–98. [PubMed: 20450490]

762. Lin VS, Lippert AR, Chang CJ. Cell-Trappable Fluorescent Probes for Endogenous Hydrogen Sulfide Signaling and Imaging H2O2-Dependent H_2S Production. Proc Natl Acad Sci U S A. 2013; 110:7131–7135. [PubMed: 23589874]

763. Tao B-B, Liu S-Y, Zhang C-C, Fu W, Cai W-J, Wang Y, Shen Q, Wang M-J, Chen Y, Zhang L-J, et al. VEGFR2 Functions As an H_2S-Targeting Receptor Protein Kinase with Its Novel Cys1045–Cys1024 Disulfide Bond Serving As a Specific Molecular Switch for Hydrogen Sulfide Actions in Vascular Endothelial Cells. Antioxid Redox Signal. 2013; 19:448–464. [PubMed: 23199280]

764. Wang Y, Zhao X, Jin H, Wei H, Li W, Bu D, Tang X, Ren Y, Tang C, Du J. Role of Hydrogen Sulfide in the Development of Atherosclerotic Lesions in Apolipoprotein E Knockout Mice. Arterioscler Thromb Vasc Biol. 2009; 29:173–179. [PubMed: 18988885]

765. Mani S, Li H, Untereiner A, Wu L, Yang G, Austin RC, Dickhout JG, Lhotak S, Meng QH, Wang R. Decreased Endogenous Production of Hydrogen Sulfide Accelerates Atherosclerosis. Circulation. 2013; 127:2523–2534. [PubMed: 23704252]

766. Bhatia M. H_2S and Inflammation: An Overview. Handb Exp Pharmacol. 2015; 230:165–180. [PubMed: 26162834]

767. Bhatia M, Wong FL, Fu D, Lau HY, Moochhala SM, Moore PK. Role of Hydrogen Sulfide in Acute Pancreatitis and Associated Lung Injury. FASEB J. 2005; 19:623–625. [PubMed: 15671155]

768. Ang AD, Rivers-Auty J, Hegde A, Ishii I, Bhatia M. The Effect of CSE Gene Deletion in Caerulein-Induced Acute Pancreatitis in the Mouse. Am J Physiol Gastrointest Liver Physiol. 2013; 305:G712–G721. [PubMed: 24008358]

769. Markó L, Szijártó IA, Filipovic MR, Kaßmann M, Balogh A, Park J-K, Przybyl L, N'diaye G, Krämer S, Anders J, et al. Role of Cystathionine Gamma-Lyase in Immediate Renal Impairment and Inflammatory Response in Acute Ischemic Kidney Injury. Sci Rep. 2016; 6:27517. [PubMed: 27273292]

770. Hui Y, Du J, Tang C, Bin G, Jiang H. Changes in Arterial Hydrogen Sulfide (H(2)S) Content during Septic Shock and Endotoxin Shock in Rats. J Infect. 2003; 47:155–160. [PubMed: 12860150]

771. Li L, Bhatia M, Zhu YZ, Zhu YC, Ramnath RD, Wang ZJ, Anuar FBM, Whiteman M, Salto-Tellez M, Moore PK. Hydrogen Sulfide Is a Novel Mediator of Lipopolysaccharide-Induced Inflammation in the Mouse. FASEB J. 2005; 19:1196–1198. [PubMed: 15863703]

772. Zhang H, Zhi L, Moore PK, Bhatia M. Role of Hydrogen Sulfide in Cecal Ligation and Puncture-Induced Sepsis in the Mouse. Am J Physiol Lung Cell Mol Physiol. 2006; 290:L1193–L1201. [PubMed: 16428267]

773. Liu Y, Kalogeris T, Wang M, Zuidema M, Wang Q, Dai H, Davis MJ, Hill MA, Korthuis RJ. Hydrogen Sulfide Preconditioning or Neutrophil Depletion Attenuates Ischemia-Reperfusion-Induced Mitochondrial Dysfunction in Rat Small Intestine. Am J Physiol Gastrointest Liver Physiol. 2012; 302:G44–G54. [PubMed: 21921289]

774. Mard SA, Neisi N, Solgi G, Hassanpour M, Darbor M, Maleki M. Gastroprotective Effect of NaHS Against Mucosal Lesions Induced by Ischemia–Reperfusion Injury in Rat. Dig Dis Sci. 2012; 57:1496–1503. [PubMed: 22271414]

775. Medeiros JVR, Bezerra VH, Gomes AS, Barbosa ALR, Lima-Junior RCP, Soares PMG, Brito GAC, Ribeiro RA, Cunha FQ, Souza MHLP. Hydrogen Sulfide Prevents Ethanol-Induced Gastric Damage in Mice: Role of ATP-Sensitive Potassium Channels and Capsaicin-Sensitive Primary Afferent Neurons. J Pharmacol Exp Ther. 2009; 330:764–770. [PubMed: 19491326]

776. Fiorucci S, Antonelli E, Distrutti E, Rizzo G, Mencarelli A, Orlandi S, Zanardo R, Renga B, Di Sante M, Morelli A, et al. Inhibition of Hydrogen Sulfide Generation Contributes to Gastric Injury Caused by Anti-Inflammatory Nonsteroidal Drugs. Gastro-enterology. 2005; 129:1210–1224.

777. Zanardo RCO, Brancaleone V, Distrutti E, Fiorucci S, Cirino G, Wallace JL. Hydrogen Sulfide Is an Endogenous Modulator of Leukocyte-Mediated Inflammation. FASEB J. 2006; 20:2118–2120. [PubMed: 16912151]

778. Wallace JL, Dicay M, McKnight W, Martin GR. Hydrogen Sulfide Enhances Ulcer Healing in Rats. FASEB J. 2007; 21:4070–4076. [PubMed: 17634391]

779. Flannigan KL, Ferraz JGP, Wang R, Wallace JL. Enhanced Synthesis and Diminished Degradation of Hydrogen Sulfide in Experimental Colitis: A Site-Specific, Pro-Resolution Mechanism. PLoS One. 2013; 8:e71962. [PubMed: 23940796]

780. Whiteman M, Li L, Rose P, Tan C-H, Parkinson DB, Moore PK. The Effect of Hydrogen Sulfide Donors on Lipopolysaccharide-Induced Formation of Inflammatory Mediators in Macrophages. Antioxid Redox Signal. 2010; 12:1147–1154. [PubMed: 19769459]

781. Fang L, Li H, Tang C, Geng B, Qi Y, Liu X. Hydrogen Sulfide Attenuates the Pathogenesis of Pulmonary Fibrosis Induced by Bleomycin in Rats. Can J Physiol Pharmacol. 2009; 87:531–538. [PubMed: 19767876]

782. Fang L-P, Lin Q, Tang C-S, Liu X-M. Hydrogen Sulfide Suppresses Migration, Proliferation and Myofibroblast Transdifferentiation of Human Lung Fibroblasts. Pulm Pharmacol Ther. 2009; 22:554–561. [PubMed: 19651225]

783. Perry MM, Hui CK, Whiteman M, Wood ME, Adcock I, Kirkham P, Michaeloudes C, Chung KF. Hydrogen Sulfide Inhibits Proliferation and Release of IL-8 from Human Airway Smooth Muscle Cells. Am J Respir Cell Mol Biol. 2011; 45:746–752. [PubMed: 21297080]

784. Fang L-P, Lin Q, Tang C-S, Liu X-M. Hydrogen Sulfide Attenuates Epithelial–mesenchymal Transition of Human Alveolar Epithelial Cells. Pharmacol Res. 2010; 61:298–305. [PubMed: 19913099]

785. Castro-Piedras I, Perez-Zoghbi JF. Hydrogen Sulphide Inhibits Ca2+ Release through InsP3 Receptors and Relaxes Airway Smooth Muscle. J Physiol. 2013; 591:5999–6015. [PubMed: 24144878]

786. Huang J, Luo Y, Hao Y, Zhang Y, Chen P, Xu J, Chen M, Luo Y, Zhong N, Xu J, et al. Cellular Mechanism Underlying Hydrogen Sulfide Induced Mouse Tracheal Smooth Muscle Relaxation: Role of BKCa. Eur J Pharmacol. 2014; 741:55–63. [PubMed: 25034810]

787. Chen Y, Wang R. The Message in the Air: Hydrogen Sulfide Metabolism in Chronic Respiratory Diseases. Respir Physiol Neurobiol. 2012; 184:130–138. [PubMed: 22476058]

788. Li H, Feng S-J, Zhang G-Z, Wang S-X. Correlation of Lower Concentrations of Hydrogen Sulfide with Atherosclerosis in Chronic Hemodialysis Patients with Diabetic Nephropathy. Blood Purif. 2015; 38:188–194.

789. Yamamoto J, Sato W, Kosugi T, Yamamoto T, Kimura T, Taniguchi S, Kojima H, Maruyama S, Imai E, Matsuo S, et al. Distribution of Hydrogen Sulfide (H_2S)-Producing Enzymes and the Roles of the H_2S Donor Sodium Hydrosulfide in Diabetic Nephropathy. Clin Exp Nephrol. 2013; 17:32–40. [PubMed: 22872231]

790. Kundu S, Pushpakumar SB, Tyagi A, Coley D, Sen U. Hydrogen Sulfide Deficiency and Diabetic Renal Remodeling: Role of Matrix Metalloproteinase-9. Am J Physiol Endocrinol Metab. 2013; 304:E1365–E1378. [PubMed: 23632630]

791. Xia M, Chen L, Muh RW, Li P-L, Li N. Production and Actions of Hydrogen Sulfide, a Novel Gaseous Bioactive Substance, in the Kidneys. J Pharmacol Exp Ther. 2009; 329:1056–1062. [PubMed: 19246614]

792. Ge S-N, Zhao M-M, Wu D-D, Chen Y, Wang Y, Zhu J-H, Cai W-J, Zhu Y-Z, Zhu Y-C. Hydrogen Sulfide Targets EGFR Cys797/Cys798 Residues to Induce Na(+)/K(+)-ATPase Endocytosis and Inhibition in Renal Tubular Epithelial Cells and Increase Sodium Excretion in Chronic Salt-Loaded Rats. Antioxid Redox Signal. 2014; 21:2061–2082. [PubMed: 24684506]

793. Lim JJ, Liu Y-H, Khin ESW, Bian J-S. Vasoconstrictive Effect of Hydrogen Sulfide Involves Downregulation of cAMP in Vascular Smooth Muscle Cells. Am J Physiol Cell Physiol. 2008; 295:C1261–C1270. [PubMed: 18787076]

794. Lu M, Liu Y-H, Ho CY, Tiong CX, Bian J-S. Hydrogen Sulfide Regulates cAMP Homeostasis and Renin Degranulation in As4.1 and Rat Renin-Rich Kidney Cells. Am J Physiol Cell Physiol. 2012; 302:C59–C66. [PubMed: 21940660]

795. Bos EM, Wang R, Snijder PM, Boersema M, Damman J, Fu M, Moser J, Hillebrands J-L, Ploeg RJ, Yang G, et al. Cystathionine γ-Lyase Protects against Renal Ischemia/Reperfusion by Modulating Oxidative Stress. J Am Soc Nephrol. 2013; 24:759–770. [PubMed: 23449534]

796. Luo Z-L, Tang L-J, Wang T, Dai R-W, Ren J-D, Cheng L, Xiang K, Tian F-Z. Effects of Treatment with Hydrogen Sulfide on Methionine-Choline Deficient Diet-Induced Non-Alcoholic Steatohepatitis in Rats. J Gastroenterol Hepatol. 2014; 29:215–222. [PubMed: 24117897]

797. Shirozu K, Tokuda K, Marutani E, Lefer D, Wang R, Ichinose F. Cystathionine γ-Lyase Deficiency Protects Mice from Galactosamine/Lipopolysaccharide-Induced Acute Liver Failure. Antioxid Redox Signal. 2014; 20:204–216. [PubMed: 23758073]

798. Peh MT, Anwar AB, Ng DSW, Atan MSBM, Kumar SD, Moore PK. Effect of Feeding a High Fat Diet on Hydrogen Sulfide (H_2S) Metabolism in the Mouse. Nitric Oxide. 2014; 41:138–145. [PubMed: 24637018]

799. Hwang S-Y, Sarna LK, Siow YL, O K. High-Fat Diet Stimulates Hepatic Cystathionine β-Synthase and Cystathionine γ-Lyase Expression. Can J Physiol Pharmacol. 2013; 91:913–919. [PubMed: 24117258]

800. Fiorucci S, Antonelli E, Mencarelli A, Orlandi S, Renga B, Rizzo G, Distrutti E, Shah V, Morelli A. The Third Gas: H_2S Regulates Perfusion Pressure in Both the Isolated and Perfused Normal Rat Liver and in Cirrhosis. Hepatology. 2005; 42:539–548. [PubMed: 16108046]

801. Zeng T, Zhang C-L, Zhu Z-P, Yu L-H, Zhao X-L, Xie K-Q. Diallyl Trisulfide (DATS) Effectively Attenuated Oxidative Stress-Mediated Liver Injury and Hepatic Mitochondrial Dysfunction in Acute Ethanol-Exposed Mice. Toxicology. 2008; 252:86–91. [PubMed: 18755235]

802. Gibson GR, Macfarlane GT, Cummings JH. Occurrence of Sulphate-Reducing Bacteria in Human Faeces and the Relationship of Dissimilatory Sulphate Reduction to Methanogenesis in the Large Gut. J Appl Bacteriol. 1988; 65:103–111. [PubMed: 3204069]

803. Suarez F, Furne J, Springfield J, Levitt M. Production and Elimination of Sulfur-Containing Gases in the Rat Colon. Am J Physiol. 1998; 274:G727–G733. [PubMed: 9575855]

804. Ohge H, Furne JK, Springfield J, Rothenberger DA, Madoff RD, Levitt MD. Association Between Fecal Hydrogen Sulfide Production and Pouchitis. Dis Colon Rectum. 2005; 48:469–475. [PubMed: 15747080]

805. Flannigan KL, McCoy KD, Wallace JL. Eukaryotic and Prokaryotic Contributions to Colonic Hydrogen Sulfide Synthesis. Am J Physiol Gastrointest Liver Physiol. 2011; 301:G188–G193. [PubMed: 21474649]

806. Ohge H, Furne JK, Springfield J, Sueda T, Madoff RD, Levitt MD. The Effect of Antibiotics and Bismuth on Fecal Hydrogen Sulfide and Sulfate-Reducing Bacteria in the Rat. FEMS Microbiol Lett. 2003; 228:137–142. [PubMed: 14612249]

807. Loubinoux J, Bronowicki J-P, Pereira IAC, Mougenel J-L, Faou AE. Sulfate-Reducing Bacteria in Human Feces and Their Association with Inflammatory Bowel Diseases. FEMS Microbiol Ecol. 2002; 40:107–112. [PubMed: 19709217]

808. Langendijk PS, Hanssen JT, Van der Hoeven JS. Sulfate-Reducing Bacteria in Association with Human Periodontitis. J Clin Periodontol. 2000; 27:943–950. [PubMed: 11140562]

809. Chassard C, Dapoigny M, Scott KP, Crouzet L, Del'Homme C, Marquet P, Martin JC, Pickering G, Ardid D, Eschalier A, et al. Functional Dysbiosis within the Gut Microbiota of Patients with Constipated-Irritable Bowel Syndrome. Aliment Pharmacol Ther. 2012; 35:828–838. [PubMed: 22315951]

810. Wang L, Zhang J, Guo Z, Kwok L, Ma C, Zhang W, Lv Q, Huang W, Zhang H. Effect of Oral Consumption of Probiotic Lactobacillus Planatarum P-8 on Fecal Microbiota, SIgA, SCFAs, and TBAs of Adults of Different Ages. Nutrition. 2014; 30:776–783. [PubMed: 24984992]

811. Sawin EA, De Wolfe TJ, Aktas B, Stroup BM, Murali SG, Steele JL, Ney DM. Glycomacropeptide Is a Prebiotic That Reduces Desulfovibrio Bacteria, Increases Cecal Short-Chain Fatty Acids, and Is Anti-Inflammatory in Mice. Am J Physiol Gastrointest Liver Physiol. 2015; 309:G590–601. [PubMed: 26251473]

812. d'Emmanuele di Villa Bianca R, Sorrentino R, Maffia P, Mirone V, Imbimbo C, Fusco F, De Palma R, Ignarro LJ, Cirino G. Hydrogen Sulfide as a Mediator of Human Corpus Cavernosum Smooth-Muscle Relaxation. Proc Natl Acad Sci U S A. 2009; 106:4513–4518. [PubMed: 19255435]

813. Qiu X, Villalta J, Lin G, Lue TF. Role of Hydrogen Sulfide in the Physiology of Penile Erection. J Androl. 2012; 33:529–535. [PubMed: 22016355]

814. Srilatha B, Adaikan PG, Moore PK. Possible Role for the Novel Gasotransmitter Hydrogen Sulphide in Erectile Dysfunction—a Pilot Study. Eur J Pharmacol. 2006; 535:280–282. [PubMed: 16527268]

815. Srilatha B, Adaikan PG, Li L, Moore PK. Hydrogen Sulphide: A Novel Endogenous Gasotransmitter Facilitates Erectile Function. J Sex Med. 2007; 4:1304–1311. [PubMed: 17655658]

816. Sparatore A, Santus G, Giustarini D, Rossi R, Del Soldato P. Therapeutic Potential of New Hydrogen Sulfide-Releasing Hybrids. Expert Rev Clin Pharmacol. 2011; 4:109–121. [PubMed: 22115352]

817. Li G, Xie ZZ, Chua JMW, Wong PC, Bian J. Hydrogen Sulfide Protects Testicular Germ Cells against Heat-Induced Injury. Nitric Oxide. 2015; 46:165–171. [PubMed: 25446250]

818. Liang R, Yu W, Du J, Yang L, Shang M, Guo J. Localization of Cystathionine Beta Synthase in Mice Ovaries and Its Expression Profile during Follicular Development. Chin Med J (Engl). 2006; 119:1877–1883. [PubMed: 17134586]

819. Patel P, Vatish M, Heptinstall J, Wang R, Carson RJ. The Endogenous Production of Hydrogen Sulphide in Intrauterine Tissues. Reprod Biol Endocrinol. 2009; 7:10. [PubMed: 19200371]

820. Srilatha B, Hu L, Adaikan GP, Moore PK. Initial Characterization of Hydrogen Sulfide Effects in Female Sexual Function. J Sex Med. 2009; 6:1875–1884. [PubMed: 19453900]

821. Wang K, Ahmad S, Cai M, Rennie J, Fujisawa T, Crispi F, Baily J, Miller MR, Cudmore M, Hadoke PWF, et al. Dysregulation of Hydrogen Sulfide Producing Enzyme Cystathionine γ-Lyase Contributes to Maternal Hypertension and Placental Abnormalities in Preeclampsia. Circulation. 2013; 127:2514–2522. [PubMed: 23704251]

822. Guzmán MA, Navarro MA, Carnicer R, Sarría AJ, Acín S, Arnal C, Muniesa P, Surra JC, Arbonés-Mainar JM, Maeda N, et al. Cystathionine Beta-Synthase Is Essential for Female Reproductive Function. Hum Mol Genet. 2006; 15:3168–3176. [PubMed: 16984962]

823. Ning N, Zhu J, Du Y, Gao X, Liu C, Li J, Wang R, Zhao W, Zhang J, Lu Y, et al. Dysregulation of Hydrogen Sulphide Metabolism Impairs Oviductal Transport of Embryos. Nat Commun. 2014; 5:1792–1798.

824. Hayden LJ, Franklin KJ, Roth SH, Moore GJ. Inhibition of Oxytocin-Induced but Not Angiotensin-Induced Rat Uterine Contractions Following Exposure to Sodium Sulfide. Life Sci. 1989; 45:2557–2560. [PubMed: 2559275]

825. Sidhu R, Singh M, Samir G, Carson RJ. L-Cysteine and Sodium Hydrosulphide Inhibit Spontaneous Contractility in Isolated Pregnant Rat Uterine Strips in Vitro. Pharmacol Toxicol. 2001; 88:198–203. [PubMed: 11322178]

826. Robinson H, Wray S. A New Slow Releasing, H_2S Generating Compound, GYY4137 Relaxes Spontaneous and Oxytocin-Stimulated Contractions of Human and Rat Pregnant Myometrium. PLoS One. 2012; 7:e46278. [PubMed: 23029460]

827. Mijušković A, Oreščanin-Dušić Z, Nikolić-Kokić A, Slavić M, Spasić MB, Spasojević I, Blagojević D. Comparison of the Effects of Methanethiol and Sodium Sulphide on Uterine Contractile Activity. Pharmacol Rep. 2014; 66:373–379. [PubMed: 24905511]

828. Volpato GP, Searles R, Yu B, Scherrer-Crosbie M, Bloch KD, Ichinose F, Zapol WM. Inhaled Hydrogen Sulfide. Anesthesiology. 2008; 108:659–668. [PubMed: 18362598]

829. Peng Y-J, Nanduri J, Raghuraman G, Souvannakitti D, Gadalla MM, Kumar GK, Snyder SH, Prabhakar NR. H_2S Mediates O2 Sensing in the Carotid Body. Proc Natl Acad Sci U S A. 2010; 107:10719–10724. [PubMed: 20556885]

830. Peng Y-J, Makarenko VV, Nanduri J, Vasavda C, Raghuraman G, Yuan G, Gadalla MM, Kumar GK, Snyder SH, Prabhakar NR. Inherent Variations in CO-H_2S-Mediated Carotid Body O2 Sensing Mediate Hypertension and Pulmonary Edema. Proc Natl Acad Sci U S A. 2014; 111:1174–1179. [PubMed: 24395806]

831. Li Q, Sun B, Wang X, Jin Z, Zhou Y, Dong L, Jiang L-H, Rong W. A Crucial Role for Hydrogen Sulfide in Oxygen Sensing via Modulating Large Conductance Calcium-Activated Potassium Channels. Antioxid Redox Signal. 2010; 12:1179–1189. [PubMed: 19803741]

832. Miller DL, Roth MB. Hydrogen Sulfide Increases Thermotolerance and Lifespan in Caenorhabditis Elegans. Proc Natl Acad Sci U S A. 2007; 104:20618–20622. [PubMed: 18077331]

833. Qabazard B, Li L, Gruber J, Peh MT, Ng LF, Kumar SD, Rose P, Tan C-H, Dymock BW, Wei F, et al. Hydrogen Sulfide Is an Endogenous Regulator of Aging in Caenorhabditis Elegans. Antioxid Redox Signal. 2014; 20:2621–2630. [PubMed: 24093496]

834. Hellmich MR, Szabo C. Hydrogen Sulfide and Cancer. Handb Exp Pharmacol. 2015; 230:233–241. [PubMed: 26162838]

835. Hellmich MR, Coletta C, Chao C, Szabo C. The Therapeutic Potential of Cystathionine β-Synthetase/Hydrogen Sulfide Inhibition in Cancer. Antioxid Redox Signal. 2015; 22:424–448. [PubMed: 24730679]

836. Szabo C, Ransy C, Módis K, Andriamihaja M, Murghes B, Coletta C, Olah G, Yanagi K, Bouillaud F. Regulation of Mitochondrial Bioenergetic Function by Hydrogen Sulfide. Part I. Biochemical and Physiological Mechanisms. Br J Pharmacol. 2014; 171:2099–2122. [PubMed: 23991830]

837. Lee ZW, Zhou J, Chen C-S, Zhao Y, Tan C-H, Li L, Moore PK, Deng L-W. The Slow-Releasing Hydrogen Sulfide Donor, GYY4137, Exhibits Novel Anti-Cancer Effects In Vitro and In Vivo. PLoS One. 2011; 6:e21077. [PubMed: 21701688]

838. Chattopadhyay M, Kodela R, Nath N, Barsegian A, Boring D, Kashfi K. Hydrogen Sulfide-Releasing Aspirin Suppresses NF-κB Signaling in Estrogen Receptor Negative Breast Cancer Cells in Vitro and in Vivo. Biochem Pharmacol. 2012; 83:723–732. [PubMed: 22209867]

839. Chattopadhyay M, Kodela R, Olson KR, Kashfi K. NOSH-Aspirin (NBS-1120), a Novel Nitric Oxide- and Hydrogen Sulfide-Releasing Hybrid Is a Potent Inhibitor of Colon Cancer Cell Growth in Vitro and in a Xenograft Mouse Model. Biochem Biophys Res Commun. 2012; 419:523–528. [PubMed: 22366248]

840. Sumi D, Ignarro LJ. Sp1 Transcription Factor Expression Is Regulated by Estrogen-Related Receptor alpha1. Biochem Biophys Res Commun. 2005; 328:165–172. [PubMed: 15670765]

841. Maor S, Mayer D, Yarden RI, Lee AV, Sarfstein R, Werner H, Papa MZ. Estrogen Receptor Regulates Insulin-like Growth Factor-I Receptor Gene Expression in Breast Tumor Cells: Involvement of Transcription Factor Sp1. J Endocrinol. 2006; 191:605–612. [PubMed: 17170218]

842. Wu D, Si W, Wang M, Lv S, Ji A, Li Y. Hydrogen Sulfide in Cancer: Friend or Foe? Nitric Oxide. 2015; 50:38–45. [PubMed: 26297862]

843. Sen S, Kawahara B, Gupta D, Tsai R, Khachatryan M, Roy-Chowdhuri S, Bose S, Yoon A, Faull K, Farias-Eisner R, et al. Role of Cystathionine β-Synthase in Human Breast Cancer. Free Radic Biol Med. 2015; 86:228–238. [PubMed: 26051168]

844. Thornburg JM, Nelson KK, Clem BF, Lane AN, Arumugam S, Simmons A, Eaton JW, Telang S, Chesney J. Targeting Aspartate Aminotransferase in Breast Cancer. Breast Cancer Res. 2008; 10:R84. [PubMed: 18922152]

845. Zhang W, Braun A, Bauman Z, Olteanu H, Madzelan P, Banerjee R. Expression Profiling of Homocysteine Junction Enzymes in the NCI60 Panel of Human Cancer Cell Lines. Cancer Res. 2005; 65:1554–1560. [PubMed: 15735045]

846. Zhao H, Li Q, Wang J, Su X, Ng KM, Qiu T, Shan L, Ling Y, Wang L, Cai J, et al. Frequent Epigenetic Silencing of the Folate-Metabolising Gene Cystathionine-Beta-Synthase in Gastrointestinal Cancer. PLoS One. 2012; 7:e49683. [PubMed: 23152928]

847. Takano N, Sarfraz Y, Gilkes DM, Chaturvedi P, Xiang L, Suematsu M, Zagzag D, Semenza GL. Decreased Expression of Cystathionine β-Synthase Promotes Glioma Tumorigenesis. Mol Cancer Res. 2014; 12:1398–1406. [PubMed: 24994751]

848. Kim J, Hong SJ, Park JH, Park SY, Kim SW, Cho EY, Do I-G, Joh J-W, Kim DS. Expression of Cystathionine Beta-Synthase Is Downregulated in Hepatocellular Carcinoma and Associated with Poor Prognosis. Oncol Rep. 2009; 21:1449–1454. [PubMed: 19424622]

849. Cao Q, Zhang L, Yang G, Xu C, Wang R. Butyrate-Stimulated H_2S Production in Colon Cancer Cells. Antioxid Redox Signal. 2010; 12:1101–1109. [PubMed: 19803745]

850. Fan K, Li N, Qi J, Yin P, Zhao C, Wang L, Li Z, Zha X. Wnt/β-Catenin Signaling Induces the Transcription of Cystathionine-γ-Lyase, a Stimulator of Tumor in Colon Cancer. Cell Signalling. 2014; 26:2801–2808. [PubMed: 25193114]

851. Pan Y, Ye S, Yuan D, Zhang J, Bai Y, Shao C. Hydrogen Sulfide (H_2S)/cystathionine γ-Lyase (CSE) Pathway Contributes to the Proliferation of Hepatoma Cells. Mutat Res, Fundam Mol Mech Mutagen. 2014; 763–764:10–18.

852. Yin P, Zhao C, Li Z, Mei C, Yao W, Liu Y, Li N, Qi J, Wang L, Shi Y, et al. Sp1 Is Involved in Regulation of Cystathionine γ-Lyase Gene Expression and Biological Function by PI3K/Akt Pathway in Human Hepatocellular Carcinoma Cell Lines. Cell Signalling. 2012; 24:1229–1240. [PubMed: 22360859]

853. Ma K, Liu Y, Zhu Q, Liu C, Duan J-L, Tan BK-H, Zhu YZ. H_2S Donor, S-Propargyl-Cysteine, Increases CSE in SGC-7901 and Cancer-Induced Mice: Evidence for a Novel Anti-Cancer Effect of Endogenous H_2S? PLoS One. 2011; 6:e20525. [PubMed: 21738579]

854. Chattopadhyay M, Kodela R, Nath N, Dastagirzada YM, Velázquez-Martínez CA, Boring D, Kashfi K. Hydrogen Sulfide-Releasing NSAIDs Inhibit the Growth of Human Cancer Cells: A General Property and Evidence of a Tissue Type-Independent Effect. Biochem Pharmacol. 2012; 83:715–722. [PubMed: 22222427]

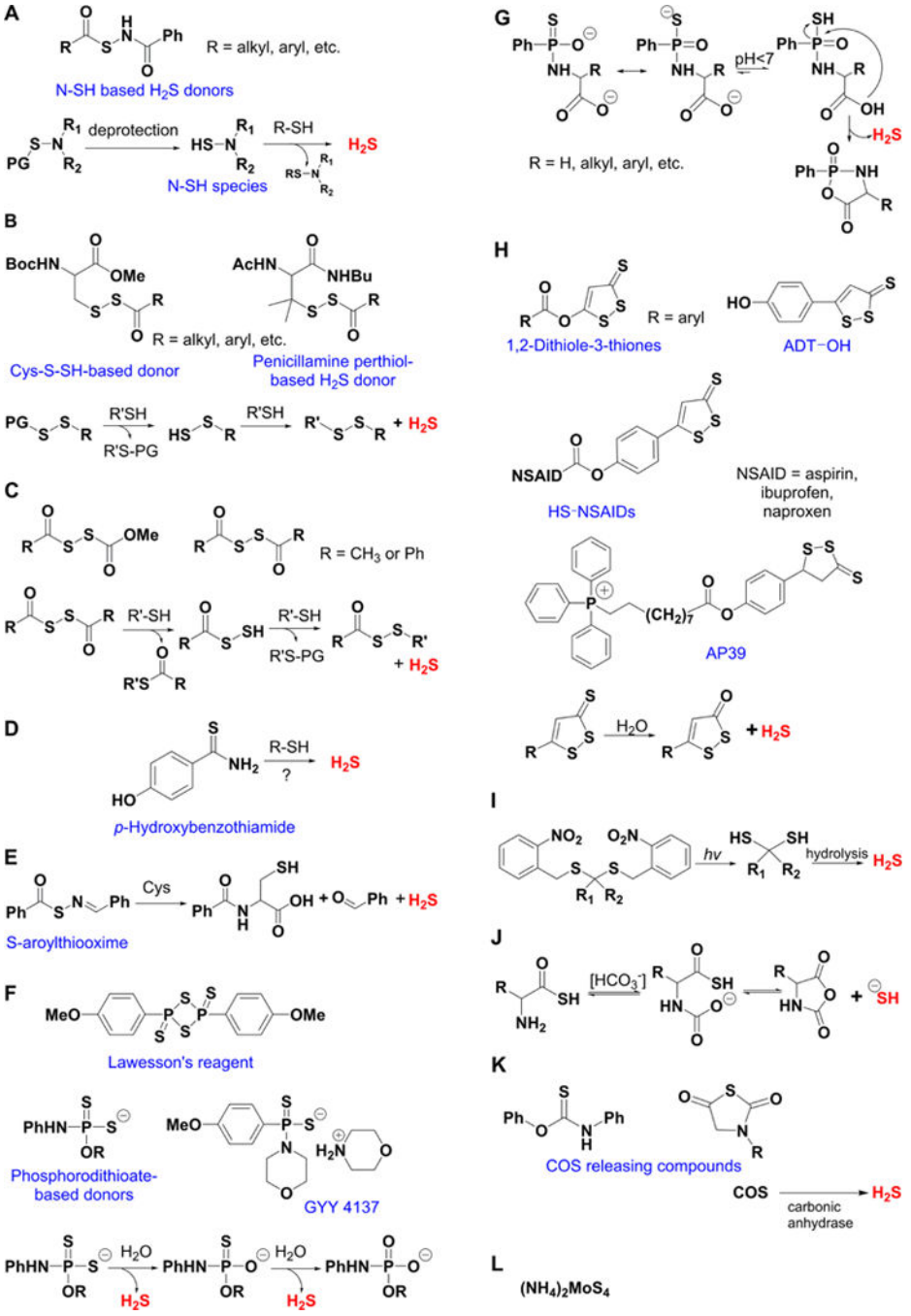

Figure 1.

Overview of different classes of H_2S donors. (A) Compounds based on the *N*-mercapto template (*N*-SH species) and the proposed mechanism for H_2S release. PG, protective group. (B) Perthiol-based compounds and proposed thiol-dependent mechanism of H_2S release. (C) Dithioperoxyanhydrides can also serve as H_2S donors upon reaction with thiols. (D) Arylthioamides release H_2S in the presence of thiols via an uncharacterized mechanism. (E) *S*-Aroylthiooximes release H_2S in the presence of aminothiols. (F) Chemical structures of Lawesson's reagent and its derivative, GYY4137, the most widely used H_2S donor, and the

proposed mechanism for H_2S release from GYY4137. (G) Phosphorothioate-based H_2S donors that release H_2S in a pH-dependent manner. (H) Another widely used class of molecules is 1,2-dithiole-3-thiones. They can be coupled to nonsteroid antiinflammatory drugs (NSAID) such as aspirin, ibuprofen, or naproxen, or to triphenylphsophonium group (AP39) which directs them to mitochondria. This class of molecules is believed to release H_2S via hydrolysis. (I) Example of photo cleavable gem-dithiol based H_2S donors, which undergo hydrolysis to release H_2S. (J) Thioamino acids release H_2S in reactions with bicarbonate. (K) COS, released by COS donors, forms H_2S in the presence of carbonic anhydrase. (L) Ammonium tetrathiomolibdate is shown to act as H_2S donor in vivo.

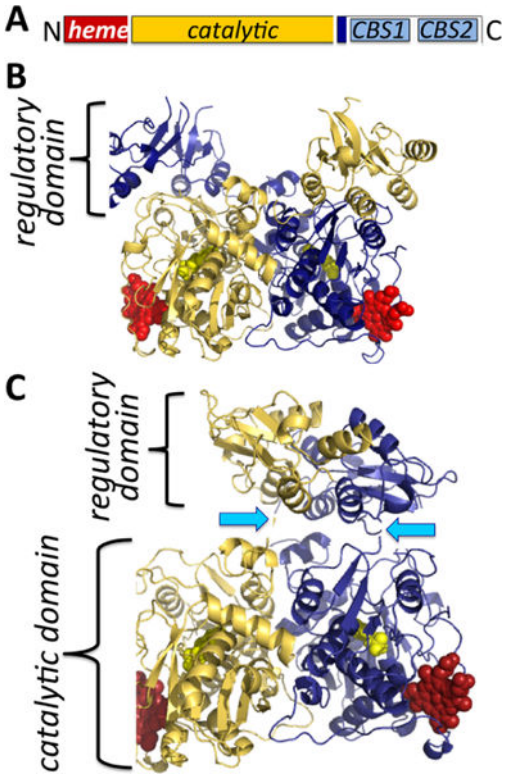

Figure 2.

Organization and structure of human CBS. (A) CBS is a modular protein with regulatory domains at its N- and C-termini. The C-terminal domain comprises a tandem repeat of two CBS domains, CBS1 and CBS2. The structures of human CBS in the absence (PDB: 4L27) (B) and presence (PDB: 4PCU) (C) of AdoMet show that a large conformational rearrangement accompanies the transition from the basal to the activated state. The protomers are shown in blue and yellow, respectively, the heme (red) and PLP (yellow) are in sphere representation, and the blue arrows point to the intervening linker region between the catalytic core and the C-terminal domain.

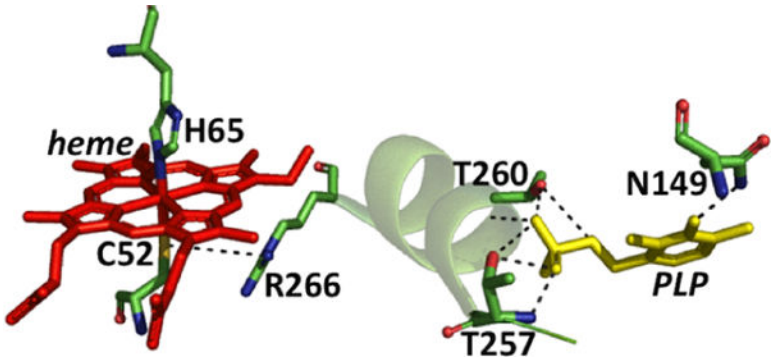

Figure 3.

Close up of the CBS structure. The interactions between the Cys52 heme ligand and Arg266 at one end of the α-helix and between Thr257 and Thr260 and the phosphate group of PLP at the other are shown. Asn149 hydrogen bonds with the C4 oxygen in PLP.

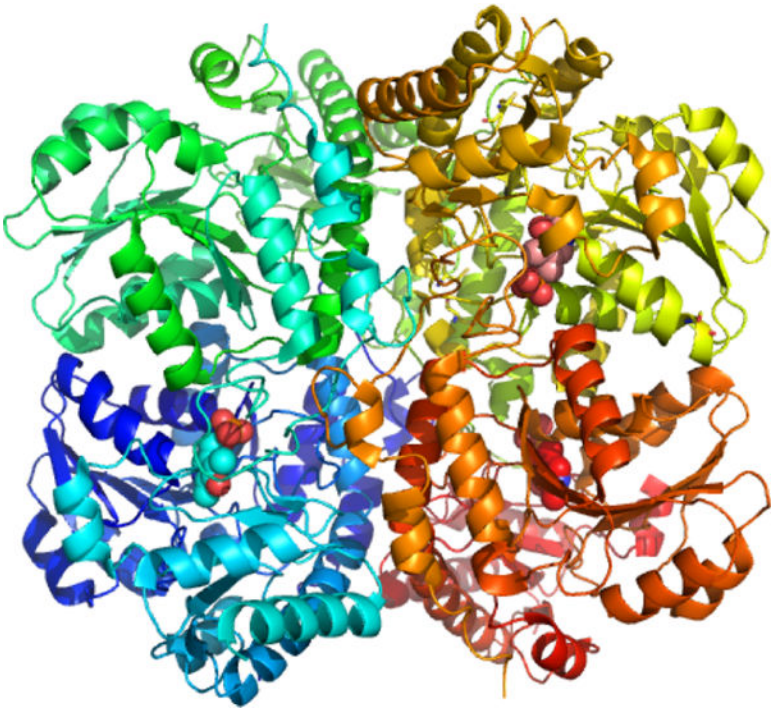

Figure 4.

Structure of human CSE (PDB: 2NMP). Each of the four monomers is shown in a different color, and the three PLPs visible in the structure are in sphere representation.

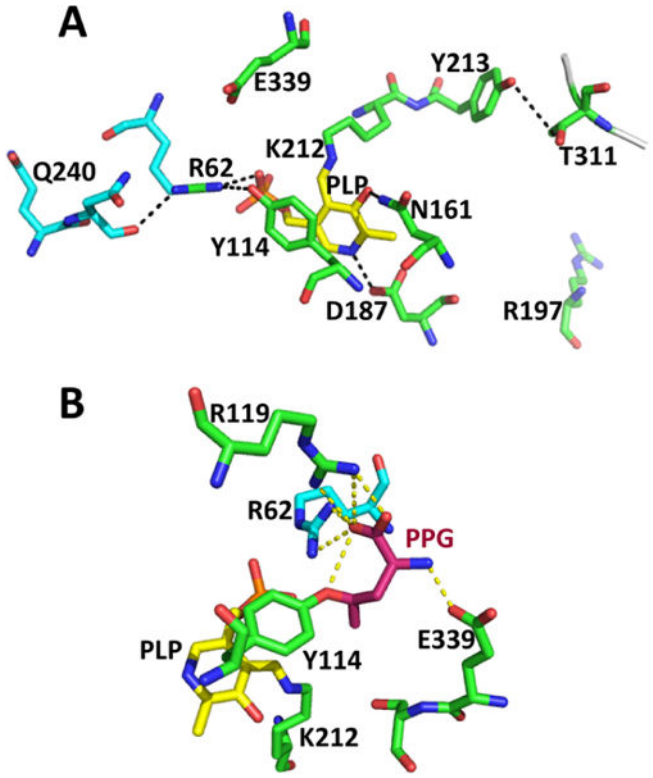

Figure 5.

Close-up of the active site structure of human CSE. (A). Interactions between PLP (yellow) and residues donated by the two subunits (in green and cyan) are highlighted (PDB: 2NMP). (B). Structure of PPG-inactivated CSE (PDB: 3COG). The coloring is the same is in panel A. PPG is covalently linked to Tyr114 and is shown in pink.

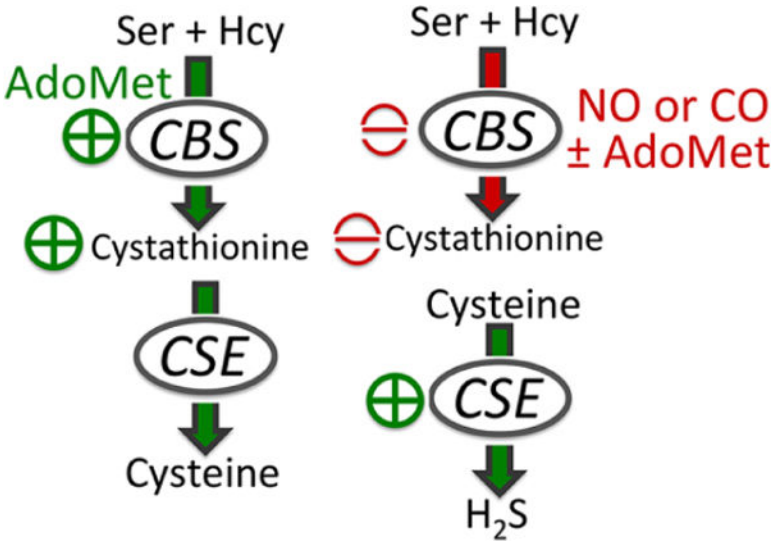

Figure 6.
Heme-regulated switching in the transsulfuration pathway from cysteine (left) to H_2S (right) synthesis.

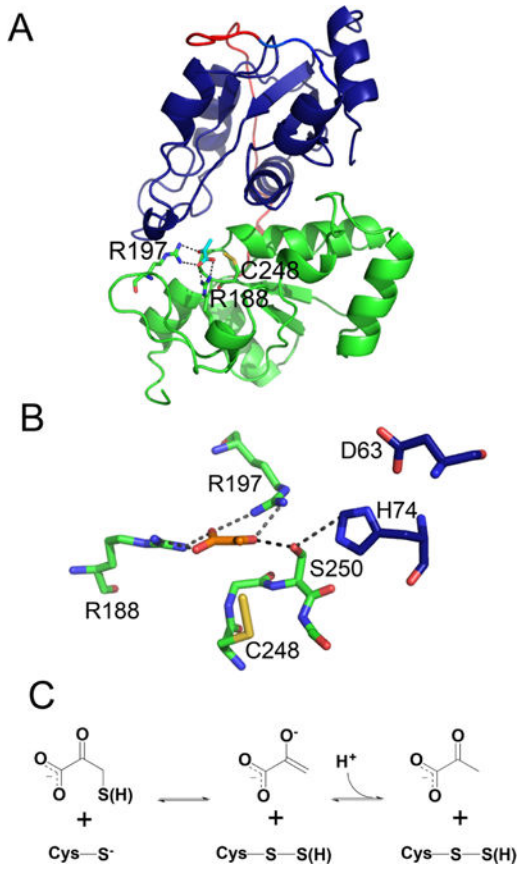

Figure 7.

Structure and mechanism of human MST. (A) The N and C-terminal domains of human MST (PDB: 4JGT) are shown in blue and green, respectively, and the linker is in red. Pyruvate (cyan) and key active site residues including Cys248 in the Cys-SSH state are shown in stick representation. (B) Close up of the active site captured in a product complex with pyruvate (orange) and Cys-SSH (PDB: 4JGT). Two residues in the catalytic triad (D63 and H74) are donated by the N-terminal domain and are shown in blue. (C) Mechanism of the reaction between the 3-mercaptopyruvate substrate and the Cys248 thiolate.

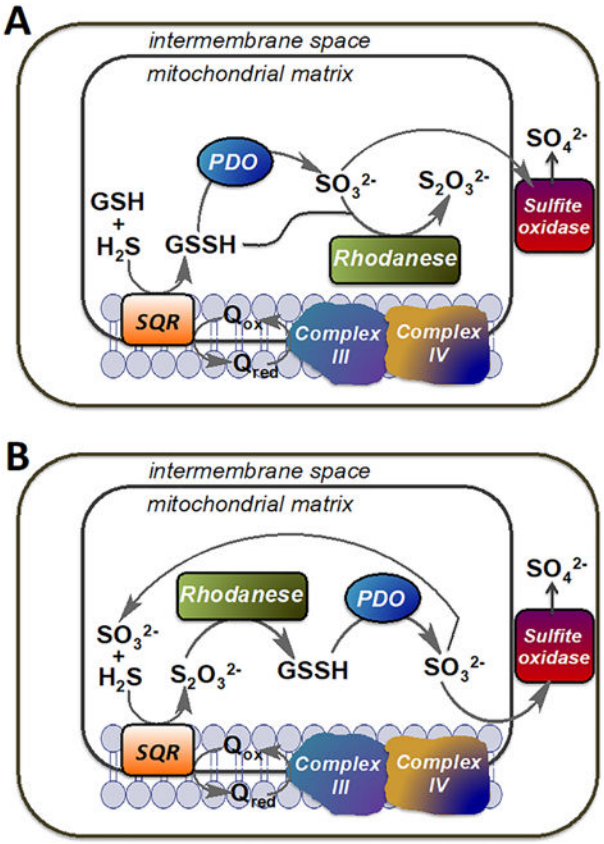

Figure 8.

Alternative models describing the organization of the mitochondrial sulfide oxidation pathway. (A) In this model, GSH is the sulfur acceptor from SQR and the product, GSSH, is utilized by either PDO or by rhodanese generating sulfite and thiosulfate, respectively. (B) In this model, sulfite is the sulfur acceptor from SQR and the product, thiosulfate, is utilized by rhodanese to generate GSSH, which is subsequently oxidized by PDO to sulfite. Sulfite is eventually oxidized to sulfate by sulfite oxidase. Q represents coenzyme Q.

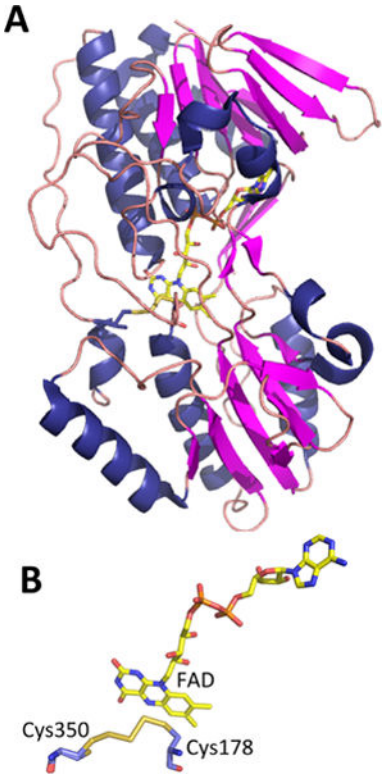

Figure 9.

Structure of SQR from *A. ambivalens*. (A). Structure of an SQR subunit (PDB: 3H8L) in which the covalently bound FAD is shown in stick representation. (B) Close-up of the active site showing FAD and a bridging trisulfide intermediate between Cys350 and Cys178.

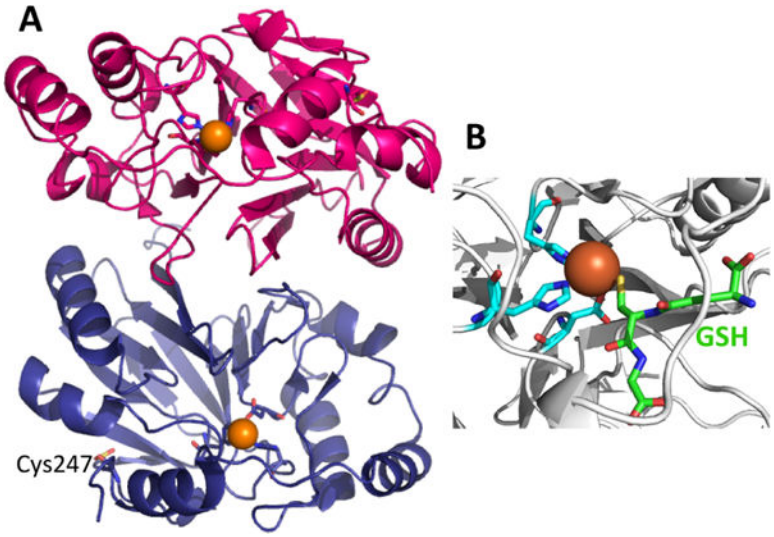

Figure 10.

Crystal structure of PDO. (A) Structure of human PDO (PDB: 4CHL) in which the protomers are shown in pink and blue, the iron ion as an orange sphere, and the coordinating histidines and aspartate in stick representation. Cys247 is oxidized as cysteine sulfinate and is also shown in stick representation. (B). Close up of the *P. putida* PDO (PDB: 4YSL) with bound GSH (green). The cysteine sulfur of GSH is proximal to the iron ion, which is coordinated by a 2His-1Asp facial triad.

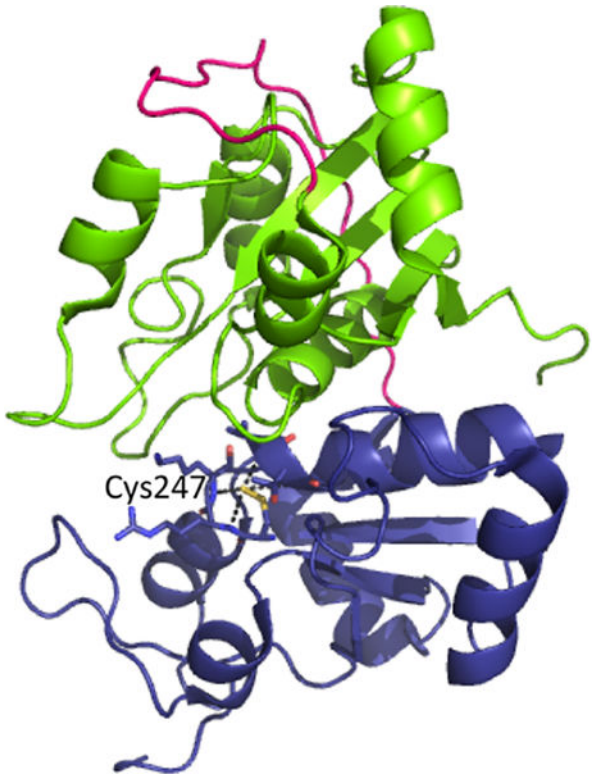

Figure 11.

Structure of bovine rhodanese (PDB: 1RHD). The N- and C-terminal domains are shown in green and blue with the intervening linker in pink. A Cys-SSH intermediate is stabilized at Cys247 in the active site, via hydrogen bonding interactions with neighboring residues.

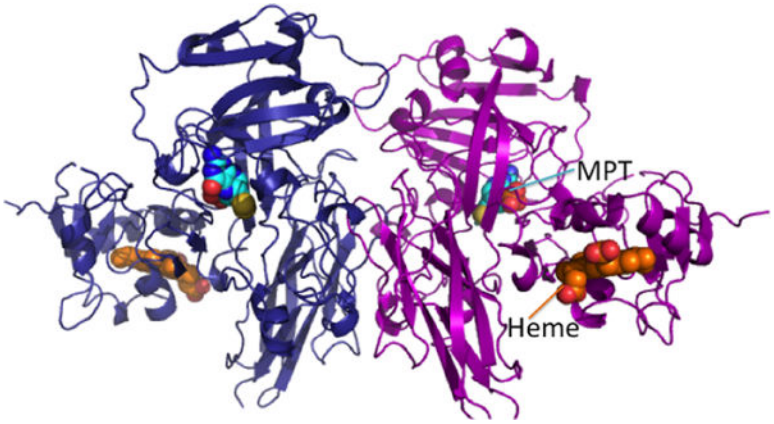

Figure 12.

Structure of dimeric chicken sulfite oxidase (PDB: 1SOX). The two subunits are shown in blue and magenta, respectively, and the heme (orange) and molybdopterin (MPT, cyan) cofactors are in sphere representation.

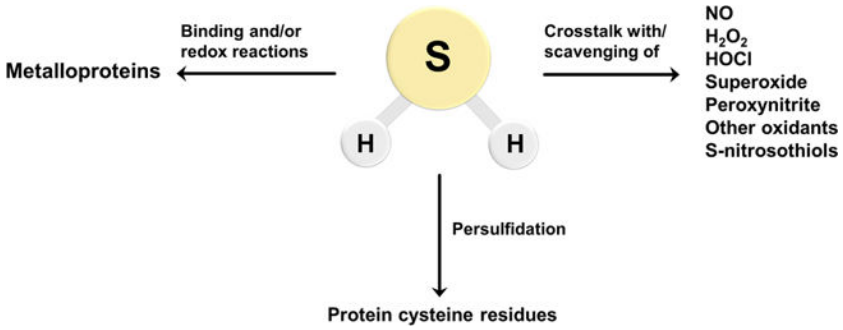

Figure 13.

Biological reactivity of H_2S. H_2S can react directly with oxidants such as superoxide, HOCl, and $ONOO^-$. It can also react with $NO^\bullet$ and S-nitrosothiols leading to the formation of other signaling species (right arrow). Metal centers in proteins can bind H_2S for delivery to specific targets, be reduced by H_2S, or catalyze sulfide oxidation chemistry (left arrow). H_2S is also involved in the modification of protein cysteine residues leading to persulfide (Cys-SSH) formation (central arrow).

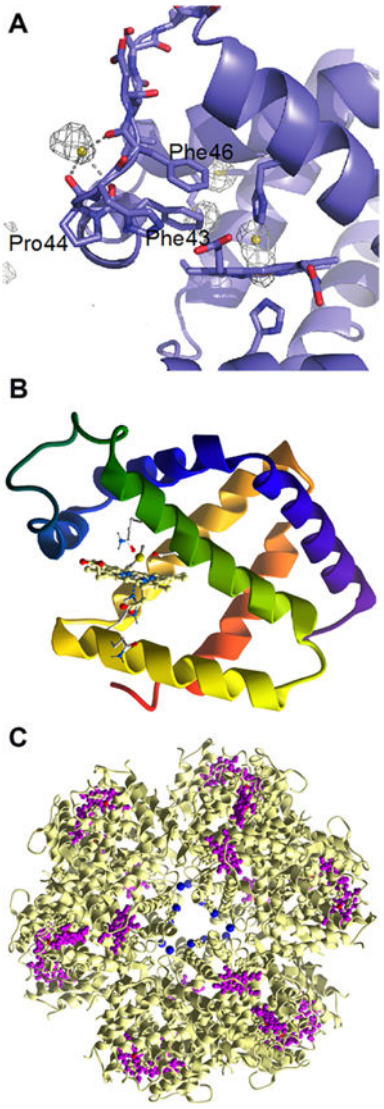

Figure 14.

Binding of H_2S to protein metal centers. (A) Structure of the α subunit of human hemoglobin showing HS^- bound at the entry/exit point of the so-called Phe path that leads to the distal face of the heme. A second sulfide is bound to the heme iron (PDB: 5UCU). (B) Close up of the heme in hemoglobin I from *Lucina pectinata* with HS^- coordinated to the iron ion (PDB: 1MOH). (C) Structure of hemoglobin-like protein C1 from *Riftia pachyptila* (PDB: 1YHU) with Zn^{2+} shown in blue and iron hemes in purple.

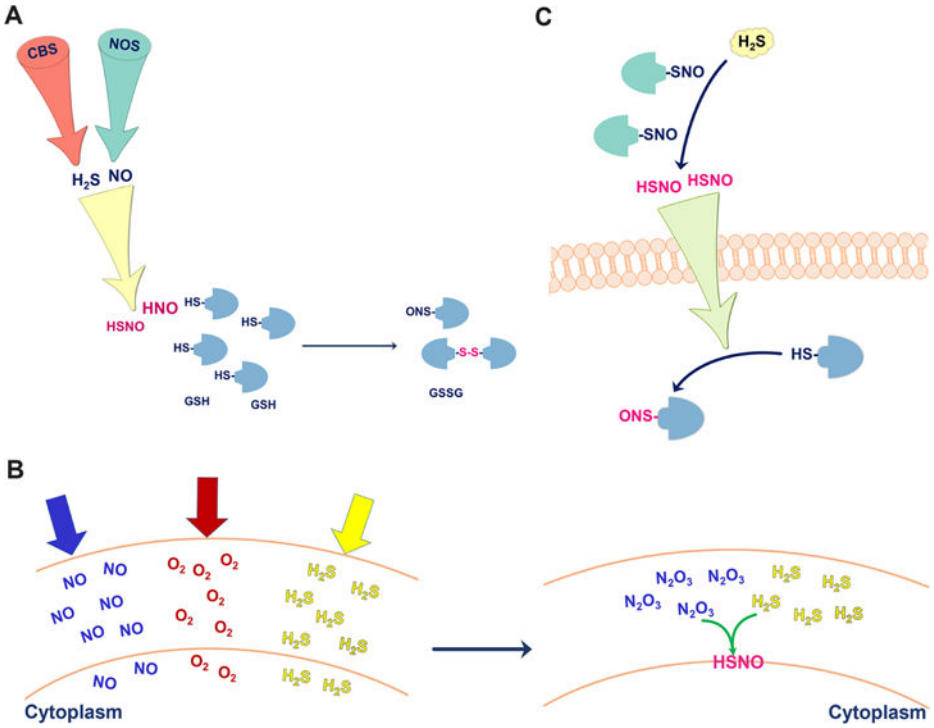

Figure 15.

Signaling aspects of $NO^{\bullet}/H_2S$ cross-talk. (A) To form HNO and minimize side reactions, H_2S and $NO_2^{\bullet}$ have to be produced in proximity. HNO (and possibly HSNO) reacts with protein thiols and glutathione. (B) All three gases, $NO^{\bullet}$, O_2, and H_2S tend to accumulate in membranes. $NO^{\bullet}$ and O_2 form N_2O_3, which readily reacts with H_2S to form HSNO. (C) HSNO formed in the reaction of protein *S*-nitrosothiols with H_2S can diffuse through the cell membrane and transfer the "NO^{+}" group to another protein target.

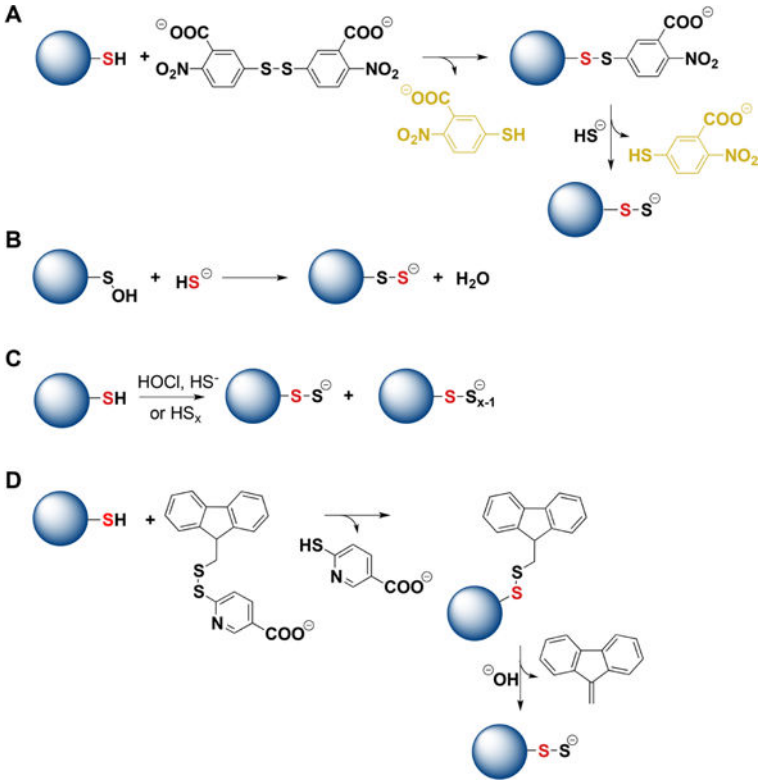

Figure 16.

Strategies for the preparation of protein persulfides. (A) Protein thiols react first with DTNB forming mixed disulfides that react with H_2S forming persulfides. Thionitrobenzoate is a good leaving group and its UV–visible absorbance can be used to estimate the yield of persulfides. (B) Protein sulfenic acids, when stable, can be used as precursors for persulfide preparation. (C) Protein thiols can be mixed with inorganic polysulfides or with a mixture of HOCl and H_2S. Besides persulfides, polythiolated products are also formed. (D) Protein thiols can react with 9-fluorenylmethyl disulfide. The products undergo alkaline hydrolysis forming persulfides.

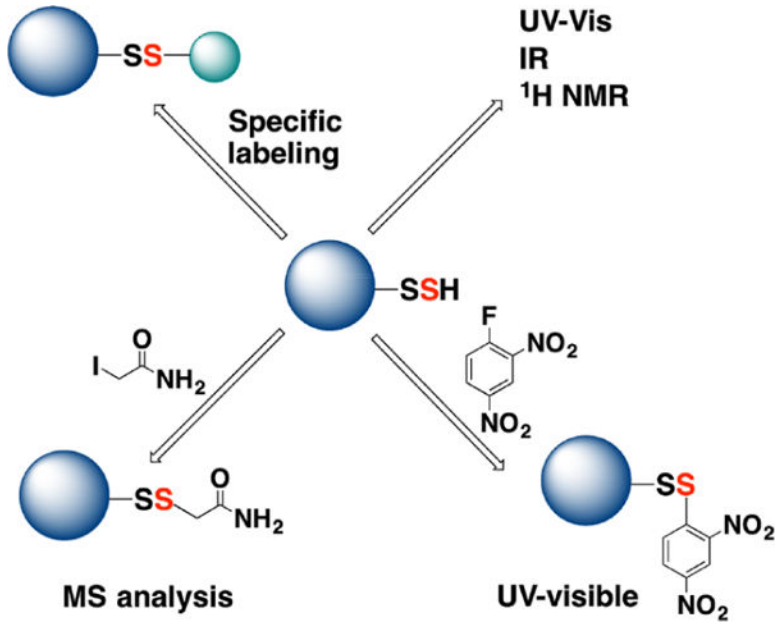

Figure 17.

Methodological approaches for the characterization of protein persulfides. (A) When pure, protein persulfides can be characterized by UV–visible, IR, and ^{1}H NMR spectroscopy. (B) Protein persulfides react with 1-fluoro-2,4-dinitrobenzene to form mixed disulfides. DTT releases 2,4-dinitrobenzenethiol, which absorbs at 408 nm under alkaline conditions. (C) Persulfides can be labeled with thiol blocking reagents such as iodoacetamide and analyzed by MS. (D) Protein persulfides can be tagged through different strategies that rely on either their electrophilic or their nucleophilic character.

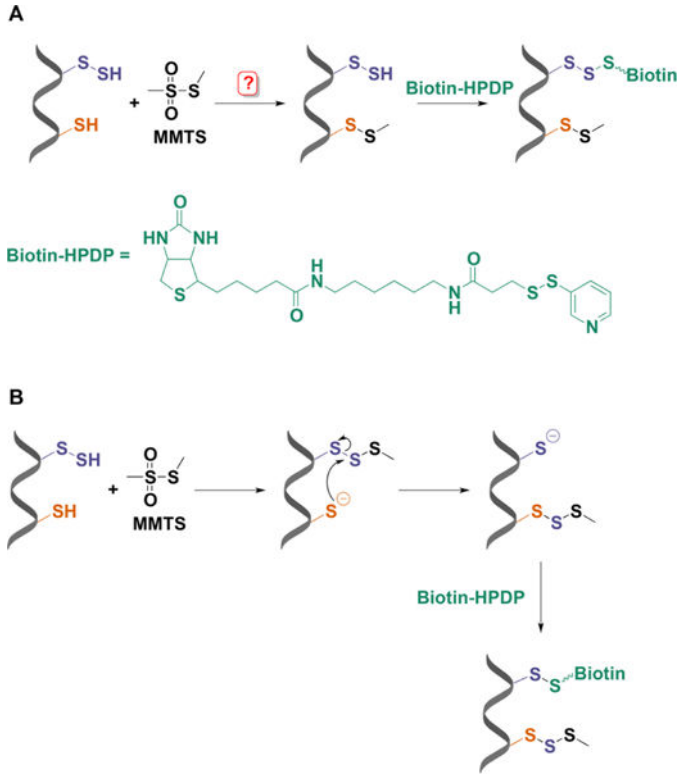

Figure 18.

Modified biotin switch assay for persulfide labeling. (A) MMTS was proposed to selectively block free thiols leaving persulfides unmodified and ready for reaction with a biotin-derivatized reactive disulfide (biotin-HPDP). (B) Mechanistic explanation for persulfide labeling with the biotin switch assay. MMTS reacts with persulfides more readily than with thiols forming a trisulfide product. This trisulfide is attacked by unreacted thiols leaving a free cysteine that can react with biotin-HPDP.

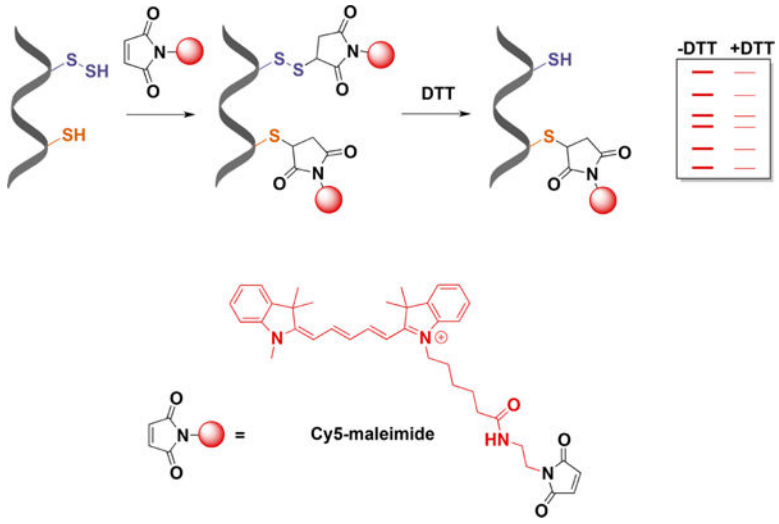

Figure 19.

Persulfide detection by differential fluorescence tagging. Both thiols and persulfides are initially blocked with Cy5-maleimide. DTT treatment then removes the fluorescent tag from the persulfides. Proteins are separated by electrophoresis, and the loss of fluorescence caused by DTT is used as a measure of persulfidation.

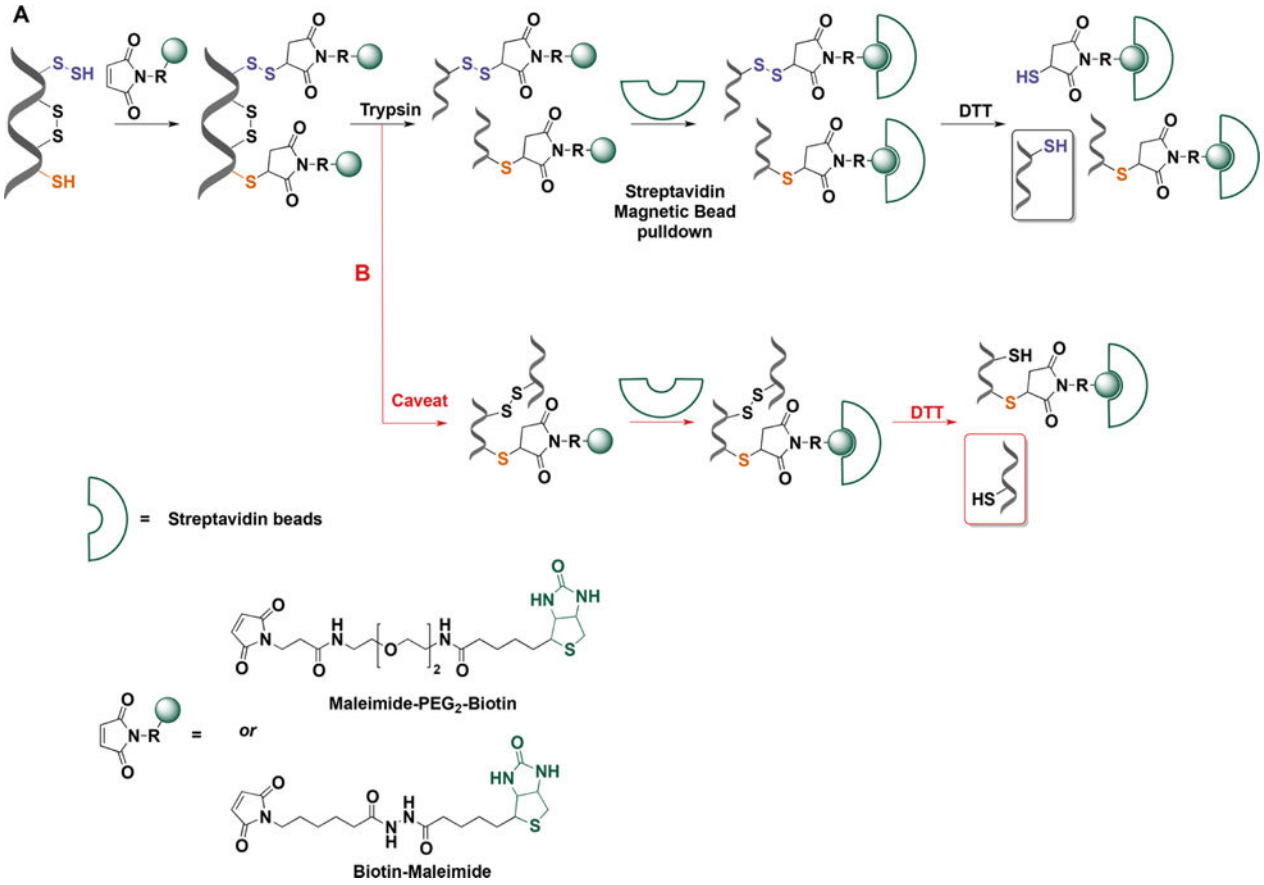

Figure 20.

Persulfide labeling with biotin-tagged alkylating reagents. (A) In the first step proteins are mixed with maleimide-biotin (or maleimide-PEG_2-biotin) to tag both thiols and persulfides. Proteins are trypsinized and the biotinylated peptides are bound to streptavidin beads. Persulfidated peptides attach to streptavidin beads via disulfide bonds. DTT treatment facilitates elution from the beads and subsequent MS analysis. (B) A possible caveat is that peptides connected by disulfide bonds and containing a thiol or persulfide could be released from the beads with DTT. However, the concentration of disulfide bonds in intracellular proteins is low and this not expected to be a quantitiatvely major drawback of the method.

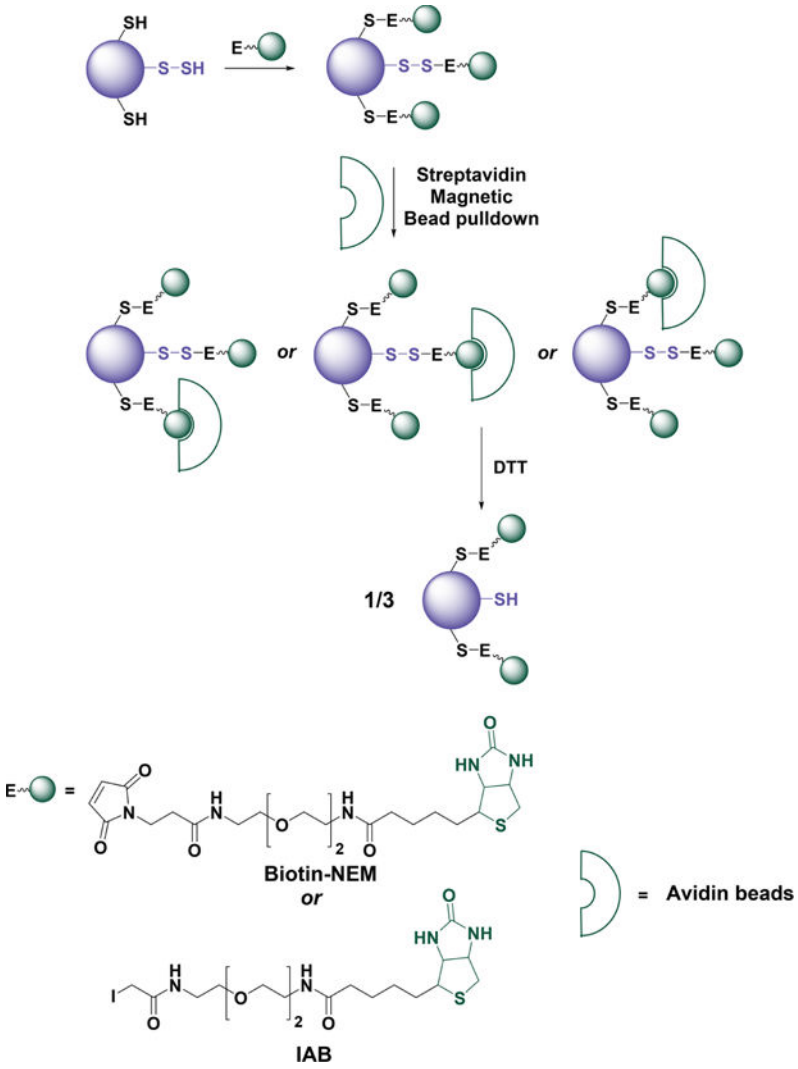

Figure 21.

Caveats of whole protein labeling with biotin-tagged alkylating reagents. Proteins containing several cysteine residues, of which only one is persulfidated, are labeled with biotin-maleimide (biotin-NEM) or biotin iodoacetamide (IAB). Since all labels have equal chances of binding to streptavidin beads, the elution with DTT will result in lower than expected yield because the protein will remain bound through the tagged thiols.

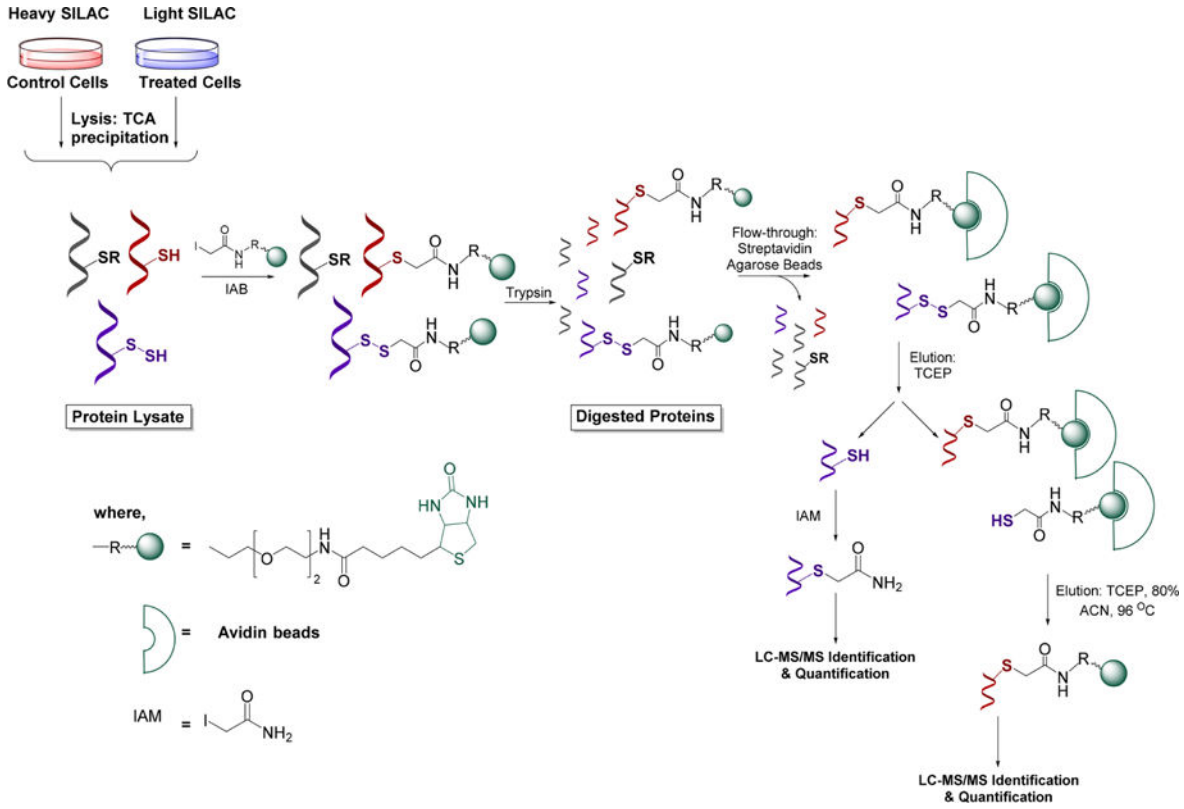

Figure 22.

qPerS-SID (quantitative persulfide site identification) approach. Control cells and H_2S-treated cells are grown in heavy and light SILAC (stable isotope labeling with amino acids in cell culture) media, respectively. After cell lysis protein extracts are mixed 1:1 and exposed to iodoacetamide-PEG-biotin to labelthiols and persulfides. Proteins are then trypsinized and labeled peptides bound to streptavidinbeads. Since persulfidated peptides attach to streptavidin beads via disulfide bonds they are eluted with TCEP (tris(2-carboxyethyl)phosphine). Released peptides are subjected to LC-MS/MS identification and quantification (enabled by the SILAC approach).

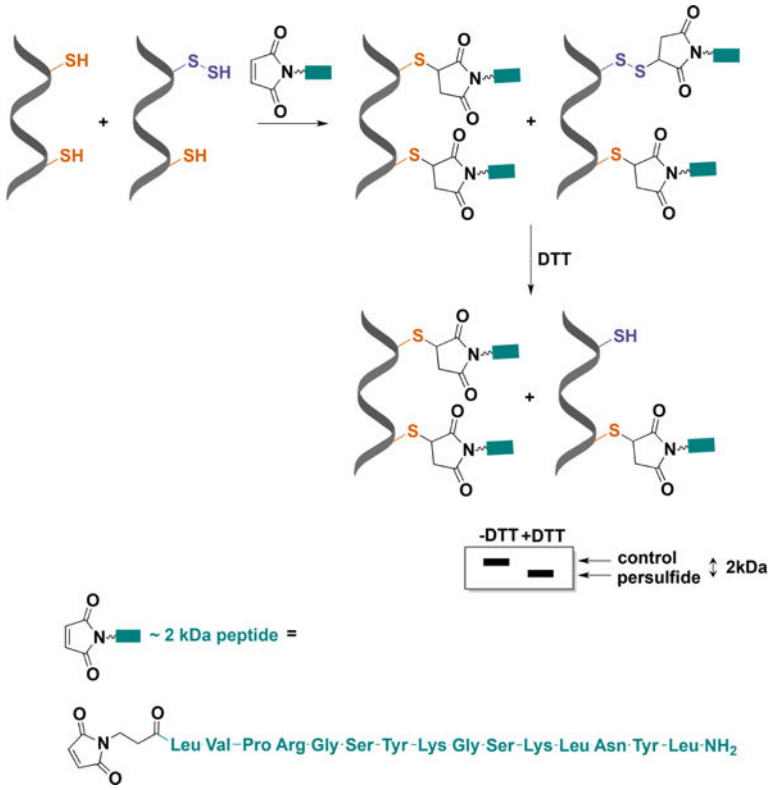

Figure 23.

Detection of protein persulfidation by differential peptide tagging. An engineered maleimide with a peptide arm and a molecular mass of ~2 kDa (MalP) reacts with both thiols and persulfides. DTT removes the mixed disulfides formed with persulfides and increases the electrophoretic mobility of the protein.

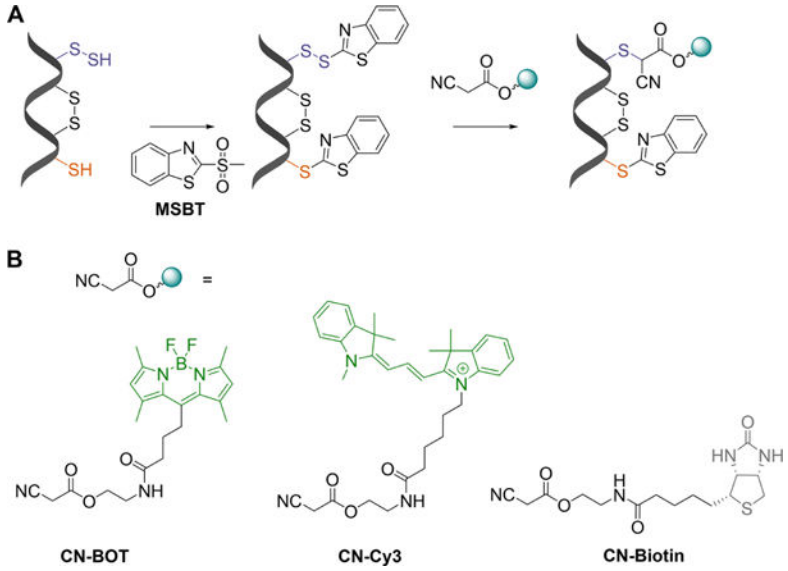

Figure 24.

Cyanoacetic acid-based tag-switch method for persulfide labeling. (A) Both persulfides and thiols are initially blocked with MSBT. The product with a persulfidated cysteine is a mixed aromatic disulfide that can be nucleophilically attacked by a cyanoacetic acid–based probe causing a tag-switch. (B) Three different tags are attached to cyanoacetic acid: BODIPY (CN-BOT), Cy3 (CN-Cy3), and biotin (CN-biotin).

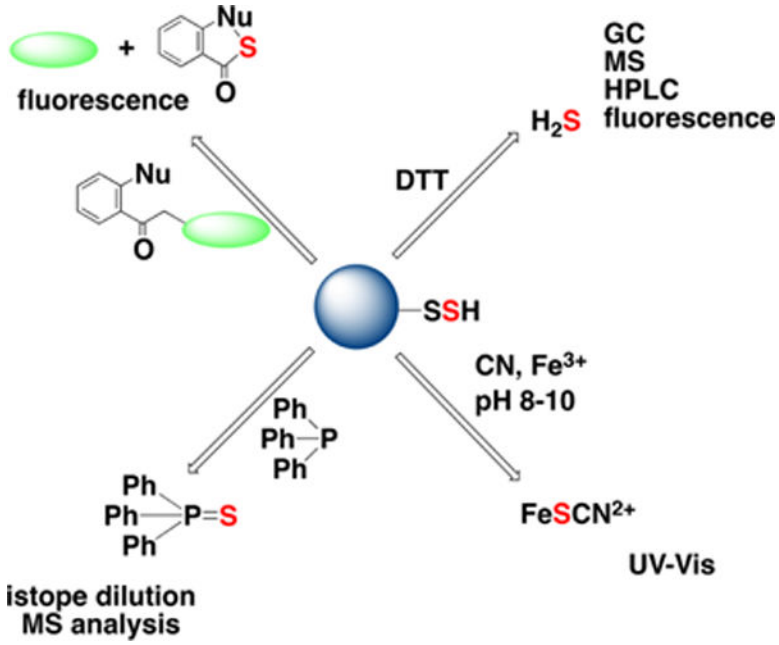

Figure 25.

Overview of methodological approaches for total sulfane sulfur detection. Sulfane sulfur compounds release H_2S upon DTT treatment. Sulfane sulfur can be detected by the cold cyanolysis method; samples are incubated in alkaline (pH 8–10) cyanide solutions to release SCN^-, which is then quantified spectrophotometrically as a complex with Fe^{3+}. Sulfane sulfur can be extracted by triarylphosphines in the form of triarylphosphine sulfide, which can be quantified by isotope dilution MS analysis. Finally, different fluorescence probes (e.g., the SSP series) can detect sulfane sulfur in protein persulfides and low molecultar weight hydropolysulfides in cells (described in greater detail in Chart 28).

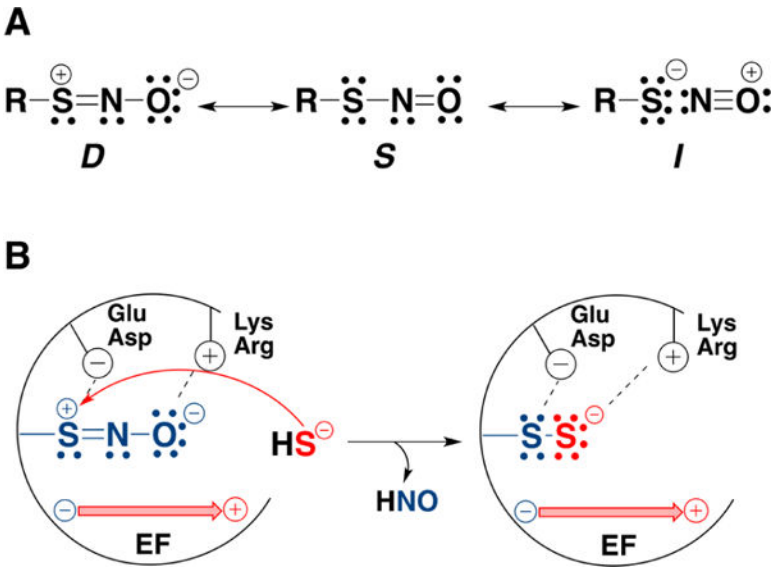

Figure 26.

Factors that might favor protein persulfidation over *trans*-nitrosation in the reaction of an *S*-nitrosothiol (RSNO) with H_2S. (A) Resonance structures of RSNO. Nucleophilic attack on the sulfur is favored in Structure *D*. (B) Interactions with the protein environment could stabilize the resonance structure *D*. Positively charged Arg or Lys residues could stabilize the NO moiety, while negatively charged Glu or Asp residues could stabilize the sulfur. In addition electric fields (EF) created by the protein environment could selectively stabilize a resonsance structure, e.g., *D*, promoting persulfidation and HNO release.

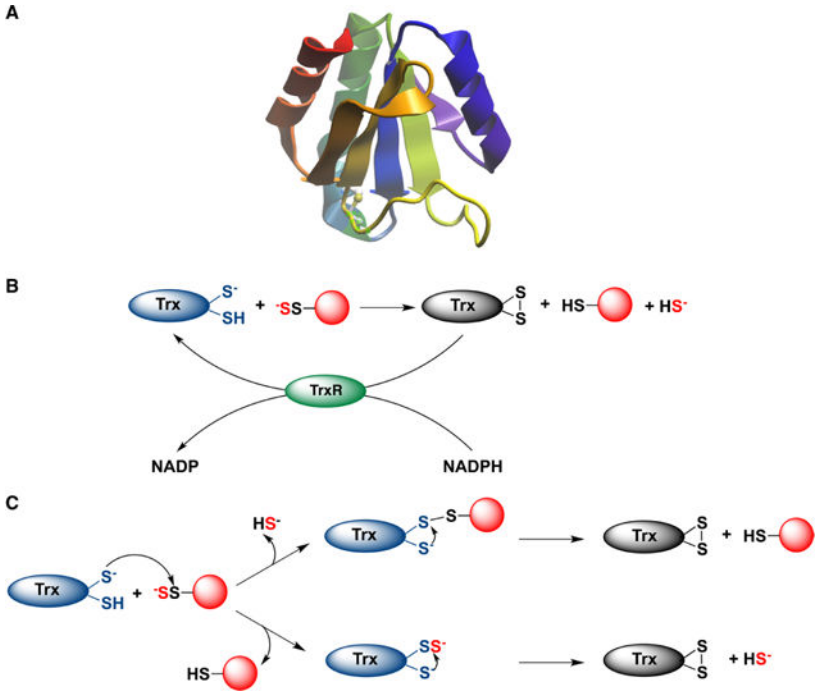

Figure 27.

Depersulfidation by thioredoxin (Trx). (A) The structure of human thioredoxin (PDB: 5DQY). (B) Thioredoxin reduces protein persulfides and releases H_2S. Oxidized Trx is reduced by thioredoxin reductase (TrxR) at the expense of NADPH. (C) Two possible mechanisms for protein depersulfidation. Top: The nucleophilic thiol attacks the inner sulfur of the protein persulfide forming a mixed protein-Trx disulfide and releasing H_2S. In the next step the resolving cysteine reduces the mixed disulfide forming fully oxidized Trx. Bottom: Trx undergoes persulfidation, forming Trx persulfide, which is reduced by the resolving cysteine with concomitant release of H_2S.

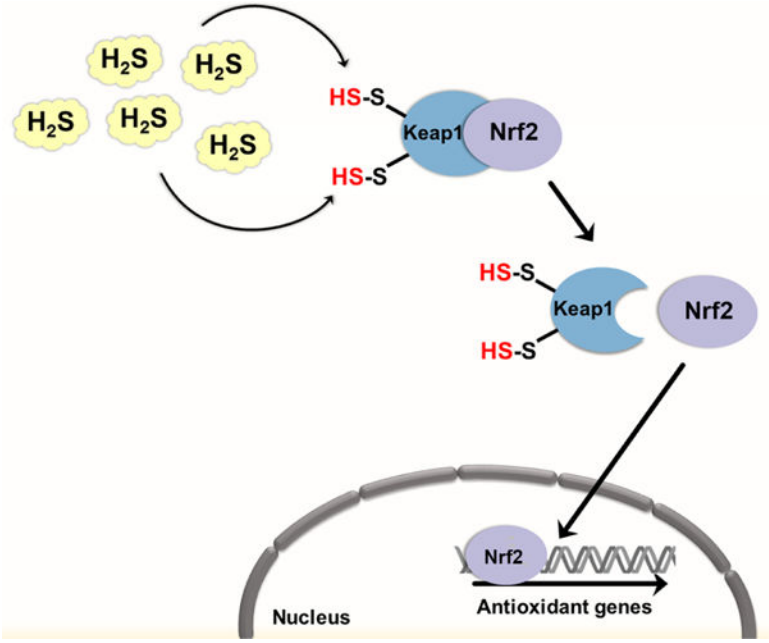

Figure 28.

H_2S may regulate cellular antioxidant defenses and prevent senescence by persulfidation of Keap1. In the cytosol, Keap1 represses Nrf-2 signaling by binding to it. Bound Nrf-2 is subjected to polyubiquitination and proteasomal degradation. Persulfidation of cysteine residues in Keap1 induces a conformational change, which results in Nrf-2 release. Nrf-2 translocates to the nucleus where it upregulates the expression of various antioxidant defense genes.

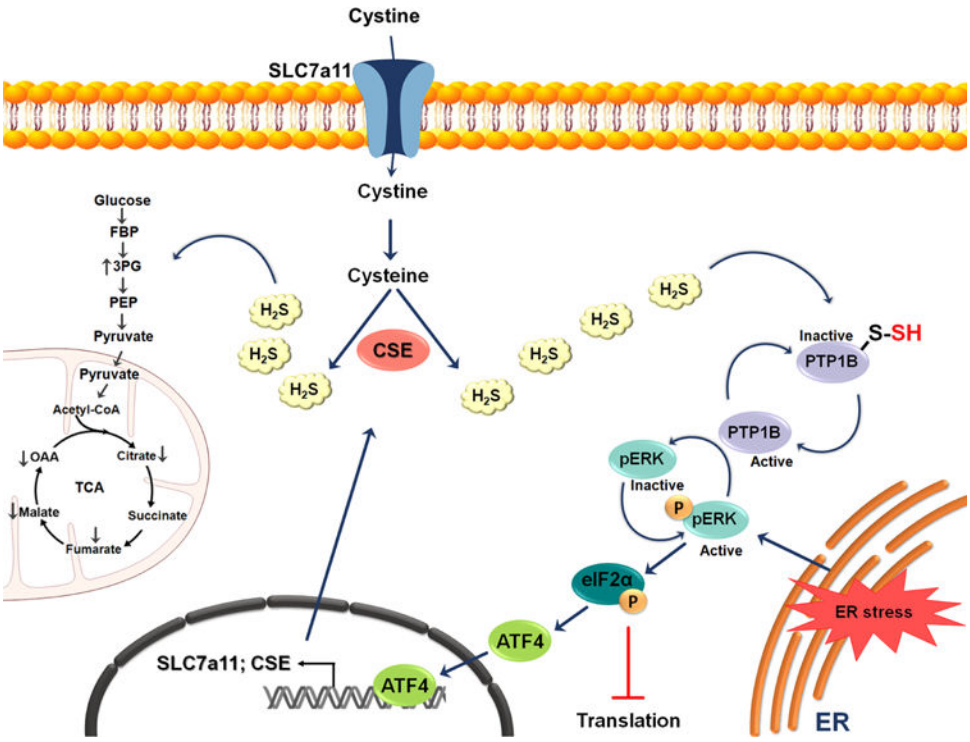

Figure 29.

Possible role of H_2S in endoplasmic reticulum (ER) stress. Under ER stress, the activity of the transcription factor ATF4 is increased, resulting in the upregulation of CSE and the cystine transporter Slc7a11. The subsequent increased production of H_2S leads to the persulfidation of protein tyrosine phosphatase 1B (PTP1B) and consequently to an increase in pERK phosphorylation. pERK activation results in global inhibition of protein translation by activation of eukaryotic translation initiation factor 2α (eIF2α). eIF2α induces ATF4 nuclear translocation. The increased production of H_2S during ER stress also results in persulfidation of glycolytic and tricarboxylic acid (TCA) cycle enzymes.

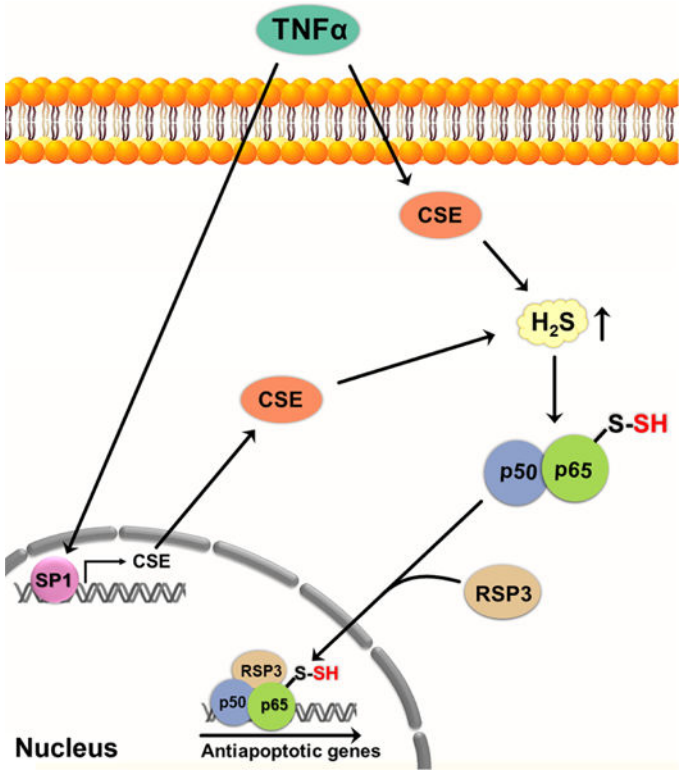

Figure 30.

Persulfidation of NF-κB may regulate apoptosis. The proinflammatory cytokine TNFα, involved in the control of inflammatory reactions, stimulates CSE transcription by activating the SP1 transcription factor, resulting in increased H_2S levels. H_2S induces persulfidation of Cys38 in the p65 subunit of NF-κB, enhancing the binding of NF-κB subunits to the coactivator RPS3. The activator complex then migrates to the nucleus where it upregulates the expression of several antiapoptotic genes. TNFα, tumor necrosis factor α; CSE, cystathionine γ lyase; p50 and p65 subunits of NF-κB; RPS3, ribosomal protein S3; SP1, specificity protein-1.

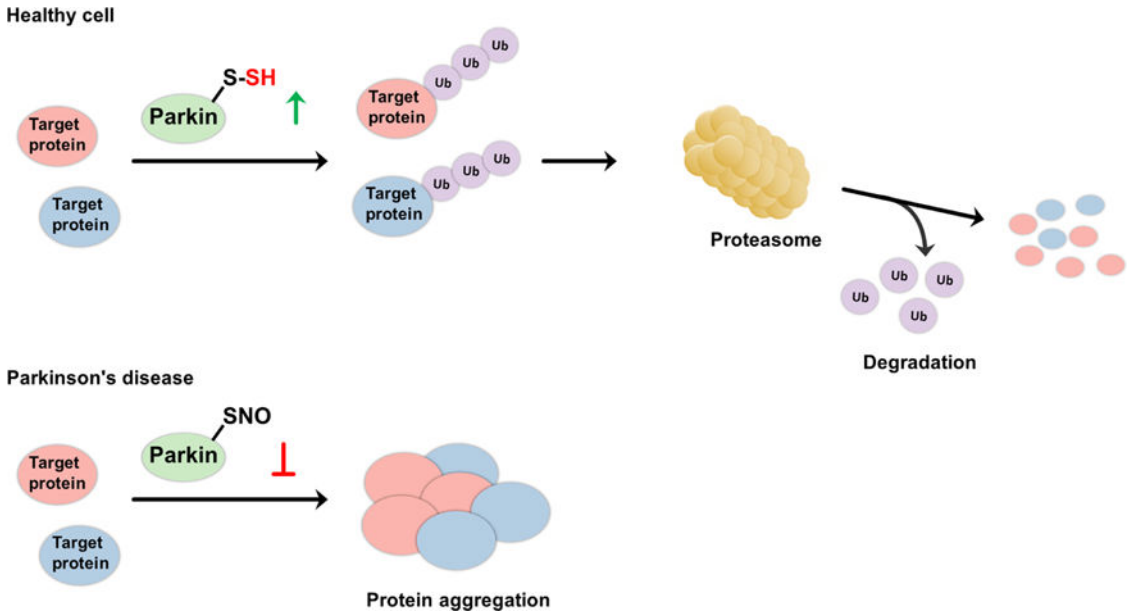

Figure 31.

Possible regulatory role of H_2S on the catalytic activity of parkin. (A) In healthy subjects, parkin, a E3 ubiquitin ligase, is persulfidated, which increases its enzymatic activity. This leads to ubiquitination of diverse substrates and their subsequent proteasomal degradation. (B) In patients with Parkinson's disease, parkin is *S*-nitrosated. The decreased catalytic activity results in protein aggregation, accumulation of toxic proteins, and cell death.

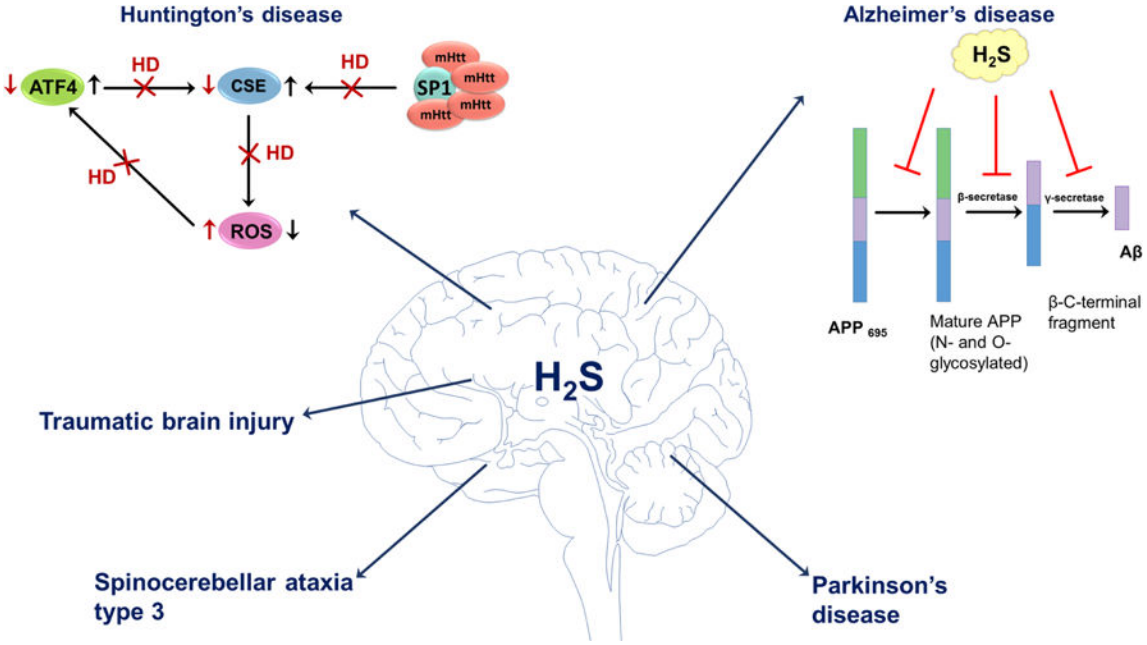

Figure 32.

Some possible physiological roles of H_2S in neurodegenerative disorders. H_2S has been shown to be involved in pathogenesis of Huntington's, Alzheimer's, and Parkinson's diseases, spinocerebellar ataxia, and traumatic brain injury. In healthy subjects, the expression of CSE is regulated by SP1 and ATF4 transcription factors. In Huntington's disease, abnormal mutated huntingtin (mHtt) protein binds to SP1 and inhibits its activity. Reduced CSE expression results in oxidative stress that subsequently affects ATF4 expression. H_2S also inhibits the production of amyloid beta (Aβ) at different catalytic steps of Aβ. The mature isoform of APP is cleaved by β- and γ-secretases forming Aβ. H_2S interferes with APP maturation and inhibits the activity of β- and γ-secretases leading to the decreased production of Aβ. In Parkinson's disease, H_2S induces persulfidation of parkin and increases E3 ubiquitin ligase activity. H_2S has beneficial effects in spinocerebellar ataxia type 3, where it regulates protein persulfidation and improves SCA3-associated tissue degeneration. In traumatic brain injury H_2S exerts antiapoptotic effects and down-regulates the expression of autophagy-related proteins, reduces brain edema and improves the recovery of motor and cognitive dysfunction.

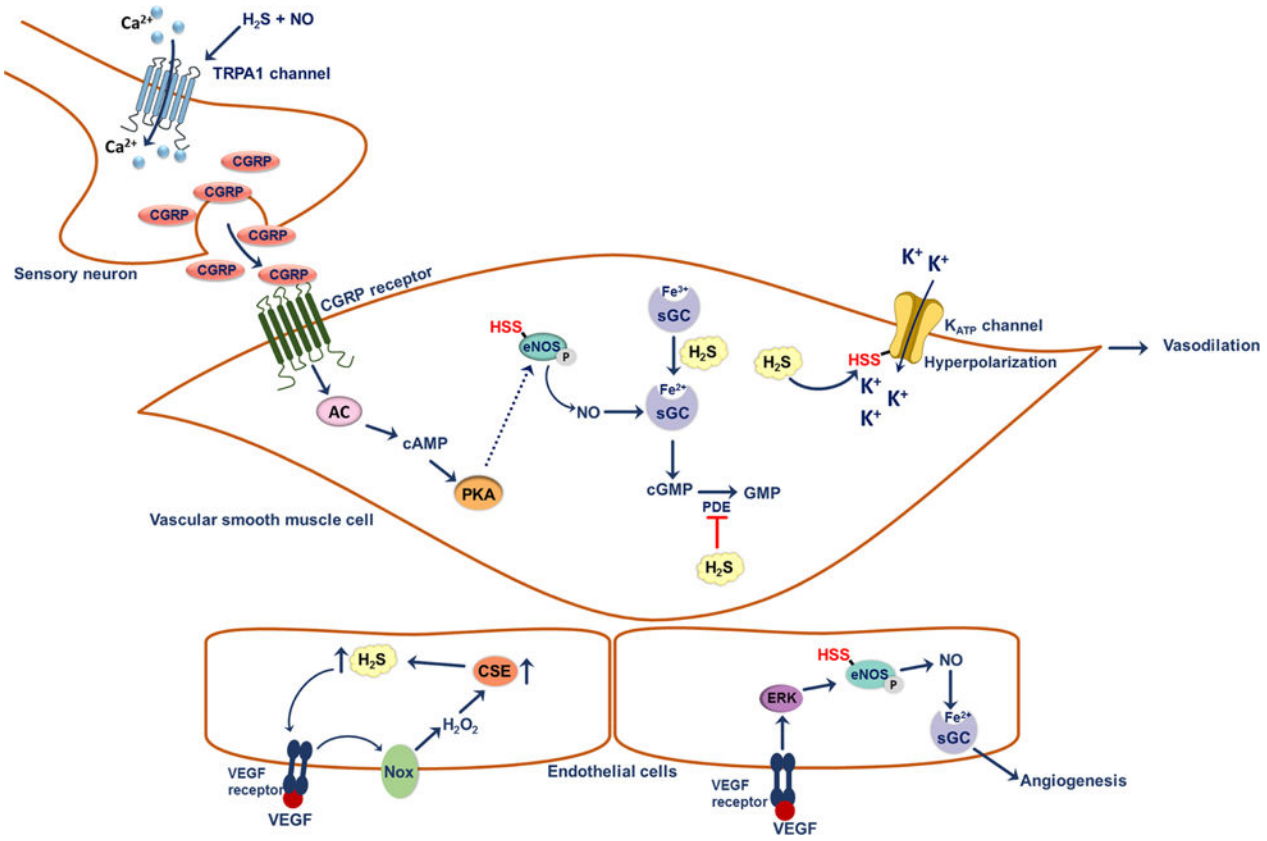

Figure 33.

Possible signaling roles of H_2S in the vascular system. At a sensory nerve ending, H_2S interacts with $NO^{\bullet}$ to give HNO. HNO activates TRPA1 channels; this results in Ca^{2+} influx and subsequent release of calcitonin gene-related peptide (CGRP). Binding of CGRP to its receptor on vascular smooth muscle cells activates the adenylate cyclase and the cyclic adenosine monophosphate (cAMP)-controlled downstream signaling pathways. As a result of elevated cAMP, protein kinase A (PKA) is activated and could potentially increase the activity of eNOS. Persulfidation of Cys443 on eNOS increases the activity of the enzyme as well as its ability to be phosphorylated, which results in increased production of $NO^{\bullet}$ and activation of soluble guanylate cyclase (sGC). H_2S potentiates the binding of $NO^{\bullet}$ to sGC by reducing ferric heme to the ferrous state. Degradation of cGMP by phosphodiesterase (PDE) is prevented by H_2S. These effects result in vasodilation of smooth muscle cells. Persulfidation of Cys43 on K_{ATP} channel enhances its activity, resulting in the influx of K^+ and hyperpolarization of vascular smooth muscle cells. H_2S also plays a role in angiogenesis. Binding of VEGF to its receptor on endothelial cells induces the production of H_2O_2 by activating NADPH oxidase (Nox). H_2O_2 supposedly increases CSE expression leading in turn, to increased H_2S production. H_2S stimulates activation of the Akt signaling cascade, which results in the phosphorylation of eNOS, increasing its activity. $NO^{\bullet}$ acts as a pro-angiogenic factor.

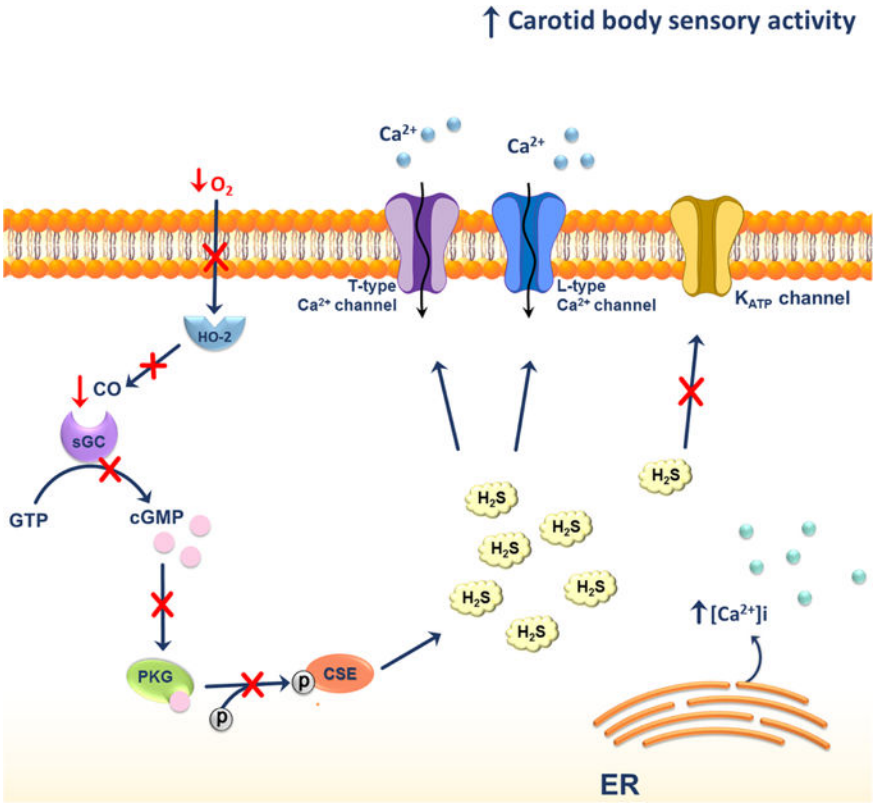

Figure 34.

Possible H_2S effects on glomus cells of carotid bodies under hypoxic conditions. Under hypoxic conditions the levels of H_2S in glomus cells of carotid bodies are elevated. This could be a result of decreased phosphorylation of CSE due to the lack of CO produced by heme oxygenase-2 (HO-2). The lack of CO results in the inhibition of cyclic guanosine monophosphate (cGMP)-stimulated activation of phosphokinase G. The overall increase in H_2S levels activates the L-type Ca^{2+} and T-type voltage-gated Ca^{2+} channels and mobilizes Ca^{2+} from the endoplasmic reticulum (ER).

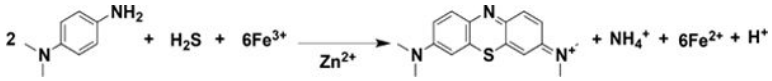

Chart 1.

Measurement of H_2S through Formation of Methylene Blue

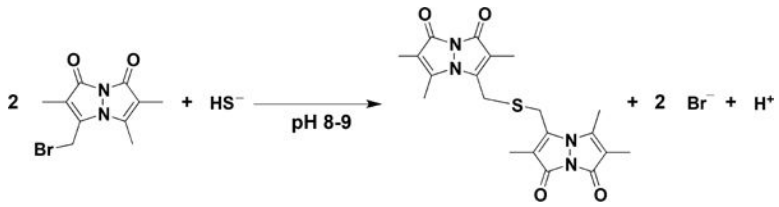

Chart 2.
Reaction of Monobromobimane with H_2S to form Dibimane Sulfide

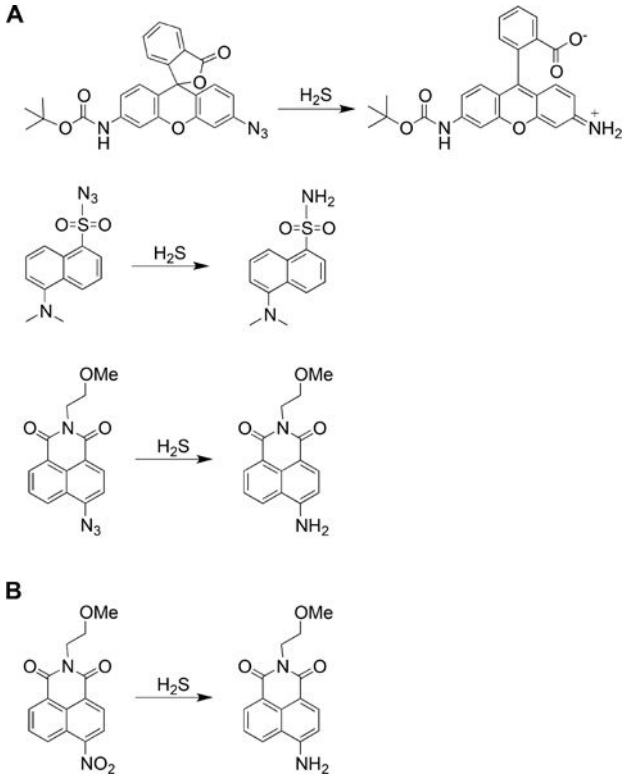

Chart 3. Examples of Fluorescent Probes for H_2S Detection Based on the Reduction of Azide or Nitro Groups[a]

[a](A) Reduction of azide groups in rhodamine (top), dansyl (middle), and naphthalimide (bottom) scaffolds. (B) Reduction of nitro group in the naphthalimide scaffold.

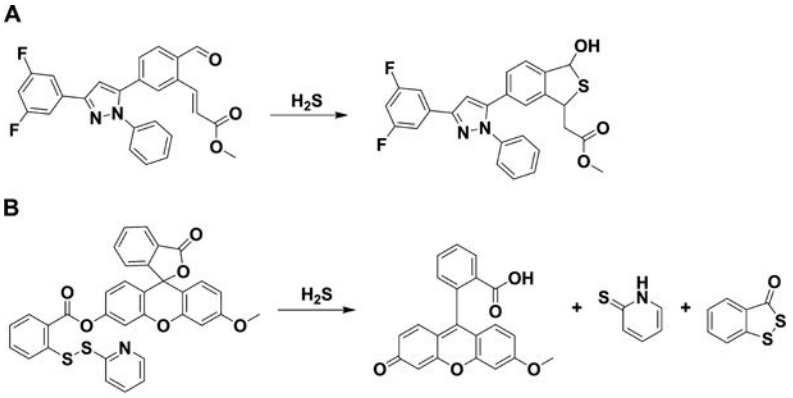

Chart 4. Examples of Fluorescent Probes for H_2S Detection Containing Two Electrophilic Centers[a]

[a](A) Probe containing an aldehyde and an acrylate group on a triaryl pyrazoline scaffold. (B) Probe containing an activated disulfide on a fluorescein scaffold.

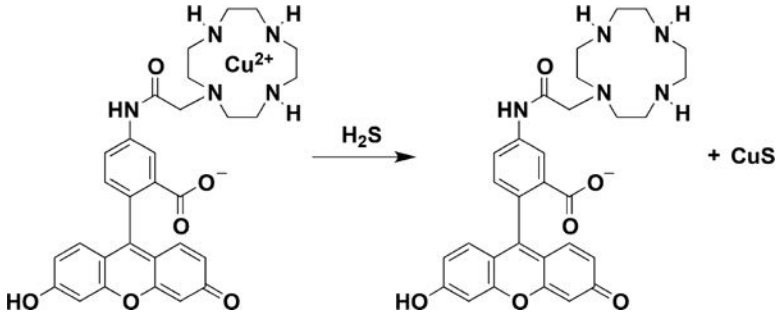

Chart 5.

Example of a Probe for H_2S Detection Based on the Release of Copper Sulfide from a Cyclen and Fluorescein Derivative

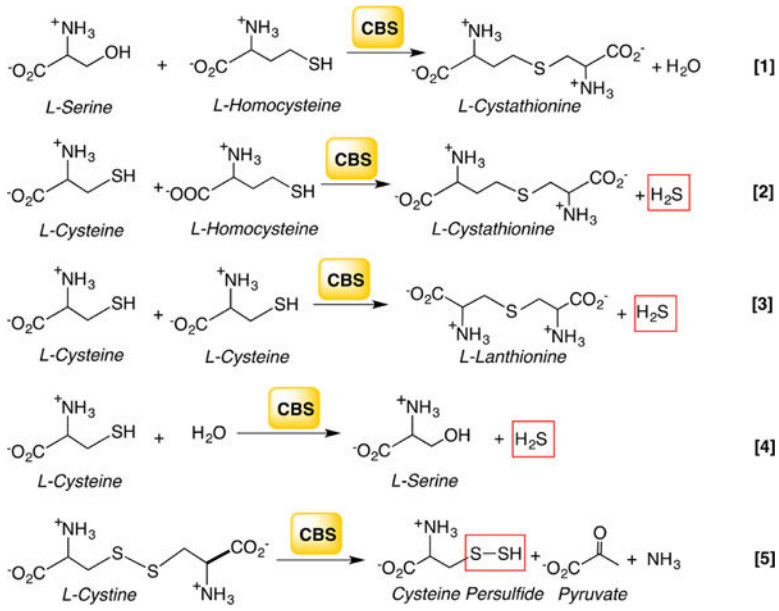

Chart 6. Reactions Catalyzed by CBS[a]

[a]Reaction 1 generates cystathionine in the canonical transsulfuration pathway. Reactions 2–4 generate H_2S from cysteine and/or homocysteine, and reaction 5 produces Cys-SSH from cystine.

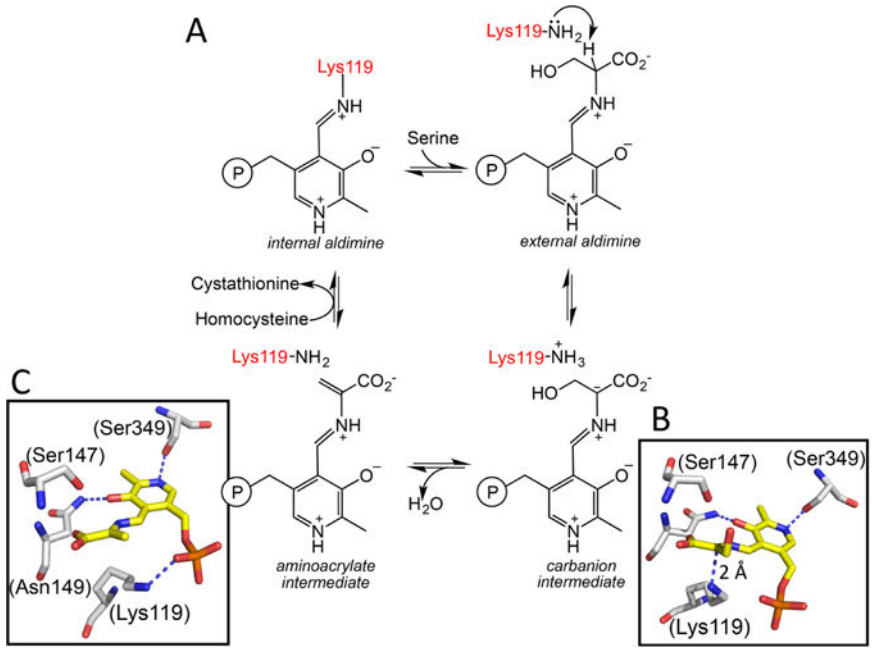

Chart 7. Reaction Mechanism of CBS and Structures of Key Intermediates[a]

[a](A) A minimal mechanism is shown for the β-replacement of serine by homocysteine to generate cystathionine and water. Structures of the carbanion (B) and aminoacrylate (C) intermediates trapped in *Drosophila* CBS (PDB: 2PC4 and 2PC3) are shown. The numbering of residues shown in parentheses in B and C are for human CBS. The corresponding residues in the fly protein are Lys88, Ser116, Asn118, and Ser318, respectively. An sp^2 hybridized α carbon and sp^2 hybridized α and β carbons are seen in the carbanion and aminoacrylate intermediates, respectively. Lys119 undergoes a major positional shift in the aminoacrylate intermediate where it is no longer required to stabilize the carbanion.

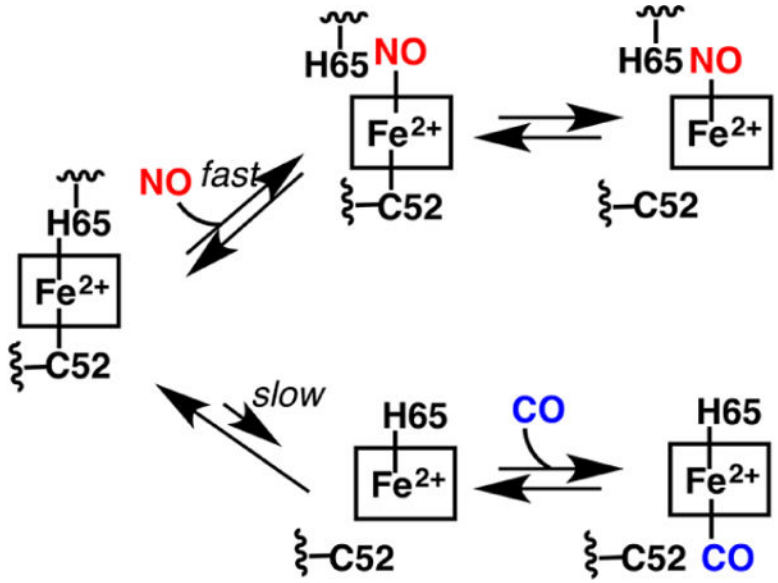

Chart 8. Binding of NO• and CO to Ferrous CBS[a]

[a]Binding of NO• is fast and predicted to occur via displacement of the His65 ligand. Binding of CO is slow and limited by the slow dissociation of the Cys52 ligand.

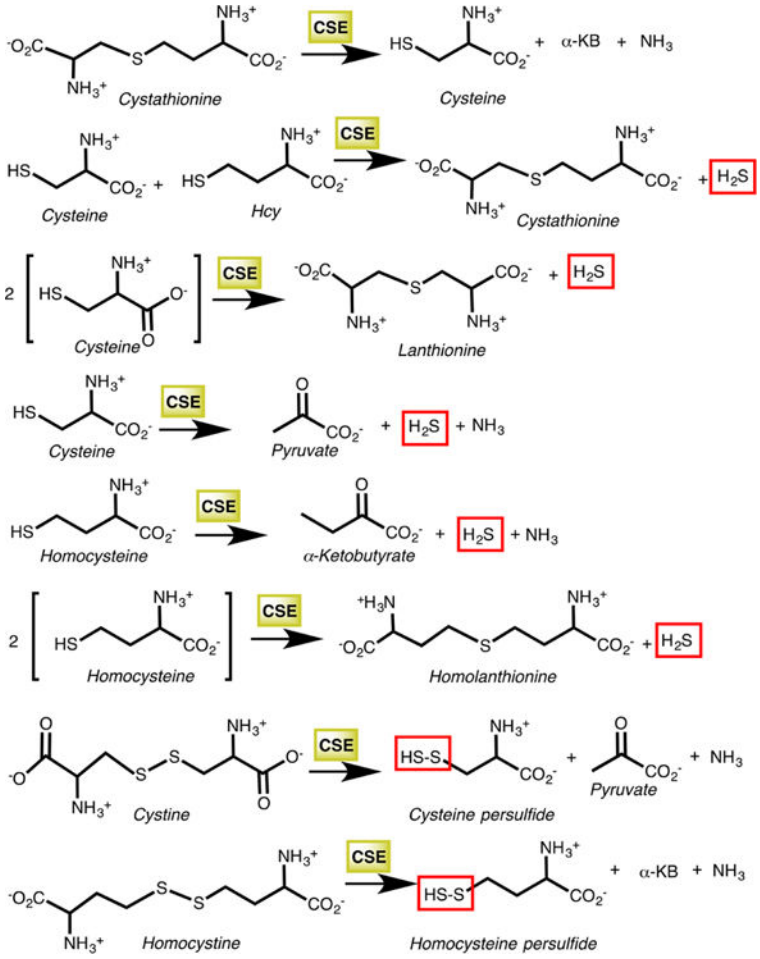

Chart 9. Reactions Catalyzed by CSE[a]

[a]The first reaction is the cleavage of cystathionine to cysteine, α-ketobutyrate (α-KB), and ammonia in the canonical transsulfuration pathway. The next five reactions produce H_2S, while the last two generate the corresponding persulfides from cystine and homocystine.

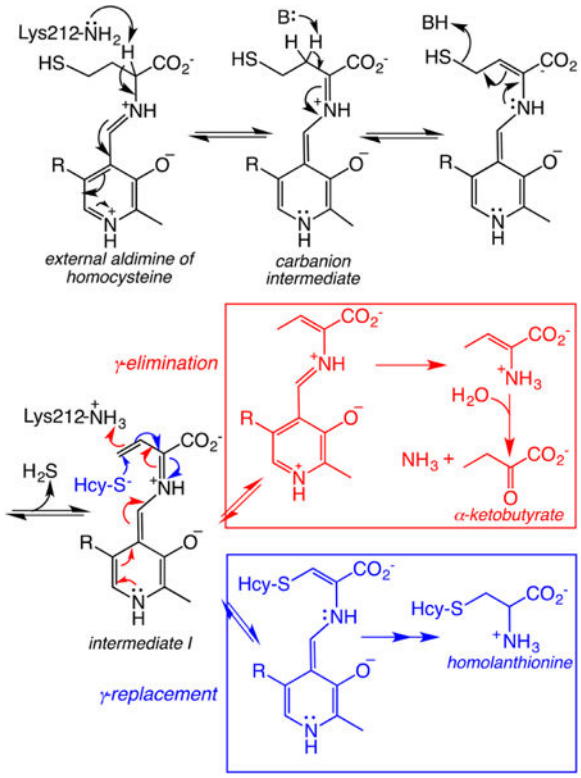

Chart 10. Outline of CSE Mechanism Illustrated for the γ-Elimination of Homocysteine (Red Box) or the γ-Replacement of Homocysteine by a Second mole of the Same Substrate (Blue Box)[a]

[a]Hcy-S$^-$ denotes homocysteine. The first few steps until intermediate I are common to both pathways.

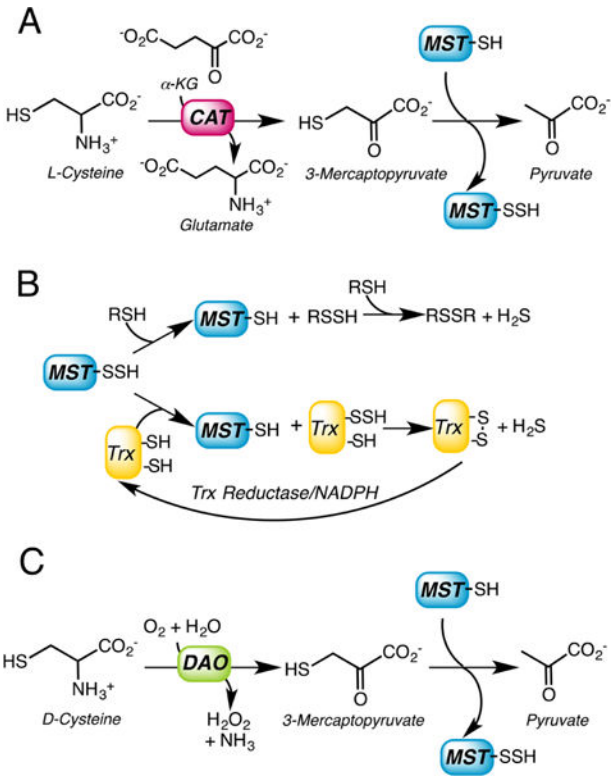

Chart 11. Reaction Catalyzed by MST[a]

[a](A) 3-Mercatopyruvate is synthesized by L-cysteine aminotransferase (CAT), which requires α-ketoglutarate as a cosubstrate. In the first half reaction, MST transfers the sulfur atom from 3-mercaptopyruvate to an active site cysteine forming a Cys-SSH intermediate. (B) In the second half reaction, the outer sulfur from Cys-SSH is transferred to a small molecule thiol acceptor (RSH) or to thioredoxin (Trx) and subsequently released as H_2S. (C) 3-Mercatopyruvate can be synthesized from D-cysteine via the action of D-amino acid oxidase (DAO).

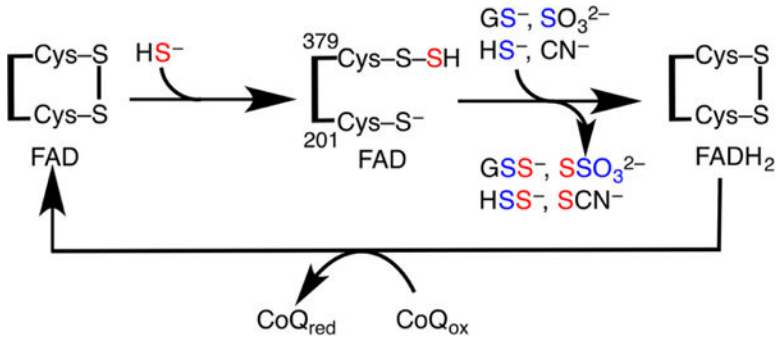

Chart 12. Overview of the Reaction Catalyzed by SQR[a]

[a]In the sulfurtransferase steps, HS^- attacks the disulfide bond in SQR forming a persulfide at Cys379 and the sulfane sulfur (in red) is transferred to an acceptor (GSH, sulfite, sulfide, or cyanide). In the electron transfer steps, two electrons are transferred from HS^- through the disulfide to FAD and then to CoQ.

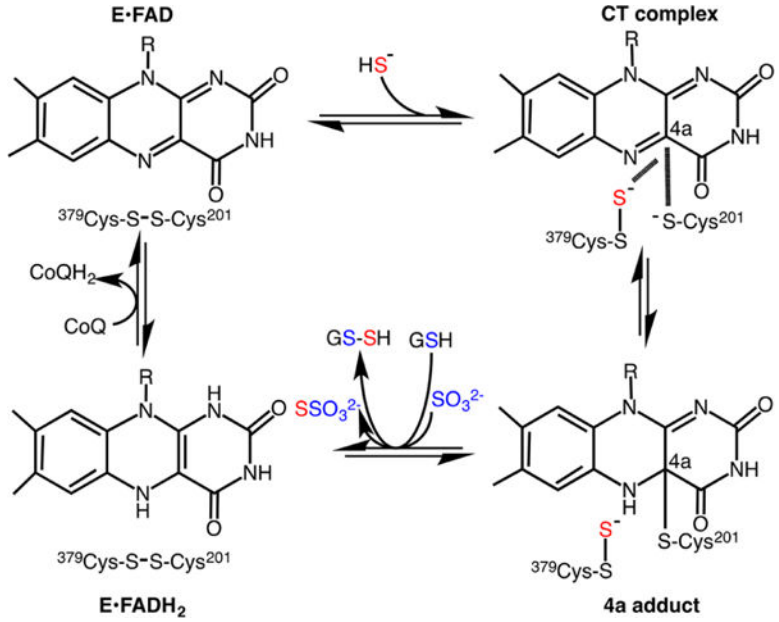

Chart 13. Postulated Reaction Mechanism of SQR[a]

[a]Nucleophilic attack of HS^- on the active site disulfide results in the formation of a Cys-SSH intermediate at Cys379 and a charge transfer (CT) complex, which collapses to a postulated 4a adduct. A sulfur acceptor viz. GSH or sulfite moves the sulfane sulfur from the active site, forming GSSH or thiosulfate ($S_2O_3^{2-}$), respectively, and restoring the active site disulfide. Electron transfer from the reduced flavin, $FADH_2$, to CoQ completes the catalytic cycle.

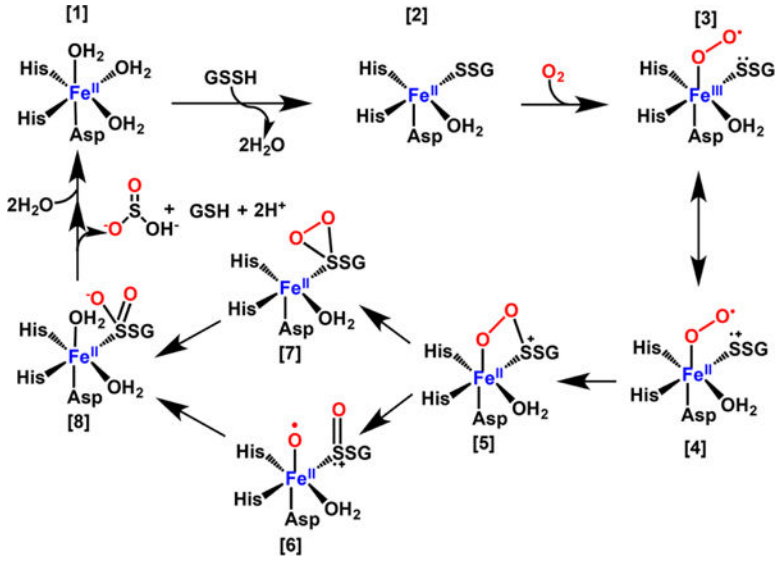

Chart 14. Postulated Reaction Mechanism of PDO[a]

[a]Binding of GSSH to the resting enzyme [1] creates a binding site for O_2 [2]. Formation of a superoxo-Fe^{III} [3] in resonance with a biradical Fe^{II} species [4] leads to formation of a cyclic peroxo-Fe^{II} species [5]. Cleavage of the O–O bond gives [6]. Alternatively, cleavage of the Fe–O bond gives [7]. Binding of H_2O [8], sets up hydrolysis and formation of the product, sulfite. Alternatively, the water that remained coordinated to the metal center could be used for the final hydrolysis step.

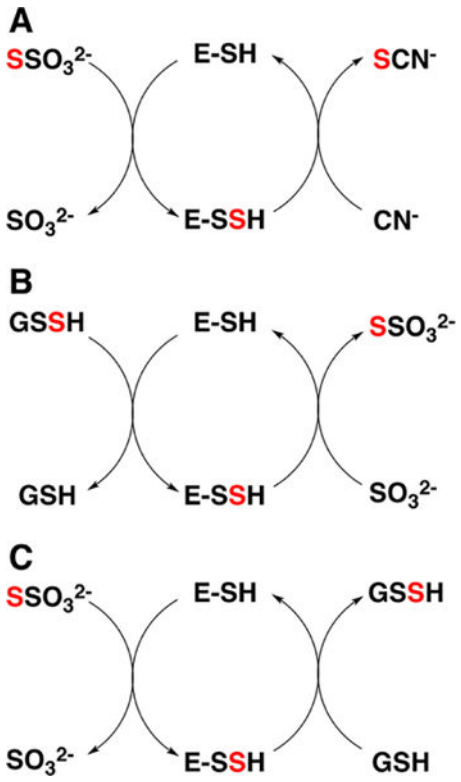

Chart 15. Reactions Catalyzed by Rhodanese[a]

[a]Rhodanese exhibits varied sulfur transferase activities including: (A) thiosulfate:cyanide sulfurtransferase, (B) GSSH:sulfite sulfurtransferase, and (C) thiosulfate:GSH sulfurtransferase. E-SSH denotes the enzyme-bound Cys-SSH intermediate. The red color traces the fate of the sulfur from the donor to the acceptor.

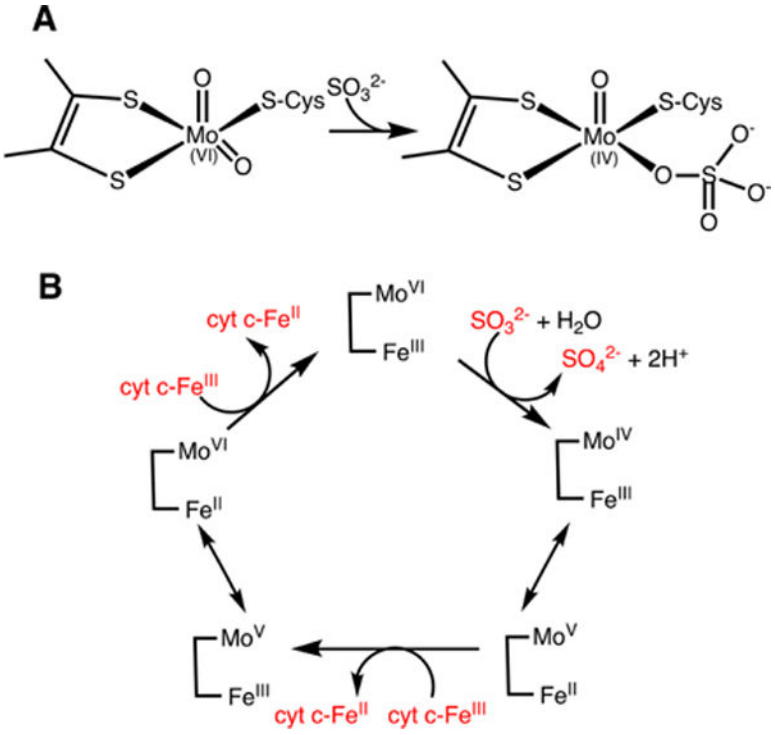

Chart 16. Molybdopterin Cofactor in Sulfite Oxidase and Redox Changes during the Catalytic Cycle[a]

[a](A) Attack of sulfite on an oxo/hydroxyl ligand reduces the molybdenum ion. (B) The reaction cycle of sulfite oxidase involves an initial two-electron reduction of the molybdenum center, which is subsequently oxidized in two one-electron steps via intramolecular electron transfer to the heme. The latter in turn, transfers electrons to the heme in cytochrome c (cyt c) in an intermolecular process.

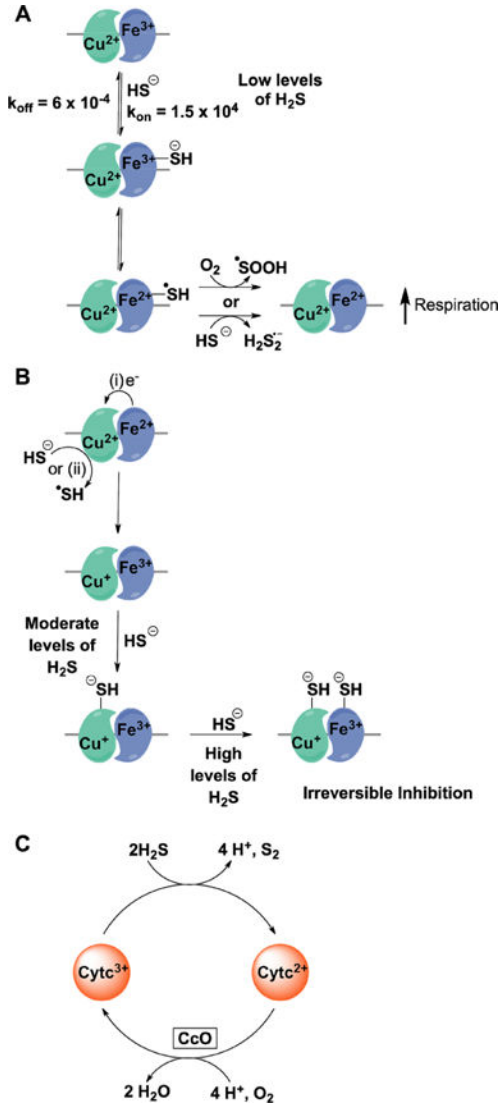

Chart 17. Interaction of H_2S with Cytochrome c Oxidase[a]

[a](A) At low concentrations, H_2S binds to ferric heme a_3 and reduces it with concomitant formation of $HS^{\bullet}$ which can react with either another molecule of H_2S or with oxygen. Reduction of heme a_3 leads to an increase in oxygen consumption. (B) At moderate levels, H_2S interacts with the Cu_B^+ center forming a stable $Cu_B–SH^-$ complex, which is difficult to oxidize. Cu_B^+ is formed by electron transfer from ferrous heme a_3 or by a direct reduction by H_2S. At higher levels of H_2S, the $Cu_B–SH^-$ complex induces a conformational change and causes further binding of H_2S to ferric heme a_3. (C) Alternatively, H_2S can reduce cytochrome c thereby increasing CcO reduction and respiration.

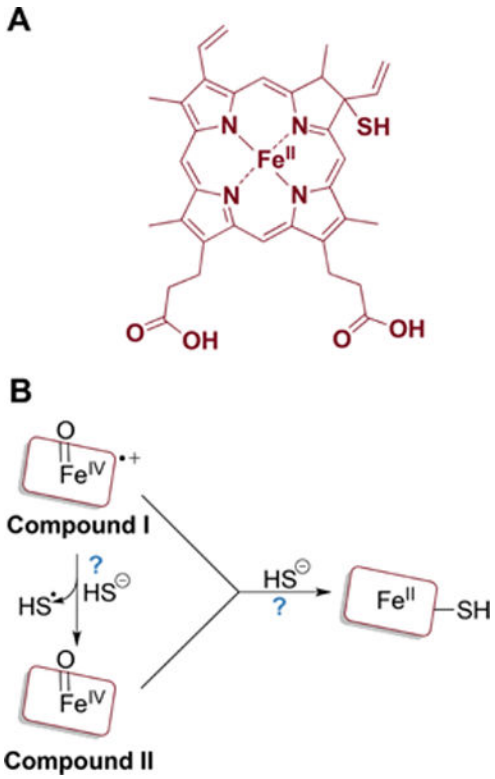

Chart 18. Sulfhemoglobin Formation[a]

[a](A) One of the proposed structures of sulfheme. (B) The mechanism of sulfheme formation is not fully understood (as denoted by the question marks) but starts with compound I or II reacting with H_2S and results in sulfur being incorporated into the porphyrin ring.

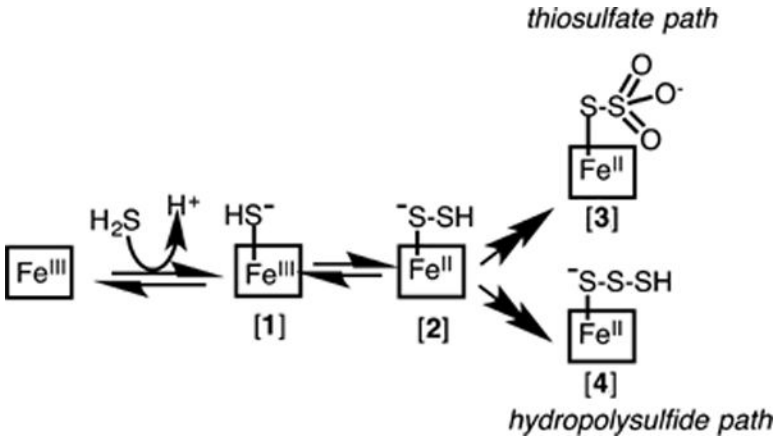

Chart 19. Minimal Reaction Mechanism for Ferric Globin-Dependent Sulfide Oxidation to Thiosulfate and Iron-Bound Hydropolysulfides[a]

[a]Details of the oxidation chemistry that lead to the products have been omitted for clarity.

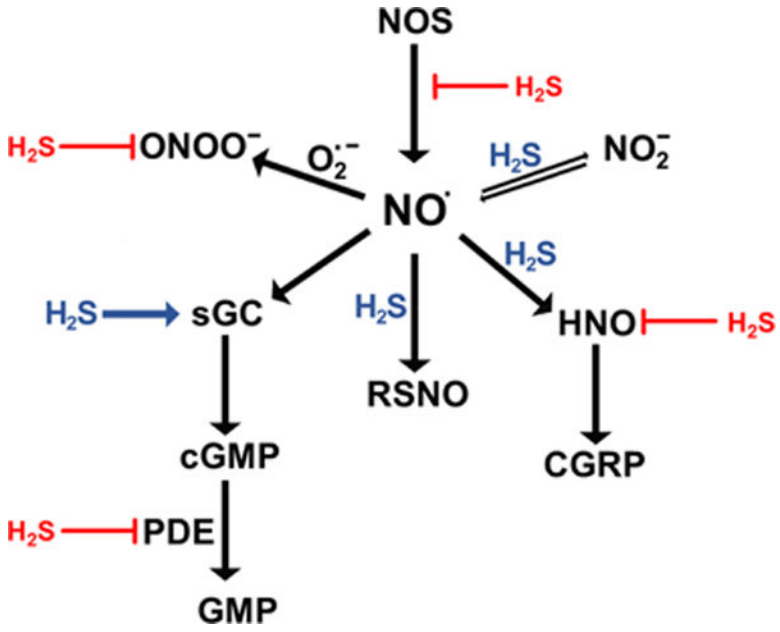

Chart 20. Interaction of H_2S with $NO^{\bullet}$ and Its Metabolites[a]

[a]$NO^{\bullet}$ signals via the classical soluble guanylate cyclase (sGC)/cyclic GMP (cGMP) cascade. H_2S can reduce sGC to increase $NO^{\bullet}$ binding and cGMP production. cGMP is deactivated by phosphodiesterase 5 (PDE), an enzyme that is inhibited by H_2S. Oxidation of $NO^{\bullet}$ to nitrosonium (NO^{+}) ion leads to modification of cysteine residues and formation of *S*-nitrosothiols (RSNO), a process that H_2S can facilitate. $NO^{\bullet}$ can be reduced by H_2S to form HNO. HNO activates the release of calcitonin gene-related peptide (CGRP), a vasodilator, but HNO can also be trapped by H_2S. $NO^{\bullet}$ is oxidized to nitrite, which can be reduced back to $NO^{\bullet}$, a process that H_2S can facilitate. $NO^{\bullet}$ reacts with superoxide to form peroxynitrite ($ONOO^{-}$). H_2S can scavenge $ONOO^{-}$.

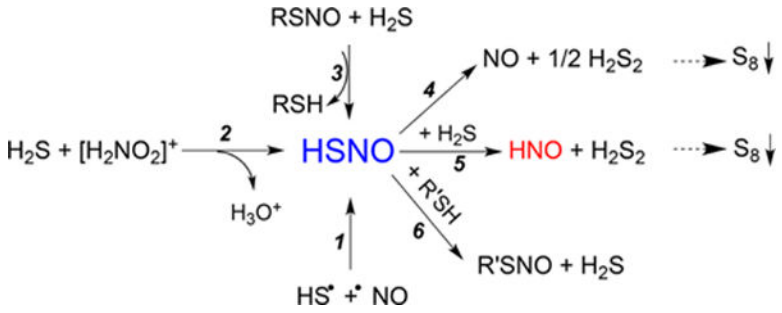

Chart 21.

Reaction Paths for HSNO Generation (1–3) and Its Biologically Relevant Reactions (4–6)

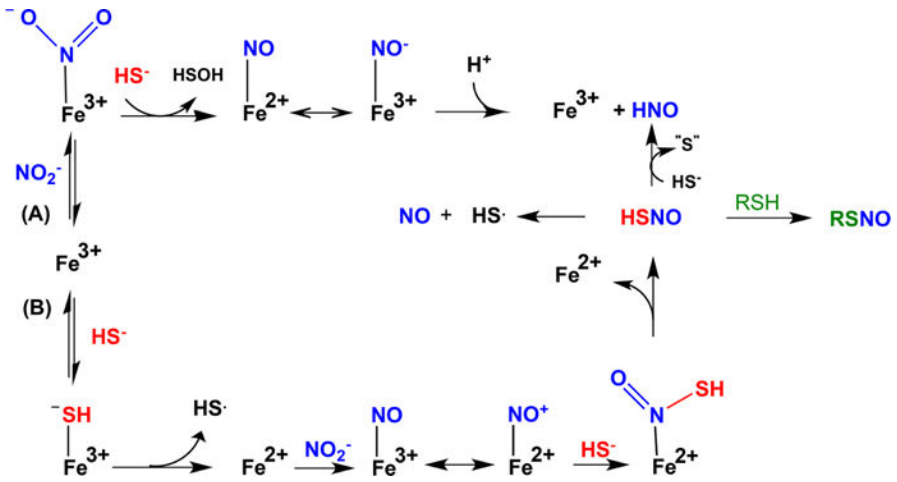

Chart 22. Proposed Reaction Mechanism for H_2S-Assisted Nitrite Reduction Catalyzed by an Iron Porphyrin Compound[a]

[a]Pathway A, which predominates when nitrite is in excess over H_2S, represents a classical oxygen atom transfer; nitrite coordination to ferric heme leads to HSOH and $[Fe^{2+}(NO)] \leftrightarrow [Fe^{3+}(NO^{-})]$, which releases HNO slowly. Pathway B predominates when H_2S is in excess over nitrite; reduction of ferric heme by H_2S is followed by nitrite reduction to $[Fe^{3+}(NO)] \leftrightarrow [Fe^{2+}(NO^{+})]$ species, which is scavenged by HS^{-} giving HSNO. Either free or coordinated HSNO causes transnitrosation of protein thiols or, in the reaction with H_2S, generates HNO.

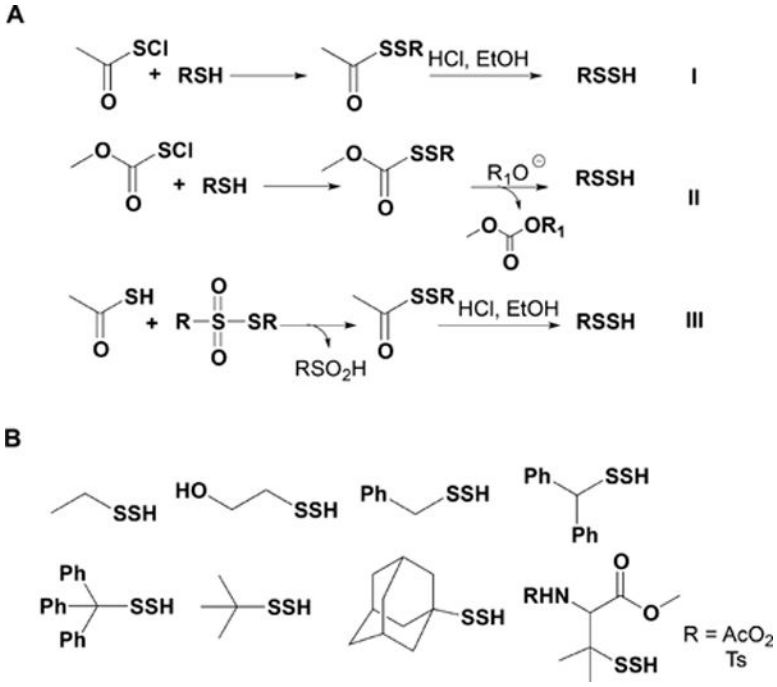

Chart 23.

Synthetic Strategies for the Preparation of Low Molecular Weight Persulfides (A) and Structures of Some of the Persulfides Prepared following These Synthetic Routes (B)

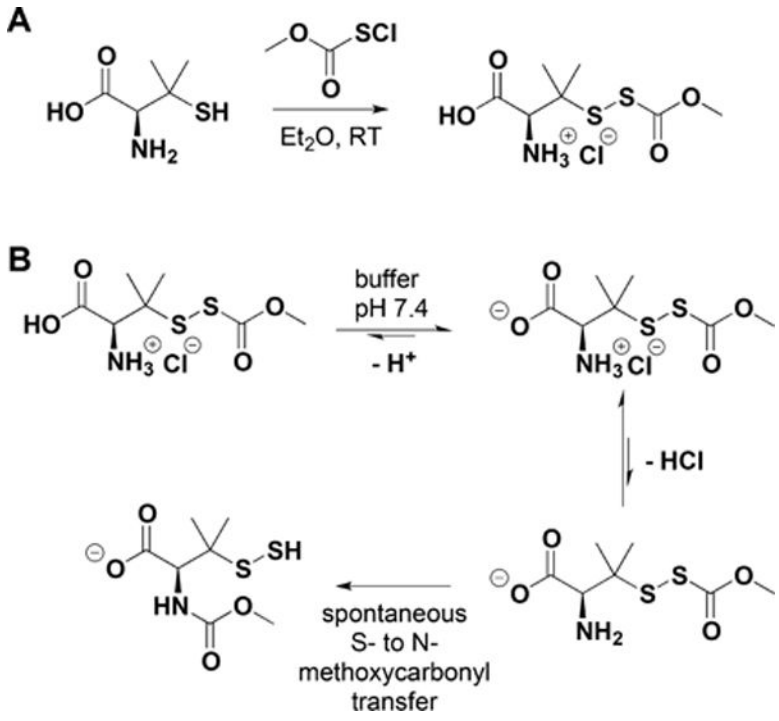

Chart 24.

Synthesis of an Acyl-Protected Disulfide of Penicillamine (A) and Its Rearrangement to *N*-Methoxycarbonyl Penicillamine Persulfide via *S*- to *N*-Methoxycarbonyl Transfer at pH 7.4 (B)

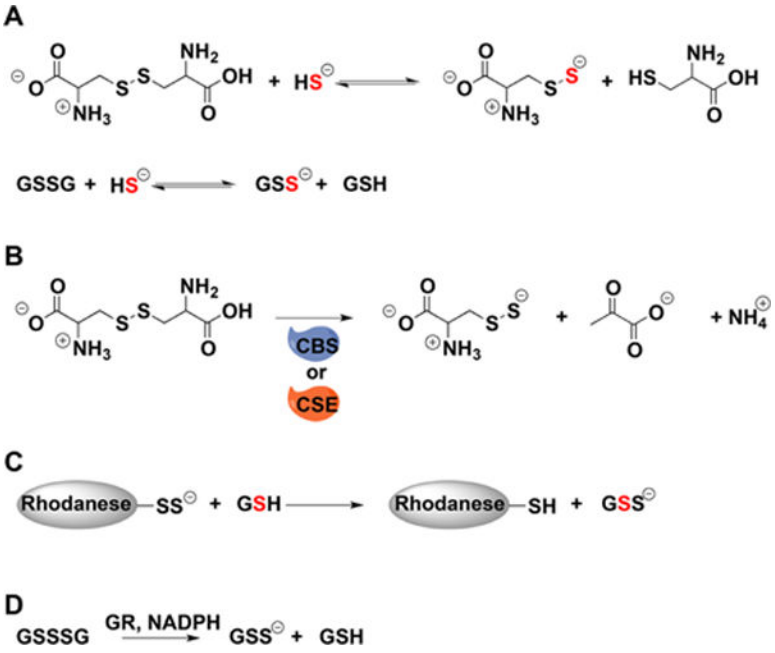

Chart 25. Strategies for the in Situ Preparation of LMW Persulfides[a]

[a](A) Cysteine and glutathione persulfides can be prepared by the reaction of H_2S with cystine and glutathione disulfide, respectively. (B) Cysteine persulfide can be generated from cystine and CSE or CBS. (C) Rhodanese can be used to transfer sulfur to glutathione. (D) Glutathione reductase (GR) uses electrons from NADPH to reduce glutathione trisulfide to persulfide and GSH.

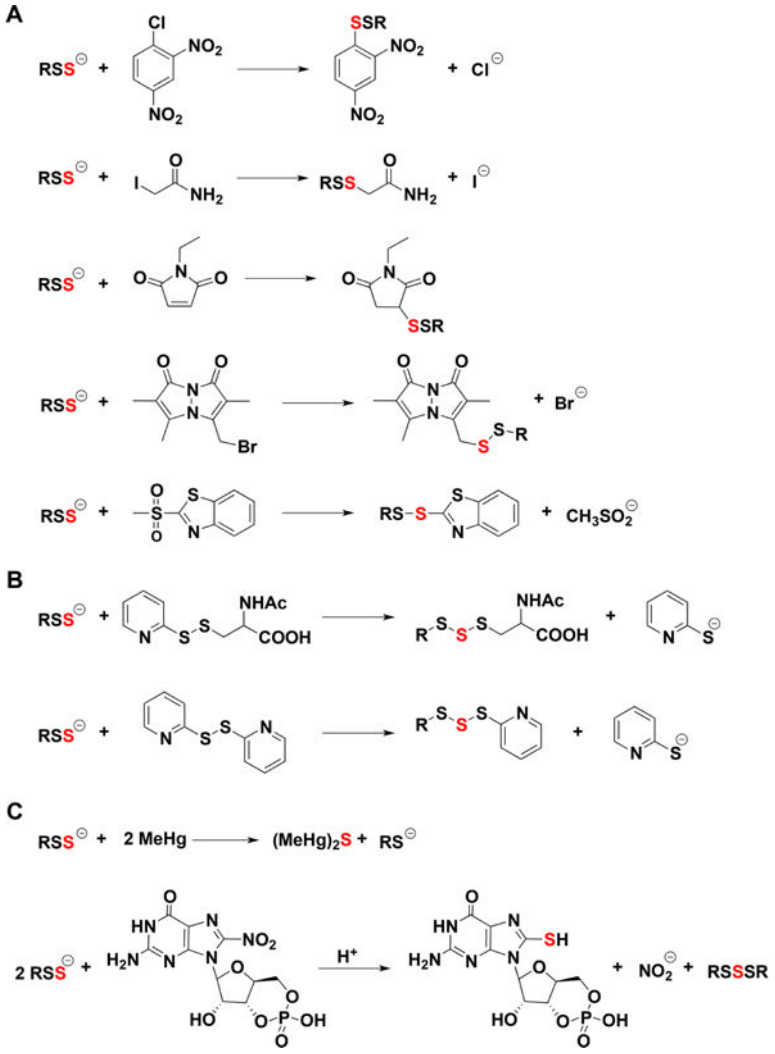

Chart 26. Reactions of Persulfides with Electrophiles[a]

[a](A) Reactions with thiol alkylating agents. (B) Reactions with disulfides. (C) Reactions with methylmercury and nitroguanosine 3′,5′-cyclic monophosphate.

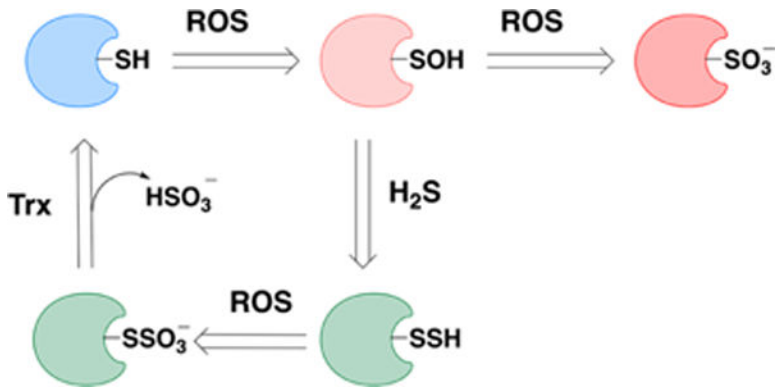

Chart 27. Protein Persulfidation Can Protect Proteins from Overoxidation[a]

[a]A thiol can be oxidized to a sulfenic acid. The latter can be reduced back to thiol or be further oxidized to sulfonate, an irreversible modification. Persulfides, if exposed further to oxidants, will form *S*-sulfocysteines ($-SSO_3^-$). Enzymes such as thioredoxin can reduce the S–S bonds and restore the native thiol.

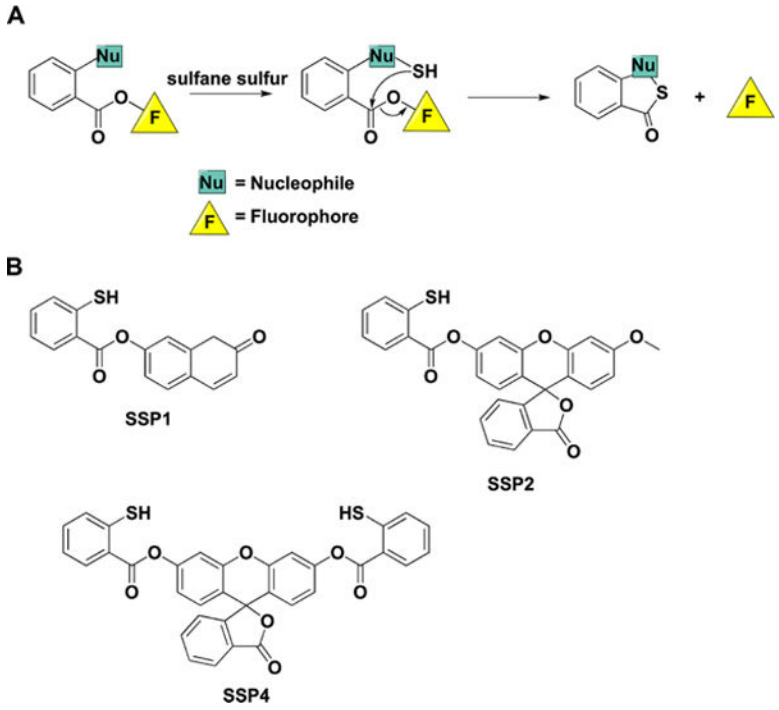

Chart 28. Fluorescent Probes for Sulfane Sulfur[a]

[a](A) Internal cyclization and fluorophore release following the initial reaction of the probe with sulfane sulfur compounds. (B) Structures of the synthetic probes that exhibit this type of chemical reactivity.

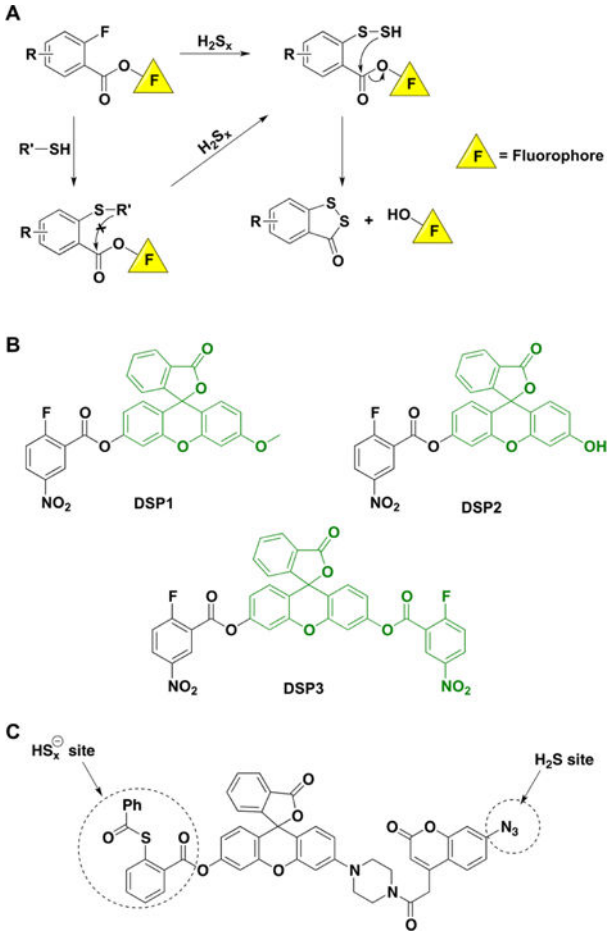

Chart 29. Electrophilic Probes that Release a Fluorophore upon Reaction with Inorganic Polysulfides[a]

[a](A) Reactions leading to fluorophore release. (B) Structures of the synthetic probes that exhibit this type of reactivity. (C) FRET-based probe for the simultaneous detection of H_2S and sulfane sulfur-containing species.

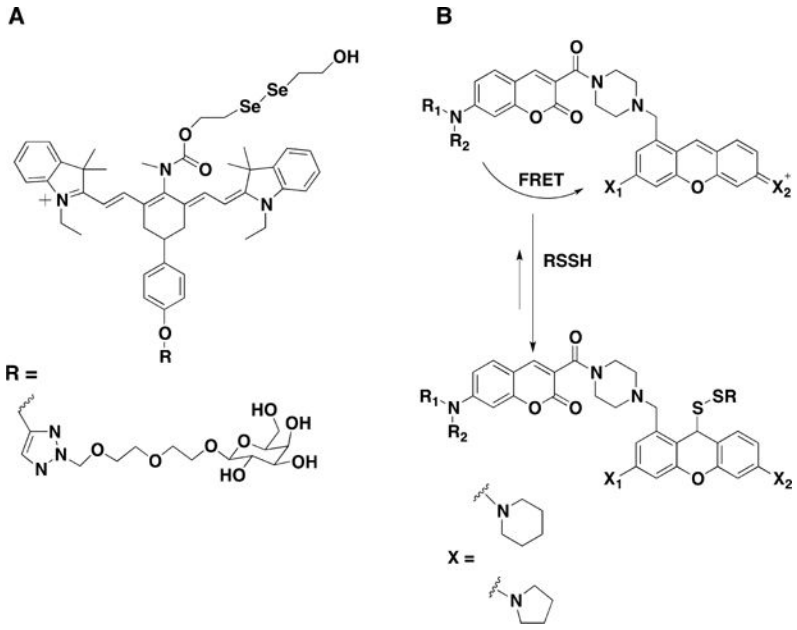

Chart 30.

Ratiometric Near-IR Fluorescence Probe for Cysteine Persulfide Detection (A) and FRET Probe Designed for Persulfide Detection (B)

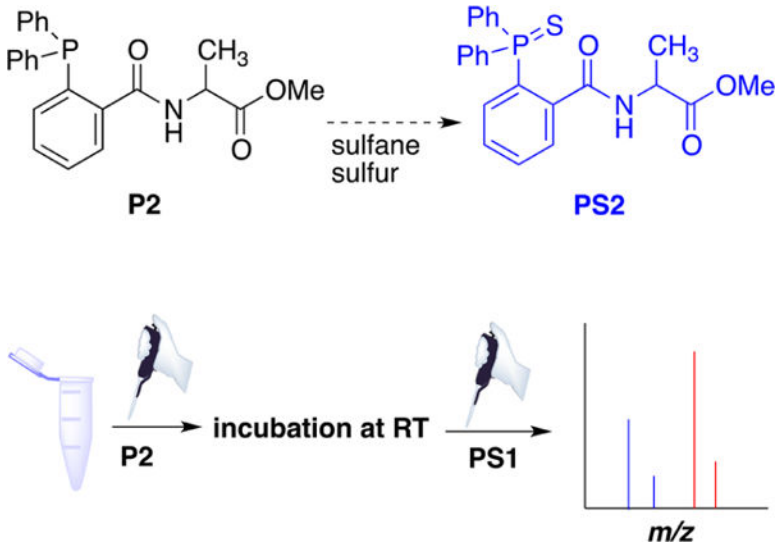

Chart 31. Isotope Dilution Mass Spectrometry Approach for the Detection of Sulfane Sulfur Using Substituted Phosphines[a]

[a]The reaction of triarylphosphine (P2) with sulfane sulfur compounds. After incubation of P2 with cell or tissue samples to form PS2, PS1 (^{13}C-labeled triarylphosphine sulfide) is added as internal standard and the samples analyzed by MS.

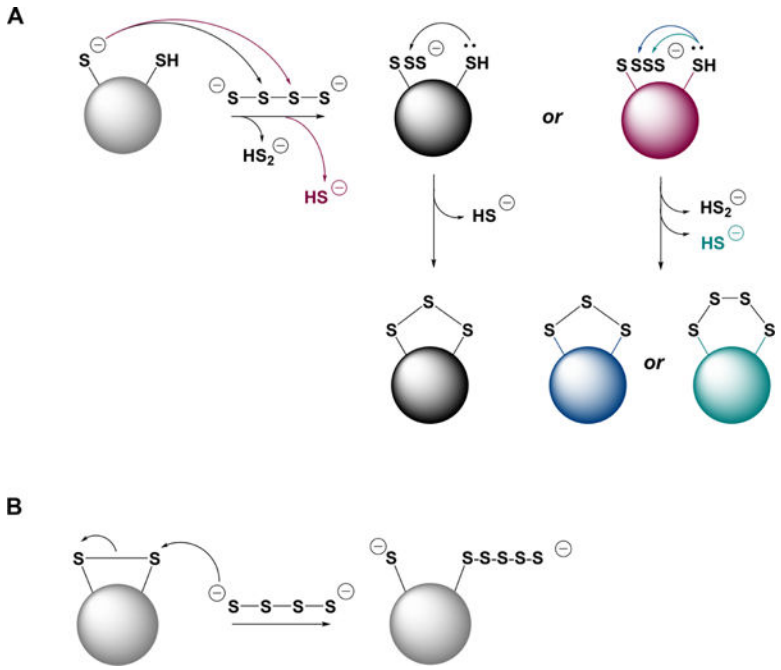

Chart 32. Reactions of Inorganic Polysulfides with Proteins[a]

[a](A) Inorganic polysulfides can react as electrophiles with a protein thiolate. The resulting polythiolated cysteine can have different numbers of S atoms and can in turn, be attacked by a proximal cysteine forming a family of products, e.g., intramolecular disulfides, trisulfides, etc. (B) Inorganic polysulfides can react as nucleophiles with an intramolecular protein disulfide forming thiol and polythiolated cysteine.

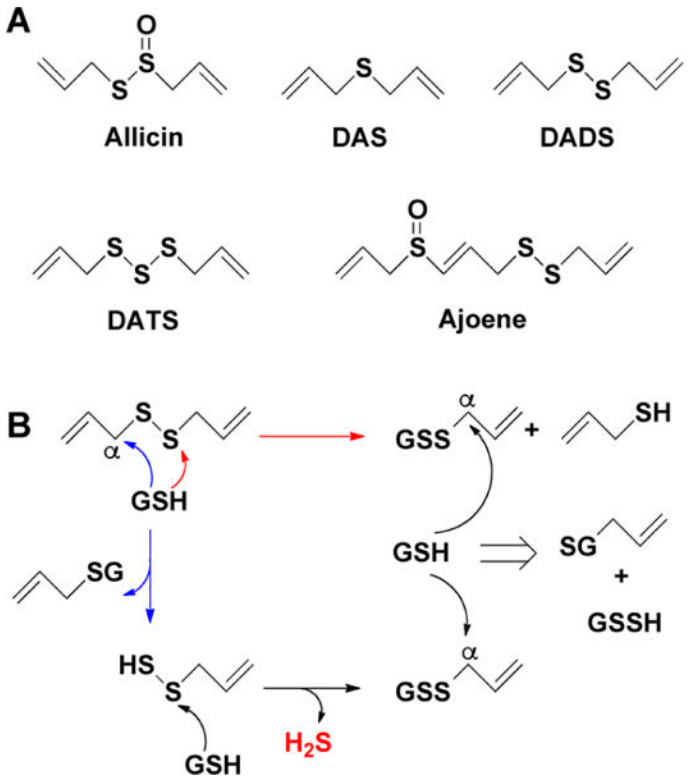

Chart 33. Active Principles of Garlic and the Mechanisms for LMW Persulfide Generation from Them[a]

[a](A) Allicin (diallyl thiosulfinate) is rapidly metabolized in aqueous solutions into diallyl sulfide (DAS), diallyl disulfide (DADS), diallyl trisulfide (DATS), and ajoene. (B) Glutathione-promoted decomposition of DADS and generation of allylpersulfide, glutathione persulfide (GSSH), and H_2S.

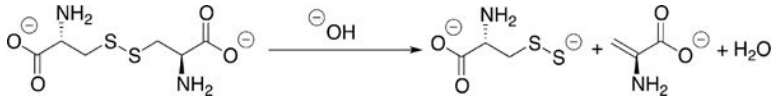

Chart 34.
Base-Promoted Persulfide Generation from Cystine

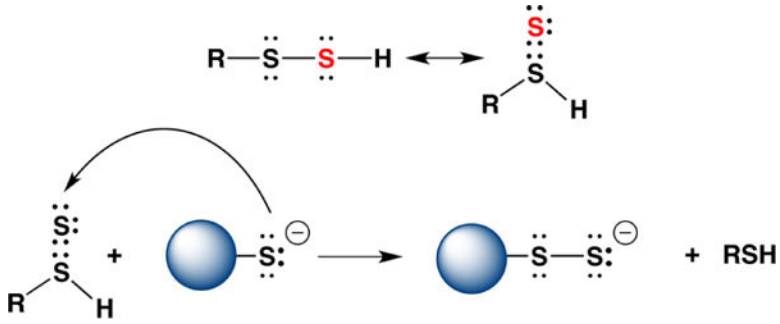

Chart 35.

Tautomerization of a Persulfide to a Thiosulfoxide as a Postulated Mechanism for Transpersulfidation

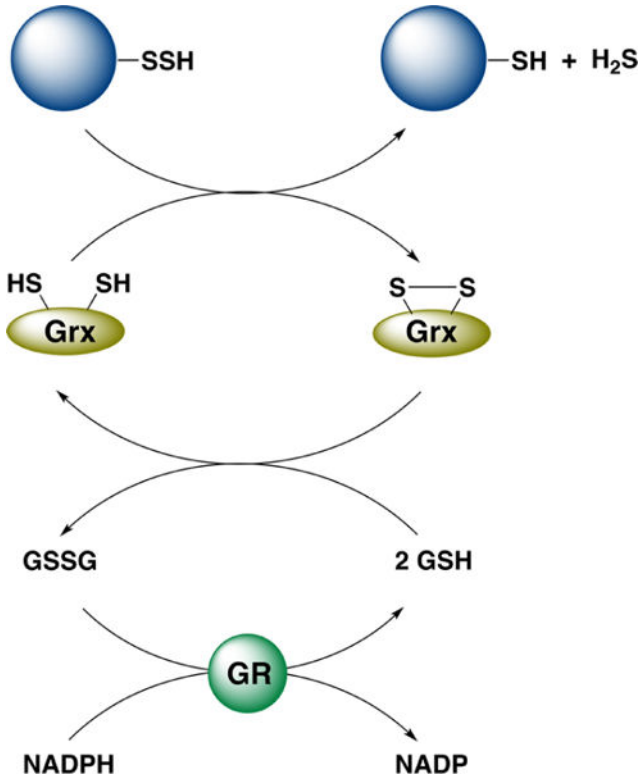

Chart 36. Glutaredoxin-Catalyzed Protein Depersulfidation[a]

[a]Glutaredoxin (Grx) reduces a protein persulfide, oxidized Grx is reduced by glutathione (GSH), and GSSG is reduced by glutathione reductase (GR) at the expense of NADPH.

Table 1

Basic Physicochemical and Thermodynamic Properties of H_2S

dipole moment	**0.97 D**
boling temperature	−60 °C
solubility (in H_2O)	110 mM/atm, 25 °C
	210 mM/atm, 0 °C
boiling temperature	−60.2 °C
density (25 °C, 1 atm)	1.36 kg/m^3
IR[a]	ν_1 2525, 2536 cm^{-1}
	ν_2 1169, 1184, 1189 cm^{-1}
	ν_3 2548 cm^{-1}
^{1}H NMR[b]	0.52 ppm
pK_1	6.98
pK_2	>17 at 25 °C
λ_{max} (HS^-)	230 nm
ε	8×10^3 M^{-1} cm^{-1}
Henry's law coefficient (298 K)	0.087135 mol solute/mol water atom
detection threshold by human nose	0.02–0.03 ppm
lethal dose	>500 ppm
$\Delta_f G°(H_2S)$	−28 kJ/mol
$\Delta_f G°(HS^-)$	+12 kJ/mol
$\Delta_f G°(S^{2-})$	+86 kJ/mol
$E°'(S^{\bullet -}, H^+/HS^-)$	+0.91 V[c]
$E°'(HS_2^-, H^+/2HS^-)$	−0.23 V[c]

[a] Values are for the crystalline phase III.

[b] Value obtained from crude sulfane oil.

[c] Versus SHE.

Table 2

Rate Constants for the Reaction of H_2S with Biologically-Relevant Oxidants

	reduction potential			kinetics of reaction with H_2S	
oxidant	**couple**	$E^{\circ\prime}$ **(V)**	**ref**	$k(M^{-1}\ s^{-1})$	**ref**
	One-Electron Oxidant				
hydroxyl radical	$HO^{\bullet}$, H^+/H_2O	+2.31	414	1.1×10^{10} (pH 7)	415,416
oxygen	$O_2(g)/O_2^{\bullet-}$	−0.35[a]	414	very slow	
carbonate radical	$CO_3^{\bullet-}$, H+/HCO_3^-	+1.77[b]	63	2.0×10^8 (pH 7, 20 °C)	65
nitrogen dioxide	$NO_2^{\bullet}/NO_2^-$	+1.04	63	1.2×10^7 (pH 7.5, 25 °C)	61
superoxide radical	$O_2^{\bullet-}$, $2H^+/H_2O_2$	+0.91	414	~208 (DMSO)	97
myeloperoxydase compound I	CI/Fe^{3+}	+1.35	421	1.1×10^6 (pH 7.4, 25 °C)	376
myeloperoxydase compound II	CII/Fe^{3+}	+0.97	421	2.0×10^5 (pH 7.4, 25 °C)	376
	Two-Electron Oxidant				
hydrogen peroxide	H_2O_2, $2H^+/2H_2O$	+1.35	414	0.48–0.73 (pH 7.4, 37 °C)	61,73
peroxynitrite	ONOOH, H^+/NO_2^-, H_2O	+1/30	422	6.7×10^3 (pH 7.4, 37 °C)	420
hypochlorite	HOCl, H^+/Cl^-, H_2O	+1.28	421	$0.8–20 \times 10^8$ (pH 7.4, 37 °C)	61,418
tauramine-chloramine	–			303 (pH 7.4, 37 °C)	61

[a] The reduction potential based on a standard state of 1 M O_2 is −0.18.[414]

[b] Extrapolated to pH 7 from $E^{\circ}(CO_3^{\bullet-}/CO_3^{2-})$ = 1.57 V assuming a pK_a of 10.32 for HCO_3^-.

Table 3

Basic Physicochemical and Thermodynamic Properties of LMW Persulfides

	values	refs
λ_{max}	335–340 nm[a]	31,494,495,501,502
IR (S–H stretch) (cm^{-1})	2490–2510	488–500
(S–S stretch) (cm^{-1})	200–500	
^{1}H NMR	2.7–3 ppm	494,495,501,502
S–S bond length	2.04 Å	495
$E^{\circ\prime}$(RSS^-, $2H^+$/RSH, HS^-)	−0.18 V[b]	64
$E^{\circ\prime}$($RSS^{\bullet}$/RSS^-)	+0.68 V[b]	64

[a]Alkaline pH, but organic solvents as well.

[b]Versus SHE.